
Distribution of Complex Chemicals in Oil-Water Systems

Muhammad Riaz

PhD Thesis

September 2011

Center for Energy Resources Engineering

Department of Chemical and Biochemical Engineering

Technical University of Denmark

DK-2800 Lyngby, Denmark

Preface

This thesis is submitted as partial fulfillment of the requirement for the PhD degree at Technical University of Denmark (DTU). The work has been carried out at the Department of Chemical and Biochemical Engineering and Center for Energy Resources Engineering (CERE) from April 2008 to September 2011 under the supervision of Professor Georgios M. Kontogeorgis, Professor Erling H. Stenby and Senior Researcher Wei Yan. The project was funded by Statoil. This work has been carried out in close collaboration with Statoil including six months external stay at Statoil Research and Development Center, Trondheim Norway.

First of all I would like to express my gratitude to Professor Georgios M. Kontogeorgis for his guidance and support on the research presented in this thesis. Your deep involvement has been very helpful in this project. You have been a source of inspiration for me throughout this project due to your passion and dedication towards research.

I am grateful to Professor Erling H. Stenby for providing me an opportunity to do my PhD project in close collaboration with oil and gas industry. Your leadership has been very productive for keeping CERE close to the industry and making it a multidisciplinary center which has helped me to broaden my research vision.

Many thanks to Senior Researcher Wei Yan for providing his guidance and valuable input in this project. I always found you helping with your unique holistic ideas about experimental work, computation and the modeling. I am thankful to Dr. Yannis for his help in handling FORTRAN codes.

I gratefully acknowledge Statoil for the financial support of the project. The experimental work presented in this thesis has been carried out at Statoil R and D where a number of people helped me during my stay in beautiful town of Trondheim. First of all I would like to thank Toril Haugum for her great help from introducing me to GC to the completion of this work. I am grateful to Dr. Lars Henrik and Dr. Kjersti O. Christensen to facilitate my stay. Thanks to Torbjørn V. Løkken for his help to find a way through challenging situations in experiments. My gratitude to Dr. Even Solbraa for his time for fruitful discussions and guidance in this project. Thanks to Dr. Stathios for having nice chats during my stay. Thanks to Dr. Nina Aas for collaboration in the first phase of this PhD project and sharing useful information about the chemicals. It has been very useful to be with all of you and getting benefit from your knowledge and experience.

Thanks to all my colleagues for nice research and social environment at CERE. Special thanks to Louise and Patricia for their support in official documentations and Christian for IT support. I always found you ready to help with smile on your faces.

Special thanks to my friends and colleagues Shafiq, Hamid (NTNU), Adeel and Wasim. I spent a decade with you and always found you very helpful. I deeply acknowledge your support during all those times we have been together. Additional thanks to Hamid for his help during my external stay in Trondheim. My thanks to Subham Paul, I have benefited from your presence in our office. I had a nice time with you.

I want to pay my humble gratitude to my parents for their love and prayers. Your wisdom and guidance bring me this far in my life and academic career. I am also grateful to my family in Pakistan for their prayers and good wishes. You always supported me and your role has been tremendous in my life and academic career. Thanks for your trust and believe in every descion I made in my life.

Thanks to my wife Amrozia. Without your love, care and understanding it was not easy for me to complete this work. You always encouraged me in the challenging moments of life. Thanks to my daughter Ayesha who born and grow with my PhD. You have always been a cool baby and a child. I always got energy from your smile and love and relaxed by nerves with your entrainment. I am thankful to both of you for accompanying me during my external stay in Trondheim

Muhammad Riaz
September 06, 2011
2800 Kgs. Lyngby Denmark

This dissertation is dedicated to my mother your love is the most precious thing for me !

Summary

The deepwater energy sector represents one of the major growth areas of the oil and gas industry today. In order to meet the challenges of hydrate formation, corrosion, scaling and foaming the oil and gas industry uses many chemicals and their use has increased significantly over the years. In order to inhibit gas hydrate formation in subsea pipelines monoethylene glycol (MEG) and methanol are injected in large amounts. It is important to know the distribution of these chemicals in oil and water systems for economical operation of a production facility and to evaluate their impact on marine life. Furthermore distribution of chemicals is important information for downstream processing of oil and gas. The purpose of this project is the experimental measurement and the thermodynamic modeling of distribution of these complex chemicals in oil-water systems.

Traditionally distribution of chemicals in oil-water system is calculated using octanol-water partition coefficients. But experiments carried out by Statoil R & D have shown that octanol-water partition coefficients (K_{ow}) do not always mimic oil-water partition coefficients ($K_{oil-water}$) and therefore calculations may not be always correct. In the first phase of this project experimental data on K_{ow} , $K_{oil-water}$ and K_{hw} (hexane-water partition coefficients) are collected and investigations were carried out to develop correlations so that $K_{oil-water}$ can be predicted using K_{ow} and K_{hw} . However, due to scarcity of experimental data and limited information about the molecular structure of production chemicals the correlation could only be obtained for few families like alcohols, glycols and alkanolamines with varying degree of reliability.

In order to develop a thermodynamic model for the distribution of chemicals in oil-water systems experimental data are required but such data with natural gas-condensate/oil systems are very rare in the literature. In this project experimental work has been carried at Statoil R & D and an experimental method has been established and tested for such measurements. The mutual solubility of two North Sea condensates, MEG and water has been measured in the temperature range of 275-326 K at atmospheric pressure. The detailed composition of condensates is measured by GC analysis and 85 components are identified up to n-nonane and hundreds of ill-defined components in decane plus fraction.

When methanol and MEG are used as gas hydrate inhibitors, the most significant disadvantage, especially for methanol, is their loss in hydrocarbon phase(s). The successful estimation of inhibitor loss would enable the inhibitors injection optimization as a function of the system parameters such as temperature and water cut. In this project the distribution of water and inhibitors (methanol,

MEG) in various phases is modeled using the CPA EoS. The hydrocarbon phase consists of mixture-1 (methane, ethane, n-butane) or mixture-2 (methane, ethane, propane, n-butane, n-heptane, toluene and n-decane). CPA can satisfactorily predict water content in the gas phase of the multicomponent systems containing mixture-1 over a range of temperature and pressure. Similarly the methanol content in gas phase of mixture-1 + water + methanol systems is predicted satisfactorily with accuracy in the range of experimental uncertainty. For VLLE of mixture-2 + water, mixture-2 + MEG + water and mixture-2 + methanol + water systems, the organic phase compositions are satisfactorily predicted whereas modeling results are relatively less satisfactory for vapor phase compositions partially due to uncertainties in the experimental data.

In addition to the multicomponent systems described above, the VLE of the binary system of methane-methanol is also investigated using CPA with satisfactory calculations of methane content of liquid phase using a single temperature independent k_{ij} over a range of temperature and pressure. The methanol content in the gas phase is satisfactorily correlated at higher temperatures and lower pressures using the same k_{ij} but deviations from experimental data are observed at lower temperatures and higher pressures. In order to extend CPA to reservoir fluids it is of interest to investigate the LLE of binary systems of hydrocarbons and water. In this work CPA is also applied to alkane + water and alkylbenzene + water systems to obtain binary interaction parameters and cross-association volumes respectively.

Finally, CPA has been extended to reservoir-fluid + MEG and reservoir-fluid + MEG + water systems. The reservoir fluid consists of three condensates and two oils from the gas fields in the North Sea. The mutual solubility of condensates and MEG is satisfactorily correlated using a single, average and temperature independent k_{ij} for all MEG-HC pairs. Similarly the mutual solubility of condensate/oil, MEG and water is predicted satisfactorily using the same average k_{ij} for MEG-HC pairs and water-HC k_{ij} from a generalized correlation as a function of carbon number. The experimental trends in mutual solubility as a function of temperature and MEG content in polar phase are predicted satisfactorily which are correct in order of magnitude according to the industrial requirements.

Resumé på dansk

Energisektoren for undervandsoperationer repræsenterer i dag et af de hurtigst voksende områder inden for olie- og gas industrien. For at imødekomme udfordringerne med korrosion, afskalning, samt hydrat- og skumdannelse anvender olie- og gas industrien store mængde kemikalier, og forbruget af disse kemikalier er stærkt stigende. For at forhindre dannelsen af gas hydrater anvender olie- og gas industrien store mængder monoethylene glycol (MEG) og methanol i deres undersøiske rørledninger. Det er vigtigt at kende distributionen af disse kemikalier i olie- og vand systemer, både for den økonomiske drift af produktionsanlæg, samt for at evaluere virkningen på marint liv. Derudover er viden om kemikaliedistributionen vigtigt for oprensningsprocesser af olie og gas. Formålet med dette projekt er at foretage eksperimentelle målinger samt at udføre termodynamisk modellering af distributionen af disse komplekse kemikalier i olie og vand systemer.

Traditionelt anvendes fordelingskoefficienter for oktanol-vand til at udregne distributionen af kemikalier i olie/vand systemer. Men eksperimentelle resultater opnået af Statoil R&D, har vist at disse oktanol-vand fordelingskoefficienter (K_{ow}) ikke altid passer sammen med olie-vand fordelingskoefficienter ($K_{oil-water}$). I dette projekts første fase, blev eksperimentelle data for K_{ow} , $K_{oil-water}$ og K_{hw} (hexane-vand fordelingskoefficient) indsamlet. Det blev undersøgt hvorvidt man kunne udvikle en korrelation til beregning af $K_{oil-water}$ ved brug af K_{ow} og K_{hw} . Dette kunne dog kun opnås for nogle få familier af kemikalier, såsom alkoholer, glykoler og alkanolaminer, og med en varierende grad af pålidelighed. Dette skyldes en stor mangel på eksperimentelle data og begrænset information omkring molekyler struktur af produktionskemikalier.

Eksperimentelle data er essentielle for udviklingen af en termodynamisk model, der er i stand til at forudsige distributionen af kemikalier i olie- og vand systemer. Data for kondensat- og oliesystemer er dog meget sjældne i litteraturen. I dette projekt er der blevet udført eksperimentelt arbejde hos Statoil R&D, hvor en eksperimentel metode er blevet etableret og testet for målinger af denne type blandinger. Den gensidige opløselighed af to Nordsø gas kondensater med MEG og vand er blevet målt i et temperatur område på 275-326 K og ved atmosfærisk tryk. Den detaljerede sammensætning er målt med GC analyse, hvor 85 komponenter er identificeret op til n-nonane og med hundredvis af udefinerede komponenter i decane plus fraktionen.

Ved brugen af methanol og MEG som gashydrat inhibitor, er den største svaghed, specielt for methanol, tabet til den kulbrinterige fase. Hvis man kunne estimere dette tab af inhibitor, ville man

være i stand til at optimere injektionen af inhibitorer som funktion af systemparametre, såsom temperatur og vandsnit.

I dette projekt anvendes tilstandsligningen CPA (Cubic Plus Association) til at modellere distributionen af vand og inhibitorer (methanol, MEG) i forskellige faser. Den kulbrinte rige fase består af mixture-1 (methane, ethane, n-butane) eller mixture-2 (methane, ethane, propane, n-butane, n-heptane, toluene and n-decane). CPA giver tilfredsstillende resultater med at forudsige vandindholdet i gasfasen af et multikomponent system indeholdende mixture-1. Ligeledes kan CPA forudsige methanolindholdet i gasfasen af en blanding af mixture-1 + vand + methanol med en nøjagtighed inden for eksperimentel usikkerhed. For yderligere væske-væske-gas systemer indeholdende mixture-2 + vand, mixture-2 + vand + MEG og mixture-2 + methanol + vand, opnås tilfredsstillende forudsigelser for sammensætningen af kulbrinte fasen, hvorimod modelleringsresultaterne er relativt mindre tilfredsstillende for sammensætningen i gas fasen, delvist på grund af usikkerheder i de eksperimentelle data.

Ud over de ovenfor beskrevne multikomponent systemer, blev gas-væske ligevægten af det binære system methanol + methane undersøgt. Her opnås tilfredsstillende resultater af methane i væskefasen, ved brug af en enkelt temperatur uafhængig k_{ij} over en række temperaturer og tryk. Her giver CPA gode resultater for methanol indholdet i gasfasen ved høje temperaturer og lave tryk ved anvendelsen af den samme k_{ij} , mens der ved lave temperaturer og høje tryk ses afvigelse fra eksperimentelle data. For at kunne anvende CPA til modellering af reservoirmedier (olie/gas etc.), har det interesse at undersøge LLE af binære systemer med kulbrinter og vand. Dette er blevet gjort i dette projekt for alkane + vand og alkylbenzene + vand med CPA, hvor der er blevet fundet de binære interaktions parametre (k_{ij}) og cross-association volumen.

CPA er blevet udvidet til at kunne anvendes på reservoir medier med MEG og MEG + vand. Reservoir medierne består af tre kondensater og 2 olier fra oliefelter i Nordsøen. Den gensidige opløselighed af kondensater og MEG bliver modelleret tilfredsstillende ved anvendelse af en enkelt gennemsnitlig og temperatur uafhængig k_{ij} for alle MEG-HC par. Beregningen af den gensidige opløselighed af kondensat/olie, MEG og vand er ligeledes tilfredsstillende ved anvendelse af den samme gennemsnitlige k_{ij} for MEG-HC par, samt en k_{ij} for vand-HC fra en generaliseret korrelation som er en funktion af kulstofantal. De eksperimentelle tendenser i den gensidige opløselighed som funktion af temperatur og MEG indhold i den polære fase er tillige fanget tilfredsstillende og lever op til industriens krav om beregnede resultater i den samme størrelsesorden som de eksperimentelle.

Nomenclature

List of Abbreviations

% AD	absolute deviation= $\left \frac{x_i^{\text{exp.}} - x_i^{\text{cal.}}}{x_i^{\text{exp.}}} \right \times 100$
% Dev	deviation= $\frac{x_i^{\text{exp.}} - x_i^{\text{cal.}}}{x_i^{\text{exp.}}} \times 100$
% AAD	average absolute deviation= $\frac{1}{NP} \sum_{i=1}^{NP} \left \frac{x_i^{\text{exp.}} - x_i^{\text{cal.}}}{x_i^{\text{exp.}}} \right \times 100$
% Global AAD	average absolute deviation= $\frac{1}{TNP} \sum_{i=1}^{NP} \left \frac{x_i^{\text{exp.}} - x_i^{\text{cal.}}}{x_i^{\text{exp.}}} \right \times 100$
ASTM	American society of testing and materials
CAS Number	(a unique numerical identifier assigned by) chemical abstracts service (to each chemical)
CHARM	chemical hazard assessment and risk management
COND-1	condensate-1
COND-2	condensate-2
COND-3	condensate-3
CPA	cubic-plus-association
eCPA	electrolyte CPA
COSMO-RS	conductor-like screening model for real solvents
ECR	Elliott combining rule
EoS	equation of state
FID	fluid ionization detector
GC	group contribution (in chapter 2) , gas chromatography (in chapter 5)
GCs	gas chromatographs
HC	hydrocarbon
HCs	hydrocarbons
HPLC	high pressure liquid chromatography
HWHYD	(a thermodynamic model developed by) Heriot-Watt (University for Gas) Hydrate
LLE	liquid-liquid equilibrium
MS	Microsoft (Office)
MeOH	methanol
MEG	monoethylene glycol
MIX-1	mixture 1
MIX-2	mixture 2
NRTL	non-random two liquid
NP	number of points
OLF	Norwegian oil operators
PNA	paraffinic, naphthenic and aromatic (content of condensate or oil)
PR	Peng Robinson (equation of state)
RF	response factor

R & D	research and development
rpm	revolution per minute
RRF	relative response factor
SAFT	statistical associating fluid theory
SARA	saturates, asphaltenes, resins and aromatic (analysis method)
SFT	State Pollution Control Authority
SCN	single carbon number
Sim Dist	simulated distillation (GC)
SRK	Soave-Redlich-Kwong (EoS)
TBP	true boiling point (distillation)
TNP	total number of points (in all phases)
UNIFAC	universal quasi-chemical functional group activity coefficient (model)
UNIQUAQ	universal quasi-chemical (model)
VLE	vapor-liquid equilibrium
VLLE	vapor-liquid-liquid equilibrium

List of Symbols

A	area of a peak (in GC chromatogram) in chapter 5
a_0	parameter in the energy term of CPA ($bar.l^2 / mol^2$)
b	co-volume parameter (l / mol)
c_1	parameter in the energy term of CPA
c_j	correction factor
C_N	carbon number, for methane N=1, for ethane N=2 and so on...
C_i^o	concentration of component i in octanol phase
C_i^w	concentration of component i in water phase
f_i	fragment of component i
$g(\rho)$	radial distribution function
h	hour
k_{ij}	binary interaction parameter (k_{ij}) in the CPA equation of state
$K_{oil-water}$	oil-water partition coefficient
K_{ow}	octanol-water partition coefficient
K_{hw}	hexane-water partition coefficient
l	liter
ml	mili liter
min	minute
m_{IS}	mass of internal standard
m_{ISTD}	mass of diluted internal standard
M	molar mass
\bar{M}	mean molar mass
P	pressure
P_c	critical pressure
P_{cm}	CPA "monomer" critical pressure

R	gas constant
s	second
SG	specific gravity
SG_0	specific gravity of n-alkanes
T	temperature
T_b	boiling point
T_c	critical temperature
T_{cm}	CPA “monomer” critical temperature
V_m	molar volume
w_i	mass fraction of component i
W_c	water cut
X_{A_i}	the fraction of A-sites of molecule i that are not bonded with other active sites
x_i	mole fraction of component i

Greek Letters

$\beta^{A_i B_j}$	association volume
$\Delta^{A_i B_j}$	association strength between site A on molecule i and site B on molecule j
$\varepsilon^{A_i B_j}$	association energy
ρ	density
ω	acentric factor
ω_m	CPA “monomer” acentric factor
μ	micro
γ^∞	infinite dilution activity coefficient

Subscript and superscript

i	component i
j	component j
IS	internal standard
+	plus fraction (of an oil or a gas condensate)
exp.	experimental
cal.	calculated
hw	hexane-water (partition coefficient)
ow	octanol-water (partition coefficient)

Contents

Preface.....	iii
Summary.....	vii
Resumé på dansk.....	ix
Nomenclature.....	xi
List of Tables.....	xix
List of Figures.....	xxiii
1 INTRODUCTION TO THE PROJECT	27
1.1 Thesis Outline	31
2 OCTANOL-WATER PARTITION COEFFICIENT	35
2.1 Introduction	35
2.2 Octanol-Water Partition Coefficient	36
2.2.1 Experimental Measurement Methods	37
2.2.1.1 Direct Methods	37
2.2.1.2 Indirect Methods	38
2.2.2 Estimation Methods	38
2.2.2.1 Empirical Direct Correlations	38
2.2.2.1.1 Hansch and Leo Model	38
2.2.2.1.2 AFC Correlation Model	38
2.2.2.1.3 ACD Method	39
2.2.2.2 Higher Order Group Contribution Methods	39
2.2.2.2.1 Gani Method	39
2.2.2.2.2 Constantinou Method	40
2.2.2.3 Thermodynamic Models	40
2.2.2.3.1 UNIFAC Methods	40
2.2.3 Octanol-Water Partition Coefficient in Oil Industry	42
2.2.4 Limitations of Octanol-Water Partition Coefficient Based Method	43
2.3 Oil-Water Partition Coefficient	43
2.3.1 Experimental Work at Statoil R & D	43
2.3.2 Parameters Affecting Oil-Water Partition Coefficients	45
2.3.3 Challenges Related to Oil-Water Partition Coefficients	47
2.3.4 Alternative Approaches to Predict $K_{oil-water}$	49
2.3.4.1 $K_{oil-water}$ via K_{ow}	49
2.3.4.2 $K_{oil-water}$ via K_{hw}	51
2.4 Conclusions	52

3	MODELING APPROACH.....	55
3.1	Introduction.....	55
3.2	The CPA EoS.....	57
3.2.1	Description of the Model	57
3.2.2	Parameters for Pure Components	58
3.2.3	Mixing and Combining Rules for the Physical Term	59
3.2.4	Combining Rules for the Association Term	59
3.2.5	Association Term for Solvating Mixtures	60
3.2.6	Association Schemes	61
3.3	Heptane Plus Characterization	63
4	MODELING OF COMPLEX WELL-DEFINED SYSTEMS.....	67
4.1	Introduction.....	67
4.2	Results and Discussion	68
4.2.1	LLE of n-Nonane and Water	68
4.2.2	LLE of Undecane and Water	69
4.2.3	LLE of Heavy Aromatic Hydrocarbons and Water	70
4.2.4	VLE of Methane and Methanol System.....	73
4.2.5	Modeling of MIX-1	77
4.2.5.1	VLE of the MIX-1 + Water System.....	78
4.2.5.2	VLE of the MIX-1 + Water + Methanol System	80
4.2.5.3	VLE of the MIX-1 + Water + MEG System	82
4.2.6	Modeling of MIX-2	84
4.2.6.1	VLE of the MIX-2 + Water System	84
4.2.6.2	VLE of the MIX-2 + Water + Methanol System	86
4.2.6.3	VLE of the MIX-2 + Water + MEG System	88
4.3	Conclusions.....	90
5	EXPERIMENTAL WORK.....	93
5.1	Introduction.....	93
5.2	Experimental Section	94
5.2.1	Materials	94
5.2.2	Methods	95
5.2.2.1	Pure Condensate Analysis	95
5.2.2.2	Mutual Solubility Measurements	102
5.2.2.2.1	Apparatus and Procedure	102
5.2.2.2.2	Mixing and Equilibrium	105
5.2.2.2.3	Sampling.....	105
5.2.2.2.4	Polar Phase Analysis.....	106
5.2.2.2.5	Hydrocarbon Phase Analysis	107

5.3	Results and Discussion	110
5.3.1	LLE of the n-Heptane + MEG System	111
5.3.2	LLE of the Condensate + MEG Systems.....	112
5.3.3	LLE of the Condensate + MEG + Water Systems.....	113
5.4	Extension of Experimental Work	116
5.4.1	Light-Oil Composition Analysis.....	117
5.4.1.1	Mutual Solubility of Reservoir-Fluids and MEG.....	123
5.4.1.2	Mutual Solubility of Light-Oil-1 and MEG.....	124
5.5	Conclusions	125
6	MODELING OF RESERVOIR FLUIDS PHASE BEHAVIOR.....	127
6.1	Introduction	127
6.2	Results and Discussion	129
6.2.1	Condensate-1	129
6.2.1.1	Condensate-1 Characterization.....	129
6.2.1.2	Mutual Solubility of Condensate-1 and MEG	130
6.2.1.3	Mutual Solubility of Condensate-1, MEG and Water	133
6.2.2	Condensate-2	137
6.2.2.1	Condensate-2 Characterization.....	137
6.2.2.2	Mutual Solubility of Condensate-2 and MEG	138
6.2.2.3	Mutual Solubility of Condensate-2, MEG and Water	140
6.2.3	Condensate-3	144
6.2.3.1	Condensate-3 Characterization.....	144
6.2.3.2	Mutual Solubility of Condensate-3 and MEG	144
6.2.3.3	Mutual Solubility of Condensate-3, MEG and Water	146
6.2.4	Light-Oil-1.....	148
6.2.4.1	Light-Oil-1 Characterization	148
6.2.4.2	Mutual Solubility of Light-Oil-1 and MEG.....	149
6.2.4.3	Mutual Solubility of Light-Oil-1, MEG and Water.....	150
6.2.5	Light-Oil-2.....	153
6.2.5.1	Light-Oil-2 Characterization	153
6.2.5.2	Mutual Solubility of Light-Oil-2 and MEG.....	153
6.2.5.3	Mutual Solubility of Light-Oil-2, MEG and Water.....	154
6.2.6	Comparison of Well-Defined-HC and Oil Systems in Presence of Water and Polar Chemical	156
6.3	Conclusions	157
7	CONCLUSIONS AND FUTURE WORK	159
7.1	Conclusions	159
7.2	Future Work Recommendations.....	163

8	BIBLIOGRAPHY	165
9	APPENDICES.....	171
9.1	Appendix A: Production Chemicals	172
9.2	Appendix B: GC Analysis.....	179
9.3	Appendix C: Thermodynamic Modeling	186
9.4	Appendix D: List of Publications.....	188

List of Tables

Table 2.1: Consumption of Chemicals in the Statoil Operated Fields in 1997 and Their Release to the Sea Water. ¹⁹	36
Table 2.2: General Rig Conditions for Oil-Water Partition Experiment. ⁶	43
Table 2.3: Discharge of Chemicals to the Sea Calculated on the Basis of Octanol-Water and Oil-Water Partition Coefficients. ⁶	47
Table 2.4: Production Chemicals in Statoil Operated Fields and Their Functions.....	49
Table 2.5: Production Chemicals in Statoil Operated Fields and Their Families.	49
Table 3.1: Applications of the CPA Equation of State (1995-2005). ⁵¹	56
Table 3.2: CPA Parameters for Associating Components Considered in This Work. The 2B Association Scheme is Used for Methanol and 4C is Used for Both Water and MEG.....	61
Table 3.3: CPA Parameters for Inert Components Used in This Work.....	62
Table 3.4: Association Schemes Based on the Terminology of Huang and Radosz. ⁵⁰	63
Table 4.1: Solubility of Water in Undecane, Experimental Data ⁹² and CPA Calculations.....	70
Table 4.2: % AAD Between Experimental and Calculated Water Solubilities in the Hydrocarbon Phase and Hydrocarbon Solubilities in the Aqueous Phase Using the Generalized Expression for the Interaction Parameter $k_{12} = -0.02(\text{carbon number}) + 0.1915$. ⁷⁷	70
Table 4.3: % AAD Between Experimental and Calculated Mutual Solubilities for Alkylbenzene and Water Using the Generalized Correlation ⁷⁷ for Binary Interaction Parameters.....	73
Table 4.4: % AAD Between Experimental ⁸⁹ and Calculated Methanol Content in Gas Phase of Methane + Methanol System and Binary Interaction Parameters (k_{ij}) Used. The $k_{ij}=0.01$ from Hemptinne ¹⁰⁰ and $k_{ij}=0.0482$ from Haghighi et al. ⁸⁹ and Temperature Dependent k_{ij} from This Work.	74
Table 4.5: % AAD Between Experimental ⁸⁹ and Calculated Solubility of Methane in Methanol in the Methane + Methanol System and Binary Interaction Parameters (k_{ij}) Used.	76
Table 4.6: % AAD Between Experimental ¹⁰¹ and Calculated Methanol Content in Gas Phase of Methane + Methanol System and Binary Interaction Parameters (k_{ij}) Used.	77
Table 4.7: Composition of MIX-1 (in Mole Fraction, x). ¹⁰²	78
Table 4.8: Temperature Dependent Binary Interaction Parameters Used for Water and Light-HC. ¹⁶	79
Table 4.9: Compositions (in Mole %) of MIX-1 + Water + Methanol System. ¹⁰²	80
Table 4.10: Binary Interaction Parameters Used in the Calculations of MIX-1 + Water + Methanol System. ...	82
Table 4.11: Composition (in Mole %) of Components in MIX-1 + Water + MEG System. ¹⁰²	83
Table 4.12: Binary Interaction Parameters Used in the Calculations for the MIX-1 + Water + MEG System. ...	84
Table 4.13: Composition of MIX-2 (in Mole Fraction, x). ¹⁰²	84
Table 4.14: Binary Interaction Parameters for Water-HC and Methanol-HC Systems.....	84
Table 4.15: Experimental ¹⁰² and Calculated Compositions of the Different Species in the Vapor Phase (in Mole Fraction, y) of the MIX-2 + Water System at 298.1 K and Various Pressures. The Vapor Phase Compositions of Methane (y_{C1}), Ethane (y_{C2}), Water (y_w), Propane (y_{C3}), n-Butane (y_{C4}), n-Heptane (y_{C7}), Toluene (y_{Tol}) and n-Decane (y_{C10}) are Presented.	85
Table 4.16: Experimental ¹⁰² and Calculated Compositions of the Different Species in the Organic Phase (in Mole Fraction, x) of the MIX-2 + Water System at 298.1 K and Various Pressures. The organic Phase Compositions of Methane (x_{C1}), Ethane (x_{C2}), Water (x_w), Propane (x_{C3}), n-Butane (x_{C4}), n-Heptane (x_{C7}), Toluene (x_{Tol}) and n-Decane (x_{C10}) are presented.	86
Table 4.17: Experimental Data ¹⁰² and CPA Calculations for Composition of Different Species in the Vapor Phase (in Mole Fraction, y) of the MIX-2 + Water + Methanol System at Various Temperatures and	

Pressures. The Vapor Phase Compositions of Methane (y_{C1}), Ethane (y_{C2}), Water (y_w), Propane (y_{C3}), n-Butane (y_{C4}), Methanol (y_{MeOH}), n-Heptane (y_{C7}), Toluene (y_{Tol}) and n-Decane (y_{C10}) are Presented.	87
Table 4.18: Experimental ¹⁰² and Calculated Composition of Different Species in the Organic Phase (in Mole Fraction, x) of the MIX-2 + Water + Methanol System at Various Temperatures and Pressures. The organic Phase Compositions of Methane (x_{C1}), Ethane (x_{C2}), Water (x_w), Propane (x_{C3}), n-Butane (x_{C4}), Methanol (x_{MeOH}), n-Heptane (x_{C7}), Toluene (x_{Tol}) and n-Decane (x_{C10}) are presented.	88
Table 4.19: Experimental ¹⁰² and Calculated Composition of Different Species in the Vapor Phase (in Mole Fraction, y) of the MIX-2 + Water + MEG System at 258 K and Various Pressures. The Vapor Phase Compositions of Methane (y_{C1}), Ethane (y_{C2}), Water (y_w), Propane (y_{C3}), n-Butane (y_{C4}), n-Heptane (y_{C7}), Toluene (y_{Tol}) and n-Decane (y_{C10}) are Presented.	89
Table 4.20: Experimental ¹⁰² and Calculated Composition of Different Species in the Organic Phase (in Mole Fraction, x) of the MIX-2 + Water + MEG System at 258 K and Various Pressures. The Organic Phase Compositions of Methane (x_{C1}), Ethane (x_{C2}), Water (x_w), Propane (x_{C3}), n-Butane (x_{C4}), n-Heptane (x_{C7}), Toluene (x_{Tol}) and n-Decane (x_{C10}) are Presented.	89
Table 5.1: Purity (in Mass Fraction, w) of the Chemicals Used in This Work.	95
Table 5.2: Characteristics of Gas Chromatographs Used in This Work. ^{110,112}	95
Table 5.3: Detailed Composition (in Mass Fraction, w , Mole Fraction, x), Molar Mass (M) and Density (ρ) of the Condensate-2. ¹¹²	98
Table 5.4: Condensed Composition (Mass Fraction, w , Mole Fraction, x), Molar Mass (M) and Density (ρ) of Condensate-2. ¹¹²	101
Table 5.5: Condensed Composition (Mass Fraction, w , Mole Fraction, x), Molar Mass (M) and Density (ρ) of Condensate-1. ¹¹⁰	102
Table 5.6: Experimental (Liquid-Liquid) Equilibrium Data for MEG (1) + Condensate (2) System Expressed in Mole Fractions, at Pressure 101.3 KPa.	110
Table 5.7: Experimental (Liquid-Liquid) Equilibrium Data (in Mole Fractions, x) for MEG (1) + Water (2) + Condensate (3) at Pressure 101.3 KPa.	111
Table 5.8: Characteristics of Sim Dist Gas Chromatograph Used for Light-Oil Compositional Analysis. ¹¹⁴	117
Table 5.9: Condensed Composition (Mass Fraction, w , Mole Fraction, x), Molar Mass (M) and Density (ρ) of Condensate-3. ¹¹⁵	117
Table 5.10: Condensed Composition (Mass Fraction, w , Mole Fraction, x), Molar Mass (M) and Density (ρ) of Light-Oil-1. ¹¹⁴	119
Table 5.11: Condensed Composition (Mass Fraction, w , Mole Fraction, x), Molar Mass (M) and Density (ρ) of Light-Oil-2. ¹¹⁵	120
Table 5.12: Overall Density, Molar Mass and C_{10+} Fraction of Condensates and Oils Investigated in This Work.	121
Table 5.13: Comparison of Compositions of Condensate-2 ¹¹² and (Pure) Condensate-3. ¹¹⁵	123
Table 6.1: The Simplified Composition (in Mole Fraction, x), Molar Mass (M) and Density (ρ) of Condensate-1 Used for the Characterization.	129
Table 6.2: Condensate-1 after Characterization and Lumping.	130
Table 6.3: Binary Interaction Parameters for LLE of MEG-HC Systems.	130
Table 6.4: Binary Interaction Parameters for LLE of Water-Hydrocarbon Systems, Based on the Generalized Expression Which is Derived Based on Data from Propane up to n-Decane: $k_{ij} = -0.026 \cdot (\text{carbon number}) + 0.1915$. ^{77,81}	132
Table 6.5: CPA Modeling of the Condensate-1 (COND-1) + MEG System and the Effect of k_{ij} on the Mutual Solubility of Condensate-1 and MEG.	133

Table 6.6: Experimental Data ¹¹⁰ and CPA Modeling for Condensate-1 + MEG + Water System at Temperature 323.15 K and Pressure 1 atm. The k_{ij} Values for the MEG-Water=-0.115, MEG-HC=0.02 and Water-HC are Taken from Table 6.4.	134
Table 6.7: Average Deviation (%) of CPA Predictions from Experimental Data for Investigated Condensate-1 (COND-1) + MEG + Water System at T=323.15 K and P=1 atm.	135
Table 6.8: The Composition of Condensate-2 from This Work and an External Laboratory.	137
Table 6.9: Characterization of Condensate-2 Using the Composition Obtained from External Laboratory.	138
Table 6.10: Condensate-2 after Characterization and Lumping Using the Composition from This Work.	138
Table 6.11: Deviations of the CPA Modeling Results from the Experimental Data for Condensate-2 + MEG and Condensate-2 + MEG + Water Systems. A Comparison in Global AAD Using Condensate-2 Composition from This Work and from External Laboratory is Presented.	140
Table 6.12: Experimental Data ¹¹² and CPA Modeling for Condensate-2 + MEG + Water System at Temperatures 303.15 and 323.15 K and Pressure 1 atm. The k_{ij} for MEG-Water=-0.115, MEG-HC=0 and Water-HC are Taken from Table 6.4. The CPA Calculations are Made Using Condensate-2 Composition Measured in This Work.	141
Table 6.13: Condensate-3 after Characterization.	144
Table 6.14: Experimental Data ¹¹⁵ and CPA Modeling for Condensate-3 + MEG + Water System at 313.15 K and Pressure 1 atm. The k_{ij} for MEG-Water=-0.115, MEG-HC=0.04 and Water-HC are Taken from Table 6.4.	146
Table 6.15: Light-Oil-1 after Characterization and Lumping.	148
Table 6.16: Deviations in CPA Calculations for Modeling of Light-Oil-1 + MEG System.	150
Table 6.17: Experimental Data ¹¹⁴ and CPA Modeling for Light-Oil-1 + MEG + Water System at 303.15 and 313.15 K and Pressure 1 atm. The k_{ij} for MEG-Water=-0.115, MEG-HC=0.02 and Water-HC are Taken from Table 6.4.	150
Table 6.18: Light-Oil-2 after Characterization and Lumping.	153
Table 6.19: Deviations in CPA Calculations for Modeling of Light-2 + MEG System.	153
Table 6.20: Experimental Data ¹¹⁵ and CPA Modeling for Light-Oil-2 + MEG + Water System at 323.15 K and Pressure 1 atm. The k_{ij} for MEG-Water=-0.115, MEG-HC=0.02 and Water-HC are Taken from Table 6.4.	154
Table 6.21: Summary of Deviations of CPA Calculations from Experimental Data and Comparison with Systems of Well-Defined-HC + MEG + Water. The k_{ij} for MEG-Water=-0.115 with Elliott Combining Rule for Condensate/Oil + MEG + Water Systems and k_{ij} =-0.028 with CR-1 Combining Rule for Well-Defined-HC + MEG + Water Systems.	156

List of Figures

Figure 1.1: Trend in the use of production chemicals on Statoil-operated fields. ⁶	28
Figure 1.2: A conceptual hydrate phase diagram. ⁷	29
Figure 1.3: Expected annual costs for hydrate inhibition alternatives. ⁸	29
Figure 1.4: A simplified sketch of MEG regeneration system. ⁷	30
Figure 2.1: CPA predictions of octanol-water partition coefficients. ¹⁴	40
Figure 2.2: Average absolute deviation (AAD) between experimental and predicted logK _{ow} values from models for complex chemicals (e.g. glycols and alkanolamines). ^{22,14} The list of 22 polyfunctional molecules considered for calculations is given in the appendix A. 6.	42
Figure 2.3: Schematic illustration of the bench-scale-rig used by Statoil for oil-water partition studies of chemicals. ⁶	44
Figure 2.4: Effect of type of crude on oil-water partition coefficient. ⁶	45
Figure 2.5: Effect of water cut on oil-water partition coefficient. ⁶	46
Figure 2.6: Correlations between octanol-water and oil-water partition coefficients (a) K _{ow} vs K _{oil-water} for methanol to 1-butanol (b) LogK _{ow} vs LogK _{oil-water} for methanol to 1-decanol.	50
Figure 2.7: Correlation between octanol-water and oil-water partition coefficients for alkanolamines.	51
Figure 2.8: Correlation between octanol-water and oil-water partition coefficients for glycols.	51
Figure 2.9: Correlation between hexane-water and oil-water partition coefficients for alcohols.	52
Figure 4.1: Mutual solubility (in mole fraction, x) of n-nonane and water as a function of temperature (K) for the n-nonane + water system. The experimental data ^{93,94} are indicated as points and the CPA calculations as lines. The $k_{ij}=-0.0425$ is obtained from generalized correlation as function of carbon number as given in Table 4.2 and $k_{ij}=-0.03$ fitted to n-nonane solubility in water.	69
Figure 4.2: Mutual solubilities (in mole fraction, x) of alkylbenzene and water for ethylbenzene + water, o-xylene + water, m-xylene + water and p-xylene + water systems. The experimental data ^{93,99} are indicated as points and CPA calculations as lines.	71
Figure 4.3: Mutual solubilities (in mole fraction, x) of alkylbenzene and water for propylbenzene + water, butylbenzene + water, pentylbenzene + water and hexylbenzene + water systems. The experimental data ⁹³ are indicated as points and CPA calculations as lines.	72
Figure 4.4: Experimental and calculated methanol content in gas phase of methane + methanol system using the CPA equation of state with $k_{ij}=0.01$. The experimental data ⁸⁹ are indicated as points and the CPA calculations as lines.	74
Figure 4.5: Methane content (in mole fraction, x) of liquid phase of methane + methanol system as a function of temperature (K) and pressure (bar). (a) For temperatures 200-273 K (b) For temperatures 290-330 K. The experimental data ¹⁰¹ are indicated as points and CPA calculations as lines. The binary interaction parameters (k_{ij}) are obtained from a generalized correlation (from this work) $k_{ij}=5.77/(T-0.001788)$ as a function of temperature (K).	75
Figure 4.6: Methanol content (in mole fraction, x) of vapor phase of methane + methanol system as a function of temperature (K) and pressure (bar). The experimental data ¹⁰¹ are indicated as points and CPA calculations as lines. The binary interaction parameters (k_{ij}) are obtained from a generalized correlation $k_{ij}=5.77/(T-0.001788)$ as a function of temperature (K) and $*k_{ij}=0.01$.	77
Figure 4.7: Water content (mole fraction, x) of the gas phase of MIX-1 + water system as a function of temperature (K) and pressure (bar). The experimental data ¹⁰² are indicated as points and the calculations using the CPA ($*k_{ij}$ =correlation given in Table 4.8 $*k_{ij}=0$) and HWHYD ¹⁰² as lines.	79
Figure 4.8: Methanol content (mole fraction, x) of the gas phase of MIX-1 + water + methanol system as a function of temperature (K) and pressure (bar). The experimental data ¹⁰² are indicated as points and	

the calculations using the CPA (k_{ij} = HC-water from correlation in Table 4.8 and HC-Methanol from Table 4.10 $k_{ij}=0$) and HWHYD ¹⁰² as lines.	81
Figure 4.9: Water content (mole fraction, x) of the gas phase of MIX-1 + water + methanol systems as a function of temperature (K) and pressure (bar). The experimental data ¹⁰² are indicated as points and the calculations using the CPA (k_{ij} = HC-water from correlation in Table 4.8 and HC-Methanol from Table 4.10 $k_{ij}=0$) and HWHYD ¹⁰² as lines.	82
Figure 4.10: Water content (mole fraction, x) of the gas phase of MIX-1 + water + MEG system as a function of temperature (K) and pressure (bar). The experimental data ¹⁰² are indicated as points and the calculations using the CPA (k_{ij} = correlation given in Tables 4.8 and 4.12 $k_{ij}=0$) and HWHYD ¹⁰² as lines.	83
Figure 5.1: Condensate chromatogram for components from propane to n-heptane.	97
Figure 5.2: Condensate chromatogram for components in C ₉ and C ₁₀ carbon fractions.	97
Figure 5.3: Equipments used at various stages of an experiment: (a). Heating oven used for mixing and attaining equilibrium at a fixed temperature (b). Mixing machine placed in lower part of heating oven (c). Two glass equilibrium cylinders placed in upper part of heating oven (d). Equilibrium cylinder showing two phases, the upper phase is condensate phase and the lower phase is polar phase consisting of MEG and water.	103
Figure 5.4: (a). Syringes (volume 10 ml each) used to withdraw samples from equilibrium cylinder (b). vials used for sample storage.	104
Figure 5.5: Chromatographs used for phase analysis: (a). condensate GC used for analysis of traces of hydrocarbon in MEG phase (b). Glycol GC used for analysis of traces of glycol in hydrocarbon phase (c). Sim Dist GC (which can be) used for analysis of traces of condensate heavier than C ₁₅	104
Figure 5.6: Karl Fisher coulometer used for the measurement of water content in hydrocarbon phase.	104
Figure 5.7: Sketch of the experimental setup used in this work. ¹¹²	105
Figure 5.8: Quantification of MEG traces in hydrocarbon phase using external standard method (a) showing peaks of external standards (MEG diluted in water) and (b) calibration curve.	108
Figure 5.9: Gas chromatogram (for glycol GC) with the quantification report of MEG in condensate (using extract phase).	109
Figure 5.10: LLE data for n-heptane + MEG and comparison to the data from literature. The data for MEG in n-heptane is from Stavely and Milward ¹⁰⁹ , Derawi et al. ¹² , Statoil ¹¹¹ and this work. ¹¹⁰ The data for n-heptane in MEG is from Derawi et al. ¹² , Statoil and this work. ¹¹⁰	111
Figure 5.11: Solubility (in mass fraction, W) of condensate-2 components in pure MEG at various temperatures.	112
Figure 5.12: Solubility (in mass fraction, W) of condensate-2 components in polar phase (MEG + water) at temperatures (a) 323.15 K and (b) 303.15 K and MEG composition in polar phase. ¹¹²	114
Figure 5.13: Comparison of the solubility (in Mole Fraction, X) of MEG in well-defined hydrocarbons (n-heptane ^{12,109,111} and benzene ¹¹) and reservoir-fluids (condensate-1 ¹¹⁰ and condensate-2 ¹¹²) as a function of temperature (K).	115
Figure 5.14: Comparison of the solubility (in Mole Fraction, X) of well-defined hydrocarbons (n-heptane ^{111,113} and benzene ¹¹) and reservoir-fluids (condensate-1 ¹¹⁰ and condensate-2) in MEG ¹¹² as a function of temperature.	115
Figure 5.15: PNA distribution of condensates (condensate-1 ¹¹⁰ , condensate-2 ¹¹² and condensate-3 ¹¹⁵) and oils (light-oil-1 ¹¹⁴ and light-oil-2 ¹¹⁵) studied.	121
Figure 5.16: Comparison of the solubility (in Mole Fraction, X) of MEG in well-defined hydrocarbons (n-heptane, ^{12,109,111} and benzene ¹¹) and reservoir-fluids (condensate-1 ¹¹⁰ , condensate-2 ¹¹² , condensate-3 ¹¹⁵ Light-Oil-1 ¹¹⁴ and light-oil-2 ¹¹⁵) as a function of temperature (K).	122

Figure 5.17: Comparison of the solubility (in Mole Fraction, x) of well-defined hydrocarbons (n-heptane ^{111,113} and benzene ¹¹) and reservoir-fluids (condensate-1 ¹¹⁰ , condensate-2, ¹¹² condensate-3 ¹¹⁵ Light-Oil-1 ¹¹⁴ and light-oil-2 ¹¹⁵) in MEG as a function of temperature (K).....	122
Figure 5.18: Comparison of solubility of aromatic content (of condensate-2 and condensate-3) in MEG for condensate-2 + MEG and condensate-3 + MEG systems at 303.15 K.	124
Figure 5.19: Comparison of mutual solubility of light-oil-1 and MEG presented in mass and mole fractions. ¹¹⁴	125
Figure 6.1: Correlation for binary interaction parameters for water-HC ⁷⁷ and MEG-HC (this work).	131
Figure 6.2: Mutual solubility (in mole fraction, x) of condensate-1 and MEG as a function of temperature (K) for the condensate-1 + MEG system. The experimental data ¹¹² are indicated as points and the CPA calculations as lines.	133
Figure 6.3: Modeling of the mutual solubility (in mole fraction, x) of condensate-1, MEG and water at temperature 323.15 K and pressure 1 atm.: (a) water in condensate (b) MEG in condensate-1 (c) condensate-1 in polar phase. The points are experimental data ¹¹⁰ and lines are modeling results with the CPA EoS using k_{ij} for MEG-water=-0.115, HC-MEG=0.02 and HC-water from the correlation of Table 6.4.	136
Figure 6.4: Mutual solubility (in mole fraction, x) of condensate-2 and MEG as a function of temperature (K) for condensate-2 + MEG system. Experimental data ¹¹² are indicated as points and the CPA calculations as lines. Modeling results are presented using condensate-2 composition from this work* and external laboratory.	140
Figure 6.5: Modeling of the mutual solubility (in mole fraction, x) of condensate-2, MEG and water at temperature 303.15 K and pressure 1 atm.: (a) water in condensate-2 (b) MEG in condensate-2 (c) condensate-2 in polar phase. The points are experimental data ¹¹² and the lines are modeling results with the CPA EoS using k_{ij} for MEG-water=-0.115, HC-MEG=0 and HC-water from the correlation in Table 6.4. The CPA calculations are made using condensate-2 composition measured in this work.	142
Figure 6.6: Modeling of the mutual solubility (in mole fraction, x) of condensate-2, MEG and water at temperature 323.15 K and pressure 1 atm.: (a) water in condensate-2 (b) MEG in condensate-2 (c) condensate-2 in polar phase. The points are experimental data ¹¹² and the lines are modeling results with the CPA EoS using k_{ij} for MEG-water=-0.115, HC-MEG=0 and HC-water from the correlation given in Table 6.4. The CPA calculations are made Using condensate-2 composition measured in this work.....	143
Figure 6.7: Mutual solubility (in mole fraction, x) of condensate-3 and MEG as a function of temperature (K) for condensate-3 + MEG system, experimental data ¹¹⁵ are indicated as points and the CPA calculations as lines.	145
Figure 6.8: Modeling of the mutual solubility (in mole fraction, x) of condensate-3, MEG and water at temperature 313.15 K and pressure 1 atm.: (a) water in condensate-3 (b) MEG in condensate-3 (c) condensate-3 in the polar phase. The points are experimental data ¹¹⁵ and the lines are modeling results with the CPA EoS using k_{ij} for MEG-water=-0.115, HC-MEG=0.04 and HC-water from the correlation in Table 6.4.....	147
Figure 6.9: Mutual solubility (in mole fraction, x) of Light-Oil-1 and MEG as a function of temperature (K) for light-oil-1 + MEG system. The experimental data ¹¹⁴ are indicated as points and the CPA calculations as lines.....	149
Figure 6.10: Modeling of the mutual (in mole fraction, x) solubility of light-oil-1, MEG and water at temperature 313.15 K and pressure 1 atm.: (a) water in light-oil-1 (b) MEG in light-oil-1 (c) light-oil-1 in polar phase. The points are experimental data ¹¹⁴ and the lines are modeling results with the CPA EoS using k_{ij} for MEG-water=-0.115, HC-MEG=0.02 and HC-water from the correlation in Table 6.4.	151
Figure 6.11: Modeling of the mutual solubility (in mole fraction, x) of light-oil-1, MEG and water at temperature 323.15 K and pressure 1 atm.: (a) water in light-oil-1 (b) MEG in light-oil-1 (c) light-oil-1 in	

polar phase. The points are experimental data ¹¹⁴ and the lines are modeling results with the CPA EoS using k_{ij} for MEG-water=-0.115, HC-MEG=0.02 and HC-water from the correlation.	152
Figure 6.12: Mutual solubility (in mole fraction, x) of light-oil-2 and MEG as a function of temperature (K) for light-oil-2 + MEG system. The experimental data ¹¹⁵ are indicated as points and the CPA calculations as lines.	154
Figure 6.13: Modeling of the mutual solubility of light-oil-2, MEG and water at temperature 323.15 K and pressure 1 atm.: (a) water in light-oil-2 (b) MEG in light-oil-2 (c) light-oil-2 in polar phase. The points are experimental data ¹¹⁵ and the lines are modeling results with the CPA EoS using k_{ij} for MEG-water=-0.115, HC-MEG=0.02 and HC-water from the correlation in Table 6.4.	155

Introduction to the Project

Deep water oil and gas exploration and production has increased significantly in recent years, with forecasts predicting that this trend will continue. This has also posed challenges for the oil and gas industry and some of these challenges are described in following paragraphs. The deepwater environment exposes the flow lines to a temperature near 4 °C, which can create production problems in subsea flow and pipework due to formation of gas hydrates. These hydrate plugs have been known to form as long as 6.2 miles and have blocked pipelines as 40 inches in diameter.¹ Some of these plugs can take weeks and even months to dissociate. Therefore these plugs cause a loss in production as well as create a severe safety and environmental hazard.¹

For long distances, the pipelines are major cost drivers. Therefore pipelines are constructed from carbon steel due to its lower cost as compared to non-corrosive materials. As a consequence the corrosion problems arise. Furthermore material selection and corrosion management are important elements in overall flow assurance evaluation.² Some risks of scale deposition occur in many operations in the petroleum industry. Scale deposition happens particularly in production, stimulation and transport. The scaling may consist of various ions (e.g. calcium carbonate and magnesium salts etc.). Also, if two chemicals that will form a precipitate are brought together, a scale is formed (e.g., if a hydrogen fluoride solution meets calcium ions).³ Corrosion and scale deposition are the two most costly problems in the oil industry. Similarly as new fields are developed, and as production conditions change at older fields, there is a constant need for demulsifiers that lead to a rapid separation (of emulsion) into oil and water.³

These challenges faced by the oil and gas industry require chemicals and their use have increased significantly over the years. These chemicals can be divided into drilling and production chemicals. As an example the production chemical usage in Statoil operated fields is shown in Figure 1.1. A similar trend can be found for drilling chemicals.⁴ This increase is not only due to the fact that new fields are brought to production. But also due to the new solutions which have been applied, for instance the use of methanol for multiphase well stream

transport from subsea wells. In addition mature fields (e.g. Gullfaks and Statfjord in the North Sea) have increased needs for chemical based treatments like well treatment or water treatment.⁵

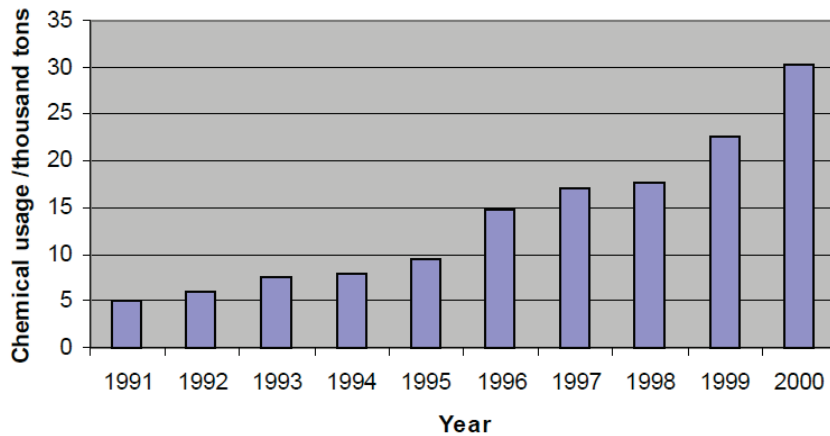


Figure 1.1: Trend in the use of production chemicals on Statoil-operated fields.⁶

The chemicals used in oil and gas production belong to different families such as glycols, alcohols, alkanolamines, polymers and salts etc. They are used as e.g. hydrate inhibitors, scale inhibitors or demulsifiers.

Corrosion inhibitors which are used for the protection of oil pipelines are often complex mixtures.³ The majority of these (corrosion) inhibitors used in oil production systems is nitrogenous and have been classified into

- Amides and imidazolines
- Salts for nitrogenous molecules with carboxylic acid
- Polyoxylated amines, amides and imidazolines

The formation of gas hydrate in subsea production facilities is often inhibited by injecting thermodynamic inhibitors. The most common of these hydrate inhibitors are methanol (MeOH) and glycols such as monoethylene glycol (MEG). Thermodynamic inhibitors suppress the point at which hydrates form, much like antifreeze for water-ice, allowing protection under the hydrate formation conditions.¹

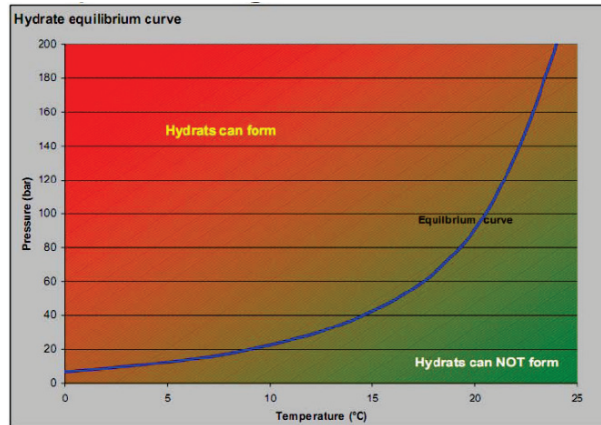


Figure 1.2: A conceptual hydrate phase diagram.⁷

A typical hydrate equilibrium phase diagram for gas hydrate is shown in Figure 1.2. This figure shows that the more the equilibrium line is shifted to the left, the more effective is the inhibitor and the larger is the safe area (conditions where hydrate formation will not take place).² Surveying the choices made by operators in oil and gas sector for recently built and planned gas-condensate tie backs, it is evident that MEG seems to be the preferred inhibitor. The list of MEG based developments can be clearly seen worldwide including Ormen Lange (Norsk hydro Norway) and Snøhvit (Statoil) in the North Sea.² It may be due to the advantage offered by MEG in economy, corrosion protection, gas dehydration, health safety and environment over methanol. However methanol on the other hand due to lower viscosity causes less pressure drop, thus reducing the pumping horse power required for injection.⁸ The expected annual costs for using MEG and methanol as hydrate inhibitors is shown in Figure 1.3. This shows that annual expected cost for using MEG as inhibitor is considerably lower than that of methanol.

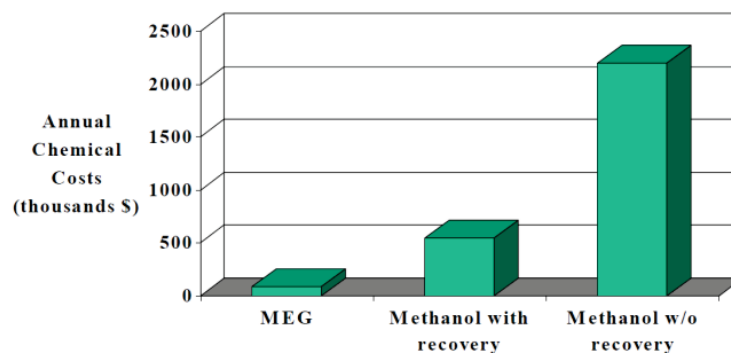


Figure 1.3: Expected annual costs for hydrate inhibition alternatives.⁸

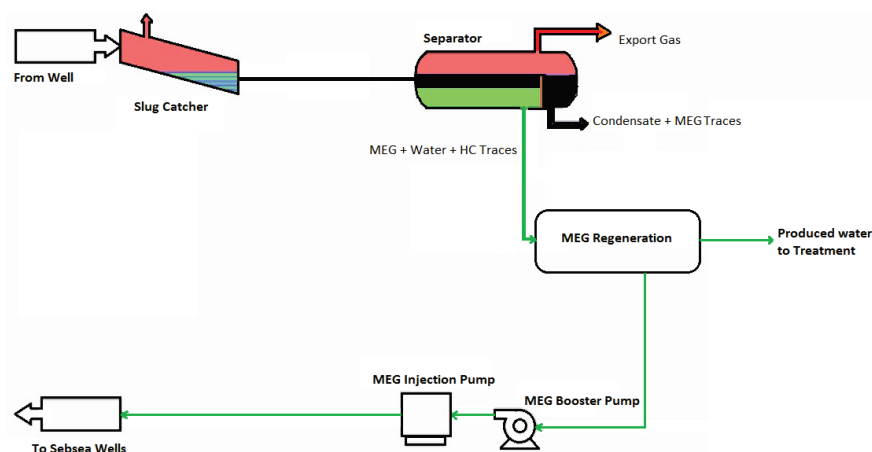


Figure 1.4: A simplified sketch of MEG regeneration system.⁷

As shown in Figure 1.4 chemicals added to the oil and gas value chain at different stages reach the well stream and then go to a series of separators and processing facilities. It is important to know the distribution of these chemicals in oil, water and gas streams because it is a key to the calculation of the amounts of chemicals required for a specific facility. It is also important information to fulfill the demand from the environmental perspective in order to know the amount of chemicals and hydrocarbons (HC) in a processed water stream for ensuring minimal impact on marine life. Furthermore it is important for design and operation of separation equipments as well as to report the chemicals and water contents of fuel oil which may be crucial for downstream processing.^{9,10}

The distribution of the chemicals can either be measured experimentally or predicted using a suitable thermodynamic model. The experimental method is expensive and challenging, partly due to the difficulties involved in measurements of such low solubilities. An evidence for this is the scarcity of such experimental data (with natural gas condensate and oil) in the literature. Data are available for only few binaries and ternaries dealing with well-defined hydrocarbons, MEG and water systems.¹¹⁻¹⁴

However for the development and validation of a thermodynamic model, experimental data are required. Those data are scarce in general, especially for gas-condensates and oil mixtures. Therefore in this PhD project experimental work was carried out at Statoil Research Center, in Norway to measure the mutual solubility data for MEG + condensate and MEG + condensate + water systems. These systems of water, hydrocarbons and chemicals represent complex mixtures containing associating /polar and non-associating compounds. The widely used equations of state (such as SRK and PR) in the oil and gas industry cannot describe such systems satisfactorily. It has been shown previously that the Cubic Plus Association (CPA) equation of

state (EoS) proposed by Kontogeorgis et al.¹⁵ is a suitable model for such mixtures.¹⁴ More applications of CPA are given in chapter 3.

The purpose of this thesis is the thermodynamic modeling and experimental measurement of distribution of complex chemicals (i.e. MEG and methanol) especially MEG in oil-water systems. The research issues to be investigated are the following:

- To identify the most important chemicals for oil and gas industry and to collect experimental data of K_{ow} and $K_{oil-water}$ and investigate if correlations exist between them.
- To perform experiments for obtaining the required (LLE) phase equilibrium data of condensate + MEG and condensate + MEG + water systems and investigate the effect of temperature, MEG content in polar phase and the type of reservoir fluid.
- Thermodynamic modeling of condensate + MEG and condensate + MEG + water systems using the CPA EoS.

1.1 Thesis Outline

The work presented in this thesis has been divided into seven chapters and their detail is given as following:

- ❖ **Chapter 1** provides introduction to the project, its industrial importance and objectives.
- ❖ **Chapter 2** presents an overview of the octanol-water partition coefficient, its environmental applications, the methods of its measurement and estimation. Then this chapter presents the use of octanol-water partition coefficients in oil industry to predict the distribution of chemicals in oil-water systems and its limitations. The last section of the chapter gives an overview of the experimental work carried out at Statoil R & D to overcome these limitations by measuring oil-water partition coefficients. Finally this chapter presents the investigations on correlations between octanol-water and oil-water partition coefficients developed for various chemical families.
- ❖ **Chapter 3** describes the thermodynamic model (the CPA EoS) considered in this work. To perform phase equilibrium calculations for a reservoir fluid with ill-defined plus fraction, a characterization method is required to estimate equation of state parameters. The characterization method used in this work is also described in this chapter.

- ❖ CPA equation of state has been applied to VLE, LLE and VLLE of mixtures containing complex, polar and associating, non-associating and solvating compounds in **chapter 4**. In the first part of the chapter mutual solubility of paraffinic/aromatic hydrocarbons and water is modeled. Furthermore VLE of the hydrate inhibitor methanol and methane has been investigated. In the next section multicomponent VLE of a hydrocarbon mixture consisting of methane, ethane and n-butane in presence of water, water + methanol and water + MEG is presented over a range of temperatures and pressure. Finally the CPA EoS has been applied to VLLE of a synthetic condensate (i.e. MIX-2 consisting of methane, ethane, propane, n-butane, n-heptane, toluene and n-decane) in presence of water, MEG and methanol. More specifically vapor and organic phase compositions of the following systems have been investigated:
 - MIX-2 + water
 - MIX-2 + water + methanol
 - MIX-2 + water + MEG
- ❖ As described earlier the experimental data for mutual solubility of reservoir fluid, MEG and water is very rare in the open literature especially for natural gas-condensates and oils. This is partly due to the difficulties involved in the measurement of such solubilities on part per million levels. In this work a method for the measurement of mutual solubility of condensate, MEG and water has been established and tested. The experimental work was carried out at Statoil R & D in Trondheim, Norway in 2009. The liquid-liquid equilibrium data for condensate + MEG and condensate + MEG + water systems have been measured over a range of temperatures and atmospheric pressure. The effect of type of condensate, temperature and MEG content in the polar phase has been investigated. This work is presented in **chapter 5**. Based on the method developed in this project the experimental work has been extended to another condensate and two oils from the North Sea which has been carried out in two master projects. The overview of this work is also included in this chapter.
- ❖ **Chapter 6** presents thermodynamic modeling of the three condensates and two oils from the North Sea. The modeling was carried out using the CPA EoS and Yan et al.¹⁶ characterization method. The modeling of each condensate and oil (in presence of water and MEG) is described in a separate subsection (subsections 6.2.1-6.2.5). The next subsection 6 presents a comparison for reservoir fluid systems modeling with that of well-defined hydrocarbons.

- ❖ Finally **chapter 7** summarizes the overall conclusions and recommendations for future work.

Octanol-Water Partition Coefficient

2.1 Introduction

In 1990, the Norwegian offshore industry started to evaluate different environmental hazards and risk assessment systems for production chemicals likely to be discharged with produced water to marine environment.¹⁷ In 1993 an initiative was taken by the Norwegian oil operators (OLF) and the State Pollution Control Authority (SFT) together with Dutch operators and authorities to develop a joint project of harmonizing environmental hazard and risk assessment of offshore chemicals. The CHARM (chemical hazard assessment and risk management) model was developed to give operators, chemical suppliers, and environmental authorities a scientific framework for analyzing the environmental hazards and risk of offshore chemicals used and discharged to the marine environment.¹⁸

During the whole development of CHARM the exposure assessment was the focal point of discussions and concerns. For assessing the environmental risk of chemicals discharged with produced water and drilling cuttings, it was necessary to understand how the environmental fate of chemicals could be predicted. This includes determination of chemical partitioning between the environmental compartments and reaction processes, as well as dispersion modeling.¹⁸

Offshore chemicals are mainly discharged through drilling and oil and gas production and process operations. In the first process chemicals are discharged with drilling cuttings and in the second with the overboard discharges of treated discharged water. The consumption and discharge of production, drilling and injection chemicals in Statoil operated fields in 1997 is shown in Table 2.1.¹⁹ For organic chemicals the octanol-water partition coefficient (K_{ow}) is a key environmental parameter often serving as a basic input parameter for environmental exposure assessments. It has been shown by many authors that there is a significant correlation between K_{ow} and the bioaccumulation potential in fish.²⁰ Chemicals used offshore comprise complex mixtures of inadequately defined substances. Due to the complexity of the processes involved, simplified methods are required to predict the amount of chemicals discharges to the sea or

become soluble in water. For this purpose the octanol-water partition coefficient is used.¹⁸ In this chapter an overview of the octanol-water partition coefficient, its application in oil and gas industry, its limitations and correlations with oil-water partition coefficients are presented.

Table 2.1: Consumption of Chemicals in the Statoil Operated Fields in 1997 and Their Release to the Sea Water.¹⁹

Chemical Group	Consumption (Ton per year)	Release to Sea (water) (Ton per year)	% Release
Drilling Chemicals	101457	51926	51
Production Chemicals	13639	5360	39
Injection Chemicals	2218	34	1.5

2.2 Octanol-Water Partition Coefficient

The octanol-water partition coefficient is the ratio of the concentration of chemical in octanol to that in water at equilibrium consisting of two largely immiscible solvents, n-octanol and water.^{18,21,22} This ratio is used as a measure of the lipophilicity of a chemical and can be defined for a chemical i as following:

$$K_{ow} = \frac{C_i^o}{C_i^w} \quad 2.1$$

where C_i^o and C_i^w are the concentration of the chemical i in the octanol-rich phase (o) and the water rich phase (w), respectively. The unit of concentration is mol/l or mol/cm³. Equation 2.1 can also be written in term of activity coefficients to use a thermodynamic model for estimation of K_{ow} as given below:²³

$$K_{ow} = 0.151 \frac{\gamma_i^{o,\infty}}{\gamma_i^{w,\infty}} \quad 2.2$$

where $\gamma_i^{w,\infty}$ and $\gamma_i^{o,\infty}$ are infinite dilution coefficients in the water and octanol phases, respectively.

For the true partition coefficient (same molecular species in both solvent, dilute solutions) symbols P and K_{ow} are used. As a general rule, P is preferred by medicinal and pharmaceutical chemists and K_{ow} is used most by the environmental and toxicological chemists. In this thesis the symbol " K_{ow} " is used for octanol-water partition coefficients. 1-Octanol is a long-chain normal alcohol (CH3CH2CH2CH2CH2CH2CH2CHOH) containing both a hydrophobic hydrocarbon chain and a hydrophilic end group. It may be considered to approximate the physicochemical environment experienced by a test chemical in living tissues.²⁴

Octanol-water partition coefficients are widely used in medicinal and environmental applications:

- To quantify structural properties of a solute such as its hydrophobicity
- For the assessment of environmental fate of the pollutants
- To approximate the partitioning of pollutants between biological tissues (membrane and fatty tissues) and water

The experimental data for octanol-water partition coefficient for about 20,000 compounds are available.^{25,26}

2.2.1 Experimental Measurement Methods

Many methods exist for the measurement of oil-water partition coefficients. They are described as direct and indirect methods. In the present context, direct means that, one or both of the immiscible phases are analyzed quantitatively for solute. Indirect means that there is no quantitative analysis. Such categorization should not be taken to imply any prejudgment on their usefulness or quality.²⁴

2.2.1.1 Direct Methods

The classical method for measurement of octanol-water partition coefficient is the shake-flask²⁷⁻²⁹ method. This is a very simple method in which the solute is dissolved in one phase, and through agitation it becomes distributed between the two phases. After separation, each phase is analyzed for the solute. The two analytical methods most often used are absorption spectrophotometry and high pressure liquid chromatography (HPLC). To use this method of measurement both the solute and the solvent should be pure in order to get reliable results. In order to facilitate the dissolution of solute in octanol and water a small volume of auxiliary solvent such as methanol can be used with heating. If a solute degrades in solution due to oxidation or reaction with the solvent, the classical shake-flask method cannot be used. Partition coefficients of unstable compounds have, however, been measured by time-dependent methods.²⁴

Various automated versions of the shake-flask method are also used including AKUFVE^{30,31} (Swedish Acronym)²⁴ and rapid mix/filter probe.³² The AKUFVE is a relatively easy and the rapid method to vary temperature, pH, and ionic strength and to observe the effects of different variables. The rapid mix/filter probe method is similar to AKUFVE. This method, in comparison to the AKUFVE method, uses centrifugation, rapid mix/ filter probe effects to separate the phases for analysis. In order to eliminate the possibility of emulsion formation sit-flask method

(another variant of shake-flask method) is used. In this method no shaking is applied. In other aspects it is similar to shake-flask method. Slow-Stirring method is used for very hydrophobic compounds for which $\log K_{ow}$ is greater than 5. This method (i.e. slow stirring) is considered as an intermediate between the shake-flask and the sit-flask methods.²⁴

2.2.1.2 Indirect Methods

These methods are based upon correlation of capacity factor of chromatography. Some of them are widely used and the relevant literature is enormous. The details of all these methods are away from the scope of present work and can be found in elsewhere.²⁴ These methods are enlisted below:

- Liquid chromatography with solid support
- Liquid chromatography without solid support
- Electrometric titration
- Activity coefficients
- Thermometric titration
- Kinetics of partitioning
- Water solubility correlation

2.2.2 Estimation Methods

The estimation methods for K_{ow} can be divided roughly into three groups¹⁴

- Empirical direct correlations
- Higher order group contribution methods
- Thermodynamic models

2.2.2.1 Empirical Direct Correlations

2.2.2.1.1 Hansch and Leo Model

In this method a molecule is regarded as being constituted of a number of chemically recognizable and common atoms or groups of atoms. The contributions of the fragments to the total $\log K_{ow}$ of molecules are estimated using a large database of reliable $\log K_{ow}$ experimental data. The basic fragment was derived from a small set of the simplest possible molecules.²⁴

2.2.2.1.2 AFC Correlation Model

It is a special correlation model which is abbreviated as KOWWIN in its computerized form. The AFC correlation model has been proposed by Melyan and Howard.³³ It is a GC (group contribution) or fragment contribution method specifically for the calculation of the octanol-water partition coefficient. The fragment can consist of the well-known organic functional groups such as alcohols, amines, etc. as well as halogens. The expression for the calculation of octanol-water partition coefficients is given by the following equation.

$$\log K_{ow} = \sum_i n_i f_i + \sum_j n_j c_j + 0.229 \quad 2.3$$

where n_j is the number of occurrence of the fragments f_i and n_i is the number of occurrences of the correction factor c_j . The fragments constant are determined by regression from reliable experimental $\log K_{ow}$ data.^{22,33}

2.2.2.1.3 ACD Method

Advanced Chemistry Development, Inc., (ACD/Labs) is a chemistry software company (founded in 1994, and headquartered in Toronto, Canada) offering solutions that integrate chemical structures with analytical chemistry information. The ACD method has not been described in the scientific literature and further information about the products and solution offered by the company can be found elsewhere.³⁴

2.2.2.2 Higher Order Group Contribution Methods

These methods include third order group contribution (GC) method of Gani¹²⁵ and second order GC method of Constantinou.¹²⁴

2.2.2.2.1 Gani Method

In this method K_{ow} is estimated using a three level group contribution estimation approach requiring molecular structure information. The group contribution values were calculated using linear regression analysis using a data set of 9560 values. The data set included compounds ranging from C_3 to C_{70} , including large and heterocyclic compounds.

The primary level uses contribution from simple first order groups that allow for the description of a wide variety of organic compounds. It cannot distinguish between isomers and therefore intended to deal with simple and nonfunctional compounds. The higher level (second and third-order groups) involve polyfunctional and structural groups that provide more information about molecular fragments whose description through first-order groups is not possible.

The second level estimation is consequently intended to deal with polyfunctional, polar or nonpolar, compounds of medium size, C_3 - C_{10} , and aromatic or cycloaliphatic compounds with only one ring and several substituent. The third level includes group that provide more structural information about molecular fragments of compounds whose description is insufficient through the first and second order groups. The third level estimation allows the property of complex heterocyclic and large polyfunctional acyclic compounds to be estimated.

2.2.2.2.2 Constantinou Method

Constantinou et al. proposed an additive property method which is based on conjugation operator and is applicable to organic compounds. This method uses two kinds of groups: first-order groups that describe the basic molecular structure of the compounds and the second order groups which are based on the conjugation theory and improves the accuracy of the predictions. In addition to octanol-water partition coefficient the other properties like total solubility parameters and flash point were also estimated using this method.

2.2.2.3 Thermodynamic Models

Thermodynamic model can also be used as an alternative approach to empirical correlations for estimating the octanol-water partition coefficient ranging from group contribution methods (UNIFAC) to advanced association models like SAFT and CPA.¹⁴ A preliminary application of CPA for prediction of $\log K_{ow}$ is shown in Figure 2.1. The quantum mechanical and statistical thermodynamic based tool COSMO-RS has also been applied for the partition coefficients of solutes in different solvents.³⁵

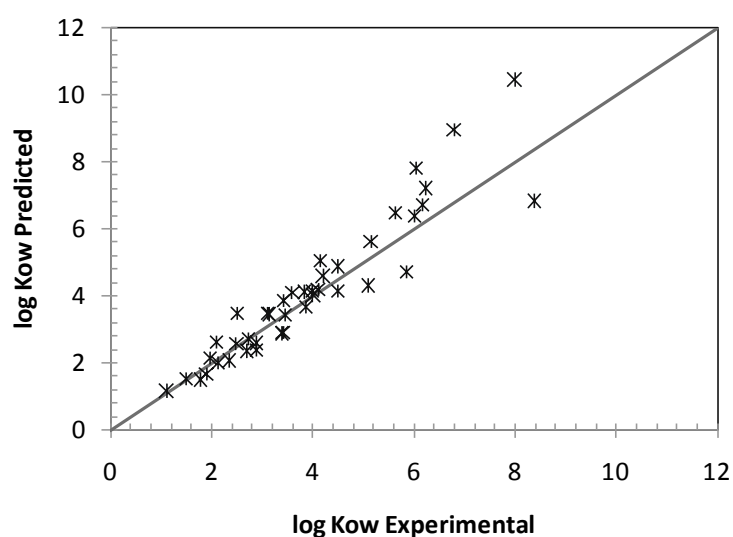


Figure 2.1: CPA predictions of octanol-water partition coefficients.¹⁴

2.2.2.3.1 UNIFAC Methods

Much effort has been put into the development of the UNIFAC and ASOG group contribution models for about 35 years. As a result the most elaborate of these methods, which are different implementations of UNIFAC and ASOG, represent the state of the art models for structure interpolating thermodynamic property prediction in the liquid phase in chemical engineering, since about 1990.²⁵

The performance of standard UNIFAC methods as well as indirect method (by activity coefficient at infinite dilution) for the calculation of K_{ow} has been presented in the literature.¹⁴ A comprehensive review of application of group contribution models such as various forms of UNIFAC (UNIFAC VLE, UNIFAC LLE, UNIFAC VLE-2, Water UNIFAC, and UNIFAC VLE-3) and AFC empirical correlation model is presented by Derawi et al.²² The difference among the various forms of the UNIFAC model is shortly described in the next section. The predicted K_{ow} is compared with experimental data for different classes of chemicals. The models are evaluated based on the average absolute deviation (AAD) given by the following equation and the summary of results is presented in Figure 2.2.

$$AAD = \frac{1}{N} \sum_{i=1}^N \left(\left| \log K_{ow}^{\text{exp},i} - \log K_{ow}^{\text{cal},i} \right| \right) \quad 2.4$$

where N is total number of points. A short description of various UNIFAC models used by Derawi et al. is given below.

Original UNIFAC VLE-1

This model is similar to original UNIFAC by Fredenslund³⁶ but it additionally uses recent revised parameters of Hansen.³⁷ The interaction parameters are determined experimentally using VLE data and they are not temperature dependent.²²

UNIFAC LLE³⁸

This model is similar to the original UNIFAC³⁶ however interaction parameters have been determined by fitting LLE experimental data.

Original UNIFAC VLE-2³⁷

This model is similar to the above two, the only difference here is that, interaction parameters are linearly temperature dependent.³⁷

Modified UNIFAC VLE-3

This model is the modified version of the original UNIFAC by Larsen developed at DTU.³⁹ The interaction parameters are temperature dependent and have different form as compared to VLE-2. Interaction parameters are determined from experimental VLE and excess enthalpy data.

WATER UNIFAC

This model is developed by Chen⁴⁰ and is similar to the original UNIFAC VLE-1, but is specially designed for aqueous systems. New interaction parameters have been determined between water molecule and other functional groups, from experimental infinite dilution activity coefficients in aqueous solutions.

The AAD for all GC models investigated is tabulated for considered poly-functional chemicals are given in Figure 2.2. The partition coefficient of 115 nonfunctional chemicals between octanol and water phase have critically evaluated by use of five UNIFAC models and AFC empirical correlation model. The AFC correlation has been shown to be superior to all UNIFAC models in all cases. However, the AFC correlation is limited to the octanol-water partitioning coefficient and cannot be employed to other partition coefficient e.g. oil-water of these chemicals. Among the various more general GC models UNIFAC LLE and WATER UNIFAC were recommended to predict the partitioning of molecules between octanol and water phase. These models were also recommended for poly-functional molecules (e.g. ethylene glycol and diethanolamine) for octanol-water partition coefficients.²²

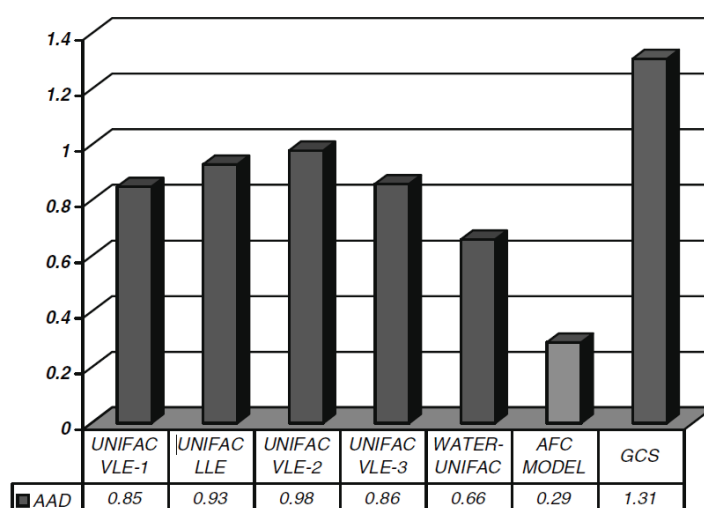


Figure 2.2: Average absolute deviation (AAD) between experimental and predicted $\log K_{ow}$ values from models for complex chemicals (e.g. glycols and alkanolamines).^{22,14} The list of 22 polyfunctional molecules considered for calculations is given in the appendix A. 6.

2.2.3 Octanol-Water Partition Coefficient in Oil Industry

In order to decide on the consequences of production chemicals with respect to environment it is important to know their amounts in the water and in the crude oil. The added production chemicals vary in complexity and they belong to different chemical families as shown in Appendix A. 1. Many of the chemicals used are mixtures of different compounds with complex or ill-defined structures. Furthermore these chemicals are generally added in such small quantities that their direct detection by analysis is extremely difficult and in many cases impossible.⁶ Therefore in order to report amount of applied production chemical discharged with the produced water to sea, it is based on octanol-water partition coefficient of chemicals.

2.2.4 Limitations of Octanol-Water Partition Coefficient Based Method

When reporting the discharge of a production chemical to sea it is assumed that the oil-water distribution will mimic the octanol-water distribution. But the work carried out at Statoil Research and Development Center in Norway has shown that this is not always the case. This has been shown by the distribution of the active components of two corrosion inhibitors reported by Knudsen in 1997.⁵ The calculation based on octanol-water partition coefficients predicted that 60-90% of active components will go into the water. But experimental results showed that less than 5% of the active components were found in the water phase whereas remaining 95% or more were found in the oil. These results were based on both the laboratory and the field data.⁶ In order to investigate the oil-water partition coefficient for other chemicals experimental work was carried out until 1999 at Statoil R & D.⁶ The details of experimental setup used in that study are given in the next section.

2.3 Oil-Water Partition Coefficient

2.3.1 Experimental Work at Statoil R & D

The experimental setup used for obtaining the oil-water partition coefficient at Statoil R & D consists of a bench scale separation rig as shown in Figure 2.3. It consists of two piston flasks with volume 600 ml each and a measuring cylinder which act as the model separator. The liquid from both flasks is pumped using hydraulic pumps. It is passed through a pressure reducing valve where the pressure is reduced to atmospheric. Pumping speeds are independent of each other but are generally kept between 0-300 ml/min. The general rig operating conditions are given in Table 2.2. They are designed to simulate the approximate conditions in an oil, water and gas separator offshore. The chemical to be analyzed is premixed with oil or water. After passing through a valve, the mixture was left to separate in measuring cylinder. The analysis technique of “radioactive labeling and scintillation” was used.⁶

Table 2.2: General Rig Conditions for Oil-Water Partition Experiment.⁶

Conditions	Characteristic
Identification	C-14 or H-3 labeled isotopes
Pressure	20-80 bar
Temperature	25-85 °C
Oil/water volume stream	3000 ml/h
Water cut	20-70
Total volume	3000 ml

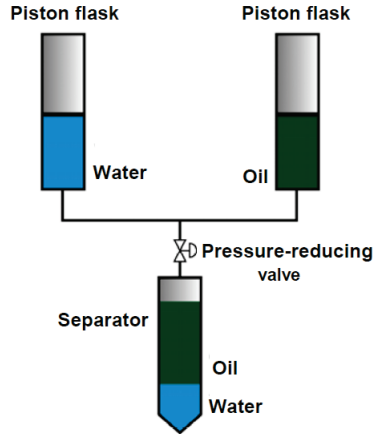


Figure 2.3: Schematic illustration of the bench-scale-rig used by Statoil for oil-water partition studies of chemicals.⁶

After measurement of the concentration of the chemical in hydrocarbon and water phase the following equations have been used for obtaining the results. The oil-water partition coefficient ($K_{oil-water}$) can be defined similar to octanol-water partition coefficient (K_{ow}) as given in equation 2.5.

$$K_{oil-water} = \frac{C_{oil}}{C_{water}} \quad 2.5$$

where C_{oil} is the concentration of chemical in the oil and C_{water} is the concentration of the chemical in the water. At Statoil concentration of chemicals in oil and water phase was measured in units of mg/l.

The water cut is given by the equation 2.6:

$$W_c = \frac{100V}{O + V} \quad 2.6$$

where V is the volume of water and O is the volume of oil.

The fraction of chemical in the crude after separation is given by equation 2.7:

$$\frac{K_{oil-water} (100 - W_c)}{W_c + 100K_{oil-water} - K_{oil-water} W_c} \quad 2.7$$

The fraction of chemical which is discharged to the sea is given by equation 2.8:

$$1 - \frac{K_{oil-water} (100 - W_c)}{W_c + 100K_{oil-water} - K_{oil-water} W_c} \quad 2.8$$

2.3.2 Parameters Affecting Oil-Water Partition Coefficients

The effect of various parameters (temperature, pressure, type of crude and concentration of chemical) on oil-water partition coefficient was also investigated. The active gradient of corrosion inhibitor PK6050, imidazoline salt was used as chemical in all those experiments. Figure 2.4 shows the effect of type of crude on the average partition coefficient. It can be seen from the figure that (crude oil from) Gullfaks and Statfjord show similar partitioning behavior whereas Heidrun crude shows higher partition coefficient of chemical. Here higher partition coefficient means the higher tendency of Heidrun crude to accumulate the chemical. This higher partition coefficient is attributed to naphthenic nature of the crude. The similar partition coefficients for Gullfaks and Statfjord are because both the crudes are similar in the composition and the character (i.e. PNA distribution).⁶

The effect of water cut on average partition coefficients is shown in Figure 2.5. It shows that partition coefficient of imidazoline salt increases with increasing water cut. This is because the salt is oil soluble and with increasing water cut the more salt is forced into the oil. It has been stated that the other parameters like temperature and the pressure (in the range given in Table 2.2) had no significant effect on the partition coefficient.⁶

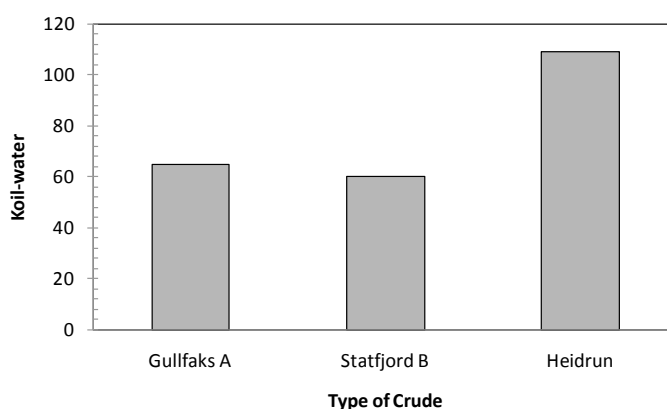


Figure 2.4: Effect of type of crude on oil-water partition coefficient.⁶

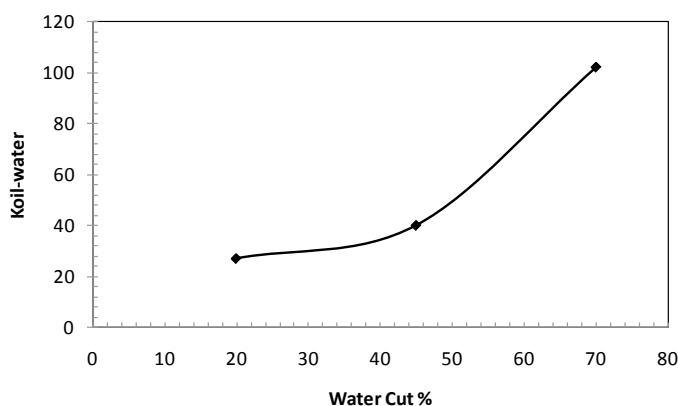


Figure 2.5: Effect of water cut on oil-water partition coefficient.⁶

On the basis of a parameter study a standard method for determining the oil-water partition coefficient was established and 45 production chemicals were tested by Statoil and the work did not continued. In standard the partition coefficient of each chemical was measured for 20% and 70% water cut. The average of two values was reported as the chemical-specific partition coefficient. The discharge of three production chemicals calculated using K_{ow} or $K_{oil-water}$ in equation 2.8 as given in Table 2.3. The partitioning trends can be summarized as given below:

- For imidazoline salt K_{ow} predicts that it is discharged 40-90% to the Sea whereas $K_{oil-water}$ shows that it is only 2% discharged in the sea. The discharge of this chemical is far lower than anticipated.
- Methyldiethanolamine (MDEA) is a much used gas treatment chemical. Use of K_{ow} predicts that the chemical is oil soluble at lower water cut and at high water cut half of the amount of chemical would be discharged. The $K_{oil-water}$ shows the opposite partitioning behavior such that hardly any of the chemical remains in the oil after oil-water partitioning.
- For methanol which is used as hydrate inhibitor, the trends in partitioning are similar for both coefficients.

The three examples given in Table 2.3 show that it is not reliable to predict oil-water partition coefficient of chemicals on the basis of octanol-water partition coefficient. Furthermore there is a need to make investigations (experimental / using thermodynamic model) to validate these results. In order to get better estimation of discharged chemicals field specific factor will be required.⁶ Also a factor accounting for temperature, pressure and chemical concentration should be evaluated. This can be achieved by extended experimental work and developing a thermodynamic model. As the systems of interest consist of polar and associating compounds therefore a model such as CPA taking association into account is believed to be a better choice.

The experimental work carried in this PhD project is given in chapter 5 and the modeling using CPA EoS is presented in chapter 6.

Table 2.3: Discharge of Chemicals to the Sea Calculated on the Basis of Octanol-Water and Oil-Water Partition Coefficients.⁶

Partitioning	Water Cut %	Discharge to Sea %
Imidazoline salt		
Oil-Water	20	1
Oil-Water	70	3
Octanol-Water	20	43
Octanol-Water	70	87
Methyldiethanolamine		
Oil-Water	20	90
Oil-Water	70	98
Octanol-Water	20	9
Octanol-Water	70	48
Methanol		
Oil-Water	20	43
Oil-Water	70	88
Octanol-Water	20	51
Octanol-Water	70	91

2.3.3 Challenges Related to Oil-Water Partition Coefficients

In this PhD project Statoil provided a list of 73 production chemicals containing different functions as given in Appendix A. 1. These chemicals have been extracted from a longer list of chemicals (i.e. from a list of 37 groups on the basis of functions). In this list chemicals are given under every function in decreasing order of use (i.e. chemical at the top is used the most and one at the bottom is used the least). This means that the most used compound within every function is the one that is listed first. For wax inhibitors (shown in Appendix A. 1) this implies that the aromatic solvent has the highest usage (in tones). The usage is an obvious criterion for choice but the factors like the environmental properties or the possible negative effects on the refinery are also important. The classification of chemicals on the basis of their function and the family are given in Tables 2.4 and 2.5 respectively.

After initial investigations on the list of chemicals following challenges have been identified:

- The molecular structure of many chemicals is unknown in order to comply with confidentiality agreement with the suppliers.
- The CAS number is not available for all compounds which make the selection of chemicals to work with more difficult. There are some compounds in the list with their

CAS number but such CAS number does not exist in the literature. This suggests that for some chemicals, the given CAS number is probably not correct.

- The compositions of the oil and the oil mixtures used in experiments are not available. Similarly overall density and molar mass (of the oil and the oil mixture used) are also not available.
- The $K_{\text{oil-water}}$ data are reported with chemical concentration units in oil and water phases as mg/l (i.e. mg of chemical / liter of oil or water) whereas in modeling results the concentration units are expressed as mole/mole (i.e. mol of chemical / mol of oil or water). In order to compare data with modeling results $K_{\text{oil-water}}$ must be in same units and to convert into the same units, density and molar mass of the oil is required which is unknown.
- There are some inconsistencies in the K_{ow} and $K_{\text{oil-water}}$ values as the diverse values are given for the same chemicals in the various industrial reports.
- All the data for $K_{\text{oil-water}}$ may not necessarily be the equilibrium data due to limited time given for the separation of oil and aqueous phases.

As it is not possible to cover all the chemicals therefore a range of chemical compounds have been selected. Methanol, butyldiglycolether and monoethylene glycol are the most important based on the usage in 2007 at Statoil. Finally it has been decided for this PhD project to focus on glycols and alcohols. More specifically methanol and MEG are of interest. For experimental work it was decided to concentrate on MEG using similar experimental setup as used by Derawi et al.¹² and Folas et al.⁷⁷ But they carried out experiments with well-defined alkanes (e.g. n-heptane) and aromatic hydrocarbons (e.g. benzene and toluene) whereas in this project reservoir fluid from the gas fields in the North Sea will be used. This implies that analytical method will require modifications due to complexity of the system of study added by reservoir fluid.

It can also be seen from the Appendix A. 1 that oil-water partition coefficients are not available for all chemicals. Investigations have been made to develop correlations between oil-water and octanol-water or hexane-water partition coefficients. These correlations are presented in the next section.

Table 2.4: Production Chemicals in Statoil Operated Fields and Their Functions.

Chemical Function	Number of components
Emulsion breakers	26
pH regulating	1
Wax inhibitors	10
Corrosion inhibitors	7
Scale inhibitors	6
Defoamer	8
Flocculant	6
Hydrate inhibitors	3
Others	6
Total components	73

Table 2.5: Production Chemicals in Statoil Operated Fields and Their Families.

Chemical Family	Number of components
Alcohols	3
Glycols and Glycolethers	6
Aromatics	4
Acetates	1
Amines	2
Acids	3
Esters	1
Polymers	26
Salts	13
Others	14
Total components	73

2.3.4 Alternative Approaches to Predict $K_{\text{oil-water}}$

In order to correlate oil-water partition coefficient with K_{ow} and K_{hw} experimental data were collected from different sources^{24,26,41} as given in appendices A. 2 and A. 3. It has been noted that experimental data for $K_{\text{oil-water}}$ are very rare and therefore correlations can only be made for a limited number of chemical families which are presented in the next sections.

2.3.4.1 $K_{\text{oil-water}}$ via K_{ow}

Figure 2.6 shows correlations between the octanol-water and oil-water partition coefficients. It can be seen from the figure that linear correlations exist between K_{ow} and $K_{\text{oil-water}}$. The octanol-water partition coefficient of n-decanol and octadecanol is estimated to be 3.7×10^3 and 5.2×10^7 respectively. Therefore the logarithm of partition (i.e. $\text{Log}K_{\text{ow}}$ and $\text{Log}K_{\text{oil-water}}$) is plotted to correlate an extended range of alcohols from methanol to octadecanol. A relatively better correlation ($R^2=0.9926$) can be obtained by excluding 2-propanol which is the only iso-alcohol in the list. The oil-water partition coefficient of 1-alcohol can be predicted from octanol-water partition coefficients using the correlation given in Figure 2.6. The correlations for two other

chemical families (i.e. glycol and alkanolamine) are shown in Figures 2.7 and 2.8 respectively. These correlations are relatively less reliable because of the limited number of data points (three points in each plot). More data are required to build more reliable correlations.

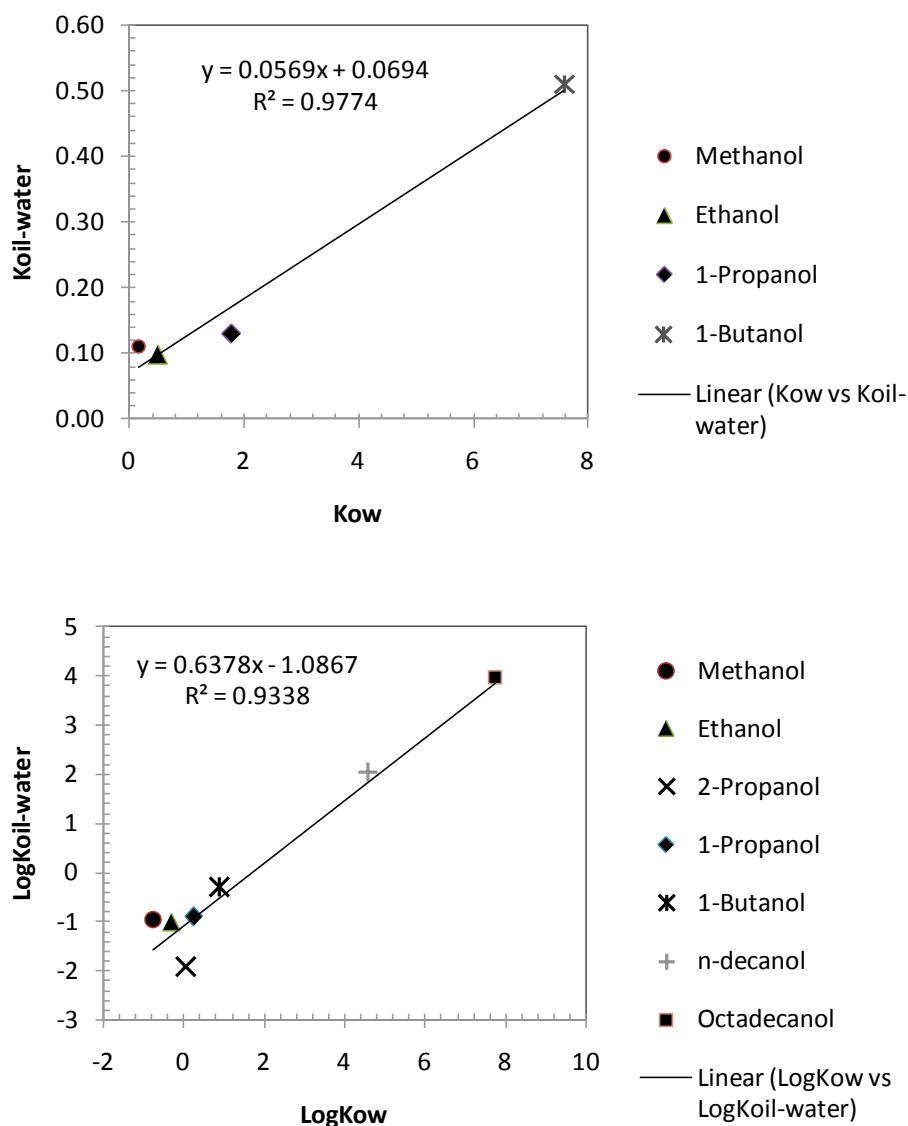


Figure 2.6: Correlations between octanol-water and oil-water partition coefficients (a) K_{ow} vs $K_{oil-water}$ for methanol to 1-butanol (b) $\text{Log}K_{ow}$ vs $\text{Log}K_{oil-water}$ for methanol to 1-decanol.

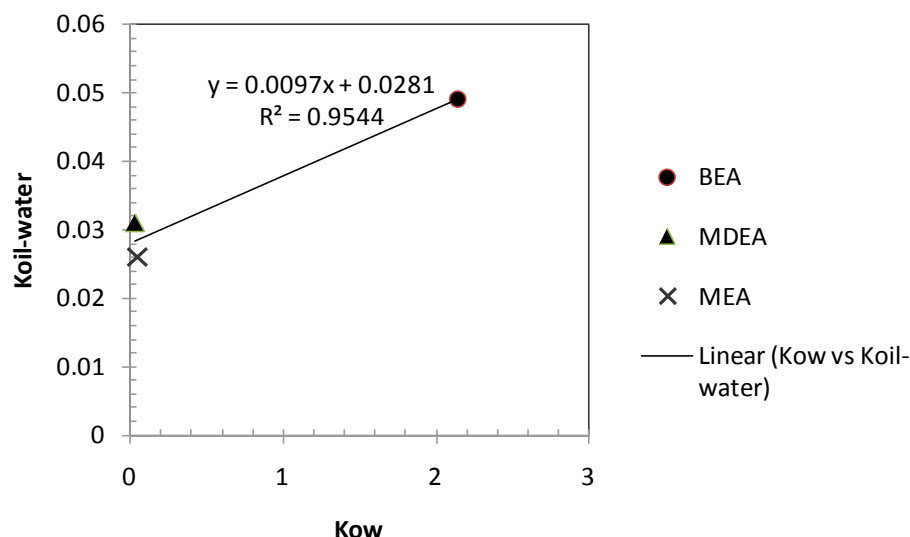


Figure 2.7: Correlation between octanol-water and oil-water partition coefficients for alkanolamines.

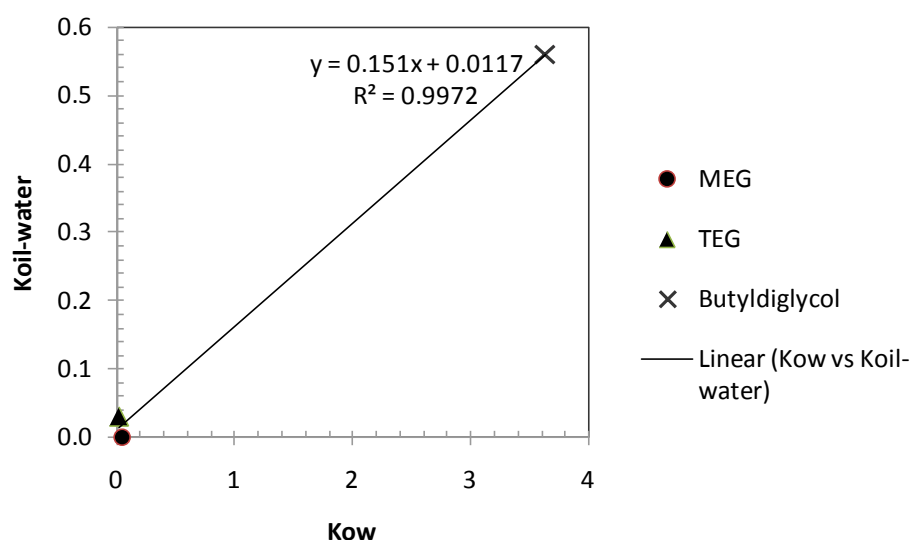


Figure 2.8: Correlation between octanol-water and oil-water partition coefficients for glycols.

2.3.4.2 $K_{oil-water}$ via K_{hw}

Similar to octanol-water partition coefficient the hexane-water partition coefficient is the ratio of the concentration of chemical in hexane to that in water in a two-phase system at equilibrium consisting of two immiscible solvents, n-hexane and water. The alkane/hexane-water can better mimic oil + water system due to the similarity of oil and n-hexane. As described earlier, that for many solutes, experimentally determined partition coefficients are available for 1-octanol and water system. But experimental data for the hexane-water partition coefficient are rarely found in the literature. Schulte et al.⁴¹ have reported hexane-water partition coefficient of 41 chemicals which contain only a few production chemicals such as

alcohols. Figure 2.9 shows a correlation between K_{hw} and $K_{oil-water}$. It can be seen from Figure 2.9 that satisfactory correlation exists between K_{hw} and $K_{oil-water}$ for the available data for alcohols. Furthermore correlations for carbon number (N_c) of alcohols vs ratio ($K_{oil-water}/K_{ow}$) or ($K_{oil-water}/K_{hw}$) are also investigated as shown in Appendix A. 4 and A. 5 respectively. It is shown that a fairly good correlations are obtained.

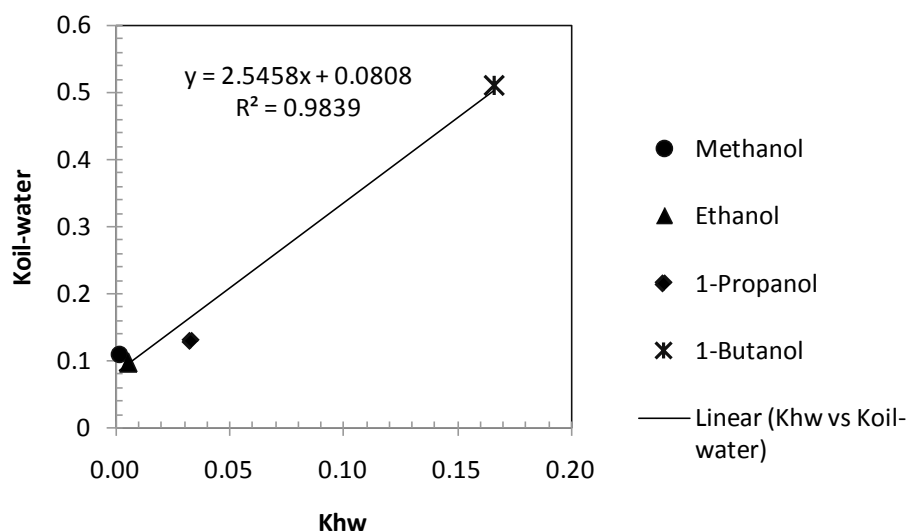


Figure 2.9: Correlation between hexane-water and oil-water partition coefficients for alcohols.

2.4 Conclusions

Many chemicals are used by oil and gas industry in drilling, production and transportation of oil and gas. These chemicals have various functions such as they are used as hydrate inhibitors, scale inhibitors, defoamers and emulsion breakers. They belong to various chemical families like glycols, alcohols, amines, polymers and salts. As a result a lot of attention has been paid to their use from oil industry itself as well as from authorities due to the environmental aspects. In order to evaluate the consequences of use of chemicals it is of crucial importance to know how much of the chemicals are discharged via the produced water and how much are dissolved in the oil. These chemicals are very complex and many of them are a mixture of different compounds with unknown molecular structure. Furthermore they are added in very small amount and their direct detection is very difficult and in some cases impossible. Therefore the octanol-water partition coefficient is used to calculate their amount in oil and water. A lot of data exist for octanol-water partition coefficients. It can also be estimated using empirical correlations, higher order group contribution methods and thermodynamic models. In such

calculations it is assumed that octanol-water partition coefficient mimics the oil-water partition coefficient but the research carried out at Statoil R and D showed that this is not always the case. In this chapter a review of experimental work carried out at Statoil R & D is presented which shows that the experimental partitioning trends of imidazoline salt and alkanolamine are opposite to those predicted using octanol-water partition coefficient. Furthermore parameters like water cut (Figure 2.5) and the type of crude (Figure 2.4) have considerable effect on oil-water partition coefficient whereas pressure and temperature have relatively lower effect.

As it is expensive to measure oil-water partition coefficient ($K_{\text{oil-water}}$) for all chemicals used by Statoil therefore it is of interest to investigate alternative approaches to estimate them from octanol-water partition coefficient (K_{ow}) or hexane-water partition coefficient (K_{hw}). In order to correlate $K_{\text{oil-water}}$ with K_{ow} or K_{hw} the experimental data were collected from different sources. It has been noted that the experimental data of $K_{\text{oil-water}}$ is very rare and the only data available are from Statoil. The experimental data of K_{ow} and K_{hw} are even not available for all the chemicals of interest in this study. K_{ow} cannot be predicted for all the chemicals as their molecular structure is not available to comply with confidentiality. Due to these reasons satisfactory correlation between $K_{\text{oil-water}}$ and K_{ow} or K_{hw} could not be built between for all families of interest. However a satisfactory linear correlation exists between $K_{\text{oil-water}}$ and K_{ow} for alcohols (methanol to octadecanol in Figure 2.6). Similarly satisfactory correlations are obtained between $K_{\text{oil-water}}$ and K_{hw} for light alcohols (methanol to 1-butanol Figure 2.9) as experimental data for K_{hw} is not available for heavy alcohols. The correlations for two other chemical families (i.e glycol and alkanolamine) are less reliable possibly because of a limited number of data points. Therefore more data and molecular structure's information are required to build such correlations.

Modeling Approach

3.1 Introduction

Different types of phase equilibrium calculations or data are needed for optimal design and operation of processes or equipments. Equations of state play an important role in chemical and petroleum engineering design, and they have assumed expanding role in the study of the phase equilibria of fluids and fluid mixtures.⁹ These widely used existing models (e.g. cubic EoS) were found to be inadequate for VLE/LLE applications, especially for mixtures containing highly immiscible compounds e.g. water + hydrocarbon LLE or water + hydrocarbon + alcohol/glycols VLE.¹⁴ The models combining EoS with excess Gibbs energy (EoS/G^E) like SRK with the Huron-Vidal mixing rule sometimes provide satisfactory results but they are dependent on the accuracy of underlying activity coefficient model like NRTL⁴² and UNIQUAC.⁴³ Such local composition models often fail to describe well mixtures with associating compounds, especially for multiphase, multicomponent equilibria. Associating components are those which are capable of hydrogen bonding e.g. alcohol, glycol, water and amines etc. Phase equilibria of complex associating systems are important for many applications, for example in the oil industry for studying of gas hydrates, calculation of the amount of hydrate inhibitors and their partitioning between water and oil, azeotropic and extractive separation. Furthermore they have many applications in environmental, polymer and chemical industry.¹⁴

Over the last two decades, substantial progress has been made regarding the development of thermodynamic models which can successfully perform phase equilibrium calculations for systems containing associating components. By extending Wertheim's theory,⁴⁴⁻⁴⁷ Chapman et al.^{48,49} proposed a general statistical associating fluid theory (SAFT) approach. Huang and Radosz⁵⁰ developed the SAFT equation of state which accounts for hard-sphere repulsive forces, dispersion forces, chain formation and association. Kontogeorgis et al.¹⁵ presented an equation of state suitable for describing associating fluids. The equation combines the simplicity of a cubic equation of state (SRK) and the theoretical background of the perturbation theory employed for the associating part.^{9,14,51} The resulting equation, called cubic plus association (CPA) equation of state is described in section 3.2. When no associating compounds are present, the CPA equation of state reduces to SRK EoS. Table 3.1 provides an overview of the

applications of the model, together with the corresponding references.⁵¹ An overview of earlier works and more recent applications have been provided elsewhere.¹⁴

Table 3.1: Applications of the CPA Equation of State (1995-2005).⁵¹

CPA variants	Applications	References
original	model presentation, pure compounds	Kontogeorgis et al. ¹⁵
original	VLE alcohol-hydrocarbons	Yakoumis et al. ⁵²
original	LLE alcohol-hydrocarbons	Voutsas et al. ⁵³
original	acetone-alcohols-alkanes	Yakoumis et al. ⁵¹
original, SAFT	a simpler equivalent form of the association term of CPA	Hendriks et al. ⁵⁴
original	LLE water-hydrocarbons	Yakoumis et al. ⁵⁵
Peng	LLE water-alkanes, water-NaCl	Wu and Prausnitz ⁵⁶
Robinson-CPA		
original	VLE, LLE water-alcohols; water-alcohol-hydrocarbons	Voutsas et al. ⁵⁷
simplified	VLE, LLE water-alcohols; water-alcohol-hydrocarbons	Kontogeorgis et al. ⁵⁸
simplified	octanol-water partition coefficients (preliminary results)	Polyzou et al. ⁵⁹
original and SAFT	LLE water-alkanes, comparison with SAFT	Voutsas et al. ⁶⁰
special PR CPA version	CO ₂ -ethanol-cresols	Pfohl et al. ⁶¹
simplified	polymer-solvent VLE	Kontogeorgis et al. ⁶²
CPA, SAFT	a computationally efficient representation of the association Wertheim term	Michelsen and Hendriks ⁶³
original/Pfhol	water-alkanes	Peeters ⁶⁴
CPA, SAFT, SRK	computing times comparison	von Solms et al. ⁶⁵
simplified	LLE glycol-alkanes	Derawi et al. ⁶⁶
simplified	VLE glycol-water, LLE glycol-water-hydrocarbons	Derawi et al. ⁶⁷
simplified	LLE water-IPA-C16-NBA	Orr ⁶⁸
simplified	methanol-water-oil, comparison of CPA with SRK-Huron Vidal	Bruinsma et al. ⁶⁹
simplified	organic acids	Derawi et al. ⁷⁰
simplified	VLE/LLE/SLE alcohol-alkanes, glycol-water SLE and VLE	Folas et al. ⁷¹
simplified	surface tension of water, alcohols (CPA + gradient theory)	Queimada et al. ⁷²
simplified	amines with alkanes and alcohols (VLE)	Kaarsholm et al. ⁷³
simplified	cross-associating systems (glycol-water, alcohol-water SLE, VLE including hydrate phases), high pressures	Folas et al. ⁷⁴
simplified	Soret coefficients of water-methanol and water-ethanol mixtures	Saghir et al. ⁷⁵
simplified	water + N ₂ , CO ₂ , methane, natural gas	Frøyna ⁷⁶
simplified	LLE water-aromatics, VLE alcohol-aromatics, LLE water-alcohol-aromatics, LLE glycol-aromatics	Folas et al. ⁷⁷
simplified	water-hydrocarbons (C ₁ -C ₄)	De Hemptinne et al. ⁷⁸

In this thesis the CPA equation of state has been applied to a variety of phase equilibria (liquid-liquid, vapor-liquid and vapor-liquid-liquid) of complex polar and associating, non-associating and solvating compounds. These chemicals include alkanes, aromatic hydrocarbons, water and polar chemicals (methanol and monoethylene glycol) used as gas-hydrate inhibitors. These investigations are presented in chapter 4.

The CPA EoS has been extended to reservoir fluids by Yan et al.¹⁶ using a characterization procedure similar to that of Pedersen et al.⁷⁹ and a set of new correlations for the critical properties. Calculations presented for reservoir-fluids + water and reservoir-fluids + water + methanol/glycols showed promising results.¹⁶ These correlations are described in section 3.3. In this thesis Yan et al. characterization method is applied to characterize three North Sea condensates and two light-oils and the results are presented in chapter 6.

3.2 The CPA EoS

3.2.1 Description of the Model

The CPA equation of state (EoS), proposed by Kontogeorgis et al.^{15,58} is an extension of the SRK EoS. It can be expressed for mixtures in terms of pressure as a sum of the SRK EoS and the contribution of association term as given by Michelsen and Hendriks⁸⁰:

$$P = \frac{RT}{V_m - b} - \frac{a(T)}{V_m(V_m + b)} - \frac{1}{2} \frac{RT}{V_m} \left(1 + \frac{1}{V_m} \frac{\partial \ln g}{\partial (1/V_m)} \right) \sum_i x_i \sum_{A_i} (1 - X_{A_i}) \quad 3.1$$

where V_m is the molar volume, X_{A_i} is the fraction of A-sites of molecule i that are not bonded with other active sites, and x_i is the mole fraction of component i . The letters i and j are used to index the molecules, whereas the letters A and B indicate the bonding sites on a given molecule.

The first two terms on the right-hand side of equation 3.1 are the same as in the SRK EoS, while the last term is the one that accounts for association. The last association term is therefore eliminated if inert (non-associating) compounds like hydrocarbons are present.

In the association part X_{A_i} is given by the equation 3.2:

$$X_{A_i} = \frac{1}{1 + \frac{1}{V_m} \sum_j x_j \sum_{B_j} X_{B_j} \Delta^{A_i B_j}} \quad 3.2$$

where $\Delta^{A_i B_j}$ is the association strength between site A on molecule i and site B on molecule j and is given by:

$$\Delta^{A_i B_j} = g(\rho) \left[\exp\left(\frac{\varepsilon^{A_i B_j}}{RT}\right) - 1 \right] b_{ij} \beta^{A_i B_j} \quad 3.3$$

with the radial distribution function $g(\rho) = 1 / (1 - 1.9\eta)$ and $\eta = (1/4)b\rho$ where η is reduced fluid density. The parameters $\varepsilon^{A_i B_j}$ and $\beta^{A_i B_j}$ are the association energy and volume between site A of molecule i and site B of molecule j , respectively.

The energy parameter in the SRK part of the equation is given by a Soave-type temperature dependency, whereas b is temperature independent:

$$a(T) = a_0 [1 + c_1 (1 - \sqrt{T_r})]^2 \quad 3.4$$

where $T_r = T / T_c$ and T_c is critical temperature.

3.2.2 Parameters for Pure Components

CPA has five pure compound parameters, three for the SRK part (a_0, b, c_1) and two in the association part ($\varepsilon^{A_i B_j}, \beta^{A_i B_j}$). They are typically obtained by fitting experimental vapor pressure and saturated liquid density data. For inert (non-self-associating) compounds (e.g. hydrocarbons) only three parameters of SRK part are required. The systematic guidelines regarding the estimation of pure component parameters can be found elsewhere.⁵¹ The pure component parameters used in this thesis are given in Tables 3.2 and 3.3. For methane and ethane T_c , P_c and ω were used.

The three parameters in SRK part correspond to a set of apparent critical temperature, pressure and acentric factor. The subscript m is used to indicate that they are the CPA “monomer” parameters rather than the experimental values. The following equations were used by Yan et al.¹⁶ to calculate T_{cm} , P_{cm} and m_m from a_0 , b and c_1 :

$$m_m = c_1 \sqrt{\frac{a_0 \Omega_B}{b R T_c \Omega_A}} \quad 3.5$$

$$T_{cm} = T_c \left(\frac{1 + 1/c_1}{1 + 1/m_m} \right)^2 \quad 3.6$$

$$P_{cm} = \frac{\Omega_B RT_{cm}}{b} \quad 3.7$$

where $\Omega_A = 0.42748$, $\Omega_B = 0.08664$ and

$$m_m = 0.480 + 1.574 \omega_m - 0.176 \omega_m^2 \quad 3.8$$

3.2.3 Mixing and Combining Rules for the Physical Term

The CPA EoS when applied to mixtures requires mixing rules only for the SRK part, while the association part is extended to mixtures in a straightforward way. The classical van der Waals one-fluid mixing rules⁵⁵ are used for a and b :

$$a = \sum_i \sum_j x_i x_j a_{ij} \quad 3.9$$

$$b = \sum_i \sum_j x_i x_j b_{ij} \quad 3.10$$

where a_{ij} and b_{ij} are calculated by the following combining rules:

$$a_{ij} = \sqrt{a_i a_j} (1 - k_{ij}) \quad 3.11$$

$$b_{ij} = \frac{b_i + b_j}{2} \quad 3.12$$

where k_{ij} in equation 3.11 is a binary interaction parameter which is fitted to experimental data.

3.2.4 Combining Rules for the Association Term

For mixtures containing more than one associating compounds such as the mixture of glycols and water, combining rules are needed for the association parameters. Different combining rules have been suggested.⁸¹ The two types of combining rules have been shown to perform better than other types:

- CR-1 combining rule proposed by Derawi et al.⁶⁷
- Elliott combining rule proposed by Suresh and Elliott⁸²

The expressions for the cross-association energy and cross-association volume parameters with CR-1 are given by equations 3.13 and 3.14 respectively.

$$\varepsilon^{A_i B_j} = \frac{\varepsilon^{A_i B_i} + \varepsilon^{A_j B_j}}{2} \quad 3.13$$

$$\beta^{A_i B_j} = \sqrt{\beta^{A_i B_i} \beta^{A_j B_j}} \quad 3.14$$

The expression for cross-association strength with the Elliott Combining Rule (ECR) is given by equation 3.15:

$$\Delta^{A_i B_j} = \sqrt{\Delta^{A_i B_i} \Delta^{A_j B_j}} \quad 3.15$$

Assuming the radial distribution function in equation 3.3 equal to unity (i.e. $g(\rho) \approx 1$) and the term $\left[\exp(\varepsilon^{A_i B_j} / RT) - 1 \right] \cong \exp(\varepsilon^{A_i B_j} / RT)$, it can be shown that the equivalent expressions for the cross-association energy and cross-association volume parameters are obtained as given in equations 3.16 and 3.17:

$$\varepsilon^{A_i B_j} = \frac{\varepsilon^{A_i B_i} + \varepsilon^{A_j B_j}}{2} \quad 3.16$$

$$\beta^{A_i B_j} = \sqrt{\beta^{A_i B_i} \beta^{A_j B_j}} \frac{\sqrt{b_i b_j}}{b_{ij}} \quad 3.17$$

The equations 3.16 to 3.17 show that the CR-1 and ECR combining rules are similar. The only difference is that the second term in equation 3.17 contains the co-volume parameters in the expression for the cross-association volume.

3.2.5 Association Term for Solvating Mixtures

CPA when applied to a mixture with a self-associating (e.g. water, glycols, alcohols) and an inert compound (olefinic or aromatic hydrocarbons) where there is the possibility of cross-association (solvation) the so-called modified CR-1 combining rules proposed by Folas et al.⁷⁷ are used. In the modified CR-1 rule, the cross association volume is fitted to the binary data whereas cross-association energy parameter is equal to the half of the association energy of associating compound.

$$\varepsilon^{A_i B_j} = \frac{\varepsilon_{\text{associating}}}{2} \quad 3.18$$

This approach has been used in chapter 4 for modeling of mutual solubility of aromatic hydrocarbons and water.

3.2.6 Association Schemes

Before estimating pure component parameters, a suitable association scheme should be chosen. The mole fraction of sites not bonded (X_{A_i}) with other active sites in equation 3.2 depends on the choice of association scheme for the components. The association scheme gives the number and types of association sites in the associating components. Huang and Radosz⁵⁰ have classified eight different association schemes and Table 3.4 provides a schematic explanation of the association schemes referred in this thesis. The pure component parameters used in this work are taken from the literature.

In this thesis methanol is described as 2B where the two lone-pairs on oxygen are considered to be a single site. The four-site (4C) association scheme is used in this work for MEG in accordance to the Derawi et al.^{67,66} Although glycols have at least 6 sites based on their chemical structure, the choice of 4C scheme is consistent with the 2B scheme for alcohol where the two lone pairs of oxygen are considered as a single site. The four site (4C) association scheme is traditionally used for water within the CPA framework.

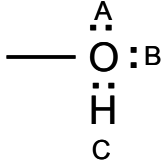
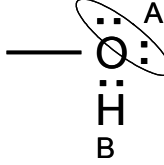
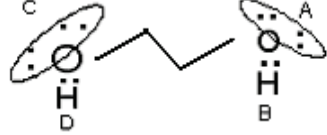
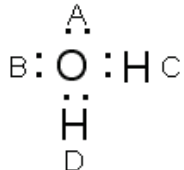
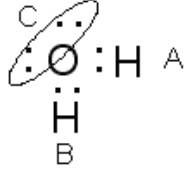
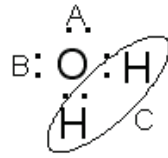
Table 3.2: CPA Parameters for Associating Components Considered in This Work. The 2B Association Scheme is Used for Methanol and 4C is Used for Both Water and MEG.

Component	a_0 ($\text{bar } l^2 \text{ mol}^{-2}$)	b ($l \text{ mol}^{-1}$)	c_1	ε ($\text{bar } l \text{ mol}^{-1}$)	$\beta \cdot 10^3$
Methanol ⁵⁸	4.053	0.03098	0.4310	245.91	16.1
MEG ⁶⁶	10.819	0.05140	0.6744	197.52	14.1
Water ⁵⁸	1.228	0.01452	0.6736	166.55	69.2

Table 3.3: CPA Parameters for Inert Components Used in This Work.

Components	a_0 ($\text{bar } l^2 \text{ mol}^{-2}$)	b ($l \text{ mol}^{-1}$)	c_1
Propane ⁵²	9.118	0.05783	0.6307
n-Butane ⁵²	13.142	0.07208	0.7077
n-Heptane ⁵²	29.178	0.12535	0.9137
n-Nonane ⁸¹	41.252	0.16035	1.0462
n-Decane ⁵²	47.389	0.17865	1.1324
Undecane ⁸¹	55.220	0.19791	1.1437
Benzene ⁵²	17.876	0.07499	0.7576
Toluene ⁵²	23.375	0.09214	0.8037
Ethylbenzene ⁷⁷	28.860	0.10872	0.8539
Propylbenzene ⁸¹	34.821	0.12685	0.9117
Butylbenzene ⁸¹	41.294	0.14440	0.9618
Pentylbenzene ⁸¹	48.415	0.16167	0.9795
Hexylbenzene ⁸¹	55.322	0.18022	1.0436
m-Xylene ⁷⁷	29.086	0.10872	0.8681
o-Xylene ⁸³	29.200	0.88000	0.1086
p-Xylene ⁷⁷	29.317	0.10980	0.8625
iso-Propylbenzene ⁸³	33.800	0.12840	0.9700
1,3,5-Trimethylbenzene ⁸³	34.800	0.12500	0.9400

Table 3.4: Association Schemes Based on the Terminology of Huang and Radosz.⁵⁰

Species	Formula	Type	Site fractions (X)
Alcohol		3B	$X^A = X^B; X^C = 2X^A - 1$ $X_1 = X^A X^B X^C$
			
Glycols		4C	$X^A = X^B = X^C = X^D$ $X_1 = X^A X^B X^C X^D$
Water		4C	$X^A = X^B = X^C = X^D$ $X_1 = X^A X^B X^C X^D$
		3B	$X^A = X^B; X^C = 2X^A - 1$ $X_1 = X^A X^B X^C$
		3B	$X^A = X^B; X^C = 2X^A - 1$ $X_1 = X^A X^B X^C$

3.3 Heptane Plus Characterization

To perform phase equilibrium calculations for a reservoir fluid using cubic equations of state, the critical temperature (T_c), the critical pressure (P_c), and the acentric factor (ω) are required for each component in the mixture. In addition, a binary interaction parameter (k_{ij}) may also be needed for each pair of components. Naturally occurring oil or condensate mixtures may contain thousands of different components. Such high numbers are impractical to handle in phase equilibrium calculations. Some components therefore must be lumped together and represented as pseudocomponents. C_{7+} characterization consists of representing

the hydrocarbons with seven and more carbon atoms (the heptane plus or C_{7+} fraction) as a convenient number of pseudo components and finding the necessary EoS parameters (T_c , P_c , ω) for each of the pseudo components.¹⁴

To characterize the C_{7+} fraction in reservoir fluids, two methods are often used: the method proposed by Pedersen et al.^{84,79} and that by Whitson et al.⁸⁵ Both methods share three common steps:

- i. Determination of the detailed molar composition in the C_{7+} fraction
- ii. Estimation of EoS parameters (T_c , P_c , ω)
- iii. Lumping of detailed C_{7+} fractions into a few pseudo components

Yan et al. proposed the modified correlations for the second step and details of the development can be found elsewhere.^{16,14} A two step perturbation method is used in order to develop correlations for the modified critical temperature (T_{cm}), critical pressure (P_{cm}) and acentric factor (ω_m) to use in the CPA. Perturbation expansion correlations were developed by Twu⁸⁶, which initially correlate the properties of normal paraffins as the reference, and then extend these correlations to petroleum fractions:

$$T_{cm0} = \frac{(1885.45947 + 0.222337924T_b)T_b}{950.853406 + T_b} \quad 3.19$$

$$\ln P_{cm0} = -4.05282558 \times 10^{-12} T_b^4 + 8.76125776 \times 10^{-9} T_b^3 - 7.4578304 \times 10^{-6} T_b^2 - 1.09972989 \times 10^{-4} T_b + 4.16059295 \quad 3.20$$

$$\omega_{m0} = \exp\left(\frac{-2553.0653 + 3.68418T_b}{608.7226 + T_b}\right) \quad 3.21$$

In the above equations, T_b and T_{cm0} are in Kelvin (K), and P_{cm0} is in bar. The subscript 0 refers to the properties of n-alkanes. Soave's correlation⁸⁷ is used to calculate the specific gravity for n-alkanes:

$$SG_0 = (1.8T_b)^{1/3} (11.7372 + 3.336 \times 10^{-3} T_b - 976.3T_b^{-1} + 3.257 \times 10^5 T_b^{-2})^{-1} \quad 3.22$$

For the perturbation step, ΔSG is used to account for the aromaticity of the fraction. Aromatic compounds generally have higher densities than normal alkanes at the same T_b . And as a

general trend, the larger ΔSG is, the higher are the differences between T_{cm} and T_{cm0} , and between P_{cm} and P_{cm0} . The final equations proposed by Yan et al.¹⁶ are:

$$\frac{T_{cm}}{T_{cm0}} = \frac{(1 - 12.0690795\Delta SG + 22.8626562\Delta SG^2 + 89.7115818\Delta SG^3)}{(1 - 12.6311386\Delta SG + 30.6779472\Delta SG^2 + 62.4698965\Delta SG^3)} \quad 3.23$$

$$\ln(P_{cm} / P_{cm0}) = \Delta SG[-677.989269 + (76624.406 - 29811.8749 / SG)\Delta SG] / (1 + 10949.2202\Delta SG + 28099.1573\Delta SG^2) \quad 3.24$$

The CPA acentric factor ω_m is not treated as a free parameter. Instead, it is back calculated by matching the T_b of the fraction. The direct vapor pressure calculation procedure proposed by Soave⁸⁴ can be used which does not need any iteration. Equation 3.21 is used only if T_b exceeds T_c for very heavy compounds.

Modeling of Complex Well-Defined Systems

4.1 Introduction

Methanol injection is an important technique for inhibiting gas hydrate formation. It makes hydrate formation thermodynamically impossible under certain conditions. However, it is often injected at higher rate than is actually necessary due to uncertainties in determining the actual requirement. It is required to keep methanol injection minimum for economical operation of the production facility and environmental aspects.⁸⁸ The cost of providing methanol, especially on offshore platforms is very high and it is a toxic substance. The current trend for gas industry is to use monoethylene glycol (MEG) over methanol for new developments. MEG has the advantage that it can be effectively recovered, regenerated and recycled.^{89,90} The operation engineers should be able to accurately calculate the injection rates of methanol and MEG needed for hydrate suspension within acceptable or desirable margins. But different commercial design programs appear to give rather different predictions of the necessary injection rate.⁸⁸ This is partly due to the reason that modeling the partitioning of methanol and MEG between gas, water and condensate (or oil) phases is a difficult task. This implies that if the partitioning calculation is in error, the overall injection rate will also be in error.⁸⁸ Therefore accurate knowledge of phase behavior of aqueous solution of methanol/MEG and hydrocarbon is crucial for safe and economical design/operation of pipelines and production/processing facilities.⁹⁰ Furthermore for modeling of mutual solubility of hydrate inhibitor, reservoir-fluid and water, accurate representation of the mutual solubility of well-defined hydrocarbon (alkane/aromatic-hydrocarbons) and water is necessary. In this way, we also obtain binary interaction parameters needed for multicomponent calculations.

Traditional thermodynamic models such as cubic equations of state perform well for vapor-liquid equilibria but are less satisfactory for liquid-liquid equilibria (LLE) and vapor-liquid-liquid equilibria (VLLE), especially for multicomponent mixtures. The same is true for activity coefficient models such as UNIFAC which can often be used for preliminary design purposes.

Advanced thermodynamic models like CPA are to some extent capable of solving such problems by explicitly accounting for association.⁹¹

In this chapter CPA has been applied to binary LLE of alkane + water and heavy aromatic + water and VLE of methane + methanol systems. Then it has been applied to a multicomponent mixture of light hydrocarbons such as methane, ethane and n-butane in presence of water and methanol/MEG over a range of temperature and pressure. Finally CPA has been applied to VLLE of a synthetic condensate, water and methanol/MEG. The synthetic condensate is a mixture (MIX-2) of methane, ethane, propane, n-butane, n-heptane, toluene and n-decane.

In this chapter methanol has been treated as two-site (2B) molecule whereas water and MEG have been treated as four site molecules (4C) according to the terminology employed in SAFT by Huang and Radosz.⁵⁰ As described in chapter 3 aromatic hydrocarbons have the ability to solvate with associating compounds (e.g. water or MEG). The solvation has been accounted for by employing the modified CR-1 combining rule in the association part of CPA. Here cross-association volume is fitted to the experimental data whereas the cross-association energy parameter is equal to half of the value of the associating compound (water, methanol, MEG etc) as given in equation 4.1:

$$\varepsilon^{A_i B_j} = \frac{\varepsilon_{\text{associating}}}{2} \quad 4.1$$

The average absolute deviation (AAD) between experimental and calculated results is calculated using the relation given in equation 4.2.

$$\%AAD = \frac{1}{NP} \sum_{i=1}^{NP} \left| \frac{x_i^{\text{exp.}} - x_i^{\text{cal.}}}{x_i^{\text{exp.}}} \right| \times 100 \quad 4.2$$

where $x_i^{\text{exp.}}$ and $x_i^{\text{cal.}}$ are experimental and calculated mole fractions respectively and NP is number of points involved in the calculation.

4.2 Results and Discussion

4.2.1 LLE of n-Nonane and Water

It has been shown in the previous work¹⁴ that CPA can satisfactorily correlate the water-alkane LLE and VLLE using a single temperature independent interaction parameter.⁷⁷ The experimental data show that the solubility of hydrocarbon in water is order of magnitude lower than that of the solubility of water in alkanes.⁹² The classical cubic equations of state fail to

describe these solubilities.¹⁴ CPA can satisfactorily correlate these solubilities at room temperature except for the minimum in the solubility which could not be described.^{14,77} Furthermore using data from light hydrocarbons (propane) to n-decane with water a generalized correlation for the binary interaction parameters as a function of carbon number has been developed.^{77,10} This correlation can satisfactorily predict the phase equilibria of water + n-alkanes systems. The modeling results are superior to a variety of SAFT variants and the Elliott-Suresh-Donohue EoS.^{77,10} But the generalized correlation has not been applied to LLE of n-nonane and water. In this work the mutual solubility of n-nonane and water is predicted using CPA EoS and the result are shown in Figure 4.1 and Table 4.2. The modeling results can be improved using a binary interaction parameter ($k_{ij}=-0.03$) fitted to n-nonane solubility in water instead of using generalized correlation and the % AAD for solubility of n-nonane in MEG decreases from 49 to 3.

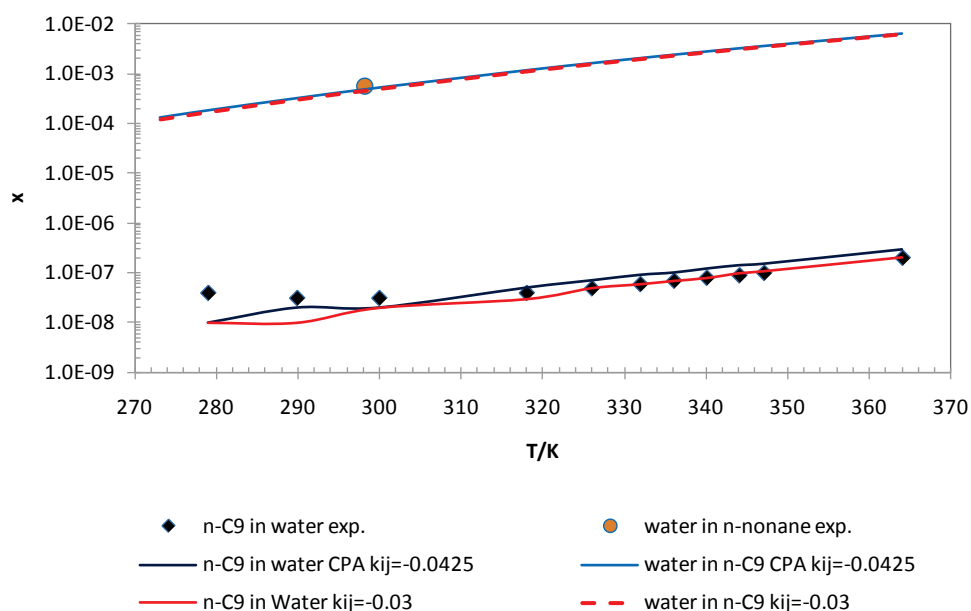


Figure 4.1: Mutual solubility (in mole fraction, x) of n-nonane and water as a function of temperature (K) for the n-nonane + water system. The experimental data^{93,94} are indicated as points and the CPA calculations as lines. The $k_{ij}=-0.0425$ is obtained from generalized correlation as function of carbon number as given in Table 4.2 and $k_{ij}=-0.03$ fitted to n-nonane solubility in water.

4.2.2 LLE of Undecane and Water

Similarly the solubility of undecane ($n\text{-C}_{11}$) in water is satisfactorily predicted using $k_{ij}=-0.0945$ from the correlation given in Table 4.2. The solubility of undecane in water is available only at 298 K and is very low (5.07×10^{-10} mole fraction) and therefore can be ignored for modeling. The calculations in Table 4.1 show that the generalized correlation given in Table 4.2 can be used up

to undecane. This can be useful for application of CPA to heavy aromatics and water system using homomorph approach. In this approach k_{ij} from n-alkanes are used for aromatic hydrocarbons with the same carbon number.

Table 4.1: Solubility of Water in Undecane, Experimental Data⁹² and CPA Calculations.

T/K	Exp.	CPA
298.00	600	587
313.20	1130	1147

Table 4.2: % AAD Between Experimental and Calculated Water Solubilities in the Hydrocarbon Phase and Hydrocarbon Solubilities in the Aqueous Phase Using the Generalized Expression for the Interaction Parameter $k_{12} = -0.02(\text{carbon number}) + 0.1915$.⁷⁷

Compounds	T/K	k_{12}	% AAD for Water in HC	% AAD for HC in Water	% AAD for Water in Vapor Phase
propane	278 - 366	0.1135	3.4	35.9	4.1
butane	310 - 420	0.0875	11.7	26.5	9.5
n-pentane	280 - 420	0.0615	13.4	28.4	-
n-hexane	280 - 473	0.0355	11.9	31.1	-
n-heptane	280 - 420	0.0095	11.5	63.3	-
n-octane	310 - 550	0.0165	9.7	44.1	1.9
n-nonane	273-364	0.0425	15.1	49.2	- this work
n-decane	290 - 566	0.0685	8.2	264	-

4.2.3 LLE of Heavy Aromatic Hydrocarbons and Water

The experimental data for liquid-liquid equilibrium of hydrocarbons and water have been evaluated and presented in a series of publications.^{93,95-98} The aromatic hydrocarbons have higher solubility (in water) as compared to paraffinic and naphthenic hydrocarbons with the same number of carbon atoms. This increased solubility is attributed to the solvation between water and aromatic hydrocarbons. The aromatic hydrocarbons are non-self-associating but there is a possibility of cross-association (solvation). For modeling of such mixtures using the CPA EoS, a solvation scheme is employed involving combining rules for the cross-associating energy and volume parameters. Using this approach the cross-association volume is fitted to the binary experimental data whereas binary interaction parameters (k_{ij}) are obtained from 'homomorph' alkanes (e.g. the k_{ij} for water and toluene are taken from n-heptane + water system). As a result only the cross-association volume is fitted to the data. In order to further improve the modeling results both the binary interaction parameter (k_{ij}) and the cross-association volume ($\beta^{A_i B_j}$) can be fitted to experimental data but in this way two adjustable parameters are used.

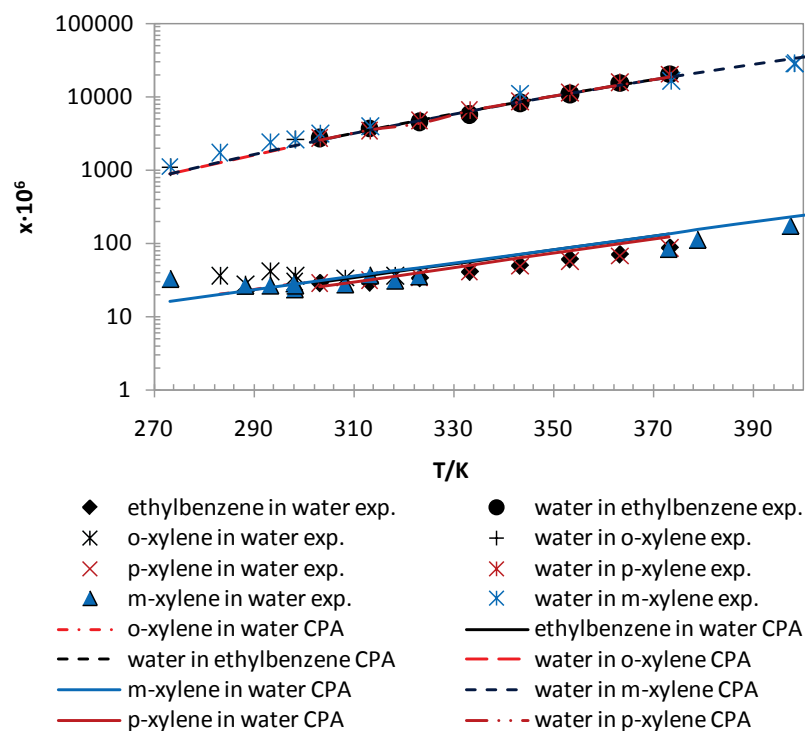


Figure 4.2: Mutual solubilities (in mole fraction, x) of alkylbenzene and water for ethylbenzene + water, o-xylene + water, m-xylene + water and p-xylene + water systems. The experimental data^{93,99} are indicated as points and CPA calculations as lines.

Modeling results for the mutual solubility of aromatic hydrocarbons and water are shown in Figures 4.2 and 4.3. The binary interaction parameters and cross-association volume used for a given temperature range with corresponding % AAD are given in Table 4.3. The mutual solubility of ethylbenzene + water and xylenes + water lies in the same range and they are correlated satisfactorily with the CPA EoS as shown in Figure 4.2.

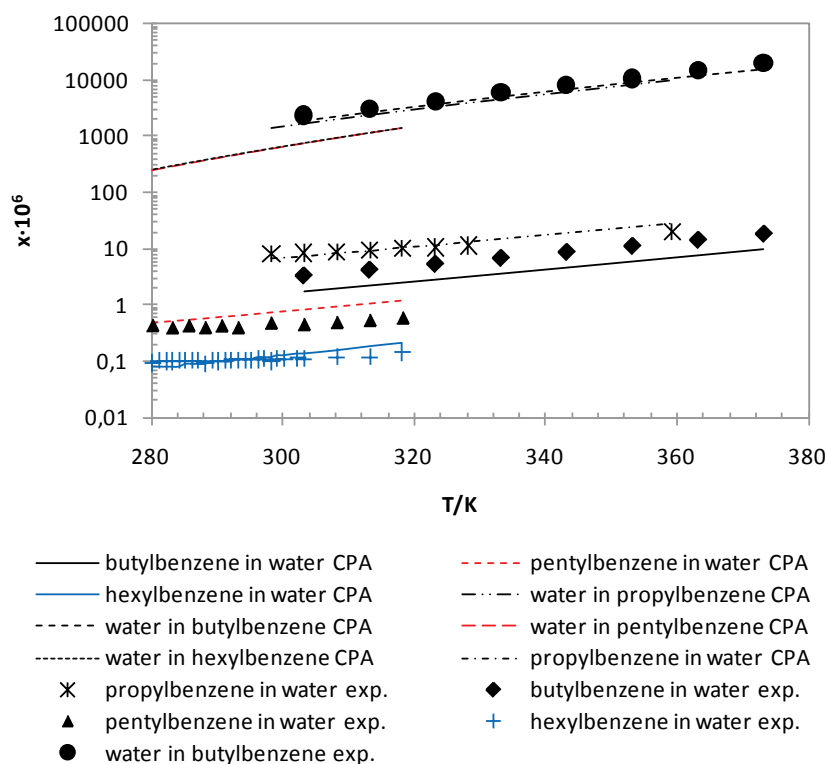


Figure 4.3: Mutual solubilities (in mole fraction, x) of alkylbenzene and water for propylbenzene + water, butylbenzene + water, pentylbenzene + water and hexylbenzene + water systems. The experimental data⁹³ are indicated as points and CPA calculations as lines.

The mutual solubility of propylbenzene to hexylbenzene and water is presented in Figure 4.3. The solubility of alkylbenzene decreases with increasing carbon number therefore the solubility of propylbenzene in water is the highest and that of hexylbenzene in water is the lowest among those presented in Figure 4.3. The CPA EoS can represent this trend satisfactorily. The cross-association volume parameter for propylbenzene, pentylbenzene and hexylbenzene are optimized on the basis of the solubility of aromatic hydrocarbons in water as the data are not available for the solubility of water in the hydrocarbon phase. The modeling of mutual solubility of alkylbenzene and water has been carried out by Oliveira et al.¹⁰ It appears that they took the water solubility values from a correlation proposed by Goral et al.⁹³ and considered it as pseudo-experimental data. The generalized correlation for k_{ij} given in Table 4.2 is applicable up to n-decane whereas the carbon numbers of pentylbenzene and hexylbenzene is higher. Therefore the k_{ij} obtained for undecane is used for both pentylbenzene + water and hexylbenzene water systems as shown in Table 4.3.

It has been observed that solubility of water in aromatic hydrocarbon is fairly constant (lie in the same range of mole fraction) for available data as shown in appendices C. 3 and C. 4. If it is

assumed that solubility of pentylbenzene and hexylbenzene will also follow this trend (i.e. overlap the solubility of water in butylbenzene). Then to capture the solubility of water in pentylbenzene and hexylbenzene non-zero cross association volume will be required. As result higher deviations for solubility of pentylbenzene and hexylbenzene in water will be obtained as shown in appendices C. 1 and C. 2.

Table 4.3: % AAD Between Experimental and Calculated Mutual Solubilities for Alkylbenzene and Water Using the Generalized Correlation⁷⁷ for Binary Interaction Parameters.

Compounds	T / K	β_{cross}	k_{ij}	% AAD for HC in water	% AAD for water in HC
ethylbenzene	303.15-373.15	0.051 ⁷⁷	-0.0165	36	6
m-xylene	273.20-543.80	0.050	-0.0165	22	21
o-xylene	273.20-318.20	0.050	-0.0165	22	18
p-xylene	303.15-373.15	0.050	-0.0165	25	6
iso-propylbenzene	273.20-353.40	0.050	-0.0425	26	5
1,3,5-trimethylbenzene	288.20-373.20	0.040	-0.0425	71	9
propylbenzene	298.10-359.00	0.030	-0.0425	15	---
butylbenzene	303.00-373.00	0.030	-0.0685	76	15
pentylbenzene	280.20-318.20	0.000	-0.0945	66	---
hexylbenzene	278.20-318.20	0.000	-0.0945	17	---

4.2.4 VLE of Methane and Methanol System

In the binary mixture of methane + methanol, methanol is self-associating and methane is an inert compound. Therefore the binary interaction parameter (k_{ij}) is the only adjustable parameter required for modeling using CPA and no combining rule is required for the association energy and volume. Figure 4.4 shows modeling results for the methanol content in vapor phase of the methane + methanol system for a range of temperatures (283.15-348.15 K) and pressures (20-200 bar). It can be seen from Figure 4.4 that CPA can describe satisfactorily the methanol content in the vapor phase using a single temperature independent $k_{ij}=0.01$ between methane and methanol. The % AAD between experimental and calculated results are presented in Table 4.4 which shows that the maximum deviation of 8% is obtained with temperature independent $k_{ij}=0.01$. Furthermore the effect of a temperature dependent k_{ij} has also been investigated which shows that the similar results are obtained. Haghighi et al.⁸⁹ proposed a higher value of binary interaction parameter ($k_{ij}=0.04869$). It has been shown in Table 4.4 that the use of a relatively high binary interaction parameter does not influence significantly the calculated methanol content in methane.

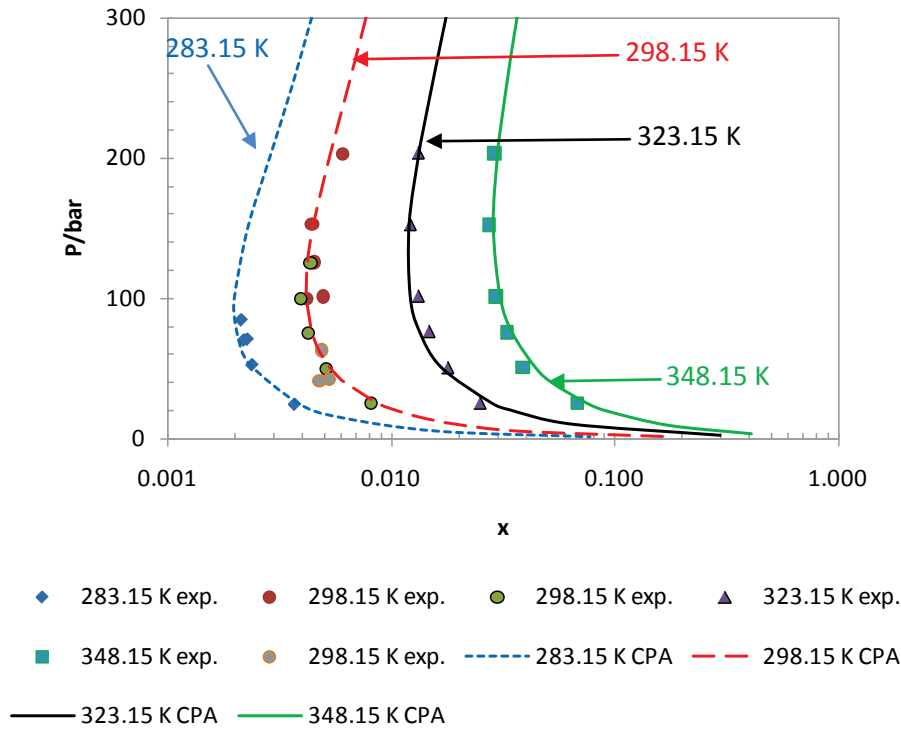


Figure 4.4: Experimental and calculated methanol content in gas phase of methane + methanol system using the CPA equation of state with $k_{ij}=0.01$. The experimental data⁸⁹ are indicated as points and the CPA calculations as lines.

Table 4.4: % AAD Between Experimental⁸⁹ and Calculated Methanol Content in Gas Phase of Methane + Methanol System and Binary Interaction Parameters (k_{ij}) Used. The $k_{ij}=0.01$ from Hemptinne¹⁰⁰ and $k_{ij}=0.0482$ from Haghighi et al.⁸⁹ and Temperature Dependent k_{ij} from This Work.

T/K	P/bar	k_{ij}	% AAD	k_{ij}	% AAD	k_{ij}	% AAD
283.15	24.74 – 84.37	0.018	5.93	0.010	5.56	0.0487	7.38
298.15	25.35 – 203.25	0.017	6.58	0.010	6.37	0.0487	7.48
323.15	25.44 – 203.31	0.016	6.17	0.010	6.11	0.0487	8.67
348.15	25.52 – 203.37	0.016	7.30	0.010	7.73	0.0487	5.74
Average			6.50		6.44		7.32

More experimental data for methane + methanol systems are available at extended temperature and pressure range. The modeling results are shown in Figures 4.5 and 4.6 whereas the % AAD between experimental and calculated results is given in Tables 4.5 and 4.6. Overall satisfactory modeling results are obtained for the methane content in liquid phase using a single temperature independent $k_{ij}=0.01$ as shown in Table 4.5. But relatively higher deviations are observed at lower temperature range (200–250 K). In order to further improve the results temperature dependent binary interaction parameter are used and a correlation is

obtained as a function of temperature as given in Figure 4.5. As a result a slight improvement in the results is obtained (see Table 4.5). Once again superior modeling results are obtained using $k_{ij}=0.01$ compared to the higher value of $k_{ij}=0.0487$ used by Haghighi et al.⁸⁹

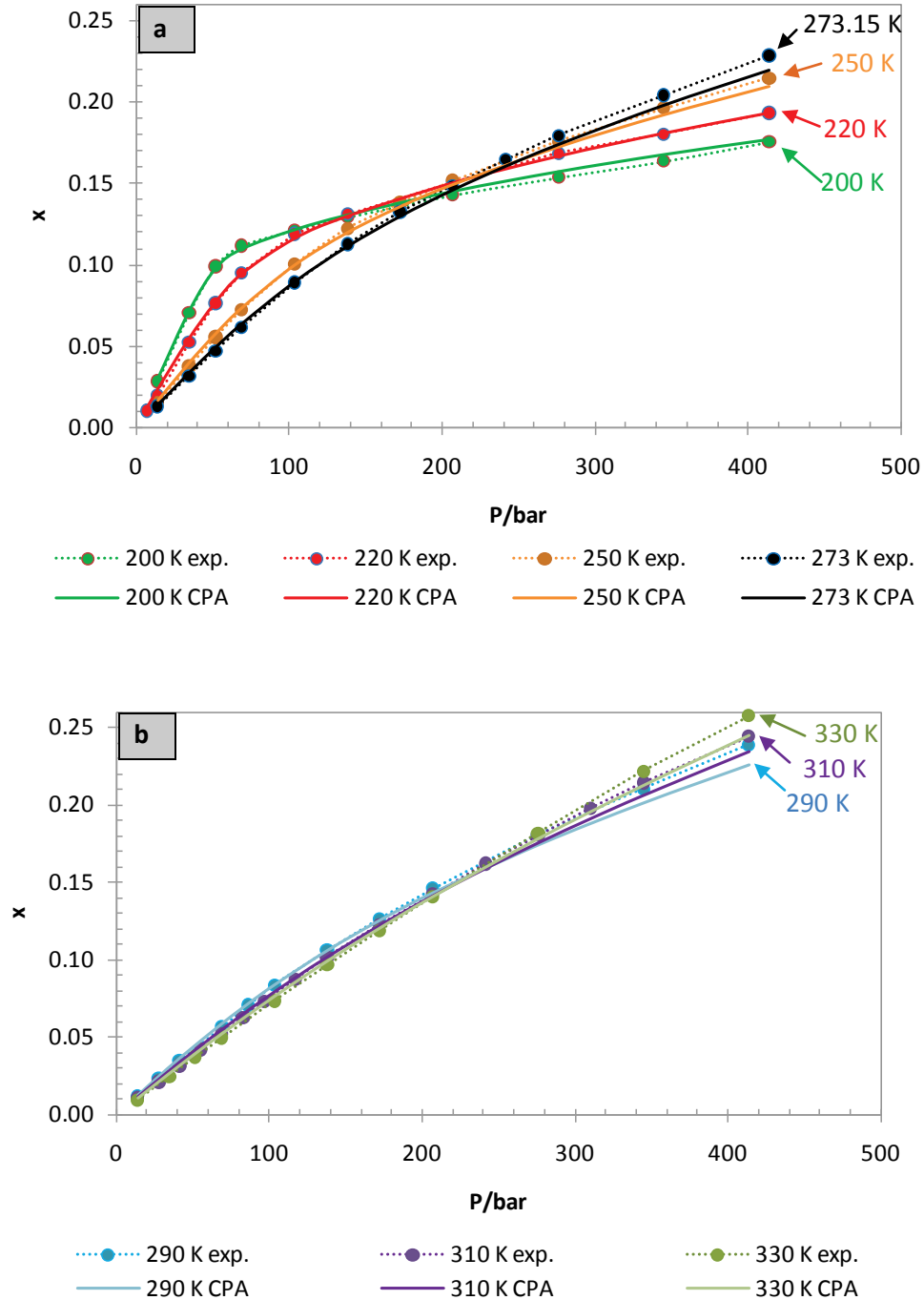


Figure 4.5: Methane content (in mole fraction, x) of liquid phase of methane + methanol system as a function of temperature (K) and pressure (bar). (a) For temperatures 200-273 K (b) For temperatures 290-330 K. The experimental data¹⁰¹ are indicated as points and CPA calculations as lines. The binary interaction parameters (k_{ij}) are obtained from a generalized correlation (from this work) $k_{ij}=5.77/(T-0.001788)$ as a function of temperature (K).

Table 4.5: % AAD Between Experimental⁸⁹ and Calculated Solubility of Methane in Methanol in the Methane + Methanol System and Binary Interaction Parameters (k_{ij}) Used.

T/K	P/bar	k_{ij}	% AAD	k_{ij}	% AAD	k_{ij}	% AAD
200	13.789 - 413.685	0.027	2.04	0.010	21.66	0.0487	19.25
220	6.895 - 413.685	0.024	3.34	0.010	15.71	0.0487	17.44
250	13.789 - 413.685	0.021	2.74	0.010	8.62	0.0487	17.30
273	13.789 - 413.685	0.019	3.15	0.010	5.80	0.0487	16.17
290	13.789 - 413.685	0.018	3.52	0.010	5.36	0.0487	14.26
310	13.789 - 413.685	0.017	3.59	0.010	4.80	0.0487	12.64
330	13.789 - 413.685	0.016	4.15	0.010	5.30	0.0487	10.99
Average			3.22		9.61		15.44

Figure 4.6 presents the methanol content in vapor phase of methane + methanol system. Satisfactory modeling results are obtained at lower pressures. At higher pressure CPA under predicts the methanol content. The deviation increases with decreasing temperature as shown in Figure 4.6 and Table 4.6. The performance of all three kinds of interaction parameters (0.01, 0.0487 and temperature dependent as given in Table 4.6) is very similar.

The deviations are partially due to the reason that the experimental data related to the methanol content in gase phase is often associated with errors as a review of data sets measured at the same temperature and pressure conditions indicated. Furthermore such data are very difficult to measure.⁸⁹

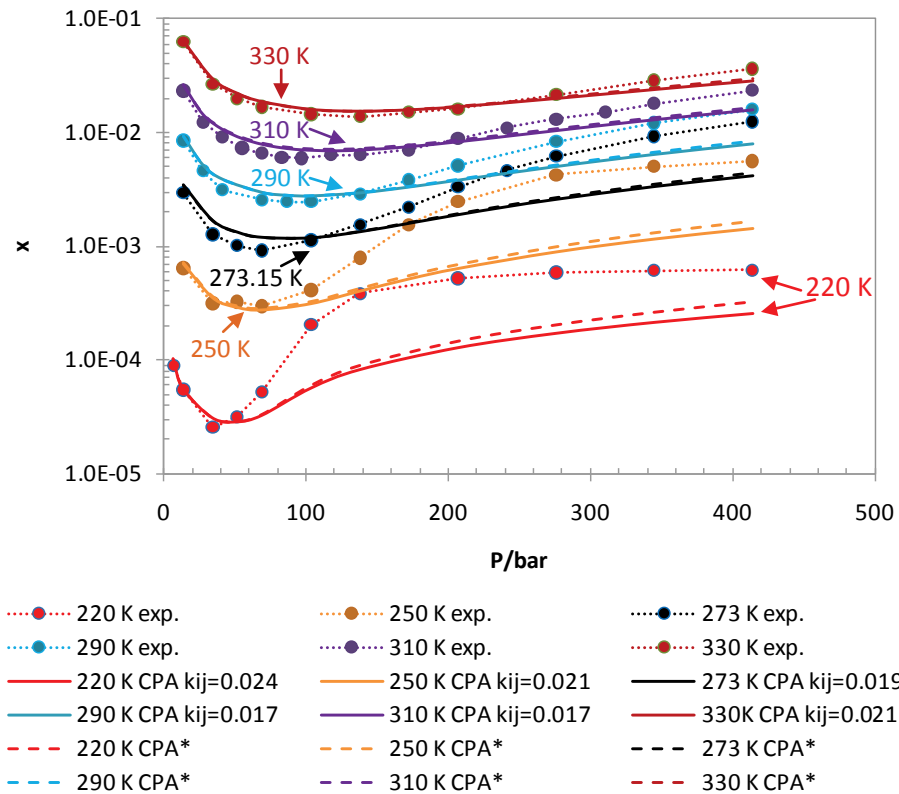


Figure 4.6: Methanol content (in mole fraction, x) of vapor phase of methane + methanol system as a function of temperature (K) and pressure (bar). The experimental data¹⁰¹ are indicated as points and CPA calculations as lines. The binary interaction parameters (k_{ij}) are obtained from a generalized correlation $k_{ij}=5.77/(T-0.001788)$ as a function of temperature (K) and $*k_{ij}=0.01$.

Table 4.6: % AAD Between Experimental¹⁰¹ and Calculated Methanol Content in Gas Phase of Methane + Methanol System and Binary Interaction Parameters (k_{ij}) Used.

T/K	P/bar	k_{ij}	% AAD	k_{ij}	% AAD	k_{ij}	% AAD
220	6.895 - 413.685	0.024	45.83	0.010	43.01	0.0487	49.66
250	13.789 - 413.685	0.021	43.64	0.010	42.28	0.0487	46.68
273	13.789 - 413.685	0.019	36.65	0.010	35.72	0.0487	39.39
290	13.789 - 413.685	0.018	22.17	0.010	21.62	0.0487	24.50
310	13.789 - 413.685	0.017	17.46	0.010	17.35	0.0487	19.16
330	13.789 - 413.685	0.016	9.81	0.010	9.64	0.0487	10.93
Average			29.26		28.27		31.72

4.2.5 Modeling of MIX-1

The composition of mixture-1 (MIX-1) is given in Table 4.7. Thermodynamic modeling of water and inhibitor (i.e. MEG, methanol) content in gas phase is carried out. More specifically the VLE of the following systems is investigated.

- MIX-1 + Water
- MIX-1 + Water + Methanol
- MIX-1 + Water + MEG

Table 4.7: Composition of MIX-1 (in Mole Fraction, x).¹⁰²

Components	x
Methane	0.94
Ethane	0.04
n-Butane	0.02

4.2.5.1 VLE of the MIX-1 + Water System

The modeling results are presented in Figure 4.7 as a function of temperature (268.15-313.14 K) and pressure (1-348 bar). It can be seen that CPA can accurately predict the water content in the gas phase of MIX-1 + water over a wide range of pressure and temperature. These results are pure predictions as no binary interaction parameters are fitted to the experimental data. The modeling results are in excellent agreement with experimental data for temperatures 283-313 K whereas at lower temperature a slight over prediction is observed. But overall satisfactory results are obtained with % AAD of 9.4 from the experimental data. These results are within the range of reported experimental uncertainty of 12%.¹⁰²

The effect of using temperature dependent k_{ij} is also investigated but no improvement has been observed and the % AAD increases from 9.4 to 16. This is consistent with the earlier investigations by Yan et al.¹⁶ as shown in Table 4.8. Here it has been shown that for mutual solubility of light hydrocarbon (i.e. methane) and water the use of temperature dependent k_{ij} improves the calculations of solubility of light hydrocarbons in water whereas the % AAD for the water content in the gas phase slightly increases.

A comparison for the calculated water content in the gas phase is also made between the CPA and HWHYD¹⁰² as given in Figure 4.7. It is shown that the CPA predictions are superior to HWHYD for a temperature range of 298-313 K whereas at lower temperatures it is reported that HWHYD fails to describe water content. The modeling results for HWHYD are taken from the literature.¹⁰²

HWHYD is an in house thermodynamic model developed at Center for Gas Hydrate Research, Heriot-Watt University, Edinburgh.¹⁰³ The model is based on uniformity of the fugacity of each component throughout all the phases^{104,105} and used to model the gas solubility, water content

and hydrate dissociation conditions. In this model, the VPT-EoS¹⁰⁶ with the NDD¹⁰⁷ mixing rules are employed in calculating fugacities in fluid phases.

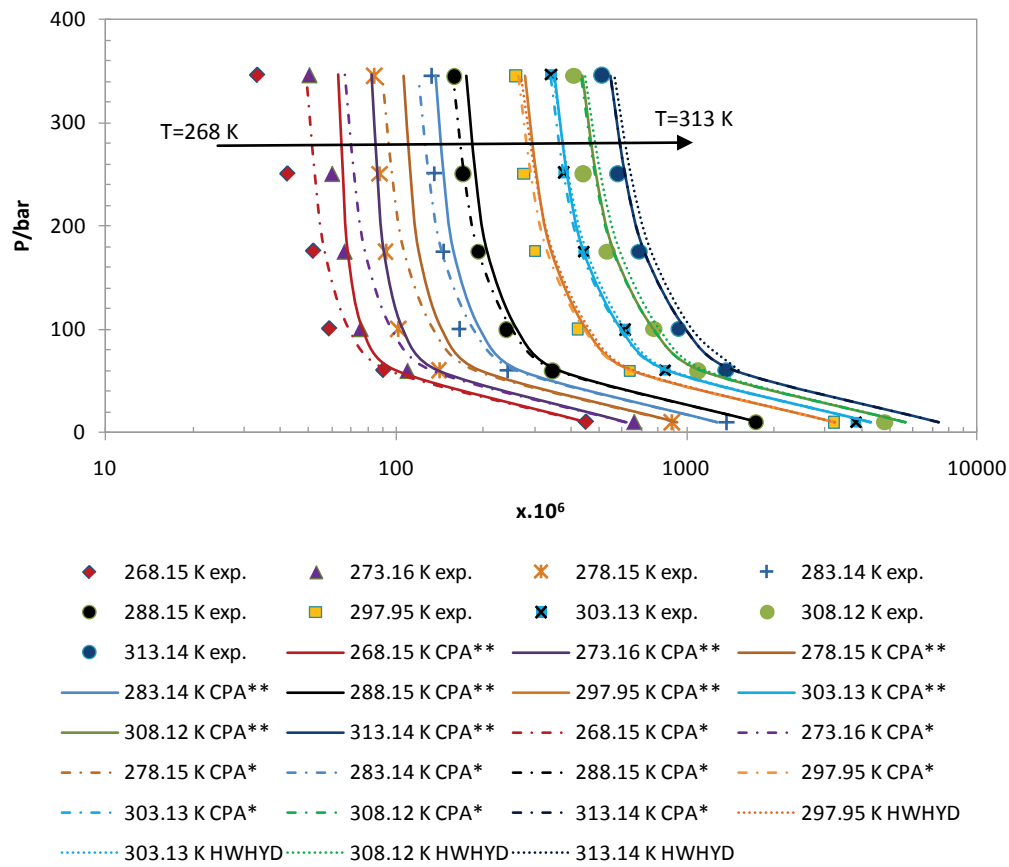


Figure 4.7: Water content (mole fraction, x) of the gas phase of MIX-1 + water system as a function of temperature (K) and pressure (bar). The experimental data¹⁰² are indicated as points and the calculations using the CPA (** k_{ij} =correlation given in Table 4.8 * $k_{ij}=0$) and HWHYD¹⁰² as lines.

Table 4.8: Temperature Dependent Binary Interaction Parameters Used for Water and Light-HC.¹⁶

Components	k_{ij}	% AAD of Hydrocarbon Solubility in Water	% AAD of Water Solubility in Hydrocarbon
Methane	0	47	4.5
	$0.6769-213.5/T$	5.6	7.4
Ethane	0	118	9.1
	$0.4497-127.2/T$	7.4	10.3
Propane	0	204	13.8
	$0.4809-130.5/T$	8.1	6.6
n-Butane	0	167	31.4
	$0.2828-73.73/T$	5.4	12.6
Average	$k_{ij}=0$	134	14.7
Average	$k_{ij}(T)$	6.6	9.2

4.2.5.2 VLE of the MIX-1 + Water + Methanol System

After MIX-1 + water, CPA is investigated for the VLE of MIX-1 + water + methanol for the temperature and pressure range of 268-298 K and 5-350 bar respectively. The compositions used for the equilibrium measurement of water and methanol content in gas phase are given in Table 4.9. In MIX-2 + Water + Methanol systems water and methanol cross-associate as well as self-associate whereas hydrocarbons are non-associating. The Elliott combining rule (ECR) is used for water and methanol. The binary interaction parameters used are given in Table 4.10. For hydrocarbons and water the temperature dependent k_{ij} values given in Table 4.8 are used (where mentioned).

The modeling results for the methanol content in gas phase of MIX-1 + Water + Methanol are shown in Figure 4.8. These results are solely based on a single binary interaction parameter between water and methanol whereas all other k_{ij} values are set equal to zero. The modeling results are quantitatively in the same range as experimental data with % AAD of 16.4. The % AAD is in the range of the reported experimental uncertainty of 15%.¹⁰² The qualitative trend of experimental and predicted methanol content in the gas phase deviates from the experimental data as shown in Figure 4.8. This deviation can be due to the reported experimental uncertainties as CPA trends for methanol content in vapor phase of methane + methanol system are consistent with data from other source shown in Figures 4.4 and 4.6. Furthermore, the trends of water content in the gas phase as a function of pressure shown by CPA are fairly consistent with that shown by the HWHYD model. Similar to the MIX-1 + Water system HWHYD is not capable of describing satisfactorily the methanol content (at lower temperature) as shown in Figure 4.8.

Investigations using non-zero binary interaction parameters between water-hydrocarbon and methanol-hydrocarbon show that the % AAD increases to 32 by using non-zero k_{ij} . Similar results (i.e. zero k_{ij} give better results) are obtained for the modeling of water content in vapor phase of MIX-1 + water system.

Table 4.9: Compositions (in Mole %) of MIX-1 + Water + Methanol System.¹⁰²

Component	Composition		
	Organic Phase	Polar Phase	Feed
Methanol	0	15.07	7.54
Water	0	84.93	42.46
Methane	94	0	47
Ethane	4	0	2
n-Butane	2	0	1

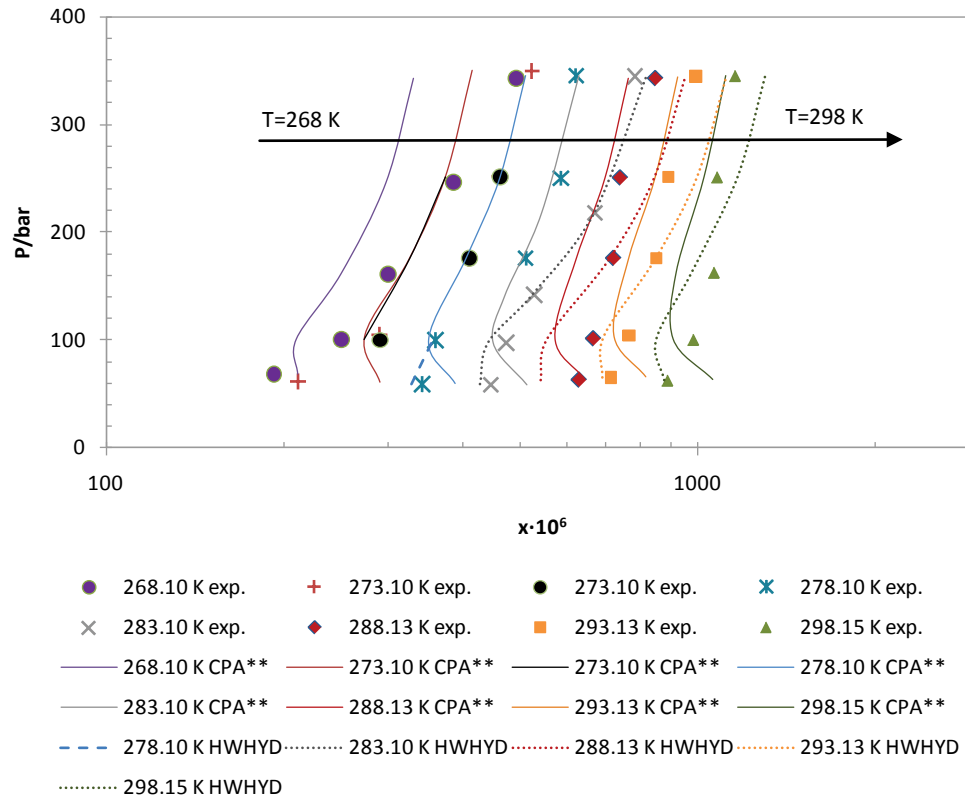


Figure 4.8: Methanol content (mole fraction, x) of the gas phase of MIX-1 + water + methanol system as a function of temperature (K) and pressure (bar). The experimental data¹⁰² are indicated as points and the calculations using the CPA (k_{ij} = HC-water from correlation in Table 4.8 and HC-Methanol from Table 4.10 * k_{ij} =0) and HWHYD¹⁰² as lines.**

In addition to the methanol content in the gas phase of MIX-1 + water + methanol systems, the experimental data for the water content in the gas phase is also available. The modeling results using the CPA EoS are given in Figure 4.9. The CPA prediction using a single temperature independent binary interaction parameter between methanol and water with ECR combining rule is in very good agreement with the experimental data. The % AAD between experimental and predicted water content is 18.91 a bit higher than experimental uncertainty of 12%.¹⁰² The deviation is mainly due to the values at lower temperatures (268 and 273 K). Using the non-zero binary interaction parameters given in Tables 4.8 and 4.10, an improvement in the results could not be obtained (% AAD 32.64) as shown in Figure 4.9. The modeling results of HWHYD are better than CPA at higher temperature whereas at lower temperature the model fails to correctly describe the water contents and the results are not reported (in the literature).¹⁰²

Table 4.10: Binary Interaction Parameters Used in the Calculations of MIX-1 + Water + Methanol System.

System	k_{ij}
Methanol-Water	-0.090 ⁷⁴
Methanol-Methane	0.010 ¹⁰⁰
Methanol-Ethane	0.020
Methanol-n-Butane	0.035 ⁸¹

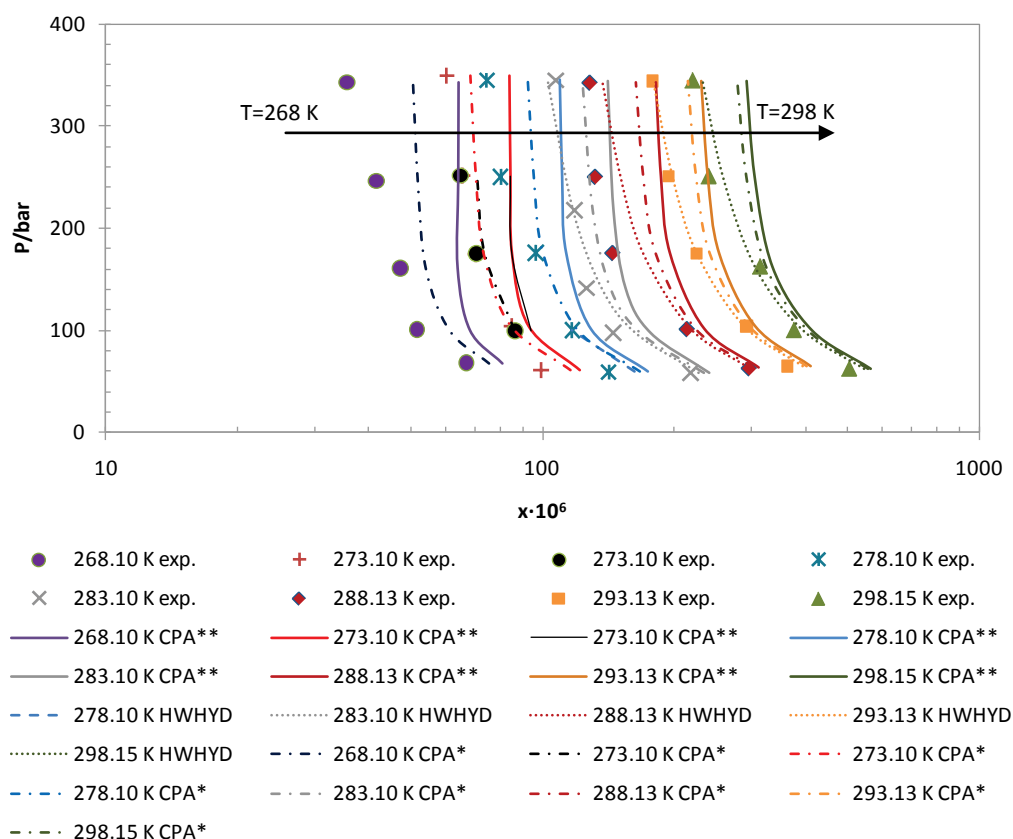


Figure 4.9: Water content (mole fraction, x) of the gas phase of MIX-1 + water + methanol systems as a function of temperature (K) and pressure (bar). The experimental data¹⁰² are indicated as points and the calculations using the CPA (k_{ij} = HC-water from correlation in Table 4.8 and HC-Methanol from Table 4.10 * k_{ij} =0) and HWHYD¹⁰² as lines.**

4.2.5.3 VLE of the MIX-1 + Water + MEG System

In this section CPA is investigated for water content in gas phase of MIX-1 + Water + MEG system. The feed as well as polar and organic phase compositions of the above system are given in Table 4.11. The modeling results are presented in Figure 4.10. It has been shown that CPA can predict satisfactorily water content using a single temperature independent $k_{ij}=-0.115$ between water and MEG using Elliott combining rule. All the other k_{ij} between water-hydrocarbon and MEG-hydrocarbon are set equal to zero. The modeling results are in good agreement (% AAD=15.07 against experimental uncertainty of 12%) with experimental data

except at lower temperature of 268.10 K. Calculations have also been made by using non-zero k_{ij} but the modeling results are inferior (% AAD=20.35) to those obtained using zero k_{ij} (except for MEG-water k_{ij}). The HWHYD model once again fails to describe satisfactorily the water content in gas phase of MIX-1 + Water + MEG at lower temperature as shown in Figure 4.10.

Table 4.11: Composition (in Mole %) of Components in MIX-1 + Water + MEG System.¹⁰²

Component	Organic Phase(MIX1)	Polar Phase	Feed
MEG	0	13	6.5
Water	0	87	43.5
Methane	94	0	47
Ethane	4	0	2
n-Butane	2	0	1

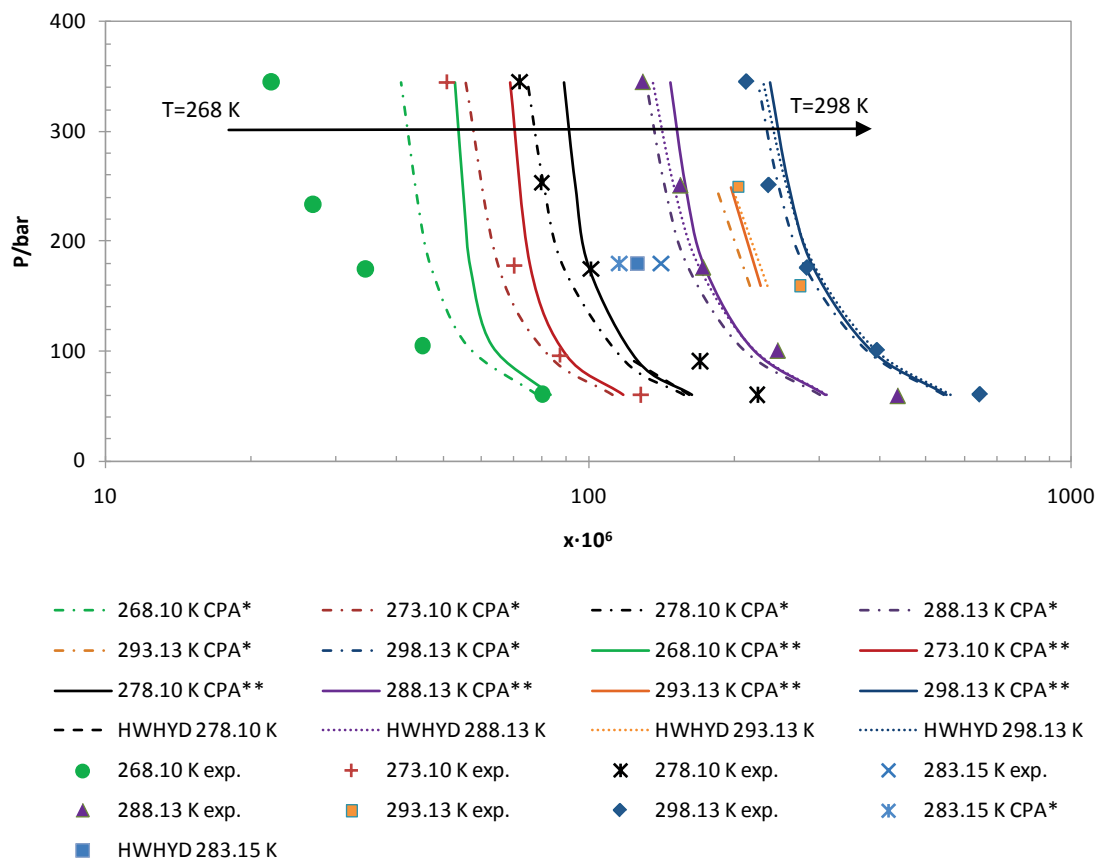


Figure 4.10: Water content (mole fraction, x) of the gas phase of MIX-1 + water + MEG system as a function of temperature (K) and pressure (bar). The experimental data¹⁰² are indicated as points and the calculations using the CPA (k_{ij} = correlation given in Tables 4.8 and 4.12 * k_{ij} =0) and HWHYD¹⁰² as lines.**

Table 4.12: Binary Interaction Parameters Used in the Calculations for the MIX-1 + Water + MEG System.

System	k_{ij}
MEG-HC	0.050 ¹⁶
MEG -Water	-0.115 ⁶⁷

4.2.6 Modeling of MIX-2

In this section modeling (for the composition in the vapor and organic phases) of mixture-2 (MIX-2) in presence of pure water, methanol + water and MEG + water is carried out using the CPA EoS. The composition of MIX-2 is given in Table 4.13 representing a synthetic condensate.

Table 4.13: Composition of MIX-2 (in Mole Fraction, x).¹⁰²

Component	x
Methane	0.195
Ethane	0.058
Propane	0.092
n-Butane	0.092
n-Heptane	0.138
Toluene	0.253
n-Decane	0.172

4.2.6.1 VLE of the MIX-2 + Water System

Experimental and predicted compositions of different species in the vapor and organic phases are given in Tables 4.15 and 4.16 respectively. In the MIX-2 + water system, water is an associating compound while all other compounds are non-associating. Therefore no combining rules are required except for toluene which is a solvating compound. The only adjustable parameter required is a binary interaction parameter (k_{ij}) between each water-hydrocarbon pair as given in Table 4.14. For toluene and water the cross-association volume is an additional parameter obtained from literature.⁷⁷

Table 4.14: Binary Interaction Parameters for Water-HC and Methanol-HC Systems.

Components	Water-HC		Methanol-HC	
	k_{ij}	$\beta^{A_i B_j}$	k_{ij}	$\beta^{A_i B_j}$
Methane	-0.1472 ¹⁶	---	0.0103 ¹⁰⁰	---
Ethane	-0.0421 ¹⁶	---	0.0204	---
Propane	-0.0237 ¹⁶	---	0.0261 ⁷⁴	---
n-Butane	-0.0023 ¹⁶	---	0.0352 ⁷⁴	---
n-Heptane	0.0095 ⁷⁷	---	0.0057 ^{71,74}	---
Toluene	0.0095 ⁷⁷	0.06 ⁷⁷	0.0348 ⁸¹	0.029 ⁷⁷
n-Decane	-0.0685 ⁷⁷	---	-0.0109 ^{71,74}	---

The modeling results for composition of various species in vapor phase of MIX-2 + water are in good agreement with experimental data at lower pressures (5.12 bar). At higher pressures there are deviations among predicted compositions and experimental data but they are correct in order of magnitude. These deviations could be partially justified by uncertainties in the experimental data.¹⁰² It has been reported that measurements in vapor phase showed scattering, mainly for heavier components and water.⁸⁹ An example of uncertainty in data is that for ethane content in vapor phase at 298 K and 20.40 bar is reported¹⁰² as 0.066 and 0.010 mole fraction (as shown in Table 4.15) giving two very different % AAD (18 and 455). As experimental measurements are easier and more reliable in organic phase, a good agreement is obtained between experimental data and the CPA calculations as shown in Table 4.16.

Table 4.15: Experimental¹⁰² and Calculated Compositions of the Different Species in the Vapor Phase (in Mole Fraction, y) of the MIX-2 + Water System at 298.1 K and Various Pressures. The Vapor Phase Compositions of Methane (y_{C1}), Ethane (y_{C2}), Water (y_w), Propane (y_{C3}), n-Butane (y_{C4}), n-Heptane (y_{C7}), Toluene (y_{Tol}) and n-Decane (y_{C10}) are Presented.

Results	y_{C1}	y_{C2}	$y_w \cdot 10^4$	y_{C3}	$y_{C4} \cdot 10^3$	$y_{C7} \cdot 10^3$	$y_{Tol} \cdot 10^4$	$y_{C10} \cdot 10^4$
T=298.10 K P=5.12 bar								
Exp.	0.636	0.143	59.820	0.147	60.56	33.120	41.700	1.290
CPA	0.645	0.151	63.032	0.137	54.55	28.503	36.432	1.145
% AD	1.4	5.5	5.4	6.8	9.8	13.9	12.6	4.6
T=298.10 K P=20.48 bar								
Exp.	0.816	0.087	19.23	0.066	23.73	14.74	18.55	0.67
CPA	0.825	0.100	16.12	0.054	17.21	9.552	12.09	0.47
% AD	1.1	14.5	16.00	17.8	27.4	35.0	34.7	21.7
T=298.10 K P=20.40 bar								
Exp.	0.81	0.09	19.95	0.010	24.24	15.76	21.04	0.58
CPA	0.822	0.101	16.61	0.056	17.616	9.71	12.30	0.47
% AD	1.4	12.5	16.74	455.4*	27.2	38.1	41.4	5.3
T=298.10 K P=35.43 bar								
Exp.	0.841	0.081	12.54	0.049	18.04	12.68	16.38	0.97
CPA	0.872	0.075	10.12	0.038	12.233	8.005	9.97	0.47
% AD	3.7	7.6	19.3	22.7	32.0	36.5	38.8	47.7
% AAD	1.9	10.0	14.36	15.63	24.1	30.9	31.9	19.8

Table 4.16: Experimental¹⁰² and Calculated Compositions of the Different Species in the Organic Phase (in Mole Fraction, x) of the MIX-2 + Water System at 298.1 K and Various Pressures. The organic Phase Compositions of Methane (x_{C1}), Ethane (x_{C2}), Water (x_w), Propane (x_{C3}), n-Butane (x_{C4}), n-Heptane (x_{C7}), Toluene (x_{Tol}) and n-Decane (x_{C10}) are presented.

Results	$x_{C1} \cdot 10^3$	$x_{C2} \cdot 10^3$	$x_w \cdot 10^4$	x_{C3}	x_{C4}	x_{C7}	x_{Tol}	x_{C10}
T=298.10 K P=4.74 bar								
Exp.	14.73	19.4	9.19	0.072	0.102	0.19	0.349	0.252
CPA	12.57	19.14	8.67	0.071	0.106	0.193	0.355	0.242
% AD	14.5	1.3	4.7	1.4	3.7	1.7	1.7	3.8
T=298.10 K P=19.35 bar								
Exp.	57.52	46.03	7.46	0.102	0.106	0.169	0.304	0.214
CPA	65.08	48.29	8.14	0.099	0.107	0.166	0.305	0.208
% AD	13.2	5.0	10.0	2.9	1.2	1.5	0.4	2.9
T=298.10 K P=33.54 bar								
Exp.	101.6	53.92	6.58	0.103	0.103	0.157	0.283	0.198
CPA	117.06	55.72	7.89	0.098	0.101	0.154	0.282	0.192
% AD	15.9	3.4	21.3	4.8	1.8	2.1	0.4	3.2
% AAD	14.5	3.2	12.0	3.0	2.2	1.8	0.8	3.3

4.2.6.2 VLE of the MIX-2 + Water + Methanol System

The CPA prediction for compositions of different species in the vapor and organic phases of MIX-2 + water + methanol system are given in Tables 4.17 and 4.18 respectively. The binary interaction parameters used for methanol-HC and water-HC are given in Table 4.14. The binary interaction parameter between water and methanol $k_{ij}=-0.090$ is used with the Elliott combining rule as in the previous case (i.e. MIX-1 + Water + Methanol). The modeling results are in good agreement with the experimental data for the compositions in organic phase. The higher deviations for water and methanol content in vapor phase are attributed to low temperature (i.e. 258 K) and experimental uncertainties as explained earlier.

Table 4.17: Experimental Data¹⁰² and CPA Calculations for Composition of Different Species in the Vapor Phase (in Mole Fraction, y) of the MIX-2 + Water + Methanol System at Various Temperatures and Pressures. The Vapor Phase Compositions of Methane (y_{C1}), Ethane (y_{C2}), Water (y_w), Propane (y_{C3}), n-Butane (y_{C4}), Methanol (y_{MeOH}), n-Heptane (y_{C7}), Toluene (y_{Tol}) and n-Decane (y_{C10}) are Presented.

Results	y_{C1}	y_{C2}	$y_w \cdot 10^4$	y_{C3}	y_{C4}	$y_{MeOH} \cdot 10^4$	$y_{C7} \cdot 10^4$	$y_{Tol} \cdot 10^4$	$y_{C10} \cdot 10^4$
T=258.64 K P=5.13 bar									
Exp.	0.7833	0.1281	1.50	0.070	0.017	6.00	3.00	4.00	--
CPA	0.7916	0.1277	3.75	0.064	0.015	11.50	2.80	3.39	0.046
% AD	1.1	0.3	150.3	9.1	13.5	91.8	6.8	15.2	---
T=258.63 K P=10.87 bar									
Exp.	0.8655	0.0884	0.80	0.036	0.009	4.00	2.00	2.00	---
CPA	0.8694	0.0874	1.83	0.035	0.008	5.75	1.56	1.88	0.028
% AD	0.5	1.1	128.3	4.9	15.1	43.8	21.8	5.8	---
T=258.67 K P=20.91 bar									
Exp.	0.9058	0.0625	---	0.025	0.006	2.00	2.00	2.00	---
CPA	0.9171	0.0569	1.01	0.021	0.005	3.32	1.14	1.35	0.025
% AD	1.3	8.9	---	17.4	22.6	66.2	42.9	32.4	---
T=258.63 K P=29.59 bar									
Exp.	0.9195	0.0515	---	0.023	0.005	3.00	3.00	3.00	ND
CPA	0.9345	0.0448	0.75	0.016	0.004	2.57	1.10	1.28	0.028
% AD	1.6	13.0	---	28.3	29.3	14.4	63.4	57.5	---
T=293.2 K P=5.60 bar									
Exp.	0.6330	0.1586	53.20	0.142	0.048	82.00	22.00	28.00	0.550
CPA	0.6693	0.1478	39.11	0.122	0.044	80.53	20.48	25.46	0.755
% AD	5.73	6.79	26.48	13.90	8.13	1.80	6.90	9.08	37.25
T= 293.20 K P=12.25 bar									
Exp.	0.7496	0.1291	26.00	0.088	0.026	26.00	12.00	15.00	0.340
CPA	0.7744	0.1214	18.37	0.073	0.023	38.97	10.66	13.21	0.429
% AD	3.3	6.0	29.3	16.6	11.0	49.9	11.2	12.0	26.2
T= 293.19 K P=20.03 bar									
Exp.	0.8154	0.1002	15.00	0.062	0.018	14.00	9.00	11.00	0.310
CPA	0.8314	0.0968	11.61	0.051	0.015	25.36	7.81	9.60	0.348
% AD	2.0	3.4	22.6	17.3	13.0	81.2	13.2	12.7	12.2
T= 293.19 K P=35.17 bar									
Exp.	0.8675	0.0728	11.00	0.043	0.013	14.00	8.00	11.00	0.870
CPA	0.8810	0.0702	7.07	0.034	0.011	16.33	6.48	7.82	0.351
% AD	1.6	3.6	35.8	19.6	15.1	16.7	19.0	28.9	59.6
T= 293.21 K P=35.05 bar									
Exp.	0.8680	0.0731	8.10	0.043	0.013	9.00	8.00	10.00	0.350
CPA	0.8807	0.0704	7.10	0.034	0.011	16.39	6.49	7.83	0.351
% AD	1.5	3.7	12.4	19.8	15.6	82.1	18.9	21.7	0.4
% AAD	2.1	5.2	57.9	16.3	15.9	49.7	22.7	21.7	15.1

Table 4.18: Experimental¹⁰² and Calculated Composition of Different Species in the Organic Phase (in Mole Fraction, x) of the MIX-2 + Water + Methanol System at Various Temperatures and Pressures. The organic Phase Compositions of Methane (x_{C1}), Ethane (x_{C2}), Water (x_w), Propane (x_{C3}), n-Butane (x_{C4}), Methanol (x_{MeOH}), n-Heptane (x_{C7}), Toluene (x_{Tol}) and n-Decane (x_{C10}) are presented.

Results	x_{C1}	x_{C2}	x_{H2O}	x_{C3}	x_{C4}	$x_{MeOH} \cdot 10^4$	x_{C7}	x_{Tol}	x_{C10}
T=258.51 K P=5.54 bar									
Exp.	0.0229	0.0399	2.1	0.1100	0.118	7.1	0.206	0.322	0.180
CPA	0.0254	0.0394	2.0	0.1006	0.115	9.7	0.177	0.319	0.221
% AD	10.9	1.3	6.0	8.5	2.7	36.3	14.0	1.0	22.6
T=293.23 K P=5.79 bar									
Exp.	0.0171	0.0265	8.7	0.0902	0.113	48.4	0.221	0.334	0.192
CPA	0.0168	0.0244	10.0	0.0806	0.110	70.8	0.188	0.338	0.234
% AD	1.6	7.8	14.6	10.6	2.7	46.4	15.1	1.1	22.1
T=293.23 K P=12.48 bar									
Exp.	0.0398	0.0424	7.5	0.1036	0.112	45.5	0.204	0.319	0.174
CPA	0.0416	0.0410	9.8	0.0963	0.110	34.8	0.174	0.312	0.216
% AD	4.4	3.3	30.3	7.1	1.1	23.5	14.9	2.1	24.4
T=293.25 K P=20.39 bar									
Exp.	0.0678	0.0511	6.5	0.1084	0.110	33.1	0.192	0.300	0.167
CPA	0.0719	0.0501	9.7	0.0992	0.107	22.7	0.164	0.295	0.204
% AD	6.0	1.9	48.7	8.5	2.8	31.3	14.5	1.7	22.4
T=293.25 K P=35.16 bar									
Exp.	0.1170	0.0561	6.7	0.1060	0.104	29.9	0.179	0.279	0.155
CPA	0.1275	0.0562	9.5	0.0968	0.100	14.9	0.151	0.272	0.188
% AD	8.94	0.26	42.08	8.65	3.70	50.33	15.55	2.59	21.43
% AAD	6.4	2.9	28.3	8.7	2.7	37.6	14.8	1.7	22.6

4.2.6.3 VLE of the MIX-2 + Water + MEG System

Finally the system of MIX-2 + Water + MEG is investigated and modeling results for the composition in vapor and organic phases are presented in Tables 4.19 and 4.20 respectively. The CPA predictions are in good agreement with experimental data especially for hydrocarbon phase composition. The data for the vapor phase content of MEG and n-decane is not reported for this mixture. Similarly data for water content in the vapor phase is not reported at the higher pressure.

Table 4.19: Experimental¹⁰² and Calculated Composition of Different Species in the Vapor Phase (in Mole Fraction, y) of the MIX-2 + Water + MEG System at 258 K and Various Pressures. The Vapor Phase Compositions of Methane (y_{C1}), Ethane (y_{C2}), Water (y_w), Propane (y_{C3}), n-Butane (y_{C4}), n-Heptane (y_{C7}), Toluene (y_{Tol}) and n-Decane (y_{C10}) are Presented.

Results	y_{C1}	y_{C2}	$y_w \cdot 10^4$	y_{C3}	y_{C4}	$y_{C7} \cdot 10^4$	$y_{Tol} \cdot 10^4$	$y_{C10} \cdot 10^4$
T=258.40 K P=5.03 bar								
Exp.	0.755	0.144	3.02	0.082	0.018	3.65	3.84	---
CPA	0.79	0.129	3.51	0.065	0.015	2.78	3.44	0.04
% AD	4.6	10.4	16.2	20.7	16.7	23.8	10.4	---
T=258.50 K P=12.37 bar								
Exp.	0.868	0.084	0.55	0.039	0.009	1.95	2.22	---
CPA	0.881	0.081	1.5	0.031	0.007	1.42	1.74	0.03
% AD	1.5	3.6	172.7	20.5	22.2	27.2	21.6	---
T=258.40 K P=20.32 bar								
Exp.	0.898	0.065	---	0.03	0.007	1.72	1.99	---
CPA	0.916	0.058	0.942	0.021	0.005	1.13	1.36	0.02
% AD	2.0	10.8	---	30.0	28.6	34.3	31.7	---
T=258.50 K P=28.91 bar								
Exp.	0.908	0.058	---	0.027	0.006	1.87	1.98	---
CPA	0.934	0.046	0.7	0.016	0.004	1.08	1.28	0.03
% AD	2.9	20.7	---	40.7	33.3	42.3	35.4	---
% AAD	2.8	11.4	---	27.0	25.2	32.0	24.8	---

Table 4.20: Experimental¹⁰² and Calculated Composition of Different Species in the Organic Phase (in Mole Fraction, x) of the MIX-2 + Water + MEG System at 258 K and Various Pressures. The Organic Phase Compositions of Methane (x_{C1}), Ethane (x_{C2}), Water (x_w), Propane (x_{C3}), n-Butane (x_{C4}), n-Heptane (x_{C7}), Toluene (x_{Tol}) and n-Decane (x_{C10}) are Presented.

Results	x_{C1}	x_{C2}	$x_w \cdot 10^4$	x_{C3}	x_{C4}	$x_{C7} \cdot 10^4$	$x_{Tol} \cdot 10^4$	$x_{C10} \cdot 10^4$
T=258.39 K P=5.72 bar								
Exp.	0.0228	0.0449	1.2	0.1157	0.12	0.168	0.319	0.209
CPA	0.026	0.04	1.1	0.101	0.114	0.176	0.320	0.220
% AD	14.0	10.9	8.3	12.7	5.0	4.8	0.3	5.3
T=258.51 K P=10.29 bar								
Exp.	0.0457	0.0561	1.1	0.1176	0.116	0.161	0.303	0.20
CPA	0.05	0.0510	1.08	0.1040	0.11	0.16	0.31	0.21
% AD	9.4	9.1	1.8	11.6	5.2	0.6	2.3	5.0
% AAD	11.7	10.0	5.0	12.2	5.1	2.7	1.3	5.2

4.3 Conclusions

In this chapter the CPA equation of state has been applied to a variety of phase equilibria (liquid-liquid, vapor-liquid and vapor-liquid-liquid) of complex polar and associating, non-associating and solvating compounds. These chemicals include alkanes, aromatic hydrocarbons, water and polar chemicals (methanol and monoethylene glycol) used as gas-hydrate inhibitors. Therefore these systems are important to oil and gas industry. The binary and multicomponent systems are studied at high pressure and low temperature. More specifically four kind of systems have been investigated: (i) LLE of heavy aromatic hydrocarbon + water and alkane + water (ii) high pressure VLE of methane + methanol (iii) VLE of hydrocarbon mixture-1 (MIX-1) + water, MIX-1 + water + methanol and MIX-1 + water + MEG (iv) VLLE of hydrocarbon mixture-2 (MIX-2) + water, MIX-2 + water + methanol and MIX-2 + water + MEG.

MIX-1 consists of 94 mol % methane, 4 mol % ethane and 2 mol % n-butane whereas MIX-2 represents a synthetic condensate consisting of 19.5 mol % methane, 5.8 mol % ethane, 9.2 mol % propane, 9.2 mol % n-butane, 13.8 mol % n-heptane, 25.3 mol % toluene and 17.2 mol % n-decane. For systems with MIX-1, water and inhibitor content of the gas phase are modeled at temperatures ranging from 268.15 K to 313.15 K and pressures ranging from 1 bar to 348 bar. For systems with MIX-2, the composition of the gas phase and the organic phase are modeled for a temperature range 258 K to 298 K and pressure 5 bar to 37 bar.

Satisfactory modeling results are obtained for the mutual solubility of alkylbenzenes and water by obtaining k_{ij} from homomorph alkanes and fitting only the cross-association volume to binary data. For higher alkylbenzenes (i.e. pentylbenzene, hexylbenzene etc.) the solubility of alkylbenzene in water can be predicted satisfactorily but for the solubility of water in alkylbenzene the experimental data are not available. Similarly, the mutual solubility of n-nonane and water as well as water in undecane has been predicted satisfactorily (against available data) using k_{ij} obtained from a generalized correlation as a function of carbon number.

For methane + methanol systems CPA can satisfactorily predict the methane content in methanol over a range of temperature and pressure and methanol content in gas phase especially at high temperature and low pressure. Equally good description is obtained by using a single temperature independent $k_{ij}=0.01$ (from de Hemptinne et al.¹⁰⁰) and $k_{ij}=0.0487$ (suggested by Haghighi et al.⁸⁹) which suggest that higher values of binary interaction parameter do not influence considerably the calculations. The deviations are observed for methanol content in vapor phase at low temperature and high pressure which can be partially explained by the reported high uncertainties in the measurements. More investigations are

required (e.g. pure component parameters) to improve the performance of the model at lower temperature (268 K) and higher pressure (200-350 bar). Furthermore correlations for light hydrocarbons and water (given in Table 4.8) are developed for temperature range of 274-473 K and may not be extrapolated reliably.

CPA can predict ($k_{ij}=0$) satisfactorily the water content in gas phase of MIX-1 + Water, MIX-1 + Water + Methanol and MIX-1 + Water + MEG systems. Methanol content in vapor phase of MIX-1 + Water + Methanol system could be correlated with % AAD of 16.4 in comparison to reported experimental uncertainty of 15%. Finally CPA can satisfactory predict organic phase composition for VLLE of MIX-2 (synthetic condensate) + water, MIX-2 + Water + Methanol and MIX-2 + Water + MEG systems but relatively less satisfactory predictions for vapor phase are obtained.

Experimental Work

Today's oil and gas production requires application of various chemicals in large amounts. In order to evaluate the effect of those chemicals on the environment, it is of crucial importance to know how much of the chemicals are discharged via produced water and how much is dissolved in the crude oil. Therefore it is of interest to develop a thermodynamic model to predict mutual solubility of oil, water and polar chemicals. But for the development and validation of the model, experimental data are required. This chapter presents new experimental liquid-liquid equilibrium (LLE) data for "condensates + monoethylene glycol (MEG)" and "condensates + MEG + water" systems at temperatures from 275 K to 323 K at atmospheric pressure. The condensates used in this work are stabilized natural-gas-condensates from offshore fields in the North Sea.

Compositional analysis of the condensates was carried out by gas chromatography and detailed separation of individual condensate's components has been carried out. For mutual solubility of MEG and condensate, several individual components peaks could be detected up to n-nonane and many components from decane plus carbon fraction. Their solubility was quantified and the sum was reported as solubility of condensate in MEG. A similar procedure was adopted for condensate, MEG and water systems but due to presence of water, solubility of condensate in the polar phase decreases.

5.1 Introduction

Chemicals are added in almost all the stages in oil and gas production. It is generally accepted that efficient and cost effective oil and gas production is not possible without the use of chemicals.^{3,6} Monoethylene glycol (MEG) is one of the most widely used production chemicals. It is used as a gas hydrate inhibitor to ensure reliable production and transportation. Other examples of chemicals include hydrate inhibitors (e.g. methanol), emulsion breakers [2-(2-butoxyethoxy)ethyl acetate, 2-ethyl hexanol] corrosion inhibitors (sodium carbonate, sodium thiosulphate and sodium bicarbonate) and scale inhibitors (potassium hydroxide).³

The purpose of this project is thermodynamic modeling of distribution of MEG in oil-water system using the CPA EoS. But for the development and validation of a thermodynamic model, experimental data are required. Those data are scarce in general, especially with condensate. Therefore experimental work was carried out at Statoil Research Center, in Norway to acquire the mutual solubility data.

Liquid-liquid equilibrium experiments were carried out to measure the mutual solubility. There are three main fluids involved in these experiments such as reservoir fluid, MEG and water. The experiments were carried out with two combinations of the fluids.

- Reservoir-fluid + MEG
- Reservoir-fluid + MEG + Water

The reservoir fluids are two gas-condensates which are obtained from offshore gas fields in the North Sea. In order to distinguish them from each other they are named as condensate-1 and condensate-2. They are also given a short name as COND-1, COND-2 respectively.

This chapter is divided into three sections namely experimental section, results and discussions and conclusions. The experimental section describes the materials and methods used to carry out experiments. Analytical techniques and equipments chosen in this work are discussed in this section. The results obtained from experimental work are described in results and discussion section. The data are analyzed and compared with the literature values of systems of well-defined hydrocarbons. Finally the trends, findings and contribution from this work are concluded.

5.2 Experimental Section

5.2.1 Materials

The chemicals used in this work are given in Table 5.1 and no further purification was carried out. The stabilized condensates were obtained from various gas fields in the North Sea. Their overall molar mass and density was measured experimentally by an external laboratory. The molar mass was measured using a freezing point depression method. The overall density and molar mass of the condensates and oils presented in this chapter is given in Table 5.12. The detailed and condensed composition of the condensate-2 is given in Tables 5.3 and 5.4 respectively. The condensed composition of condensate-1 is given in Table 5.5. The details of the methods used for composition measurement are given in the coming sections.

Table 5.1: Purity (in Mass Fraction, w) of the Chemicals Used in This Work.

Chemicals	Specific Purity $10^2 \times w$	Water Contents $10^2 \times w$	Supplier
Monethylene glycol	>99.78	<0.119	Acros Organics
1-Dodecane	>99.99	<0.001	MERCK
Carbon disulphide	>99.78	<0.119	Acros Organics
1-Heptene	>99.99	<0.100	Sigma-Aldrich
n-Nonane	>99.99	<0.100	MERCK
Ethylbenzene	>99.99	<0.100	MERCK
n-Heptane	>99.99	<0.100	MERCK

5.2.2 Methods

5.2.2.1 Pure Condensate Analysis

The compositional analysis (of pure condensate) was carried out by gas chromatograph-2 (GC-2) with specifications given in Table 5.2. The ASTM standard D5134 Qualitative Reference Naphtha Standard¹⁰⁸ given in appendix B. 3 was used to identify the components in the FID-GC analysis.

Table 5.2: Characteristics of Gas Chromatographs Used in This Work. ^{110,112}

Characteristic	GC-1 (Glycol GC)	GC-2 (Condensate GC)
Column Name	CP-Wax 52 CB	HP-PONA
Column Type	Polar Column	Non-polar Column
Column Length	30 m	50 m
Column Internal Diameter	0.53 mm	0.20 mm
Column Film Thickness	1 μm	0.50 μm
Injection Volume	0.20 nm^3	0.10 nm^3
Carrier Gas	Helium	Helium
Detector Type	FID ¹	FID ¹
Rate of Carrier Gas	0.075 $\mu\text{m}^3 \cdot \text{s}^{-1}$	0.015 $\mu\text{m}^3 \cdot \text{s}^{-1}$
Injection Temperature	548 K	473 K
Detection Temperature	533 K	523 K

A standard temperature program ASTM D5134 was used for GC-2.¹⁰⁸ The initial column temperature was (308 ± 0.5) K and it was held at this level for 1800 seconds (s). Then the temperature was ramped at the rate of 2 K per 60 s to 473 K and kept at this temperature for 180 s. In the final stage, the temperature was increased to 573 K within 180 s and kept there for 720 s. The total time for the temperature program was 8400 s. The temperature programs for both GCs are also shown in appendices B. 1 and B. 2.

For quantification of components an internal standard 1-heptene was used. The internal standard is usually a component which is not present in an analyte sample and its peak does

¹ Flame ionization detector

not overlap with any of others component's peak. A weighed amount of the internal standard (0.014-0.016 mass fraction of condensate) was added in the condensate sample.

The condensate sample is injected into a heated zone, vaporized and transported by a carrier gas into a non-polar column HP-PONA. The column partitions the components usually according to their boiling points similar to distillation. The eluted compounds are carried by a carrier gas (helium in this case) into a detector where the component concentration is related to the area under the detector response curve. Each component in the condensate appears as a peak and its amount can be calculated using equation 5.1.

$$w_i = \frac{w_{IS} \times A_i \times RRF_i}{A_{IS}} \quad 5.1$$

where w_i is the concentration of the component i (in mass fraction) in condensate sample which is required to quantify, w_{IS} is the mass fraction of internal standard, A_{IS} is the area of the internal standard peak, A_i is the area of component i and RRF_i is the relative response factor of component i .

In this work a macro was used in MS Excel which contains molar mass, density and RRF of each component in the condensate. It takes the overall molar mass, density of the condensate, mass of internal standard (m_{IS}) and the area of its peak (A_{IS}) as input. It generates a report for mass and molar composition of the condensate based on input information.

A gas chromatographic analysis of the liquid sample of condensate-2 for the fraction C₄-C₉ (where subscript 4 and 9 represent carbon number of a hydrocarbon fraction) is given in Table 5.3. Approximately 85 components peaks were identified by their retention time. Peaks eluting after n-nonane were not identified individually since they are beyond the scope of ASTM D5134.

Additionally above n-nonane some normal paraffins could also be identified. The condensed composition reports of the condensates up to decane plus fraction (C₁₀₊) are given in Table 5.4 and Table 5.5. Here components in the light end e.g. i-butane, n-butane, i-pentane and n-pentane are presented as individual compounds whereas heavier hydrocarbons are grouped in to carbon number fractions (C_N). All the components detected by GC between the two neighboring normal paraffins are grouped together. They are measured and reported as a single carbon number (SCN) fraction, equal to that of the higher normal paraffin. For example all the components eluting between n-hexane and n-heptane in a GC chromatogram are classified as C₇ fraction. The carbon number of a fraction is determined according to the boiling

Table 5.3: Detailed Composition (in Mass Fraction, w , Mole Fraction, x), Molar Mass (M) and Density (ρ) of the Condensate-2.¹¹²

Peak	Component	$w \cdot 10^2$	$x \cdot 10^2$	$M/\text{g} \cdot \text{mol}^{-1}$	$\rho/\text{g} \cdot \text{cm}^{-3}$
1	i-Butane	0.008	0.015	58.122	0.5633
2	n-Butane	0.287	0.528	58.122	0.5847
3	i-Pentane	6.885	10.201	72.151	0.6246
4	n-Pentane	8.217	12.174	72.151	0.6309
5	2, 2-Dimethylbutane	0.408	0.506	86.178	0.6539
6	Cyclopentane	0.696	1.061	70.135	0.7502
7	2, 3-Dimethylbutane	3.316	4.113	86.178	0.6662
8	3-Methylpentane	1.926	2.389	86.178	0.6688
9	n-Hexane	5.015	6.221	86.178	0.6638
10	2, 2-Dimethylpentane	0.164	0.175	100.205	0.6739
11	Methylcyclopentane	2.580	3.227	84.162	0.7534
12	2,4-Dimethylpentane	0.249	0.266	100.205	0.6771
13	2,2,3-Trimethylbutane	0.049	0.052	100.200	0.6901
14	Benzene	2.454	3.358	78.114	0.8842
15	3,3-Dimethylpentane	0.088	0.094	100.205	0.6936
16	Cyclohexane	2.977	3.781	84.162	0.7831
17	2-Methylhexane	1.463	1.561	100.205	0.6829
18	2,3-Dimethylpentane	0.410	0.437	100.205	0.6951
19	1,1-Dimethylcyclopentane	0.228	0.248	98.189	0.7590
20	3-Methylhexane	1.535	1.638	100.205	0.6915
21	<i>cis</i> -1,3-Dimethylcyclopentane	0.487	0.530	98.189	0.7493
22	<i>trans</i> -1,3-Dimethylcyclopentane	0.446	0.486	98.189	0.7532
23	3-Ethylpentane	0.082	0.087	100.200	0.6982
24	<i>trans</i> -1,2-Dimethylcyclopentane	0.801	0.872	98.189	0.7559
25	n-Heptane	3.725	3.974	100.205	0.6880
26	Methylcyclohexane + <i>cis</i> -1,2-Dimethylcyclopentane	5.026	5.472	98.189	0.7737
27	1,1,3-Trimethylcyclopentane + 2,2-Dimethylhexane	0.270	0.257	112.216	0.7526
28	Ethylcyclopentane	0.295	0.321	98.189	0.7708
29	2,5-Dimethylhexane + 2,2,3-Trimethylpentane	0.195	0.182	114.232	0.7200
30	2,4-Dimethylhexane	0.222	0.208	114.232	0.7045
31	1- <i>trans</i> -2- <i>cis</i> -4-Trimethylcyclopentane	0.229	0.218	112.216	0.7668
32	3,3-Dimethylhexane	0.065	0.061	114.232	0.7141
33	1- <i>trans</i> -2- <i>cis</i> -3-Trimethylcyclopentane	0.226	0.215	112.216	0.7701
34	2,3,4-Trimethylpentane	0.021	0.020	114.230	0.7191
35	Toluene + 2,3,3-Trimethylpentane	3.457	4.011	92.143	0.8714
36	1,1,2-Trimethylcyclopentane	0.068	0.064	114.232	0.7660
37	2,3-Dimethylhexane	0.142	0.133	114.232	0.6912
38	3-Ethyl-2-methylheptane	0.042	0.039	114.232	0.7193

Table 5.3 continued...

Peak	Component	$w \cdot 10^2$	$x \cdot 10^2$	$M/g \cdot mol^{-1}$	$/g \cdot cm^{-3}$
39	2-Methylpentane	1.248	1.168	114.232	0.7019
40	4-Methylheptane + 3-Ethyl-3-methylpentane	0.395	0.370	114.232	0.7046
41	<i>cis</i> -1,3-Dimethylcyclohexane	0.901	0.858	112.216	0.7701
42	3-Ethylheptane + <i>cis</i> -2- <i>trans</i> -3-Trimethylcyclopentane	0.858	0.803	114.232	0.7099
43	3-Ethylhexane + <i>trans</i> -1,4-Dimethylcyclohexane	0.503	0.479	112.216	0.7668
44	1,1-Dimethylcyclohexane	0.139	0.132	112.216	0.7809
45	2,2,5-Trimethylhexane + <i>trans</i> -1,3-ethylmethylcyclopentane	0.113	0.094	128.259	0.7072
46	<i>cis</i> -1,3-Ethylmethylcyclopentane	0.109	0.104	112.216	0.7724
47	<i>trans</i> -1,2-Ethylmethylcyclopentane	0.174	0.166	112.216	0.7649
48	1,1-Ethylmethylcyclopentane + 2,2,4-Trimethylhexane	0.021	0.018	128.259	0.7110
49	<i>trans</i> -1,2-Dimethylcyclohexane	0.420	0.400	112.216	0.7799
50	<i>Trans</i> -1,3-Dimethylcyclohexane + <i>cis</i> -1,4-Dimethylcyclohexane	0.261	0.218	128.259	0.7900
51	n-Octane	2.590	2.242	114.23	0.7065
52	2,4,4-Trimethylhexane + Propylcyclopentane	0.018	0.017	112.216	0.7765
53	Unidentified C ₉ naphthene	0.019	0.016	126.243	0.7900
54	Unidentified C ₉ naphthene	0.017	0.014	126.243	0.7900
55	<i>cis</i> -1,2-Ethylmethylcyclopentane + 2,3,5-Trimethylhexane	0.043	0.041	112.216	0.7900
56	2,2-Dimethylheptane	0.123	0.103	128.259	0.7144
57	<i>cis</i> -1,2-Dimethylcyclohexane	0.028	0.027	112.216	0.8003
58	2,4-Dimethylheptane	0.123	0.103	128.259	0.7192
59	Ethylcyclohexane + Propylcyclopentane	0.879	0.796	118.000	0.7900
60	4,4-Dimethylheptane	0.028	0.023	128.259	0.7721
61	2,6- Dimethylheptane + C ₉ naphthene	0.781	0.651	128.259	0.7089
62	4-Ethyl-2-methylhexane	0.053	0.044	128.259	0.7195
63	2,5-Dimethylheptane	0.362	0.302	128.259	0.7208
64	1,1,3-Trimethylcyclohexane	0.037	0.031	126.243	0.7749
65	Unidentified C ₉ naphthene	0.027	0.023	126.243	0.7900
66	Ethylbenzene	0.519	0.523	106.168	0.8714
67	3,5-Dimethylheptane + 3,3-Dimethylheptane	0.213	0.178	128.259	0.7262
68	Unidentified C ₉ naphthene	0.050	0.042	126.243	0.7900
69	Unidentified C ₉ naphthene	0.014	0.012	126.243	0.7900
70	m-Xylene	1.437	1.447	106.168	0.8642
71	p-Xylene	0.444	0.447	106.168	0.8611
72	2,3-Dimethylheptane	0.074	0.062	128.259	0.7260
73	3,4-Dimethylheptane* + Unidentified C ₉	0.042	0.035	128.259	0.7314
74	3,4-Dimethylheptane*	0.011	0.009	128.259	0.7314

Table 5.3 continued...

Peak	Component	$w \cdot 10^2$	$x \cdot 10^2$	$M/\text{g} \cdot \text{mol}^{-1}$	$\rho/\text{g} \cdot \text{cm}^{-3}$
75	4-Ethylheptane + Unidentified C ₉	0.016	0.013	128.258	0.7241
76	4-Methyloctane	0.433	0.361	128.259	0.7160
77	2-Methyloctane	0.433	0.361	128.259	0.7095
78	2,2,3-Trimethylhexane + C ₉ naphthene	0.031	0.026	128.260	0.7257
79	3-Ethylheptane + C ₉ naphthene	0.072	0.060	128.258	0.7225
80	3-Methyloctane	0.538	0.448	128.259	0.7170
81	o-Xylene	0.593	0.597	106.168	0.8844
82	Unidentified C ₉ naphthene	0.039	0.033	126.243	0.7900
83	Unidentified C ₉ naphthene	0.025	0.021	126.243	0.7900
84	Unidentified C ₉ naphthene	0.015	0.013	126.243	0.7900
85	n-Nonane	2.014	1.679	128.259	0.7214
	Decanes Plus (C ₁₀₊)	27.964	14.966	199.749	0.8364

*stereo isomers

The densities of the components given in Table 5.3 are the pure component densities recommended by American Petroleum Institute for use in the calculation of the densities of carbon fractions (e.g. C₆, C₇ etc.) in oil and condensate at standard conditions. The molar mass (M) and density (ρ) of a carbon fraction are calculated by equations 5.2 and 5.3 respectively:¹⁰⁹

$$M_{C_N} = \frac{w_{C_N}}{\sum_{i=1}^{N_{C_N}} \frac{w_i}{M_i}} \quad 5.2$$

$$\rho_{C_N} = \frac{w_{C_N}}{\sum_{i=1}^{N_{C_N}} \frac{w_i}{\rho_i}} \quad 5.3$$

where w_{C_N} is the mass fraction of components in a carbon fraction C_N and N_{C_N} is the number of components in the C_N fraction. w_i , M_i and ρ_i is mass fraction, molar mass and density of component i respectively.

The density of the plus fraction (ρ_+) and the molar mass of plus fraction (M_+) is calculated by equations 5.4 and 5.5 respectively:¹⁰

$$M_+ = \frac{M_{oil} \times w_+}{1 - M_{oil} \sum_{i=1}^{N-1} \frac{w_i}{M_i}} \quad 5.4$$

$$\rho_+ = \frac{\rho_{oil} \times w_+}{1 - \rho_{oil} \sum_{i=1}^{N-1} \frac{w_i}{\rho_i}} \quad 5.5$$

where M_{oil} and ρ_{oil} are respectively the average molar mass and the overall density of the oil or condensate sample and w_+ is the mass fraction of the plus fraction.

The components in each carbon fraction can further be divided into paraffinic (P), naphthenic (N) and aromatic (A) contents known as PNA distribution of an oil or condensate. The PNA distribution of each carbon fraction (C₄-C₉) in condensate-2 is given in Table 5.4. The overall PNA distribution on the basis of mass fraction shows that the condensate-2 is paraffinic (0.60 mass fraction) in nature whereas naphthenic (0.28 mass fraction) and aromatic (0.12 mass fraction) components are also present (see Figure 5.15). This PNA distribution is based only on the components in C₂ to C₉ carbon fraction as the components above n-nonane cannot be identified using the GC method used for condensate-1 and condensate-2 in this work.

Table 5.4: Condensed Composition (Mass Fraction, w , Mole Fraction, x), Molar Mass (M) and Density (ρ) of Condensate-2.¹¹²

Component	$w \cdot 10^2$	$x \cdot 10^2$	$M/g \cdot mol^{-1}$	$\rho/g \cdot cm^{-3}$
Light End Total	15.396	22.917	71.819	0.6271
i-Butane (P)	0.008	0.015	58.122	0.5633
n-Butane (P)	0.287	0.528	58.122	0.5847
i-Pentane (P)	6.885	10.200	72.151	0.6246
n-Pentane (P)	8.214	12.174	72.151	0.6309
Hexanes Total	11.360	14.289	84.987	0.6697
Hexanes (P)	10.664	13.228	86.178	0.6651
Hexanes (N)	0.696	1.0610	70.135	0.7502
Heptanes Total	17.738	20.837	91.003	0.7423
Heptanes (P)	7.765	8.284	100.205	0.6876
Heptanes (N)	7.519	9.195	87.420	0.7650
Heptanes (A)	2.454	3.358	78.114	0.8842
Octanes Total	17.989	18.433	104.325	0.7655
Octanes (P)	4.920	4.604	114.232	0.7054
Octanes (N)	9.613	9.819	104.656	0.7655
Octanes (A)	3.457	4.011	92.143	0.8714
Nonanes Total	9.552	8.558	119.315	0.7692
Nonanes (P)	4.476	3.731	128.259	0.7205
Nonanes (N)	2.082	1.813	122.772	0.7546
Nonanes (A)	2.994	3.015	106.168	0.8689
Decanes Plus	27.964	14.966	199.749	0.8205

Similar to condensate-2 composition of condensate-1 was also analyzed and the condensed composition is presented in the Table 5.5. After measuring the composition of the pure condensates, the next step is the measurement of mutual solubility for condensate + MEG and condensate + MEG + water systems which is presented in the next section.

Table 5.5: Condensed Composition (Mass Fraction, w , Mole Fraction, x), Molar Mass (M) and Density (ρ) of Condensate-1.¹¹⁰

Component	$10^2 \times w$	$10^2 \times x$	$M/\text{g}\cdot\text{mol}^{-1}$	$\rho/\text{g}\cdot\text{cm}^{-3}$
Light End Total	13.795	23.872	65.098	0.6038
Ethane	0.001	0.004	30.070	0.3567
Propane	0.351	0.896	44.090	0.5067
i-Butane (P)	1.229	2.382	58.122	0.5621
n-Butane (P)	4.031	7.813	58.122	0.5831
i-Pentane (P)	3.524	5.502	72.151	0.6231
n-Pentane (P)	4.659	7.275	72.151	0.6299
Hexanes Total	7.770	10.292	85.00	0.6662
Hexanes (P)	7.321	9.572	86.178	0.6617
Hexanes (N)	0.448	0.720	70.135	0.7481
Heptanes Total	13.016	16.046	91.400	0.7362
Heptanes (P)	6.124	6.885	100.200	0.6888
Heptanes (N)	5.811	7.601	86.100	0.7681
Heptanes (A)	1.081	1.559	78.100	0.8831
Octanes Total	15.293	16.632	103.600	0.7686
Octanes (P)	4.343	4.271	114.54	0.7069
Octanes (N)	7.968	8.715	103.00	0.7655
Octanes (A)	2.982	3.646	92.100	0.8714
Nonanes Total	9.363	8.903	118.500	0.7806
Nonanes (P)	4.373	3.840	128.300	0.7229
Nonanes (N)	1.999	1.889	119.200	0.7944
Nonanes (A)	2.991	3.174	106.200	0.8721
Decanes Plus	40.766	24.254	189.400	0.8464

5.2.2.2 Mutual Solubility Measurements

5.2.2.2.1 Apparatus and Procedure

The apparatus used in this work for the measurement of mutual solubility is shown in Figure 5.3 to Figure 5.6. The apparatus shown in Figure 5.3 consist of

- Air heated oven:** The heating oven consists of two compartments, the lower compartment was used for mixing of fluids (in a mixing machine) and the upper compartment was used for settling of the mixtures (in a glass equilibrium cylinder) to attain equilibrium. The objective of the oven is to carry out mixing and separation at a desired temperature. A required temperature is attained inside the oven by circulation of hot air.
- Mixing machine:** The mixing machine was used for the mixing of condensate + MEG/water mixtures. MEG and condensate are transferred in a 450 ml glass bottle with a cap on it. The bottles are tightened on mixing machine and mixing can be carried out

at a desired rpm. The mixing machine was placed in the lower compartment of the heating oven.

- c. **Equilibrium cylinders:** Two glass cylinders are shown which were used to equilibrate mixture with volume (approximately) 600 ml each. They have holes fitted with septum to facilitate the sampling.
- d. **Equilibrium cylinder:** The mixture of MEG and condensate is shown after separation. The upper dark phase is the condensate phase and the lower (colorless) phase is the MEG or aqueous phase.

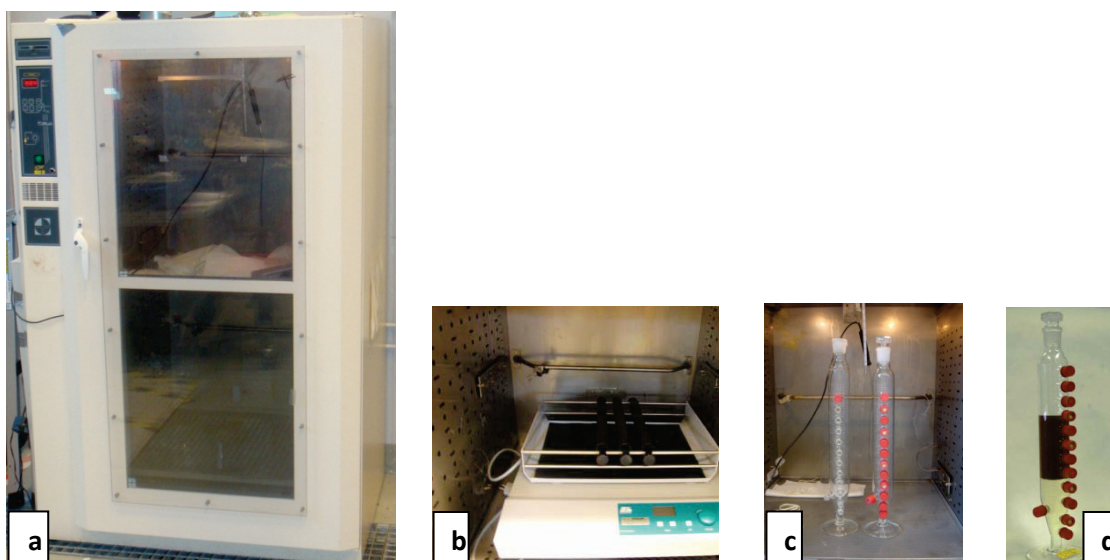


Figure 5.3: Equipments used at various stages of an experiment: (a). Heating oven used for mixing and attaining equilibrium at a fixed temperature (b).Mixing machine placed in lower part of heating oven (c).Two glass equilibrium cylinders placed in upper part of heating oven (d). Equilibrium cylinder showing two phases, the upper phase is condensate phase and the lower phase is polar phase consisting of MEG and water.

The samples from the two phases in equilibrium cylinder are withdrawn using a special kind of glass syringe as shown in Figure 5.4a. Each syringe is 10 ml in volume and has a nob to lock the fluid inside in order to avoid the spillage of condensate sample. The vials used to hold and preserve the samples are shown in Figure 5.4b. These vials were also used to extract MEG and hydrocarbon traces using appropriate solvents.

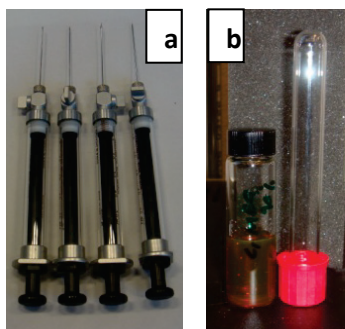


Figure 5.4: (a). Syringes (volume 10 ml each) used to withdraw samples from equilibrium cylinder (b). vials used for sample storage.

The gas chromatograph (GC) used to analyze MEG traces in hydrocarbon phase and hydrocarbon traces in polar phase are shown in Figure 5.5. The condensate GC was used to analyze hydrocarbon traces in polar phase (Figure 5.5a) and glycol GC was used to analyze MEG traces in hydrocarbon phase (Figure 5.5b). The water content in hydrocarbon phase was analyzed using Karl Fisher coulometer shown in Figure 5.6.



Figure 5.5: Chromatographs used for phase analysis: (a). condensate GC used for analysis of traces of hydrocarbon in MEG phase (b). Glycol GC used for analysis of traces of glycol in hydrocarbon phase (c). Sim Dist GC (which can be) used for analysis of traces of condensate heavier than C₁₅.



Figure 5.6: Karl Fisher coulometer used for the measurement of water content in hydrocarbon phase.

The sketch of the experimental setup used in this work is shown in Figure 5.7. A similar setup has been used in the previous work by Folas et al.⁷⁷ and Derawi et al.¹² for the experimental study of liquid-liquid equilibria of well-defined hydrocarbons and polar compounds. In this work modifications were made in the analytical methods because the hydrocarbon phase is a

reservoir fluid of higher complexity as compared to well-defined hydrocarbons. The modifications are described in next sections.

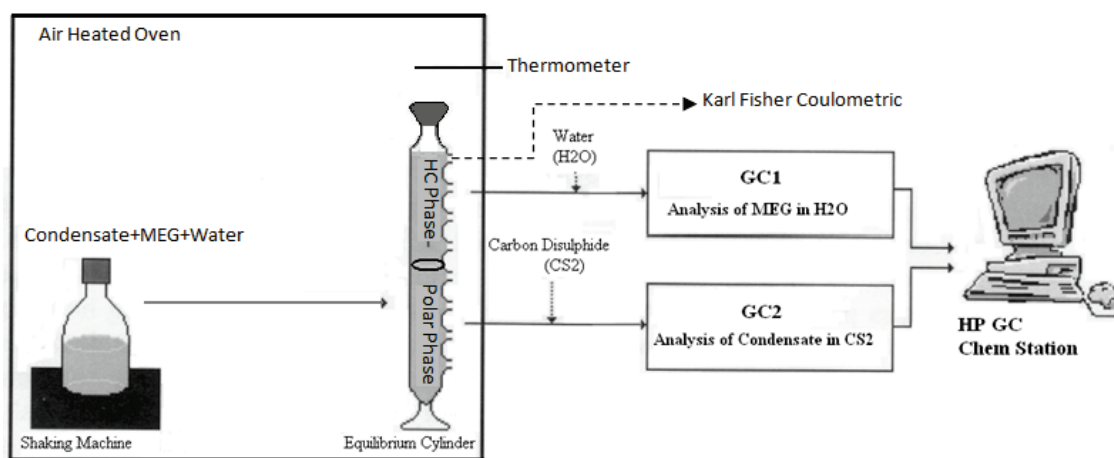


Figure 5.7: Sketch of the experimental setup used in this work.¹¹²

5.2.2.2.2 Mixing and Equilibrium

MEG, condensate and water were mixed at a fixed temperature for up to 24 hours using a mixing machine in an air heated oven. For the MEG + condensate systems, approximately equal mass of MEG and condensate were added for mixing. In the MEG + condensate + water systems the feed mixtures contain condensate 0.50 mass fraction and the polar compounds were also 0.50 mass fraction. The polar phase consists of MEG and water where the composition of MEG ranges from 0.40 mass fraction to 0.80 mass fraction which is of interest to the industrial applications in the North Sea.

After mixing the mixture was transferred to two identical glass equilibrium cylinders and it was kept for at least 18 hours to attain equilibrium. The equilibrium cylinders contain holes and caps fitted with septa for sampling. Both mixing and separation were carried out in an air heated oven which was used at the temperature range from 275 K to 323 K in this work. A DOSTMANN P500 thermometer (± 0.1 K) was used for temperature measurement.

5.2.2.2.3 Sampling

After equilibrium, samples from the two phases were withdrawn manually using a syringe and a needle. The needle and the syringe were preheated to avoid phase separation due to temperature gradient. Two Agilent gas chromatographs (GCs) with different column specifications were used for composition analysis: one for the polar phase while another for the condensate phase. The characteristics of gas chromatographs used in this work are given in Table 5.2. The gas chromatographs are connected to a computer with the Chem Station package for data acquisition and quantification.

5.2.2.2.4 Polar Phase Analysis

For the polar phase analysis, hydrocarbons traces were extracted using the solvent extraction method. The solvent used in this work for the extraction of hydrocarbons from the polar phase is carbon disulphide (CS_2) in which hydrocarbons are soluble but MEG has negligible solubility. The amount of CS_2 added for extraction was 0.30-0.40 mass fraction in the condensate sample. The CS_2 was mixed with the sample from the polar phase for about 900 s and left for separation of the two phases. The extract phase is then analyzed on the condensate GC using the standard temperature program ASTM standard D5134 (as for pure condensate analysis) with an internal standard 1-heptene diluted in 1-dodecane. The internal standard was diluted in order to have its concentration in range of the extracted hydrocarbon components. This will result in more accurate response factor and finally more accurate quantification of HC components. The peaks of 1-heptene and 1-dodecane should not overlap with any of the HC components peaks for safe quantification. The concentration of component i in the polar phase can be calculated using equation 5.6.

$$w_i = A_i \times RF \left[\left(\frac{m_{ISTD} + m_{sample}}{m_{sample}} \right) \left(\frac{m_{CS_2}}{m_{polar}} \right) \right] \quad 5.6$$

where w_i : mass fraction (in ppm) of HC component i in polar phase; A_i : area of HC component i obtained from GC chromatogram; RF : response factor of 1-heptene, m_{ISTD} : mass of diluted internal standard (i.e. $m_{1-heptene} + m_{1-dodecane}$) added in sample; m_{sample} : mass of sample taken from CS_2 extract phase; m_{CS_2} : mass of carbon disulphide added for extraction; m_{polar} : mass of sample taken from polar phase.

The term $(m_{ISTD} + m_{sample}) / m_{sample}$ is multiplied to normalize the concentration of HC traces in CS_2 , and the term (m_{CS_2} / m_{polar}) is used to normalize the concentration of HC traces in polar phase. The response factor can be calculated using equation 5.7.

$$RF = \frac{w_{1-heptene} \times 10^6}{A_{1-heptene}} \quad 5.7$$

where $A_{1-heptene}$ is area of 1-heptene peak and $w_{1-heptene}$ is the mass fraction of the 1-heptene in the mixture of internal standard and the sample given by equation 5.8.

$$w_{1-heptene} = \frac{m_{1-heptene}}{m_{ISTD} + m_{sample}} \quad 5.8$$

5.2.2.2.5 Hydrocarbon Phase Analysis

The MEG traces from the condensate phase were extracted using water and analyzed on the glycol GC. The initial column temperature was 353 K and was held for 120 s. The temperature was then increased linearly to 523 K in 1020 s. The temperature 523 K was held for 360 s. The total time for the temperature program is 1500 s. A graphical representation of temperature program is shown in appendix B. 2.

For the condensate phase analysis, the mass of water added for extraction of MEG was approximately (0.30-0.40) mass fraction of the mass of the sample. Water and the condensate were mixed for about 900 s in order to accelerate the extraction process. After mixing, some drops of the condensate remained trapped in the water phase which makes sampling for GC vial difficult. Therefore the mixture of water and condensate was kept in an oven for about 1800 s at temperature about 303.15 K. This helps the separation of both phases and condensate free sampling for GC analysis becomes possible. After separation, the condensate will form the upper phase and the water containing extracted MEG will be the lower phase. The samples for GC analysis were taken from the lower phase, using a plastic syringe with a long needle. The water sample for GC analysis should not have the condensate drops because it causes problem for the glycol GC. This is because the column temperature is too low to elute the heavy hydrocarbons present in the condensate.

The traces of MEG in condensate were quantified using multiple point external standard method. Several external standards were made covering the expected analyte (i.e. MEG) concentration range. A linear calibration curve was constructed using linear least squares method. In order to construct the calibration curve, the standards were run before and after the actual samples. This was done in order to account for the drift in the signal of the GC's detector if it occurs during the GC analysis. Figure 5.8 shows peaks of external standard in a GC chromatogram (left side) and a linear calibration curve (right side) obtained using area of the external standards peaks against the known concentration of MEG (in external standards).

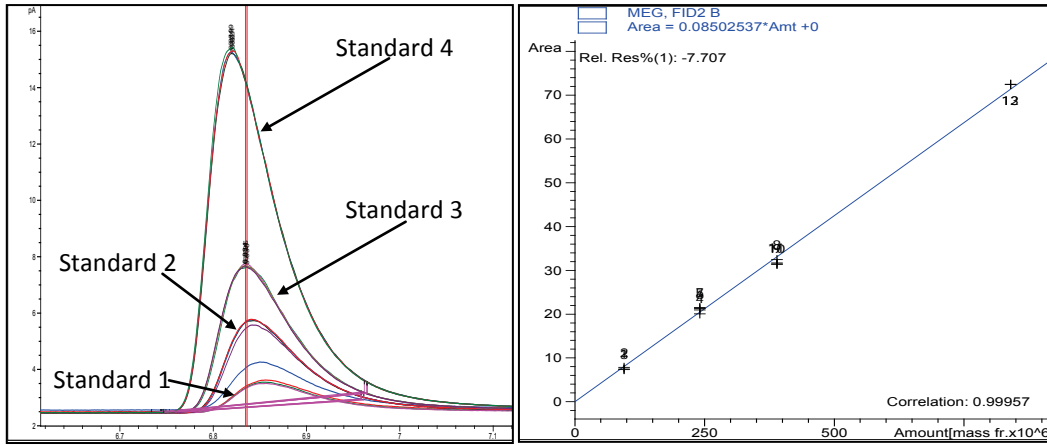


Figure 5.8: Quantification of MEG traces in hydrocarbon phase using external standard method (a) showing peaks of external standards (MEG diluted in water) and (b) calibration curve.

The MEG is quantified automatically by the HP Chem Station Package using (response factor i.e. mass fraction/area or) linear calibration curve which was constructed using external standard. A sample report of MEG quantification is shown in Figure 5.9. It is shown in this report that MEG peak is appearing after 6.8 minutes (i.e. retention time) in the chromatogram. The concentration of MEG is calculated to be 314 mass ppm using area under the curve and response factor. The normalized mass fraction of MEG in condensate phase is calculated using equation 5.9 as given below:

$$w_{MEG} = A_{MEG} \times RF_{MEG} \left(\frac{m_{water}}{m_{condensate\ sample}} \right) \quad 5.9$$

where w_{MEG} is the concentration of MEG (in mass ppm) in condensate, A_{MEG} is area of MEG peak, RF_{MEG} is the response factor of MEG in water (mass ppm/area) given by the following equation:

$$RF_{MEG} = \frac{w_{MEG\ std}}{A_{MEG}} \quad 5.10$$

where $w_{MEG\ std}$ is the known concentration of MEG in the external standard given by equation 5.11:

$$w_{MEG\ std} = \left(\frac{m_{MEG}}{m_{water} + m_{MEG}} \right) 10^6 \quad 5.11$$

The term $(m_{\text{water}} / m_{\text{condensate sample}})$ is used in equation 5.9 to normalize the amount of MEG in condensate sample where $m_{\text{condensate sample}}$ is the mass of condensate sample (taken from equilibrium cylinder) and m_{water} is the mass of water added for extraction of MEG from condensate sample.

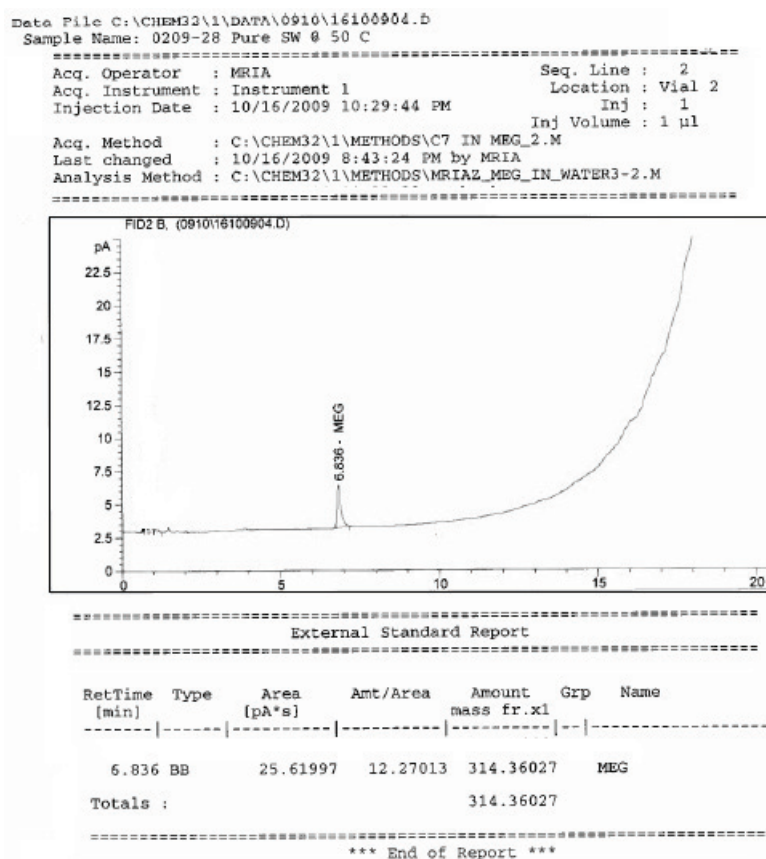


Figure 5.9: Gas chromatogram (for glycol GC) with the quantification report of MEG in condensate (using extract phase).

The water content of the condensate phase was analyzed using a Karl Fisher Coulometer which provides very fast and reliable results, especially for systems with very low solubilities. In this work the apparatus Mettler Toledo DL37 Coulometric titrator for determining the amount of water in the condensate phase was used. Before the analysis of the condensate sample for water content, external standards were analyzed in order to check the reliability of measurement. Four samples were measured for each temperature and the mean value was reported as the condensate phase water content.

For the MEG + condensate system the average uncertainty in the measurement of solubility of MEG in condensate is $(\pm 16 \times 10^{-6})$ mole fraction and for condensate in MEG is $(\pm 153 \times 10^{-6})$ mole

fraction. For the MEG + condensate + water system the average uncertainty for water in condensate is ($\pm 31 \times 10^{-6}$) mole fraction and for MEG in condensate is ($\pm 7 \times 10^{-6}$) mole fraction.

5.3 Results and Discussion

Table 5.6 presents mutual solubilities for two systems such as condensate-1 + MEG and condensate-2 + MEG. These measurements are carried out at various temperatures and atmospheric pressure. The mutual solubilities for MEG, water and condensate are presented in Table 5.7. At each temperature the mutual solubilities were measured for various feed compositions.

Table 5.6: Experimental (Liquid-Liquid) Equilibrium Data for MEG (1) + Condensate (2) System Expressed in Mole Fractions, at Pressure 101.3 KPa.

Temperature <i>K</i>	MEG Solubility in Hydrocarbon $10^6 \times x_1$	Hydrocarbon Solubility in MEG $10^6 \times x_2$
MEG(1) + COND-1(2)¹¹⁰		
275.15	53	---
283.15	74	---
303.15	250	4590
308.15	335	---
313.15	431	4524
318.15	---	5170
323.15	722	4937
326.55	711	---
MEG(1) + COND-2 (2)¹¹²		
275.15	51	---
283.15	87	---
303.15	290	4879
308.15	355	---
313.15	470	5325
318.15	---	5860
323.15	581	6084

Table 5.7: Experimental (Liquid-Liquid) Equilibrium Data (in Mole Fractions, x) for MEG (1) + Water (2) + Condensate (3) at Pressure 101.3 KPa.

Feed			Polar Phase			Hydrocarbon Phase		
x_1	x_2	x_3	x_1	x_2	$10^6 \times x_3$	$10^6 \times x_1$	$10^6 \times x_2$	$10^2 \times x_3$
MEG(1) + Water(2) + COND-1(3)¹¹⁰ T=323.15 K								
0.1324	0.6843	0.1833	0.1621	0.8378	69	61	1218	99.8721
0.3041	0.4488	0.2472	0.4037	0.5960	417	172	946	99.8882
0.4992	0.1909	0.3098	0.7222	0.2765	1793	381	402	99.9217
MEG(1) + Water(1) + COND-2(3)¹¹² T=323.15 K								
0.1312	0.6783	0.1905	0.1621	0.8378	91	82	1309	99.8610
0.2345	0.5386	0.2269	0.3032	0.6965	311	158	1119	99.8723
0.3865	0.3329	0.2805	0.5366	0.4622	1181	328	784	99.8888
MEG(1) + Water(2) + COND-2(3)¹¹² T=303.15 K								
0.1312	0.6783	0.1905	0.1621	0.8378	67	36	806	99.9158
0.2345	0.5386	0.2269	0.3033	0.6966	189	73	635	99.9292
0.3865	0.3329	0.2805	0.5370	0.4625	508	103	394	99.9502

5.3.1 LLE of the n-Heptane + MEG System

The experimental work was initiated with the well-defined system of n-heptane + MEG and a similar procedure was adopted as in a previous work.¹² The experimental results from this work are given in Figure 5.10¹¹⁰ in comparison with the experimental data from the literature. The solubility data of n-heptane in MEG is in good agreement with those of Stavely et al.¹⁰⁹ and Derawi et al.¹² On the other hand solubility data of MEG in n-heptane is slightly lower than those from Stavely et al.¹⁰⁹ and Derawi et al.¹²

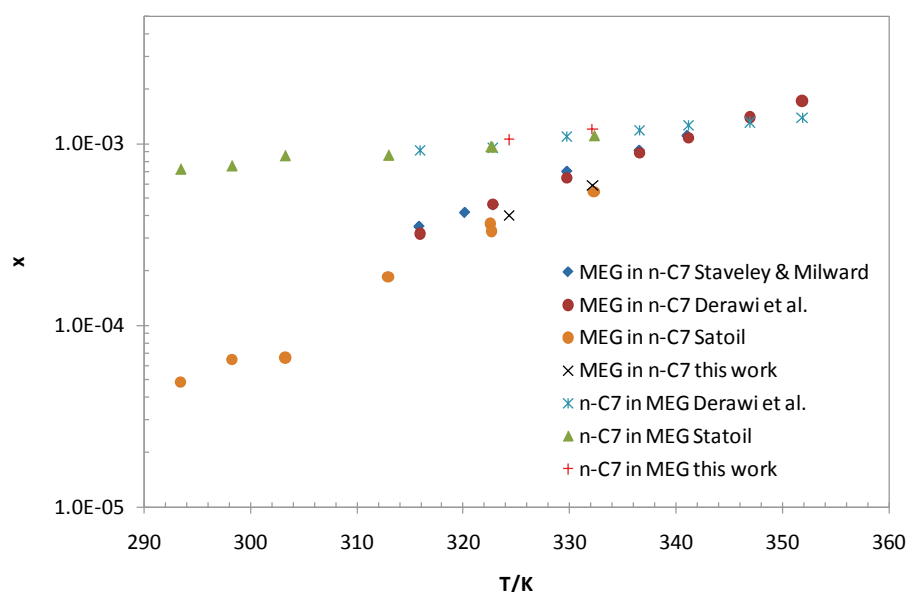


Figure 5.10: LLE data for n-heptane + MEG and comparison to the data from literature. The data for MEG in n-heptane is from Stavely and Milward¹⁰⁹, Derawi et al.¹², Statoil¹¹¹ and this work.¹¹⁰ The data for n-heptane in MEG is from Derawi et al.¹², Statoil and this work.¹¹⁰

5.3.2 LLE of the Condensate + MEG Systems

For MEG + condensate-2 system mutual solubilities were measured in the temperature range 275.15-323.15 K. The reported solubility of condensate in MEG is the sum of solubilities of all condensate's components. About 75 components were detected from GC analysis up to n-nonane and 32 of them with the highest solubilities are shown in Figure 5.11. In this figure each column represents a condensate's component and the height of the column represents its solubility (in mass fraction) in the polar phase. The last block of the columns represents the sum of the solubilities of all the components at a specific temperature. Figure 5.11 shows that in each carbon fraction the solubility of the aromatic hydrocarbons is the highest. Aromatic components are shown to contribute approximately half of the total solubility. The solubility of MEG and condensate increases with increasing temperature and the effect of temperature can also be seen at individual component level as given in Figure 5.11.¹¹⁰ The mutual solubility of condensate-2 and MEG at several temperatures is given in Table 5.6.

Mutual solubility of condensate-1 and MEG is very similar to that of condensate-2 and MEG as shown in Table 5.6 and Figure 5.13 and Figure 5.14.¹¹⁰ This is partially due to the reason that the condensate-1 and condensate-2 are similar to each other with similar PNA distribution. But they have different decane plus fraction which have very small contribution in (total) solubility of condensate in MEG as shown in Figure 5.11.

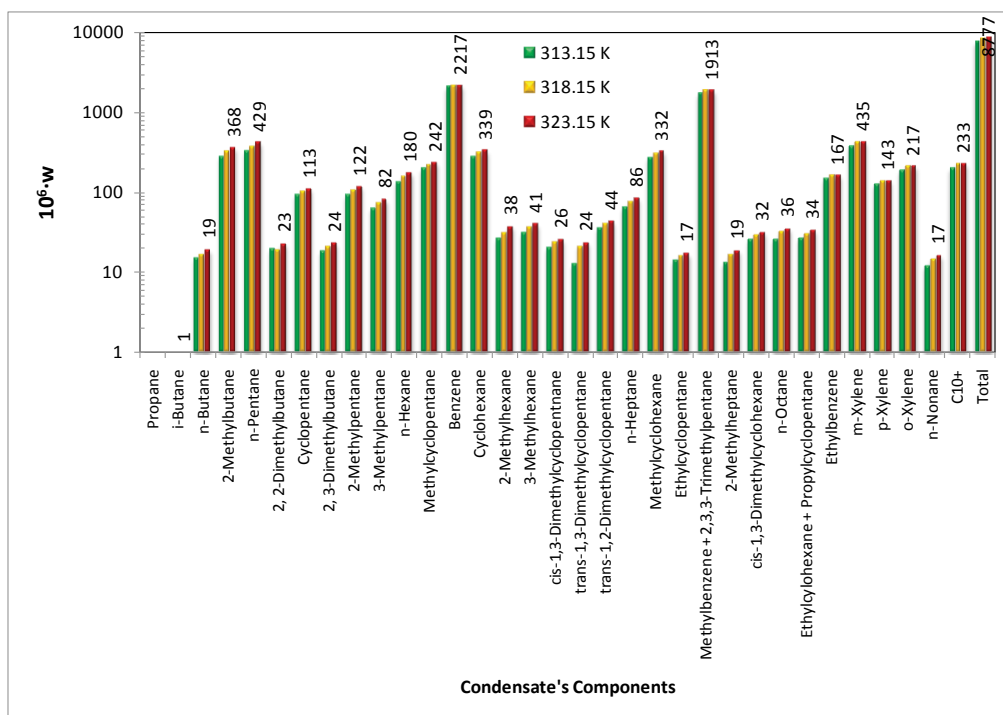


Figure 5.11: Solubility (in mass fraction, W) of condensate-2 components in pure MEG at various temperatures.

5.3.3 LLE of the Condensate + MEG + Water Systems

For the MEG + water + condensate-2 systems, the mutual solubilities were measured at 303.15 and 323.15 K for three different feed compositions. The solubility of condensate-2 in polar phase (MEG + water) at 323.15 K and 303.15 K is shown in Figure 5.12. This figure shows that the solubility of condensate increases with increasing MEG content in polar phase. This behaviour can be explained by lesser polarity of MEG than water which means higher affinity between MEG and condensate than between water and condensate. The mutual solubility of MEG, water and condensate increases with increasing temperature. It is observed that the solubility of aromatic hydrocarbons (i.e. benzene, toluene etc.) is much higher than that of paraffinic and naphthenic hydrocarbons. The sum of solubilities of benzene and toluene contribute almost half of the total solubility of condensate in polar phase (in this specific example). This is an indication of solvation between polar chemical and aromatic hydrocarbons.

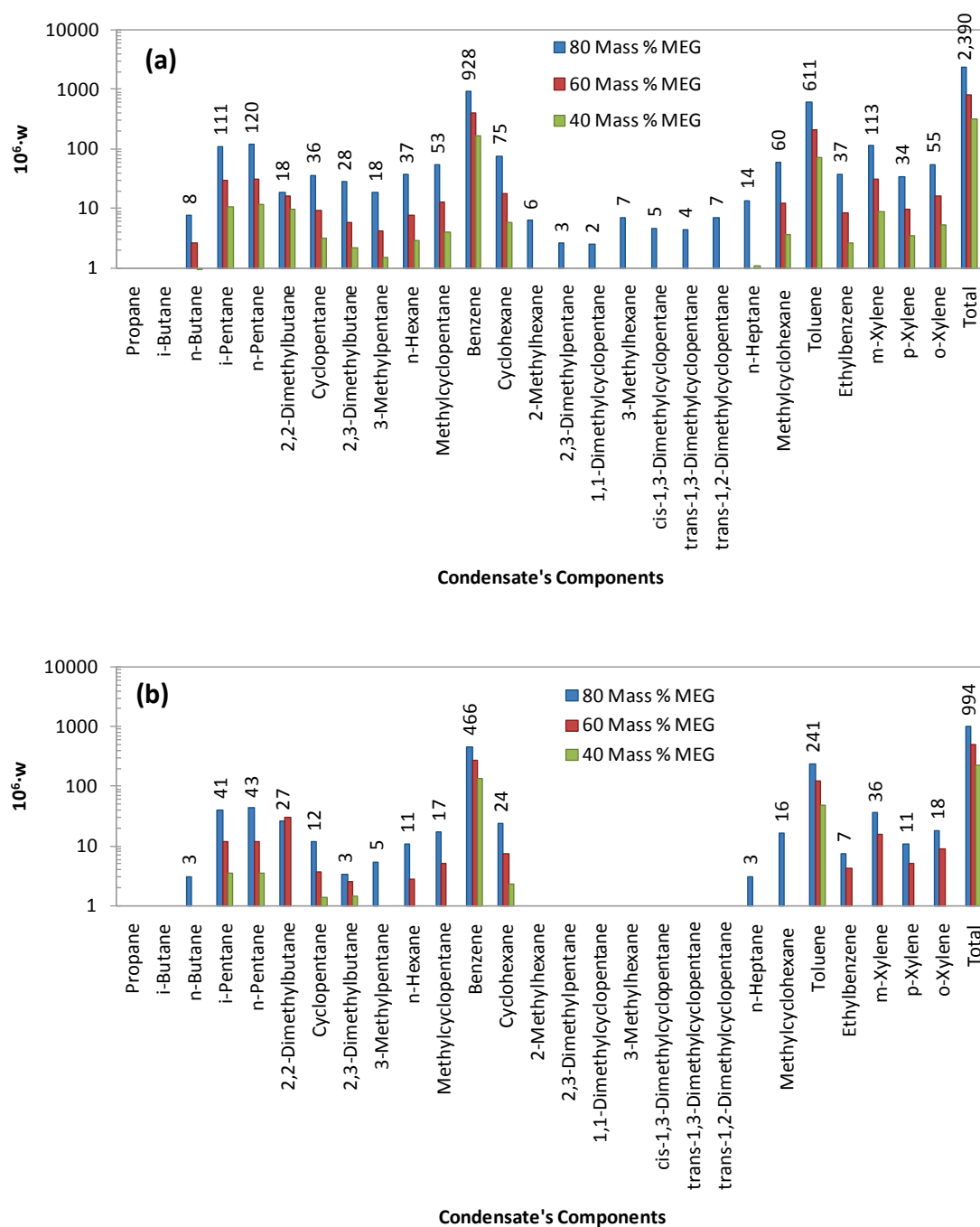


Figure 5.12: Solubility (in mass fraction, w) of condensate-2 components in polar phase (MEG + water) at temperatures (a) 323.15 K and (b) 303.15 K and MEG composition in polar phase.

112

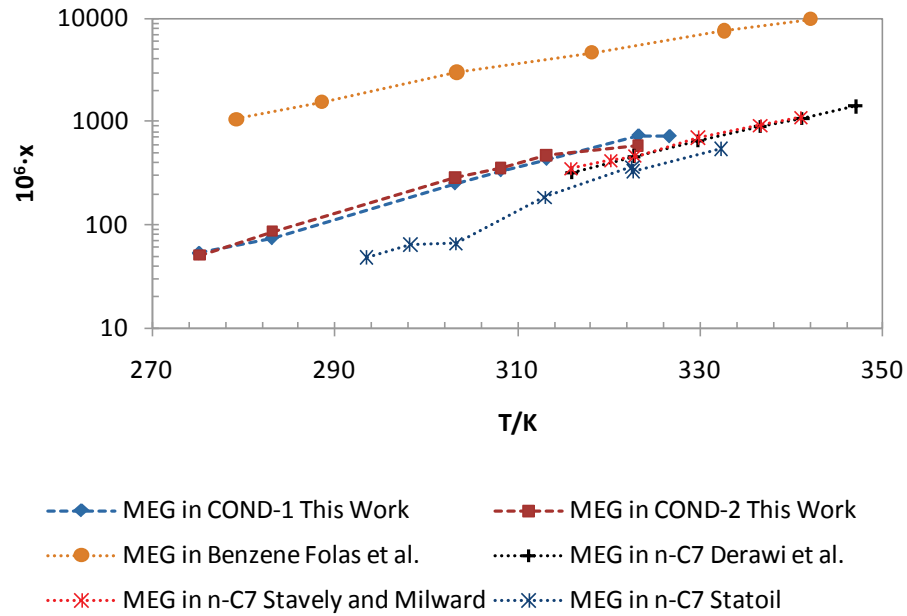


Figure 5.13: Comparison of the solubility (in Mole Fraction, x) of MEG in well-defined hydrocarbons (n-heptane^{12,109,111} and benzene¹¹) and reservoir-fluids (condensate-1¹¹⁰ and condensate-2¹¹²) as a function of temperature (K).

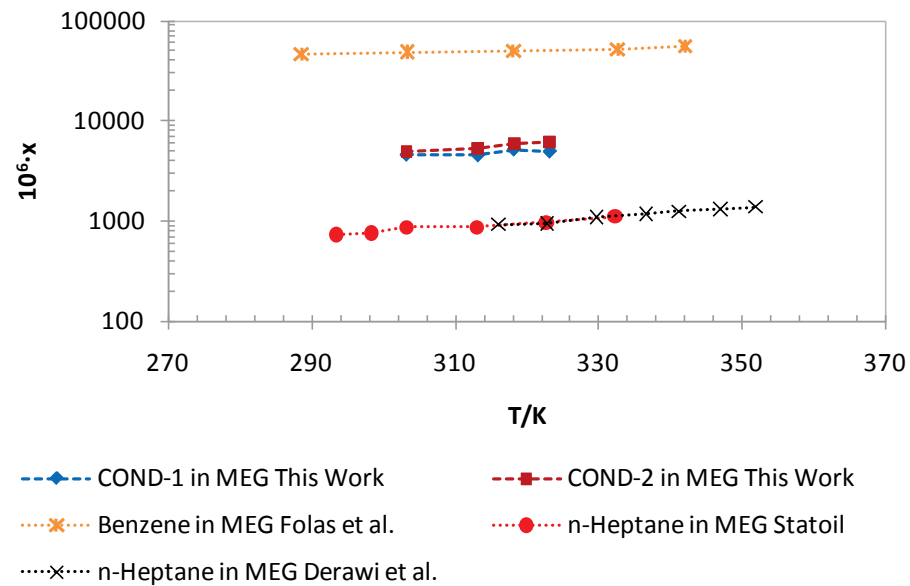


Figure 5.14: Comparison of the solubility (in Mole Fraction, x) of well-defined hydrocarbons (n-heptane^{111,113} and benzene¹¹) and reservoir-fluids (condensate-1¹¹⁰ and condensate-2) in MEG¹¹² as a function of temperature.

The experimental data were measured in mass fraction. In order to compare with the modeling results, it is required to convert these values into molar composition. Here we need the average molar mass of the condensate dissolved in the polar phase which is different from the molar mass of the original condensate in the feed. This is because the components in the original

condensate will partition in different ratios between the condensate phase and the polar phase. The average molar mass \bar{M} of the dissolved condensate in the polar phase was calculated by equation 5.12:

$$\bar{M} = \sum_{i=1}^{i=n} x_i M_i \quad 5.12$$

where x_i is the normalized mole fraction of condensate component i in polar phase and M_i is the molar mass of component i .

A condensate and an oil typically contains paraffinic (P) naphthenic (N) and aromatic (A) compounds. The solubility of MEG in a specific carbon fraction (e.g. C₇) will be the highest in the aromatic HC (e.g. benzene) and the lowest in the paraffinic HC (e.g. n-heptane). The same is also true for the solubility of HC in MEG. As condensates and oils contain both paraffinic and aromatic hydrocarbons, it is expected that the solubility of MEG in condensate should lie between the solubility of MEG in benzene and the solubility of MEG in heptane. This is illustrated in Figure 5.13 and Figure 5.14 where it is shown that the solubility of MEG and condensate lie between the values for the solubilities in the aromatic C₇ (benzene^{11,109}) and the paraffinic C₇ (heptane).¹²

In this PhD project experimental method for the measurement of mutual solubility of reservoir-fluid + MEG and reservoir-fluid + MEG + water systems has been established and tested. New experimental data has been measured for liquid-liquid equilibrium of reservoir fluid in the presence of MEG and water. The data has been measured using two condensates (condensate-1 and condensate-2). There is a need of new data with other condensates and light-oils to further investigate the effect of type of reservoir fluid on mutual solubility. To obtain more data the experimental work has been extended to condensate-3, light-oil-1 and light-oil-2 in two master theses projects.^{114,115} In the next section trends in their data are presented and compared with other related systems.

5.4 Extension of Experimental Work

The composition of condensate-3 given in Table 5.9 was measured using condensate GC. For compositional analysis of light-oil-1 and light-oil-2 Sim Dist GC was used and its characteristics are given in Table 5.8. The more details of the method are given in next section.

Table 5.8: Characteristics of Sim Dist Gas Chromatograph Used for Light-Oil Compositional Analysis.¹¹⁴

Characteristic	GC3 (Sim Dist)
Column Name	Varian Capillary Column CP-Sil 5CB
Column Type	Non-polar Column
Column Length	25 m
Column Internal Diameter	0.53 mm
Column Film Thickness	2 μm
Injection Volume	0.10 nm^3
Carrier Gas	Helium
Detector Type	FID

Table 5.9: Condensed Composition (Mass Fraction, w , Mole Fraction, x), Molar Mass (M) and Density (ρ) of Condensate-3.¹¹⁵

Component	$10^2 \times w$	$10^2 \times x$	$M/\text{g}\cdot\text{mol}^{-1}$	$\rho/\text{g}\cdot\text{cm}^{-3}$
Light End Total	16.51	24.010	64.183	0.5993
Propane	0.490	1.040	44.100	0.5080
i-Butane (P)	3.260	5.230	58.122	0.5630
n-Butane (P)	3.940	6.330	58.122	0.5850
2,2-Dimethylpropane	0.110	0.140	72.151	0.5970
i-Pentane (P)	4.420	5.720	72.151	0.6250
n-Pentane (P)	4.290	5.550	72.151	0.6310
Hexanes Total	12.620	13.980	84.460	0.6693
Hexanes (P)	11.500	12.480	86.178	0.6623
Hexanes (N)	1.110	1.500	70.135	0.7500
Heptanes Total	25.740	26.650	90.180	0.7463
Heptanes (P)	6.230	5.810	100.205	0.6873
Heptanes (N)	18.390	19.510	88.030	0.7612
Heptanes (A)	1.120	1.340	78.110	0.8840
Octanes Total	24.240	21.810	103.790	0.7616
Octanes (P)	6.260	5.120	114.230	0.7078
Octanes (N)	15.900	14.580	101.800	0.7720
Octanes (A)	2.080	2.110	92.143	0.8710
Nonanes Total	8.400	6.690	117.240	0.7857
Nonanes (P)	2.720	1.990	127.880	0.7208
Nonanes (N)	3.270	2.580	118.160	0.7878
Nonanes (A)	2.410	2.120	106.168	0.8711
Decanes Plus	12.490	6.860	169.90	0.8120

5.4.1 Light-Oil Composition Analysis

As described earlier, for the compositional analysis of the condensates the ASTM D 5134 standard was used. This method can identify the components up to C_9 . But this method is not suitable if the composition of individual carbon fractions above C_{15} (in a condensate) is of interest. On the other hand light oil with higher percentage of C_{10+} fraction (e.g. $C_{10+} = 91.45$

mass % for light-oil-2) cannot be analyzed using ASTM D 5134 and condensate GC. To overcome this limitation, simulated distillation (Sim Dist) GC was used. The Sim Dist is a gas chromatograph similar to the GC-1 and GC-2 but can reach to a higher temperature by simulating a distillation.

By running oil sample on Sim Dist we obtain several peaks with their retention time on chromatogram. The conversion of the chromatographic retention time scale to the boiling point scale is obtained by using a standard mixture of n-alkanes with known boiling points. A mixture of n-paraffins was used with carbon number C_5 to C_{40} covering a temperature range 303.15 K to 873.15 K. After running the standard mixture, a calibration curve is obtained. The calibration curve represents retention time as a function of boiling point and is fitted to a polynomial. When an unknown sample is examined, the retention time is converted to corresponding boiling points by using calibration curve's correlation. Finally the composition of each carbon fraction in the sample is obtained. Light-oil-1, light-oil-2 and condensate-3 were analyzed up to C_{40} using Sim Dist. The condensed composition of light-oil-1 and light-oil-2 is given in Tables 5.10 and 5.11 respectively.

Table 5.10: Condensed Composition (Mass Fraction, w , Mole Fraction, x), Molar Mass (M) and Density (ρ) of Light-Oil-1.¹¹⁴

Component	$10^2 \times w$	$10^2 \times x$	$M/\text{g}\cdot\text{mol}^{-1}$	$\rho/\text{g}\cdot\text{cm}^{-3}$
Light End Total	0.922	4.240	59.132	0.5772
Methane	0.001	0.040	16.040	0.3000
Ethane	0.030	0.300	30.070	0.3580
Propane	0.130	0.810	44.100	0.5080
i-Butane (P)	0.090	0.410	58.122	0.5630
n-Butane (P)	0.220	1.020	58.122	0.5847
2,2-Dimethylpropane	0.001	0.020	72.150	0.5970
i-Pentane (P)	0.200	0.720	72.151	0.6246
n-Pentane (P)	0.250	0.900	72.151	0.6309
Hexanes Total	0.610	1.920	84.900	0.6679
Hexanes (P)	0.570	1.770	86.180	0.6628
Hexanes (N)	0.040	0.150	70.130	0.7500
Heptanes Total	1.710	4.920	92.140	0.7371
Heptanes (P)	0.550	1.450	100.200	0.6875
Heptanes (N)	1.120	3.350	89.160	0.7598
Heptanes (A)	0.040	0.120	78.110	0.8840
Octanes Total	2.500	6.210	107.140	0.7482
Octanes (P)	1.030	2.390	114.230	0.7073
Octanes (N)	1.350	3.460	103.790	0.7723
Octanes (A)	0.120	0.360	92.140	0.8710
Nonanes Total	2.810	6.090	123.240	0.7513
Nonanes (P)	1.820	3.790	128.110	0.7212
Nonanes (N)	0.670	1.490	120.160	0.7875
Nonanes (A)	0.320	0.810	106.170	0.8730
Decanes Plus	91.450	76.640	317.300	0.9283

Table 5.11: Condensed Composition (Mass Fraction, w , Mole Fraction, x), Molar Mass (M) and Density (ρ) of Light-Oil-2.¹¹⁵

Component	$10^2 \times w$	$10^2 \times x$	$M/\text{g}\cdot\text{mol}^{-1}$	$\rho/\text{g}\cdot\text{cm}^{-3}$
Light End Total	9.650	20.680	71.819	0.6271
Ethane	0.040	0.170	30.070	0.3580
Propane	0.770	2.350	44.100	0.5080
i-Butane (P)	0.790	1.830	58.124	0.5630
n-Butane (P)	2.780	6.470	58.124	0.5850
2,2-Dimethylpropane (P)	0.020	0.030	72.151	0.5970
i-Pentane (P)	2.190	4.100	72.151	0.6250
n-Pentane (P)	3.060	5.730	72.151	0.6310
Hexanes Total	5.290	8.410	85.170	0.6668
Hexanes (P)	5.020	7.880	86.180	0.6628
Hexanes (N)	0.270	0.530	70.130	0.7500
Heptanes Total	9.300	13.690	91.820	0.7360
Heptanes (P)	3.930	5.300	100.200	0.6877
Heptanes (N)	4.660	7.160	87.970	0.7617
Heptanes (A)	0.710	1.230	78.110	0.8840
Octanes Total	11.020	14.270	104.450	0.7594
Octanes (P)	4.440	5.260	114.230	0.7069
Octanes (N)	4.600	6.100	101.890	0.7722
Octanes (A)	1.980	2.910	92.140	0.8710
Nonanes Total	7.330	8.380	118.100	0.7811
Nonanes (P)	3.060	3.230	128.100	0.7207
Nonanes (N)	1.910	2.150	119.720	0.7856
Nonanes (A)	2.360	3.000	106.170	0.8719
Decanes Plus	57.410	34.570	224.700	0.8462

The properties such as overall density, molar mass and decane plus fraction of condensates and light oils used are given in Table 5.12 and Figure 5.15. The PNA distribution (in mass %) is calculated on the basis of known composition up to n-nonane using the following relations for paraffinic, naphthenic and aromatic contents respectively.

$$P = \frac{100(\text{mass}\%)_P}{\left[100 - (\text{mass}\%)_{C_{10+}}\right]} \quad 5.13$$

$$N = \frac{100(\text{mass}\%)_N}{\left[100 - (\text{mass}\%)_{C_{10+}}\right]} \quad 5.14$$

$$A = \frac{100(\text{mass}\%)_A}{\left[100 - (\text{mass}\%)_{C_{10+}}\right]} \quad 5.15$$

where subscripts P, N and A represent paraffinic, naphthenic and aromatic hydrocarbons respectively and C_{10+} represents decane plus fraction.

The density and the molar mass of the condensates (condensate-1 and condensate-2) are close to each other with varying decane plus fraction. The light oils have higher molar mass, density and decane plus fraction than that of condensates as shown in Table 5.12.

Table 5.12: Overall Density, Molar Mass and C_{10+} Fraction of Condensates and Oils Investigated in This Work.

Reservoir Fluid	References	Density ($\text{g}\cdot\text{cm}^{-3}$)	Molar Mass ($\text{g}\cdot\text{mol}^{-1}$)	C_{10+} (mass %)
Condensate-1	This Work ¹¹⁰	0.7562	112.70	40.77
Condensate-2	This Work ¹¹²	0.7385	106.90	27.96
Condensate-3	Yussuf ¹¹⁵	0.7210	97.37	12.49
Light-Oil-1	Frost ¹¹⁴	0.9060	266.00	91.45
Light-Oil-2	Yussuf ¹¹⁵	0.7784	135.20	57.41

Figure 5.15 shows PNA distribution of condensates and oils presented in this chapter based on the compositions given in Tables 5.4 and 5.11. The PNA distribution has been calculated on the basis of known composition from C_1 to C_9 , assuming same PNA distribution in plus fraction. It can be seen from Figure 5.15 that condensate-1 and condensate-2 are very similar on the basis of their PNA distribution. The paraffinic content is higher than the naphthenic and the aromatic in both the condensates. Therefore they can be called as overall paraffinic in nature. The condensate-3 has less aromatic and more naphthenic content than that of condensate-1 and condensate-2. The aromatic content of light-oil-1 is lower than that of the condensates presented in this chapter.

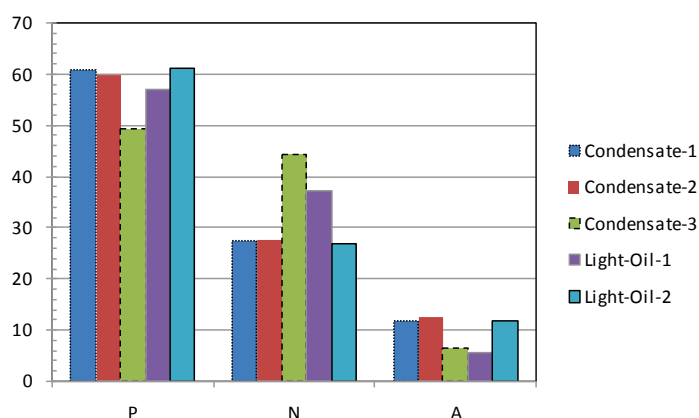


Figure 5.15: PNA distribution of condensates (condensate-1¹¹⁰, condensate-2¹¹² and condensate-3¹¹⁵) and oils (light-oil-1¹¹⁴ and light-oil-2¹¹⁵) studied.

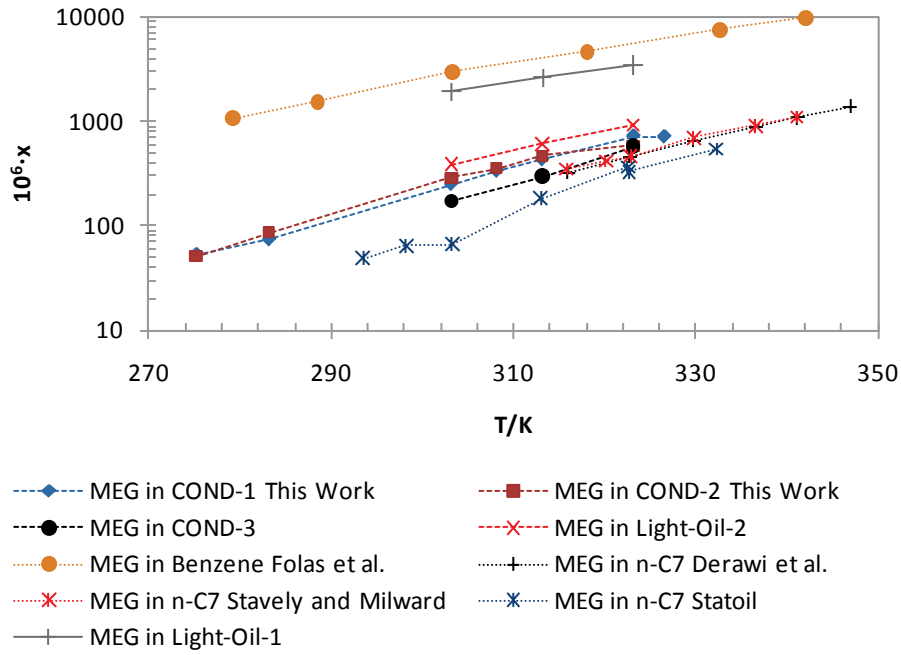


Figure 5.16: Comparison of the solubility (in Mole Fraction, x) of MEG in well-defined hydrocarbons (n-heptane^{12,109,111} and benzene¹¹) and reservoir-fluids (condensate-1¹¹⁰, condensate-2¹¹², condensate-3¹¹⁵ Light-Oil-1¹¹⁴ and light-oil-2¹¹⁵) as a function of temperature (K).

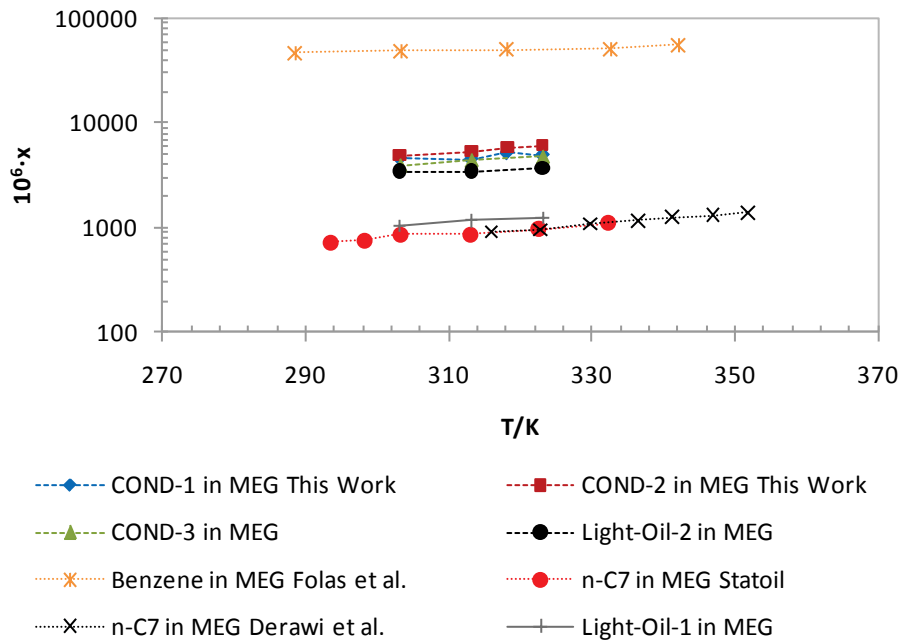


Figure 5.17: Comparison of the solubility (in Mole Fraction, x) of well-defined hydrocarbons (n-heptane^{111,113} and benzene¹¹) and reservoir-fluids (condensate-1¹¹⁰, condensate-2¹¹², condensate-3¹¹⁵ Light-Oil-1¹¹⁴ and light-oil-2¹¹⁵) in MEG as a function of temperature (K).

5.4.1.1 Mutual Solubility of Reservoir-Fluids and MEG

It is shown in Figures 5.16 and 5.17 that similar to condensate-1 and condensate-2 mutual solubility of light-oil-1, light-oil-2 and condensate-3 lies between the values for the solubilities of benzene + MEG and n-heptane + MEG systems. Furthermore the solubility of condensate-3 in MEG is lower than that of condensate-2 (in MEG). This is because the aromatic content (i.e. benzene, toluene and xylene) of condensate-3 is lower than that of condensate-2 as shown in Table 5.13. This is illustrated in Figure 5.18 which shows that the solubility contribution of benzene, toluene, xylene and ethylbenzene from condensate-3 in MEG is lower than the contribution from the condensate-2 at the same temperature of 303.15 K.

It is shown that aromatic hydrocarbons (in C₇ to C₉ carbon fractions) play a dominant role in mutual solubility. The more aromatic the condensate is the higher will be the solubility and vice versa. This is clear from the fact that even though condensate-3 is lighter (lower C₁₀₊ fraction) than condensate-2 as shown in Table 5.12 and it has more naphthenic content as shown in Figure 5.15 the mutual solubility of condensate-3 and MEG is lower than that of condensate-2 and MEG.

Table 5.13: Comparison of Compositions of Condensate-2¹¹² and (Pure) Condensate-3.¹¹⁵

Components	Condensate-2 Mass %	Condensate-3 Mass %
Light End Total	15.396	16.09
Ethane	0.00	0.03
Propane	0.00	0.49
i-Butane (P)	0.008	3.26
n-Butane (P)	0.287	3.94
i-Pentane (P)	6.885	4.53
n-Pentane (P)	8.214	4.29
Hexanes Total	11.360	12.62
Hexanes (P)	10.664	11.50
Hexanes (N)	0.696	1.10
Heptanes Total	17.738	25.74
Heptanes (P)	7.765	6.23
Heptanes (N)	7.519	18.39
Heptanes (A)	2.454	1.12
Octanes Total	17.989	24.24
Octanes (P)	4.920	6.26
Octanes (N)	9.613	15.90
Octanes (A)	3.457	2.08
Nonanes Total	9.552	8.40
Nonanes (P)	4.476	2.72
Nonanes (N)	2.082	3.27
Nonanes (A)	2.994	2.41
Decanes Plus	27.964	12.49

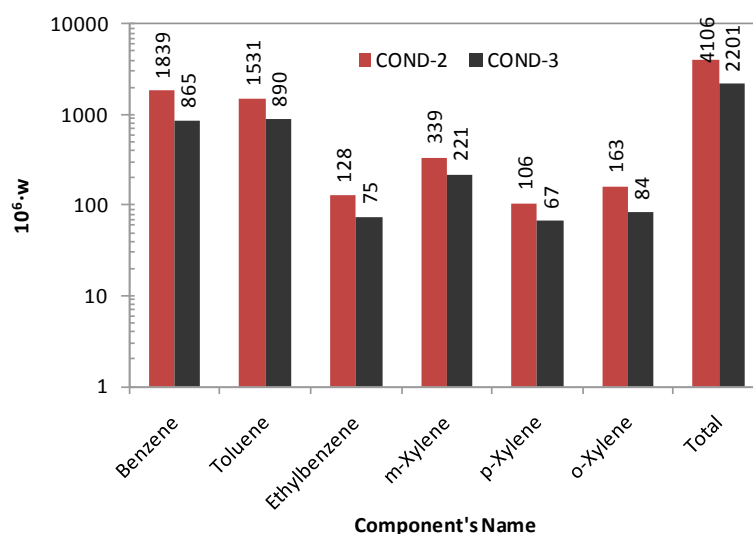


Figure 5.18: Comparison of solubility of aromatic content (of condensate-2 and condensate-3) in MEG for condensate-2 + MEG and condensate-3 + MEG systems at 303.15 K.

5.4.1.2 Mutual Solubility of Light-Oil-1 and MEG

The light-oil-1 is very different from light-oil-2 and the other condensates. It has much higher C_{10+} fraction and density as given in Table 5.12. It has lower aromatic content as compared to condensate-1, condensate-2 and light-oil-2, as shown in Figure 5.15. It should also be mentioned that the PNA distribution (like other reservoir fluids in this work) is based on C_2 - C_9 fractions. The solubility of MEG in light-oil-1 is higher than the three condensates and light-oil-2 as shown in Figure 5.16. This may be due to the reasons that Light-oil-1 is more naphthenic than condensate-1, condensate-2 and light-oil-2. Furthermore plus fraction may be more aromatic than the known C_2 - C_9 carbon fractions. This may also be due to the experimental error as light-oil-1 was very difficult to handle for mutual solubility experiments due to its higher viscosity and density (e.g. more than two days were required to attain the equilibrium).

Solubility of light-oil-1 in MEG is lower than the solubility of the condensates and light-oil-2. This may be because light-oil-1 has higher fraction of heavy hydrocarbons. Due to the higher molar mass of light-oil-1 (266 g.mole^{-1}) than MEG ($62.07 \text{ g.mole}^{-1}$), the trends of solubility are reversed when converted from mass fraction to mole fraction as shown in Figure 5.19 (i.e. the solubility of light-oil-1 in MEG is higher than the solubility of MEG in light-oil-1 in mass fraction but the solubility of light-oil-1 in MEG is lower than the solubility of MEG in light-oil-1 in mole fraction).

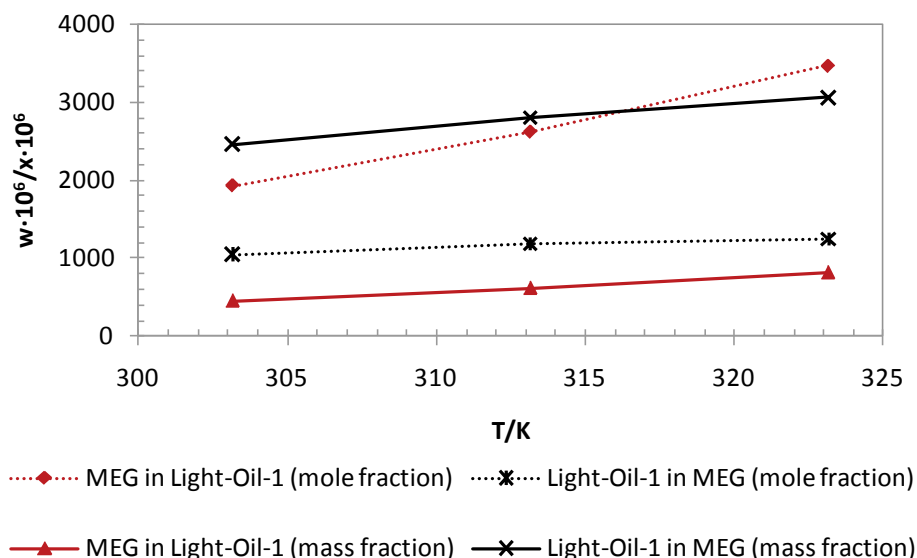


Figure 5.19: Comparison of mutual solubility of light-oil-1 and MEG presented in mass and mole fractions.¹¹⁴

5.5 Conclusions

In this chapter new experimental data for mutual solubility of North Sea condensates + MEG systems are presented. To evaluate the effect of water on mutual solubility condensates + MEG + water systems are experimentally investigated and the data are presented. The experimental work was carried out for liquid-liquid equilibrium in the temperature range of 275.15 to 323.15 K at atmospheric pressure.

A method for the measurement of the mutual solubility of condensates/oil, MEG and water has been established and tested. The detailed composition was measured using ASTM D5134 and 85 to 90 components were detected and identified up to n-nonane. The paraffinic naphthenic and aromatic contents in each carbon fraction and in the overall reservoir fluids are calculated. The detailed chromatographic analysis of reservoir fluid (i.e. condensate-2) and calculation methods used are presented.

In the reservoir-fluid + MEG systems, the mutual solubility increases with increasing temperature. The solubility of aromatic hydrocarbons is much higher than that of naphthenic and paraffinic hydrocarbons in each carbon fraction. Benzene and toluene contribute a major part to the solubility of reservoir fluid in MEG. Therefore the more aromatic (in C₇-C₉ carbon fraction) the condensate is the higher will be the solubility and vice versa. In the reservoir-fluid + MEG + water system, the mutual solubility of MEG and condensate decreases with increasing water content in the polar phase and the solubility of some of the components become

negligible. The mutual solubility increases with increasing temperature. The solubility of aromatic hydrocarbon is higher than that of naphthenic and paraffinic hydrocarbons. The aromatic components like benzene and toluene contribute almost half of the total solubility of condensate in MEG.

The data presented in this chapter are new data and no data could be found for such systems to make a comparison. However the reproducibility of the data is satisfactory.

Modeling of Reservoir Fluids

Phase Behavior

Prediction of the mutual solubility of reservoir fluids, MEG and water is important for the oil industry to ensure production and processing as well as to satisfy environmental regulations. The CPA equation of state has been successfully applied in the past to well-defined systems containing associating compounds.^{14,81} It has also been extended to reservoir fluids in presence of water and polar chemicals using a Pedersen like characterization method with modified correlations for critical temperature, pressure and acentric factor.¹⁶ In this chapter CPA is applied to the modeling of reservoir-fluid + MEG and reservoir-fluid + MEG + water systems. The reservoir fluids consist of three condensates and two light-oils obtained from the offshore gas fields in the North Sea. Satisfactory correlations and predictions are obtained for the mutual solubility of MEG and reservoir fluids. Similarly modeling results for reservoir-fluid + MEG + water systems are in good agreement with the experimental data. Generally the modeling results for reservoir-fluid + MEG + water systems are as good as for well-defined hydrocarbon + MEG + water systems using the CPA equation of state.

6.1 Introduction

As the exploitable oil resources decrease, more sophisticated recovery methods are employed in the oil industry to produce the remaining resources. One result of using more sophisticated recovery methods is that oil field chemicals are more widely used, especially in the offshore oil production. These chemicals belong to different families like alcohols, glycols, alkanolamines, surfactants and polymers. They have various functions, e.g., methanol and MEG are used as gas hydrate inhibitors, surfactants are used to lower interfacial tension between crude oil and microemulsion and polymers in a polymer-waterflooding process act primarily as thickeners. Over the last years, the use of these chemicals has increased considerably.^{3,6}

The knowledge of the phase equilibria of aqueous mixtures with hydrocarbons and chemicals is important for environmental purposes since hydrocarbons must be removed from gas processing, refinery and petrochemical plant wastewater streams and from sea or fresh water

when oil spills occurs. For this purpose, the solubility and volatility of hydrocarbons is required to describe their phase distribution through the removal process. Such information is also important in the design and operation of separation equipments. In addition, it is also useful in predicting the water and the chemical contents of the fuels.⁸³

Most phase equilibrium calculations on oil and gas mixtures are performed using a cubic equation of state, for example, the Soave-Redlich-Kwong (SRK) or Peng-Robinson (PR) EoS.¹¹⁶ However, systems containing reservoir fluids and polar/associating compounds (e.g. water, glycols and methanol etc.) are hard to describe using the conventional EoS especially at high temperature and pressure conditions.¹⁶ The CPA equation of state has been very successful in describing such complex systems.¹⁴

The CPA equation of state (EoS), proposed by Kontogeorgis et al.¹⁵, is an extension of the conventional SRK EoS. The equation combines the simplicity of a cubic equation of state and Wertheim's theory for the association part.⁹ It gives a better description of systems containing associating compounds compared with the empirical or semi-empirical modifications of cubic EoS, and reduces to the SRK EoS for non-associating compounds.¹⁶ In previous studies CPA has been extensively tested for well-defined systems containing associating compounds, most of which have already been summarized by Kontogeorgis et al.^{14,51,117}

The CPA EoS has been extended to reservoir fluids by Yan et al.¹⁶ using a characterization procedure similar to that of Pedersen et al.⁷⁹ and a set of new correlations for the critical properties for CPA. Calculations presented¹⁶ for reservoir-fluids + water and reservoir fluids/water/methanol/glycols showed promising results. However, data are available for very few systems, especially for gas-condensates, and more data are required for an extensive investigation and full validation of the model.¹⁴ Therefore an experimental work has been carried out at Statoil research center to get more data. A method of measurement of mutual solubility of reservoir fluid, MEG and water has been established and tested in this work.^{110,112} The details of experimental work are given in chapter 5. Initially two North Sea condensates were investigated in this work and LLE data was produced for condensate-1/condensate-2 + MEG and condensate-1/condensate-2 + MEG + water systems. Based on the experimental method established in this work^{110,112} the experimental work was extended to a third condensate (condensate-3) and two light-oils (light-oil-1 and light-oil-2) as a part of master thesis projects.^{114,115} In this chapter thermodynamic modeling of mutual solubility of the above systems is carried out using the CPA EoS and the characterization method of Yan et al.¹⁶

This chapter is divided into three sections. The first section provides the introduction to the work, its scope, various tools which are generally used and their limitations and the capabilities. The second section presents results and discussion of modeling of the condensates and the oils and a comparison for reservoir fluids systems modeling with that of well-defined hydrocarbons systems. Finally the third section presents the conclusions.

6.2 Results and Discussion

6.2.1 Condensate-1

The composition of condensate-1 is given in Table 5.5 with density, molar mass and PNA distribution of carbon fractions (C_6 to C_9). The experimental data for LLE of condensate-1 + MEG and condensate-1 + MEG + Water systems are given in Tables 5.6 and 5.7 respectively. The following sections will focus on the characterization and the modeling using the CPA equation of state.

6.2.1.1 Condensate-1 Characterization

The composition of condensate-1 is further simplified as given in Table 6.1 where carbon fractions (C_6 to C_9) are presented without their PNA distribution.

Table 6.1: The Simplified Composition (in Mole Fraction, x), Molar Mass (M) and Density (ρ) of Condensate-1 Used for the Characterization.

Components	$10^2 \times x$	$M/\text{g}\cdot\text{mol}^{-1}$	$\rho/\text{g}\cdot\text{cm}^{-3}$
Ethane	0.004		
Propane	0.896		
i-Butane	2.382		
n-Butane	7.813		
i-Pentane	5.502		
n-Pentane	7.275		
C_6	10.292		
C_7	16.046	91.40	0.7362
C_8	16.632	103.60	0.7686
C_9	8.903	118.50	0.7806
C_{10+}	24.254	189.40	0.8464
Average density			0.7562
Average molar mass		112.7	

Using information from Table 6.1 and Pedersen et al.⁷⁹ method of characterization with the modified correlation of Yan et al.¹⁶ for critical temperature, critical pressure and acentric factor, the condensate-1 has been characterized. The results obtained after lumping are given in Table 6.2.

Table 6.2: Condensate-1 after Characterization and Lumping.

Components	Mole %	T_{cm} (K)	P_{cm} (bar)	ω_m
Ethane	0.004	305.4	48.8	0.098
Propane	0.896	378.6	47.2	0.105
i-Butane	2.382	415.8	40.1	0.151
n-Butane	7.813	436.3	43.6	0.158
i-Pentane	5.502	460.4	33.8	0.227
n-Pentane	7.275	479.4	38.0	0.217
C ₆	10.292	522.3	34.9	0.244
C ₇	16.046	560.8	35.9	0.230
C ₈	16.632	593.5	35.0	0.254
C ₉	8.903	621.2	32.3	0.293
C ₁₀	5.038	647.8	30.4	0.325
C ₁₁	3.992	671.7	28.9	0.354
C ₁₂	3.162	694.8	27.4	0.383
C ₁₃	2.506	715.4	26.3	0.409
C ₁₄	1.985	735.9	25.1	0.436
C ₁₅ - C ₁₅	2.819	764.6	23.5	0.476
C ₁₇ - C ₁₈	1.769	798.1	21.9	0.522
C ₁₉ - C ₂₂	1.808	835.3	20.3	0.570
C ₂₃₊	1.176	911.3	17.2	0.698

6.2.1.2 Mutual Solubility of Condensate-1 and MEG

The hydrocarbon fractions that constitute the condensate cover a wide range from light to heavy carbon fractions and therefore different k_{ij} for each pair (MEG-HC) should be used. The k_{ij} are usually obtained from well-defined binary systems (e.g. n-hexane-MEG, n-heptane-MEG, etc.). The MEG-HC systems previously studied with the CPA EoS are given in Table 6.3 along with the interaction parameter used.

Table 6.3: Binary Interaction Parameters for LLE of MEG-HC Systems.

System	k_{ij}
MEG-methane ¹¹⁸	0.134
MEG-n-hexane ⁶⁶	0.059
MEG-n-heptane ⁶⁶	0.047
MEG-methylcyclohexane ⁶⁶	0.061
MEG-n-nonane ¹¹⁵	0.010

It can be seen from Table 6.3 that the interaction parameters are available for few hydrocarbon (paraffinic and naphthenic) components and MEG due to scarcity of experimental data and possible difficulty involved in measurement of such low solubilities. In this work as a first step a simple strategy is adopted i.e. to use the same k_{ij} for all MEG-HC pairs. The k_{ij} values used are temperature independent. Furthermore a correlation has been developed (for MEG-

HC) similar to the one given in Table 6.4 (for water-HC). This correlation is given by the following equation 6.1.

$$k_{ij} = -0.0153 \cdot (\text{carbon number}) + 0.1503 \quad (6.1)$$

where k_{ij} is the binary interaction parameter between MEG and hydrocarbons given as function of carbon number as shown in Figure 6.1.

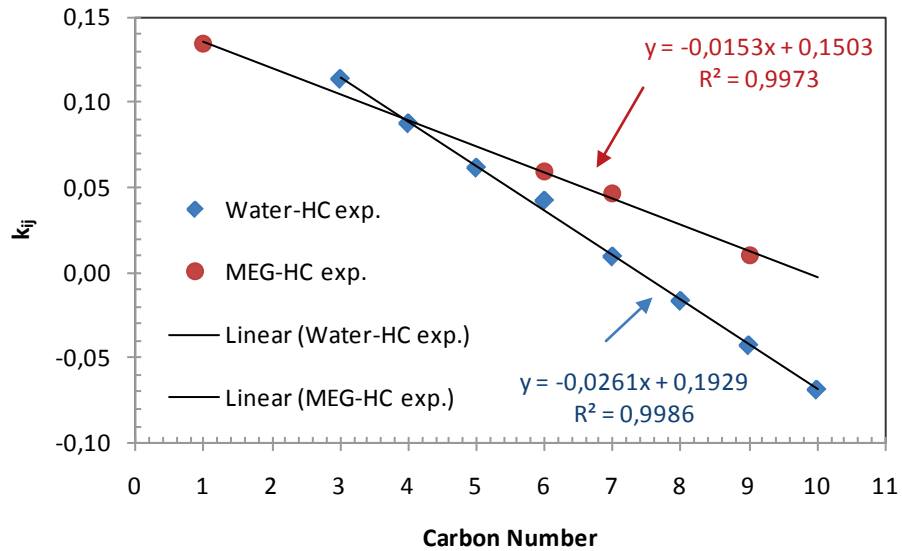


Figure 6.1: Correlation for binary interaction parameters for water-HC⁷⁷ and MEG-HC (this work).

The binary interaction parameters between water and hydrocarbons are obtained from a generalized expression using the equation given in Table 6.4⁷⁷. Table 6.4 shows % AAD in the solubility of water in the hydrocarbon as well as the solubility of HC in the water for various water-alkane systems.

Table 6.4: Binary Interaction Parameters for LLE of Water-Hydrocarbon Systems, Based on the Generalized Expression Which is Derived Based on Data from Propane up to n-Decane: $k_{ij} = -0.026 \cdot (\text{carbon number}) + 0.1915$.^{77,81}

Hydrocarbon	T range (K)	k_{ij}	% AAD in x_{HC}	% AAD in x_w
Propane	278 - 366	0.1135	35.9	3.4
Butane	310 - 420	0.0875	26.5	11.7
n-pentane	280 - 420	0.0615	28.4	13.4
n-hexane/cyclohexane	280 - 473	0.0422 ^a	---	---
n-heptane	280 - 420	0.0095	63.3	11.5
n-octane	310 - 550	-0.0165	44.1	9.7
n-nonane	290 - 566	-0.0425 ^b	---	---
n-decane	290 - 566	-0.0685	264	8.2
n-C ₁₀ to n-C ₂₃ +	---	-0.0685 ^c	---	---

^a Average of n-hexane and cyclohexane

^b Using generalized correlation

^c Same as for n-decane

In condensate-1 + MEG system, MEG is a self-associating compound whereas hydrocarbons are inert or non-associating. The only binary interaction parameter therefore required is that between MEG and each hydrocarbon (fraction from C₃ to C₂₃) whereas no combining rules are required.

The CPA correlations for the mutual solubility of condensate-1 and MEG along with the experimental data are shown in Figure 6.2. The mutual solubility of MEG and condensate-1 is estimated satisfactorily even with zero binary interaction parameters (pure prediction). The modeling results can be improved using a smaller non-zero interaction parameter ($k_{ij}=0.02$). It has also been observed that use of a non-zero binary interaction parameter is required for obtaining simultaneous good fitting of the solubility of HC in the polar phase and MEG in hydrocarbon phase. Similar trends have been observed in the work for well-defined hydrocarbons and polar compounds (MEG, water) systems.¹¹⁹ In the previous work of Yan et al.¹⁶ an average $k_{ij}=0.05$ has been used for all MEG and hydrocarbon pairs for modeling of the reservoir fluid, MEG and water systems. Using average binary interaction parameter of 0.05 between MEG and hydrocarbons, CPA under-estimates the mutual solubility of MEG and condensate-1 as shown in Table 6.5. This may be due to the presence of aromatics in the condensate-1. The % AAD for the mutual solubility for condensate-1 + MEG system is given in Table 6.5 along with the binary interaction parameter used.

A preliminary calculations for mutual solubility of condensate-1 and MEG are also made using k_{ij} obtained from the correlations given in equation 6.1. The modeling results show that the solubility of MEG in condensate-1 is in good agreement with experimental data but the

solubility of condensate-1 in MEG is under-predicted. The prediction of solubility of condensate-1 in MEG can be improved by taking in to account the cross-association volume and the energy for MEG and aromatic hydrocarbons (i.e. benzene, toluene and xylene) present in the condensate. But it shown in Figure 6.2 that satisfactory modeling results are obtained using existing characterization method (of Yan et al.) without explicitly taking aromaticity into account and using an average k_{ij} for all MEG-HC pairs.

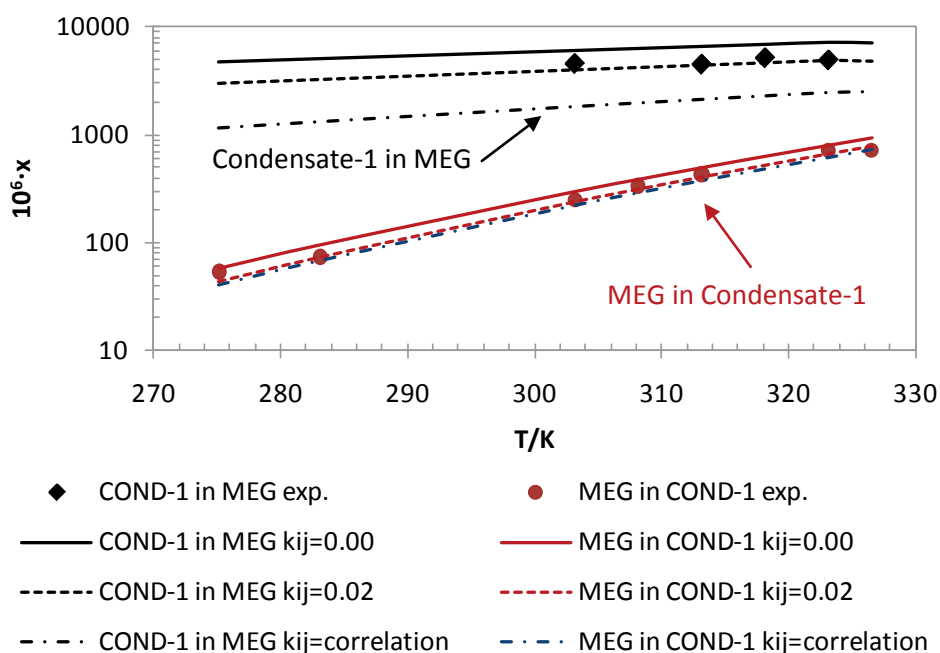


Figure 6.2: Mutual solubility (in mole fraction, x) of condensate-1 and MEG as a function of temperature (K) for the condensate-1 + MEG system. The experimental data¹¹² are indicated as points and the CPA calculations as lines.

Table 6.5: CPA Modeling of the Condensate-1 (COND-1) + MEG System and the Effect of k_{ij} on the Mutual Solubility of Condensate-1 and MEG.

k_{ij} of MEG-HC	% AAD (COND-1 in MEG)	% AAD (MEG in COND-1)
0.05	48	28
0.02	7	7
0.00	39	16

6.2.1.3 Mutual Solubility of Condensate-1, MEG and Water

In the condensate-1 + MEG + water system, in addition to self-association, we have two compounds (MEG, water) which cross-associate. The Elliott combining rule is used for the MEG and water with $k_{ij}=-0.115$ taken from the previous work.⁶⁷ The modeling results using an average binary interaction parameter (same as for COND-1 + MEG system) for all MEG-HC pairs

and for water-HC from the correlation are given in Table 6.6. CPA satisfactorily predicts the mutual solubility of condensate-1, MEG and water. The modeling results are correct in order of magnitude for most of the data points (except one) presented in Table 6.6. The deviations between experimental data and calculations are summarized in Table 6.7.

Table 6.6: Experimental Data¹¹⁰ and CPA Modeling for Condensate-1 + MEG + Water System at Temperature 323.15 K and Pressure 1 atm. The k_{ij} Values for the MEG-Water=-0.115, MEG-HC=0.02 and Water-HC are Taken from Table 6.4.

Component	Feed (mole fraction)	Polar Phase (mole ppm)			Hydrocarbon Phase (mole ppm)		
		Exp.	Cal.	% Dev.	Exp.	Cal.	% Dev.
MEG	0.1324	---	---	---	61	104	-70
Water	0.6843	---	---	---	1218	1102	10
COND-1	0.1833	69	39	43	---	---	---
MEG	0.3041	---	---	---	172	276	-61
Water	0.4488	---	---	---	946	764	19
COND-1	0.2472	417	311	26	---	---	---
MEG	0.4992	---	---	---	381	482	-27
Water	0.1909	---	---	---	402	363	10
COND-1	0.3098	1793	1773	1	---	---	---

The solubility of water in condensate-1 decreases with increasing MEG mole fraction in the polar phase. The solubility of MEG in condensate and condensate in polar phase increases with increasing MEG content in the polar phase as shown in Figure 6.3. These experimental trends are well captured using the CPA EoS even for this complex mixture containing associating and non-associating fluids. The hydrocarbon phase is also a complex North Sea condensate with numerous well-defined and ill-defined components with paraffinic, naphthenic and aromatic nature. Investigation are also made using various other combinations for k_{ij} as shown in Table 6.7. It is shown that the better predictions are obtained for condensate-1 + MEG + water system using $k_{ij}=0.02$ for all MEG-HC pairs and for water-HC from the Table 6.4.

In contrast to CPA, classical EoS are not sufficient to describe the phase behavior of water and hydrocarbon mixtures. Binary interaction parameters of the order of 0.5 have often been used.¹²⁰ Various approaches have been used. Søreide and Whitson have used the classical Peng-Robinson EoS¹²¹ with temperature dependent binary interaction parameters and different binary interaction parameters for the hydrocarbon and the aqueous phase.¹²² Kabadi and Damer have used a modified SRK EoS for water + hydrocarbon systems which gives satisfactory results for the mutual solubility of hydrocarbons and water. But it can not model satisfactorily mixtures with hydrate inhibitors such as MEG and methanol.¹²³

Table 6.7: Average Deviation (%) of CPA Predictions from Experimental Data for Investigated Condensate-1 (COND-1) + MEG + Water System at T=323.15 K and P=1 atm.

k_{ij}		% AAD			
		<i>Polar Phase</i>	<i>Hydrocarbon Phase</i>		<i>Global</i>
<i>Water-HC</i>	<i>MEG-HC</i>	<i>COND-1</i>	<i>MEG</i>	<i>Water</i>	
From Table 6.4	0.02	24	52	13	30
From Table 6.4	0.00	27	93	12	44
0.00	0.00	39	86	17	47

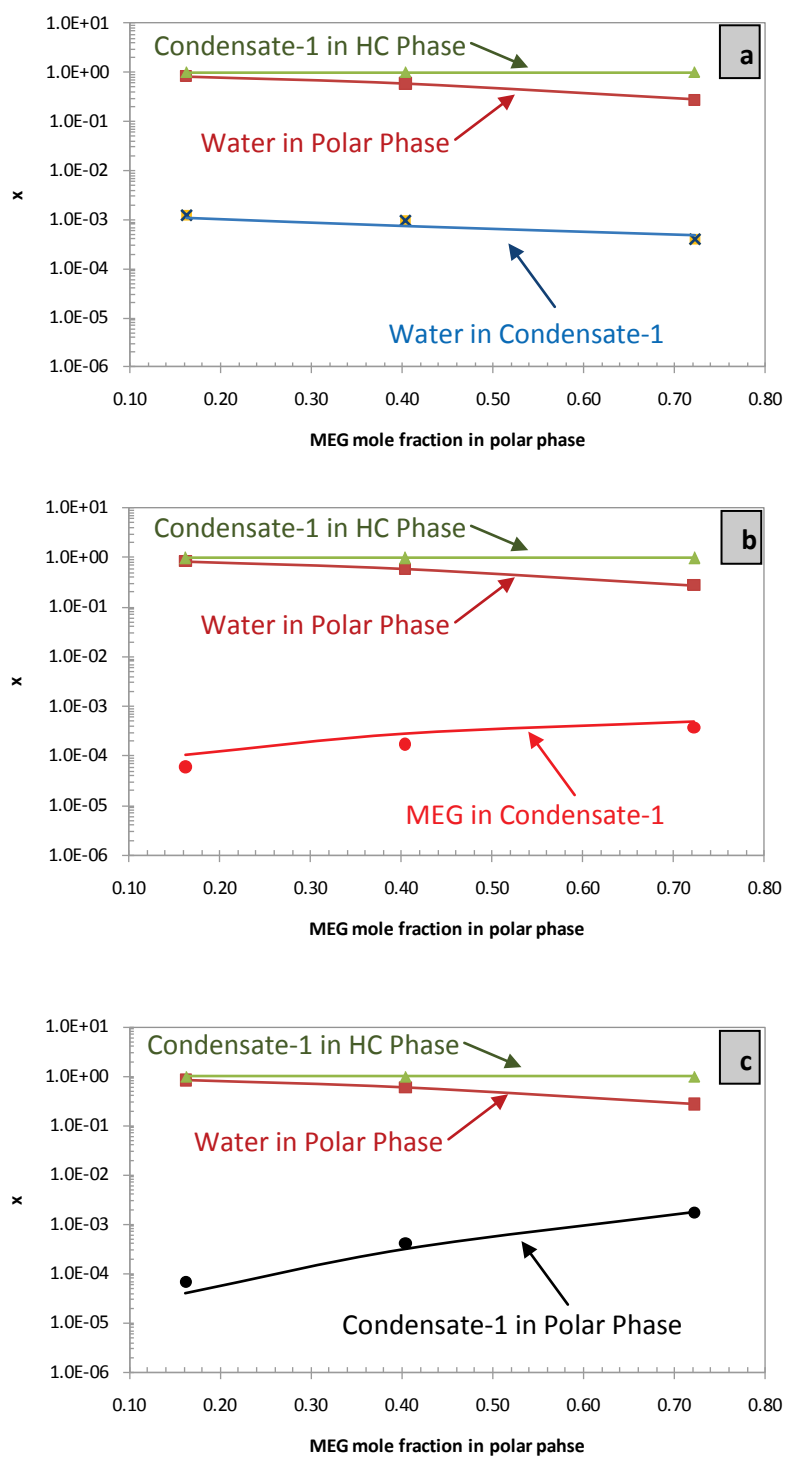


Figure 6.3: Modeling of the mutual solubility (in mole fraction, x) of condensate-1, MEG and water at temperature 323.15 K and pressure 1 atm.: (a) water in condensate (b) MEG in condensate-1 (c) condensate-1 in polar phase. The points are experimental data¹¹⁰ and lines are modeling results with the CPA EoS using k_{ij} for MEG-water=-0.115, HC-MEG=0.02 and HC-water from the correlation of Table 6.4.

6.2.2 Condensate-2

The detailed composition of condensate-2 is given Table 5.3 and condensed composition is given in Table 5.4. The composition of condensate-2 was analyzed in this work (at Rotvoll Laboratory, Statoil R and D) and by an external laboratory. The two compositions are different from each other with different decane plus fraction as shown in Table 6.8. The overall PNA distribution is the same using either of those compositions. The modeling is carried out using both compositions to investigate the effect and the results are presented in the following sections.

Table 6.8: The Composition of Condensate-2 from This Work and an External Laboratory.

Component	*This Work $w \cdot 100$	External Lab $w \cdot 100$
Light End Total	15.396	18.220
i-Butane (P)	0.008	0.010
n-Butane (P)	0.287	0.340
i-Pentane (P)	6.885	8.090
n-Pentane (P)	8.214	9.780
Hexanes Total	11.360	14.31
Hexanes (P)	10.664	13.38
Hexanes (N)	0.696	0.93
Heptanes Total	17.738	21.17
Heptanes (P)	7.765	8.74
Heptanes (N)	7.519	9.41
Heptanes (A)	2.454	3.02
Octanes Total	17.989	22.46
Octanes (P)	4.920	7.48
Octanes (N)	9.613	10.45
Octanes (A)	3.457	4.53
Nonanes Total	9.552	13.37
Nonanes (P)	4.476	5.89
Nonanes (N)	2.082	3.41
Nonanes (A)	2.994	4.07
Decanes Plus	27.964	10.47

6.2.2.1 Condensate-2 Characterization

Condensate-2 is characterized using both compositions. The components properties are given in Tables 6.9 and 6.10 using the condensate-2 composition from this work and from the external laboratory respectively. As the composition results from the external laboratory showed lower decane plus fraction, no lumping has been carried out. But for higher decane plus fraction as shown from this work some of the carbon fractions are lumped together as shown in Table 6.10.

Table 6.9: Characterization of Condensate-2 Using the Composition Obtained from External Laboratory.

Components	Mole %	T_{cm} (K)	P_{cm} (bar)	ω_m
i-Butane	0.020	415.8	40.1	0.151
n-Butane	0.550	436.3	43.6	0.158
i-Pentane	10.712	460.4	33.8	0.227
n-Pentane	12.973	479.4	38.0	0.217
C ₆	16.123	522.3	34.9	0.244
C ₇	22.294	562.5	36.6	0.225
C ₈	20.674	592.8	34.7	0.256
C ₉	10.772	620.7	32.1	0.294
C ₁₀	1.708	646.6	30.1	0.328
C ₁₁	1.212	670.0	28.4	0.359
C ₁₂	0.860	692.5	26.9	0.390
C ₁₃	0.610	712.7	25.6	0.417
C ₁₄	0.433	732.7	24.4	0.446
C ₁₅	0.307	752.7	23.2	0.476
C ₁₆	0.218	770.1	22.2	0.502
C ₁₇	0.155	787.2	21.3	0.528
C ₁₈₊	0.378	835.0	19.2	0.599

Table 6.10: Condensate-2 after Characterization and Lumping Using the Composition from This Work.

Components	Mole %	T_{cm} (K)	P_{cm} (bar)	ω_m
i-Butane	0.015	415.8	40.1	0.151
n-Butane	0.527	436.3	43.6	0.158
i-Pentane	10.200	460.4	33.8	0.227
n-Pentane	12.174	479.4	38.0	0.217
C ₆	14.289	522.3	34.9	0.244
C ₇	20.837	562.4	36.5	0.226
C ₈	18.433	592.7	34.7	0.256
C ₉	8.558	617.9	31.2	0.302
C ₁₀	2.695	642.8	29.0	0.339
C ₁₁	2.210	665.2	27.1	0.373
C ₁₂ -C ₁₃	3.297	695.9	24.8	0.421
C ₁₄	1.218	725.2	22.8	0.469
C ₁₅	0.999	744.4	21.5	0.503
C ₁₆ -C ₁₇	1.490	768.6	20.1	0.547
C ₁₈ -C ₂₀	1.372	801.0	18.4	0.604
C ₂₁ -C ₂₄	0.924	841.4	16.5	0.680
C ₂₅₊	0.762	914.0	13.5	0.829

6.2.2.2 Mutual Solubility of Condensate-2 and MEG

The modeling results for the mutual solubility of condensate-2 and MEG are shown in Figure 6.4 as a function of temperature. The results presented are in very good agreement with the experimental data. The results are pure predictions as no binary interaction parameters have

been used. A comparison of the modeling results using both compositions is also made as given in Table 6.11. The results are equally good using either of the condensate's compositions as shown in Figure 6.4. The results obtained using the condensate's composition measured in this work are slightly superior to those of external laboratory composition.

The first difference between the two compositions given in Table 6.8 is the decane plus fraction. The analysis from this work shows $C_{10+}=27.964$ (mass %) whereas the external laboratories composition shows $C_{10+}=10.47$ (mass %). The phenomena of getting similar results using the two different compositions (of decane plus) for condensate-2 can be explained by the experimental observations described in chapter 5. The hydrocarbons in C_4 - C_9 carbon fractions contribute a main part in the solubility of condensate-2 in MEG as shown in Figures 5.11 and 5.12 (chapter 5). For example at temperature 323.15 K the total solubility of condensate-2 in pure MEG is 8777 mass ppm. Here the contribution from decane plus fraction is only 233 mass ppm. This provides a clear indication that the solubility of decane plus fraction in MEG is negligible as compared to the total solubility.

Moreover both compositions show similar PNA distribution (P=60 mass %, N=28 mass % and A=12 mass %). It has been observed that aromatic hydrocarbons in C_6 - C_9 carbon fractions play a dominant role in the mutual solubility of condensate in MEG as shown in Figures 5.11 and 5.12. Here almost half of the solubility of condensate-2 in MEG is due to benzene and toluene. As both compositions show similar PNA distribution equally good results are obtained.

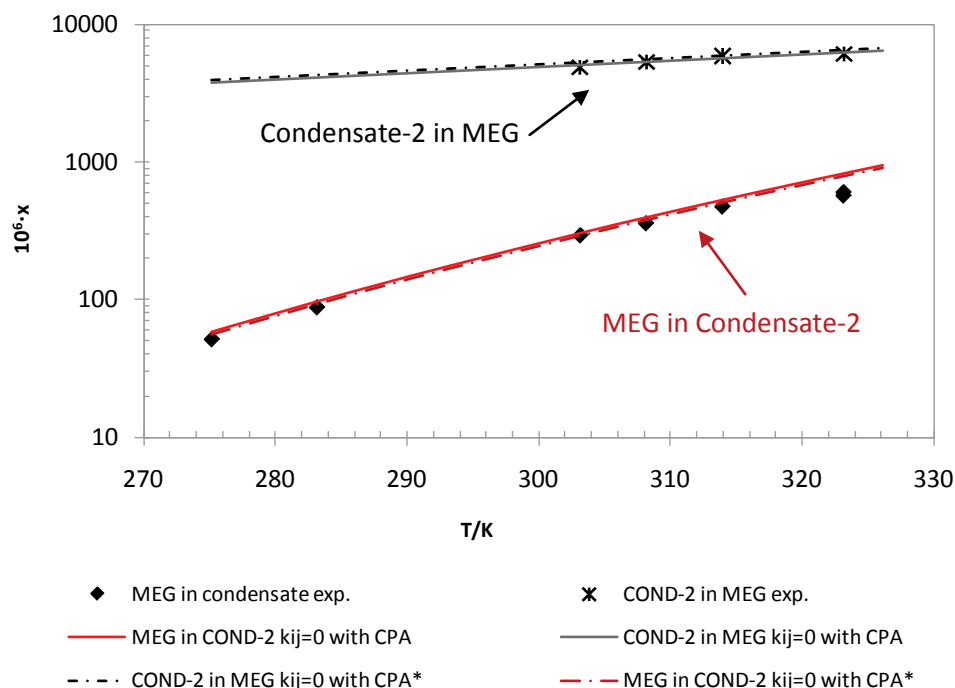


Figure 6.4: Mutual solubility (in mole fraction, x) of condensate-2 and MEG as a function of temperature (K) for condensate-2 + MEG system. Experimental data¹¹² are indicated as points and the CPA calculations as lines. Modeling results are presented using condensate-2 composition from this work* and external laboratory.

Table 6.11: Deviations of the CPA Modeling Results from the Experimental Data for Condensate-2 + MEG and Condensate-2 + MEG + Water Systems. A Comparison in Global AAD Using Condensate-2 Composition from This Work and from External Laboratory is Presented.

System	T/K	Global % AAD	
		This Work	External Lab
Condensate-2 + MEG	275.15-323.15	17	29
Condensate-2 + MEG + Water	303.15	43	42
Condensate-2 + MEG + Water	323.15	44	43

6.2.2.3 Mutual Solubility of Condensate-2, MEG and Water

The modeling results for the condensate-2 + MEG + water system at temperatures 303.15 and 323.15 K are given in Table 6.12. At each temperature three feed composition are used to investigate the effect of MEG mole fraction in polar phase on mutual solubility. This complex mixture of associating (MEG, water) and non-associating compounds (condensate's components) is modeled with the CPA EoS using temperature independent k_{ij} for water-HC obtained from the correlation of Table 6.4 and no interaction parameters are used between MEG and hydrocarbons. The CPA EoS can satisfactory predict mutual solubilities, in most cases the results are in the correct order of magnitude. The modeling results are equally satisfactory

using same k_{ij} at the higher temperature of 323.15 K. The CPA predictions are once again equally good using condensate-2 composition from this work and from the external laboratory as shown in Table 6.11.

Table 6.12: Experimental Data¹¹² and CPA Modeling for Condensate-2 + MEG + Water System at Temperatures 303.15 and 323.15 K and Pressure 1 atm. The k_{ij} for MEG-Water=-0.115, MEG-HC=0 and Water-HC are Taken from Table 6.4. The CPA Calculations are Made Using Condensate-2 Composition Measured in This Work.

Component	Feed (mole fraction)	Polar Phase (mole ppm)			Hydrocarbon Phase (mole ppm)		
		Exp.	Cal.	% Dev.	Exp.	Cal.	% Dev.
T=303.15 K							
MEG	0.1312	---	---	---	36	46	-27
Water	0.6783	---	---	---	806	446	45
COND-2	0.1905	67	15	78	---	---	---
MEG	0.2345	---	---	---	73	93	-27
Water	0.5386	---	---	---	635	362	43
COND-2	0.2269	189	73	61	---	---	---
MEG	0.3865	---	---	---	103	166	-61
Water	0.3329	---	---	---	394	240	39
COND-2	0.2805	508	497	2	---	---	---
T=323.15 K							
MEG	0.1312	---	---	---	82	127	-55
Water	0.6783	---	---	---	1309	1081	17
COND-2	0.1905	91	25	72	---	---	---
MEG	0.2345	---	---	---	158	254	-61
Water	0.5386	---	---	---	1119	883	21
COND-2	0.2269	311	115	63	---	---	---
MEG	0.3865	---	---	---	328	450	-37
Water	0.3329	---	---	---	784	588	25
COND-2	0.2805	1181	700	41	---	---	---

The CPA EoS satisfactorily describes the following data trends as shown in Figures 6.5 and 6.6 at temperatures 303.15 and 323.15 K respectively.

- The solubility of water in condensate-2 decreases with increasing MEG mole fraction in the polar phase.
- The solubility of MEG in condensate-2 increases with increasing MEG mole fraction in the polar phase.
- The solubility of condensate-2 in the polar phase increases with increasing MEG mole fraction in the polar phase.

A better prediction of the solubility of water in condensate-2 is obtained at 323.15 K as compared to 303.15 K. This may be due to the limitations of CPA for describing the solubility of water in hydrocarbons at lower temperature.¹⁴ But overall promising modeling results are obtained for the complex system of condensate-2 + MEG + Water.

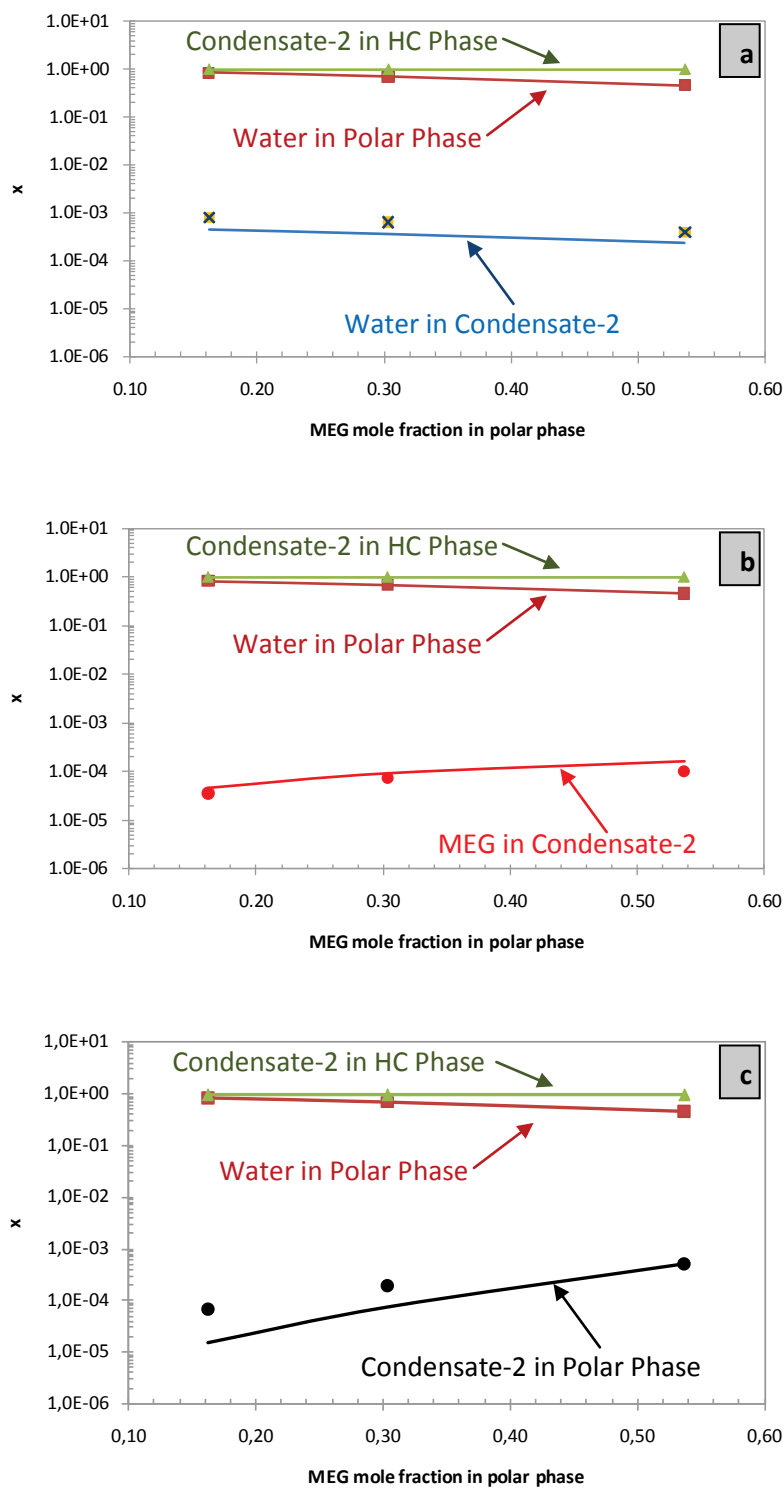


Figure 6.5: Modeling of the mutual solubility (in mole fraction, x) of condensate-2, MEG and water at temperature 303.15 K and pressure 1 atm.: (a) water in condensate-2 (b) MEG in condensate-2 (c) condensate-2 in polar phase. The points are experimental data¹¹² and the lines are modeling results with the CPA EoS using k_{ij} for MEG-water=-0.115, HC-MEG=0 and HC-water from the correlation in Table 6.4. The CPA calculations are made using condensate-2 composition measured in this work.

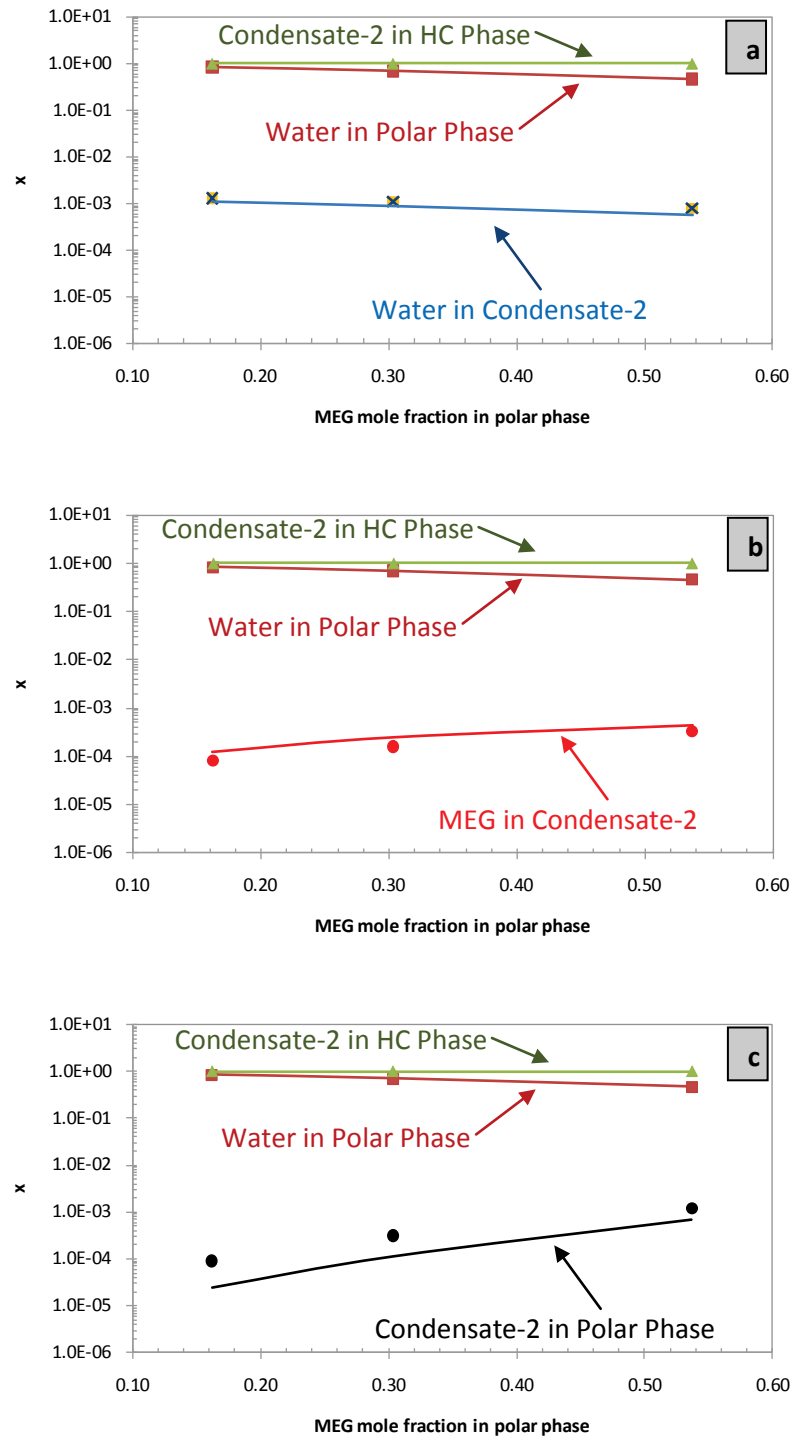


Figure 6.6: Modeling of the mutual solubility (in mole fraction, x) of condensate-2, MEG and water at temperature 323.15 K and pressure 1 atm.: (a) water in condensate-2 (b) MEG in condensate-2 (c) condensate-2 in polar phase. The points are experimental data¹¹² and the lines are modeling results with the CPA EoS using k_{ij} for MEG-water=-0.115, HC-MEG=0 and HC-water from the correlation given in Table 6.4. The CPA calculations are made Using condensate-2 composition measured in this work.

6.2.3 Condensate-3

The composition of condensate-3 is given in Table 5.9 which shows that it is a lighter condensate compared to the condensate-1 and the condensate-2. It has a lower overall molar mass and overall density as compared to the condensate-1 and the condensate-2, as shown in Table 5.12. The PNA distribution of condensate-3 is given in Figure 5.15 in comparison to the other condensates which shows that it is more naphthenic and has lower aromatic content than that of the condensate-1 and the condensate-2.

6.2.3.1 Condensate-3 Characterization

The properties of condensate-3 after characterization are given in Table 6.13. Due to lower decane plus fraction lumping is not required for desired number of pseudo components in the characterized mixture. For a systematic study of phase behavior, the number of pseudo components in the characterized mixture is kept the same for all condensates investigated in this work.

Table 6.13: Condensate-3 after Characterization.

Components	Mole %	T_{cm} (K)	P_{cm} (bar)	ω_m
Ethane	0.000	305.4	48.8	0.098
Propane	1.040	378.6	47.2	0.105
i-Butane	5.230	415.8	40.1	0.151
n-Butane	6.330	436.3	43.6	0.158
i-Pentane	5.860	460.4	33.8	0.227
n-Pentane	5.550	479.4	38.0	0.217
C ₆	13.980	522.3	34.9	0.244
C ₇	26.650	562.8	36.7	0.225
C ₈	21.810	591.6	34.3	0.259
C ₉	6.690	622.7	32.8	0.289
C ₁₀	2.005	647.2	30.2	0.327
C ₁₁	1.419	669.1	28.2	0.362
C ₁₂	1.004	690.2	26.3	0.397
C ₁₃	0.711	709.0	24.8	0.428
C ₁₄	0.503	727.6	23.3	0.462
C ₁₅	0.356	746.3	21.9	0.497
C ₁₆	0.252	762.5	20.8	0.527
C ₁₇	0.178	778.3	19.7	0.559
C ₁₈₊	0.432	821.9	17.3	0.648

6.2.3.2 Mutual Solubility of Condensate-3 and MEG

The modeling result for the mutual solubility of condensate-3 and MEG are shown in Figure 6.7 in comparison to the experimental data.¹¹⁵ CPA correlates very satisfactorily the solubilities in both phases using a single, temperature independent k_{ij} between all MEG-HC pairs. With zero

binary interactions parameter (prediction) CPA satisfactorily describes the trend of mutual solubility as a function of temperature but the solubilities in both phases are over predicted.

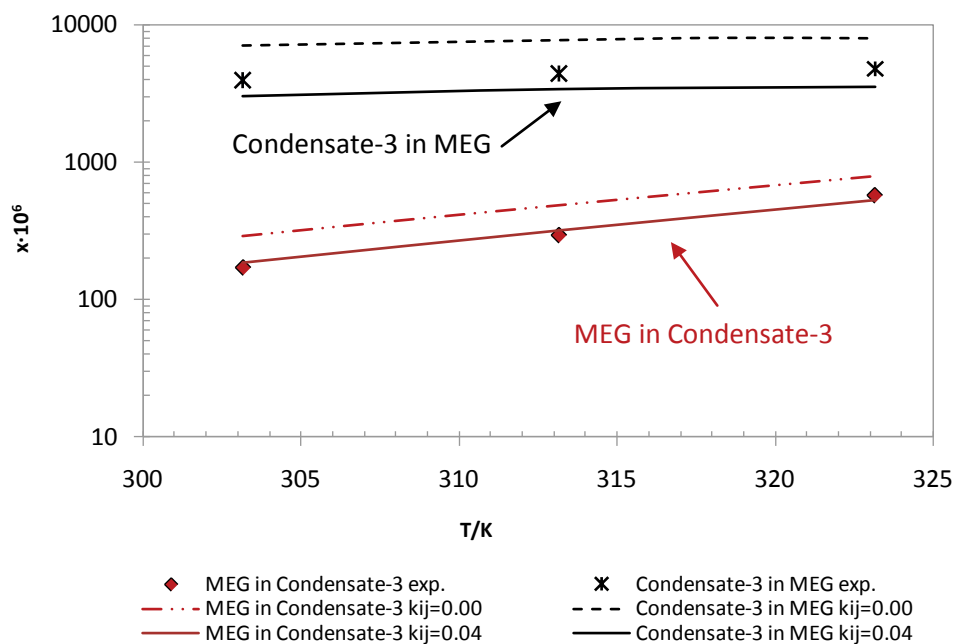


Figure 6.7: Mutual solubility (in mole fraction, x) of condensate-3 and MEG as a function of temperature (K) for condensate-3 + MEG system, experimental data¹¹⁵ are indicated as points and the CPA calculations as lines.

Despite of the fact that the condensate-3 is lighter and more naphthenic than the condensate-1 and the condensate-2, the mutual solubility of condensate-3 and MEG is less than that for the condensate-1 + MEG and condensate-2 + MEG systems. This can be explained by the lower aromatic content of condensate-3 than that of condensate-1 and condensate-2 as shown in Figure 5.18. In this figure a comparison is provided for the solubility of aromatic hydrocarbons (present in condensate-2 and condensate-3) in MEG at 303.15 K. It can be seen that the main difference in the solubility of condensate-3 compared to condensate-2 is due to the lower aromatic content (in pure condensate) and consequently the lower mutual solubility of condensate-3 and MEG.

6.2.3.3 Mutual Solubility of Condensate-3, MEG and Water

For the condensate-3 + MEG + water system the modeling results are given in Table 6.14. Once again using a single average, temperature independent k_{ij} obtained from condensate-3 + MEG system and water-HC k_{ij} from the correlation of Table 6.4 excellent modeling results are obtained. Similar to the condensate-1 and the condensate-2 the experimental trends for the solubility as a function of MEG mole fraction in the polar phase are satisfactorily captured with very good accuracy as shown in Figure 6.8 and Table 6.14.

Table 6.14: Experimental Data¹¹⁵ and CPA Modeling for Condensate-3 + MEG + Water System at 313.15 K and Pressure 1 atm. The k_{ij} for MEG-Water=-0.115, MEG-HC=0.04 and Water-HC are Taken from Table 6.4.

Component	Feed (mole fraction)	Polar Phase (mole ppm)			Hydrocarbon Phase (mole ppm)		
		Exp.	Cal.	% Dev.	Exp.	Cal.	% Dev.
MEG	0.1279	---	---	---	53	50	6
Water	0.6578	---	---	---	796	668	16
COND-3	0.2143	62	31	50	---	---	---
MEG	0.2238	---	---	---	91	100	-10
Water	0.5331	---	---	---	673	543	19
COND-3	0.2430	180	118	35	---	---	---
MEG	0.3534	---	---	---	178	173	3
Water	0.3446	---	---	---	480	367	23
COND-3	0.3019	711	507	29	---	---	---

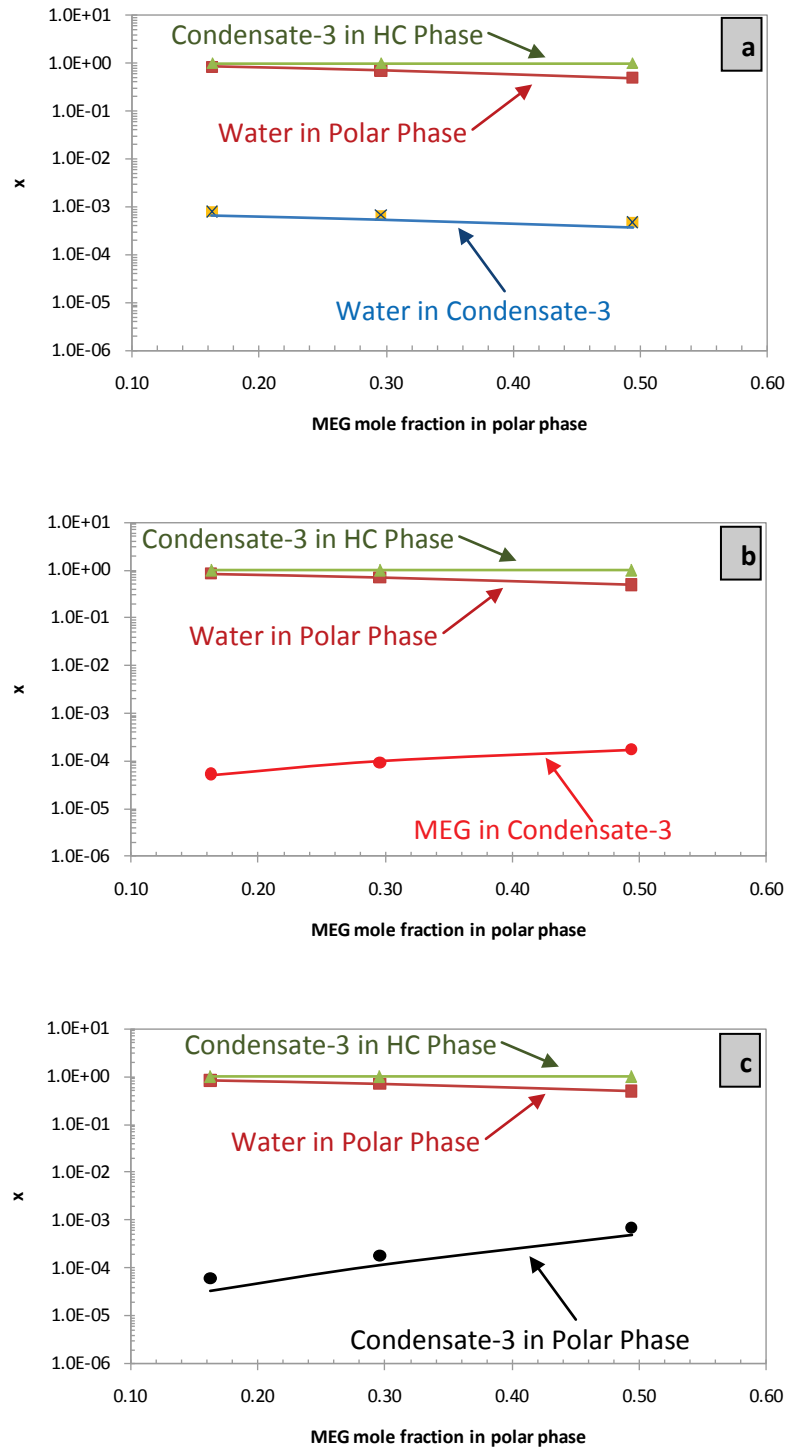


Figure 6.8: Modeling of the mutual solubility (in mole fraction, x) of condensate-3, MEG and water at temperature 313.15 K and pressure 1 atm.: (a) water in condensate-3 (b) MEG in condensate-3 (c) condensate-3 in the polar phase. The points are experimental data¹¹⁵ and the lines are modeling results with the CPA EoS using k_{ij} for MEG-water=-0.115, HC-MEG=0.04 and HC-water from the correlation in Table 6.4.

In the preceding sections the CPA modeling of condensate + MEG and the condensate + MEG + water systems has been presented. Overall satisfactory results are obtained. The modeling results for two light oils with MEG, and MEG + water will be presented in the coming sections. The light oils have relatively higher overall molar mass and average density. Furthermore, light oils have higher decane plus fraction as compared to condensate-1, condensate-2 and condensate-3. The characterization method used for light oils is the same as for the condensates and similar modeling strategy is adopted for light-oil + MEG and light-oil + MEG + water systems.

6.2.4 Light-Oil-1

The composition of light-oil-1 is given in Table 5.10 which shows that it has 91.45 mass % decane plus fraction. This means that we have a PNA distribution of only 9.55 mass % of light-oil-1 and the details of many components are unknown. The PNA distribution based on components in C_1 - C_9 is shown in Figure 5.15.

6.2.4.1 Light-Oil-1 Characterization

The molar composition and critical properties of light-oil-1 after characterization and lumping are given in Table 6.15.

Table 6.15: Light-Oil-1 after Characterization and Lumping.

Components	Mole %	T_{cm} (K)	P_{cm} (bar)	ω_m
Methane	0.040	190.6	46.0	0.008
Ethane	0.300	305.4	48.8	0.098
Propane	0.810	378.6	47.2	0.105
i-Butane	0.410	415.8	40.1	0.151
n-Butane	1.020	436.3	43.6	0.158
i-Pentane	0.740	460.4	33.8	0.227
n-Pentane	0.900	479.4	38.0	0.217
C_6	1.920	522.3	34.9	0.244
C_7	4.920	561.0	36.0	0.229
C_8	6.210	587.8	33.0	0.269
C_9	6.090	612.4	29.5	0.317
C_{10} - C_{13}	19.315	675.8	26.4	0.389
C_{14} - C_{17}	14.476	759.9	22.6	0.490
C_{18} - C_{20}	8.423	815.9	20.6	0.556
C_{21} - C_{24}	8.740	861.8	19.0	0.612
C_{25} - C_{29}	7.913	909.7	17.3	0.702
C_{30} - C_{34}	5.518	953.3	15.9	0.775
C_{35} - C_{41}	5.039	1001.1	14.5	0.796
C_{42} - C_{52}	4.203	1056.1	12.8	0.848
C_{53+}	3.012	1145.8	9.5	0.912

6.2.4.2 Mutual Solubility of Light-Oil-1 and MEG

The modeling results and the experimental data for the mutual solubility of light-oil-1 + MEG system are shown in Figure 6.9. As mentioned earlier light-oil-1 has much higher overall molar mass as compared the other condensates and as compared to light-oil-2 as shown in Table 5.12. The mutual solubilities are measured experimentally in mass fraction and to compare with the modeling results, they are converted to mole fraction. The mutual solubility trend is reversed for light-oil-1, that is the solubility of MEG (in mole fraction) is higher than that of the solubility of light-oil-2 in MEG whereas in mass fraction, the solubility of light-oil-1 in MEG is higher than that of the solubility of MEG in light-oil-1 as shown in Figure 5.19.

It can be seen that the solubility of light-oil-1 in MEG is satisfactorily correlated using an average $k_{ij}=0.02$ for all MEG-HC pairs. Prediction ($k_{ij}=0$) of the solubility of light-oil-1 in MEG using CPA is in good agreement with the experimental data. But the solubility of MEG in light-oil-2 is underestimated and the deviations from experimental data are given in Table 6.16. For further investigation of this modeling behavior other characterization method such as the Whitson et al.⁸⁵ method needs to be tested. On the other hand more data is required for oil with higher decane plus fraction and reliable measurement of PNA distribution in decane plus fraction is necessary. If the analysis shows that the decane plus fraction has considerably higher aromatic content, solvation should be added to account for the increased solubility of MEG in light-oil-1.

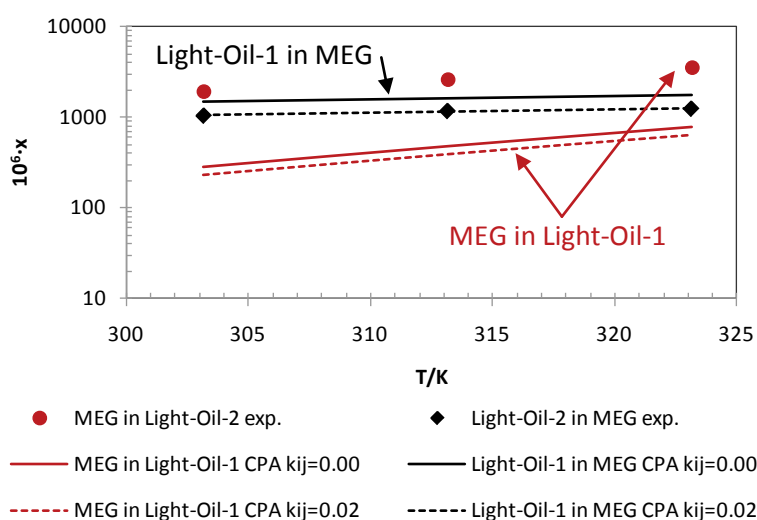


Figure 6.9: Mutual solubility (in mole fraction, x) of Light-Oil-1 and MEG as a function of temperature (K) for light-oil-1 + MEG system. The experimental data¹¹⁴ are indicated as points and the CPA calculations as lines.

Table 6.16: Deviations in CPA Calculations for Modeling of Light-Oil-1 + MEG System.

k_{ij} of MEG-HC	% AAD (Light-Oil-1 in MEG)	% AAD (MEG in Light-Oil-1)
0.02	1	85
0.00	39	82

6.2.4.3 Mutual Solubility of Light-Oil-1, MEG and Water

In the previous section the modeling results for light-oil-1 + MEG are presented showing higher deviations for the solubility of MEG in light-oil-1. In this section modeling results for light-oil-1 + MEG + water are presented in Table 6.17 using an average k_{ij} (for all MEG-HC pairs) obtained from Light-Oil-1 + MEG system. Here the modeling results are in very good agreement with the experimental data and in contrast to the light-oil-1 + MEG system deviations are lower for the prediction of solubility of MEG in oil and water in oil. This further highlights the need of more data for light-oil-2 + MEG system.

Table 6.17: Experimental Data¹¹⁴ and CPA Modeling for Light-Oil-1 + MEG + Water System at 303.15 and 313.15 K and Pressure 1 atm. The k_{ij} for MEG-Water=-0.115, MEG-HC=0.02 and Water-HC are Taken from Table 6.4.

Component	Feed (mole fraction)	Polar Phase (mole ppm)			Hydrocarbon Phase (mole ppm)		
		Exp.	Cal.	% Dev.	Exp.	Cal.	% Dev.
T=313.15 K							
MEG	0.2422	---	---	---	270	107	61
Water	0.6543	---	---	---	908	699	23
Light-Oil-1	0.1035	117	49	58	---	---	---
MEG	0.4511	---	---	---	493	209	58
Water	0.4115	---	---	---	722	454	37
Light-Oil-1	0.1374	230	189	18	---	---	---
T=323.15 K							
MEG	0.2674	---	---	---	363	196	46
Water	0.6287	---	---	---	1443	1017	29
Light-Oil-1	0.1040	129	66	49	---	---	---
MEG	0.4349	---	---	---	568	323	43
Water	0.4487	---	---	---	1022	734	28
Light-Oil-1	0.1164	239	186	22	---	---	---

For light-oil-1 + MEG + water systems CPA can satisfactorily predict the experimental trends and describe solubilities in both phases with reasonable accuracy as shown in Figures 6.10 and 6.11. These results are as good as for the investigated systems of condensates in the preceding sections.

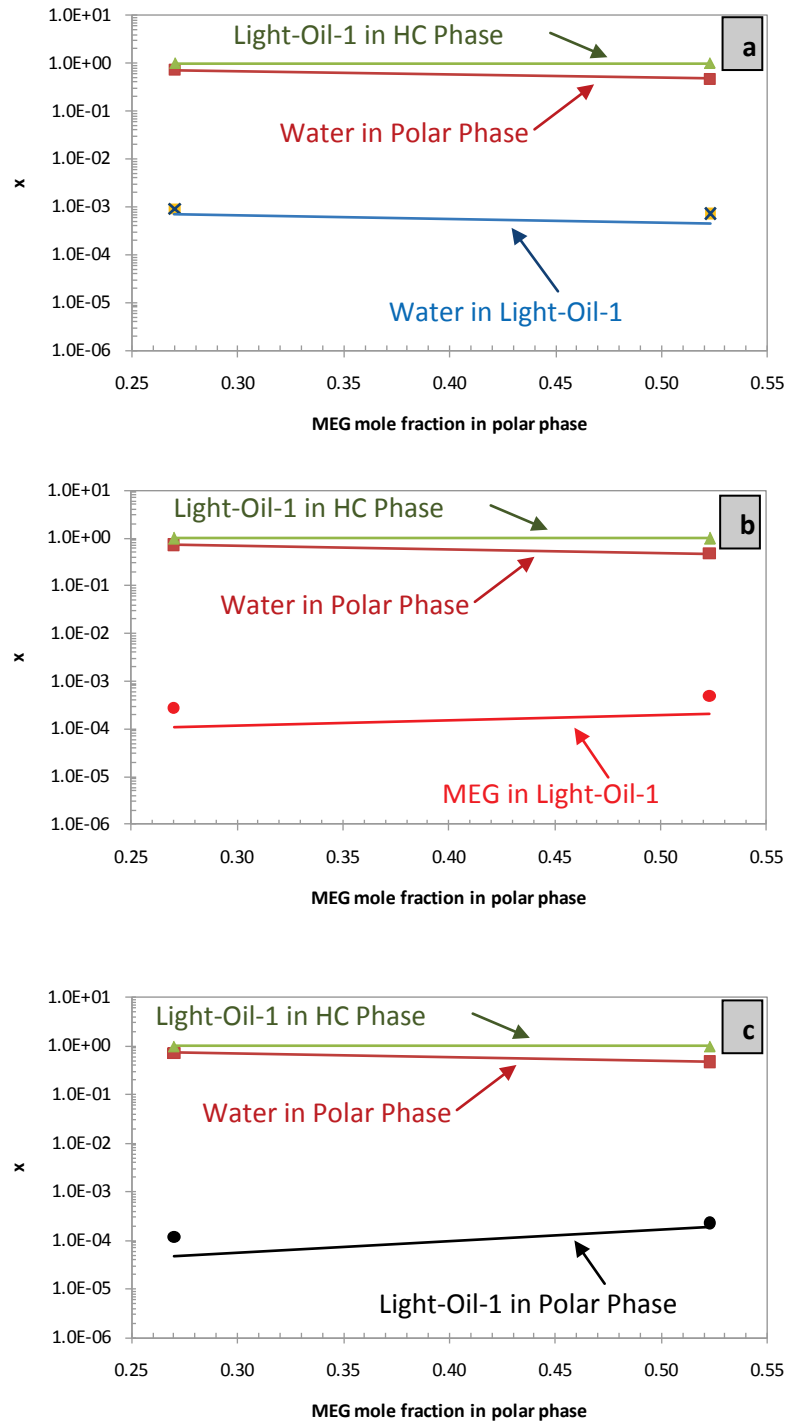


Figure 6.10: Modeling of the mutual (in mole fraction, x) solubility of light-oil-1, MEG and water at temperature 313.15 K and pressure 1 atm.: (a) water in light-oil-1 (b) MEG in light-oil-1 (c) light-oil-1 in polar phase. The points are experimental data¹¹⁴ and the lines are modeling results with the CPA EoS using k_{ij} for MEG-water=-0.115, HC-MEG=0.02 and HC-water from the correlation in Table 6.4.

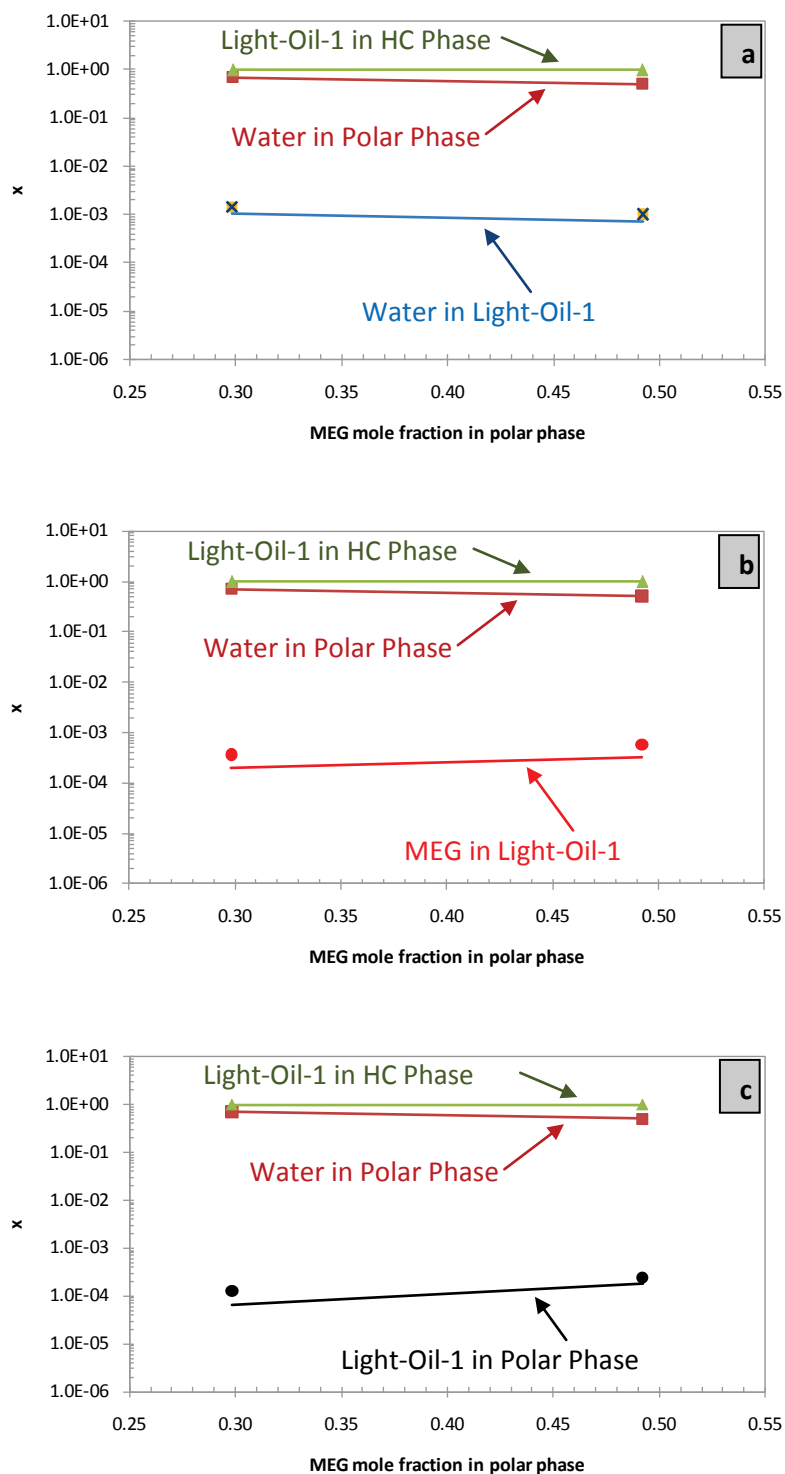


Figure 6.11: Modeling of the mutual solubility (in mole fraction, x) of light-oil-1, MEG and water at temperature 323.15 K and pressure 1 atm.: (a) water in light-oil-1 (b) MEG in light-oil-1 (c) light-oil-1 in polar phase. The points are experimental data¹¹⁴ and the lines are modeling results with the CPA EoS using k_{ij} for MEG-water=-0.115, HC-MEG=0.02 and HC-water from the correlation.

6.2.5 Light-Oil-2

The composition of light-oil-2 is given in Table 5.11. It is lighter than light-oil-1 and heavier than the condensates investigated in this work, as shown in Table 5.12.

6.2.5.1 Light-Oil-2 Characterization

The properties of light-oil-2 after characterization and lumping are given in Table 6.18.

Table 6.18: Light-Oil-2 after Characterization and Lumping.

Components	Mole %	T_{cm} (K)	P_{cm} (bar)	ω_m
Ethane	0.170	305.4	48.8	0.0980
Propane	2.350	378.6	47.2	0.1048
i-Butane	1.830	415.8	40.1	0.1508
n-Butane	6.470	436.3	43.6	0.1575
i-Pentane	4.130	460.4	33.8	0.2270
n-Pentane	5.730	479.4	38.0	0.2172
C ₆	8.410	522.3	34.9	0.2439
C ₇	13.690	560.8	35.9	0.2300
C ₈	14.270	591.0	34.1	0.2605
C ₉	8.380	621.4	32.3	0.2924
C ₁₀ -C ₁₁	8.781	657.5	29.1	0.3447
C ₁₂	3.515	690.8	26.4	0.3948
C ₁₃ -C ₁₄	5.658	719.5	24.4	0.4395
C ₁₅ -C ₁₆	4.221	756.8	21.9	0.5022
C ₁₇ -C ₁₈	3.149	788.1	20.0	0.5563
C ₁₉ -C ₂₁	3.289	818.4	18.5	0.6079
C ₂₂ -C ₂₄	2.119	853.3	16.8	0.6723
C ₂₅ -C ₃₀	2.246	895.8	14.9	0.7558
C ₃₁₊	1.593	975.3	11.9	0.9185

6.2.5.2 Mutual Solubility of Light-Oil-2 and MEG

Correlation and prediction of the mutual solubility of light-oil-2 and MEG are shown in Figure 6.12 in comparison to the experimental data. It can be seen that the modeling results are in good agreement with the experimental data using a single non-zero $k_{ij}=0.02$ for all MEG-HC binaries. The deviations in calculations are given in Table 6.19 showing that CPA can describe the system with satisfactory accuracy.

Table 6.19: Deviations in CPA Calculations for Modeling of Light-2 + MEG System.

k_{ij} of MEG-HC	% AAD (Light-Oil-2 in MEG)	% AAD (MEG in Light-Oil-2)
0.02	13	36
0.00	65	21

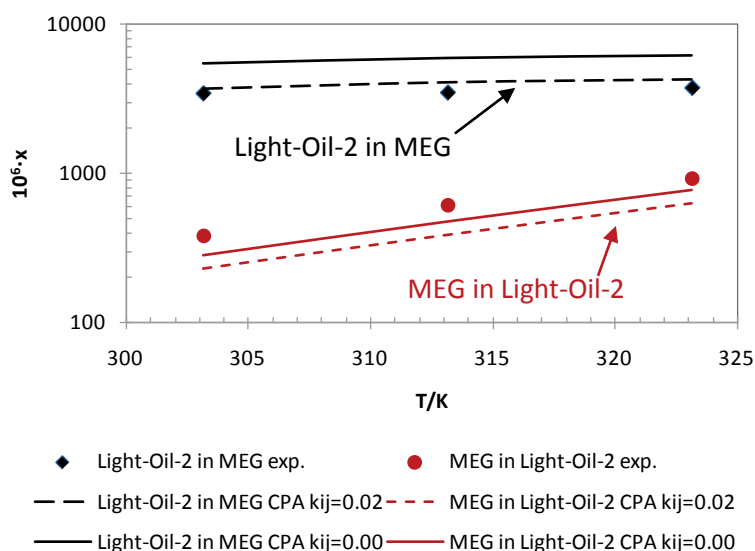


Figure 6.12: Mutual solubility (in mole fraction, x) of light-oil-2 and MEG as a function of temperature (K) for light-oil-2 + MEG system. The experimental data¹¹⁵ are indicated as points and the CPA calculations as lines.

6.2.5.3 Mutual Solubility of Light-Oil-2, MEG and Water

The CPA predictions for the mutual solubilities for the light-oil-2 + MEG + water systems are given in Table 6.20 showing that the results are correct in order of magnitude in most cases. Furthermore trends in solubilities as a function of MEG mole fraction in the polar phase are very well described as shown in Figure 6.13.

Table 6.20: Experimental Data¹¹⁵ and CPA Modeling for Light-Oil-2 + MEG + Water System at 323.15 K and Pressure 1 atm. The k_{ij} for MEG-Water=-0.115, MEG-HC=0.02 and Water-HC are Taken from Table 6.4.

Component	Feed (mole fraction)	Polar Phase (mole ppm)			Hydrocarbon Phase (mole ppm)		
		Exp.	Cal.	% Dev.	Exp.	Cal.	% Dev.
T=323.15 K							
MEG	0.1377	---	---	---	238	109	54
Water	0.7055	---	---	---	1744	1149	34
Light-Oil-2	0.1567	125	42	66	---	---	---
MEG	0.2459	---	---	---	529	199	62
Water	0.5676	---	---	---	1351	939	30
Light-Oil-2	0.1864	270	143	47	---	---	---
MEG	0.4074	---	---	---	549	352	36
Water	0.3507	---	---	---	917	622	32
Light-Oil-2	0.2418	686	659	4	---	---	---

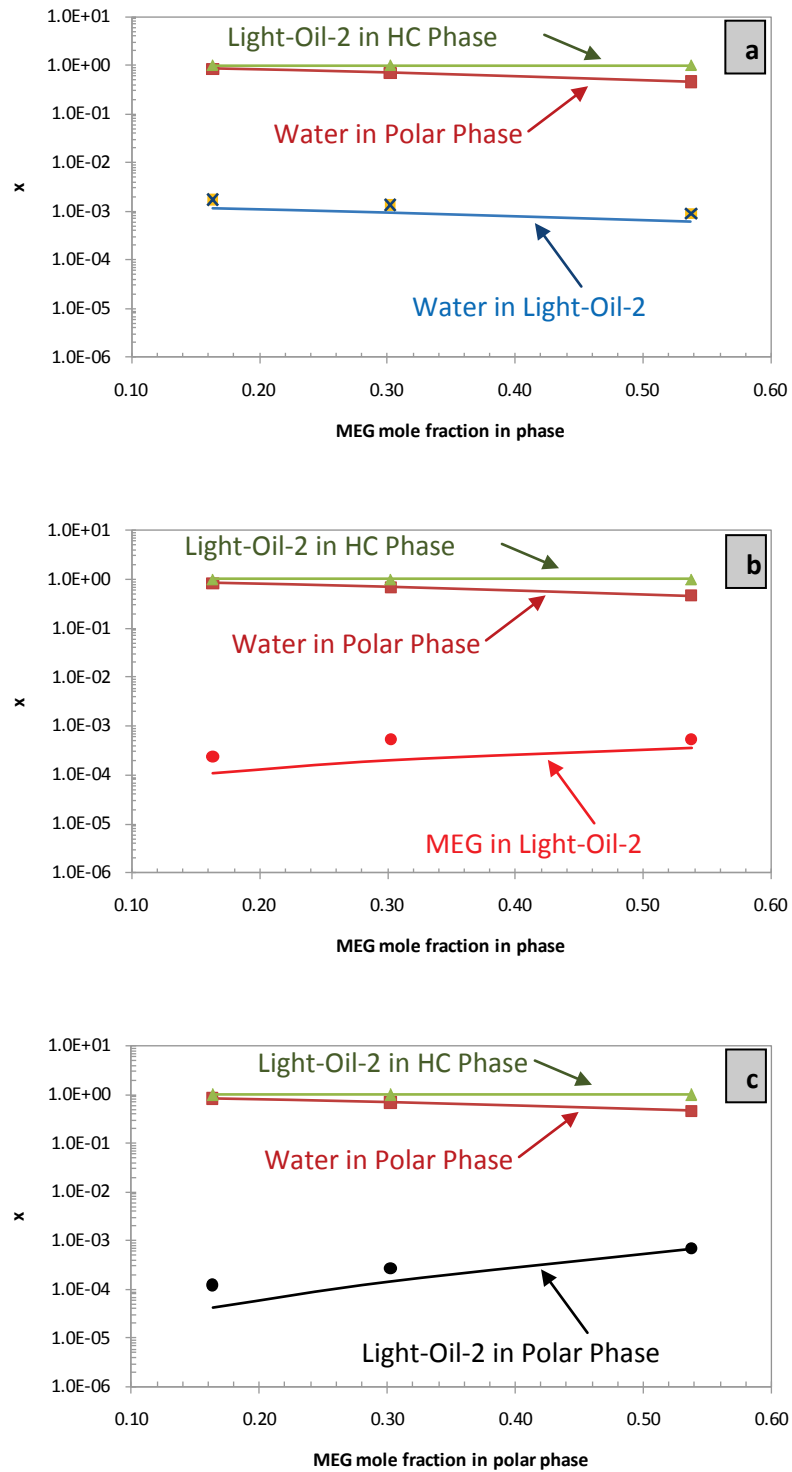


Figure 6.13: Modeling of the mutual solubility of light-oil-2, MEG and water at temperature 323.15 K and pressure 1 atm.: (a) water in light-oil-2 (b) MEG in light-oil-2 (c) light-oil-2 in polar phase. The points are experimental data¹¹⁵ and the lines are modeling results with the CPA EoS using k_{ij} for MEG-water=-0.115, HC-MEG=0.02 and HC-water from the correlation in Table 6.4.

6.2.6 Comparison of Well-Defined-HC and Oil Systems in Presence of Water and Polar Chemical

This section presents a comparison of CPA predictions for condensates/oils + MEG + water systems with well-defined hydrocarbons + MEG + water. A summary of deviations for such systems in each phase with interaction parameters and combining rules used is given in Table 6.21. Modeling work related to oils and condensates is carried out in this project whereas for the systems with well-defined hydrocarbons is from literature.¹²⁴ For the oil/condensate + MEG + water systems in general solubility of MEG is over predicted whereas the solubilities of water and condensates are under predicted. These deviations can be explained by the high complexity of the system due to presence of polar non-polar compounds and the very low solubilities on part per million (ppm) levels. Such solubilities are challenging for the measurements and the modeling.

Table 6.21: Summary of Deviations of CPA Calculations from Experimental Data and Comparison with Systems of Well-Defined-HC + MEG + Water. The k_{ij} for MEG-Water=-0.115 with Elliott Combining Rule for Condensate/Oil + MEG + Water Systems and k_{ij} =-0.028 with CR-1 Combining Rule for Well-Defined-HC + MEG + Water Systems.

% AAD			k_{ij}	
HC in Polar Phase	MEG in HC Phase	Water in HC Phase	MEG-HC	Water-HC
Condensate-1 + MEG + Water T=323.15 K				
24	52	13	0.02	From Table 6.4
Condensate-2 + MEG + Water T=303.15 K				
47	38	42	0.00	From Table 6.4
Condensate-2 + MEG + Water T=323.15 K				
59	51	21	0.00	From Table 6.4
Condensate-3 + MEG + Water T=313.15 K				
36	6	20	0.04	From Table 6.4
Light-Oil-1 + MEG + Water T=313.15 K				
38	60	30	0.02	From Table 6.4
Light-Oil-1 + MEG + Water T=323.15 K				
36	43	29	0.02	From Table 6.4
Light-Oil-2 + MEG + Water T=323.15 K				
39	52	32	0.02	From Table 6.4
2,2,4-Trimethylpentane + MEG + Water ¹²⁴ T=283-333 K				
82	83	43	-0.00028	-0.0687
n-hexane + MEG + Water ¹²⁴ T=283-333 K				
44	42	44	0.059	0.0355

Overall the predictive performance of the model is satisfactory. CPA can satisfactorily describe the temperature dependency of mutual solubility for condensates/oils + MEG systems with a single temperature independent k_{ij} as well as with $k_{ij}=0$. In the condensates/oil + MEG + water systems CPA can describe both the temperature and composition dependency of solubility and

these trends are consistent for all the systems investigated in this work. Finally the results with condensates and oil related systems are as good as for well-defined hydrocarbon systems. Even in well-defined systems we have three components whereas in case of condensates and oils numerous hydrocarbons involved which are both well-defined and ill-defined.

6.3 Conclusions

In this work the cubic plus association (CPA) equation of state (EoS) has been applied to the modeling of the mutual solubility of reservoir fluids, monoethylene-glycol (MEG) and water. The reservoir fluid consists of three condensates and two light-oils. The condensates and the oils used in this work are from different offshore gas fields in the North Sea. For characterization of the reservoir fluid Yan et al. correlations are applied.

The CPA EoS is applied to the liquid-liquid equilibrium of reservoir-fluid + MEG and reservoir-fluid + MEG + water systems in a temperature range 275-326 K and atmospheric pressure. For reservoir-fluid + MEG systems excellent correlations are obtained for the mutual solubility of reservoir fluid and MEG as a function of temperature using solely a single average, temperature independent k_{ij} for all MEG-hydrocarbon pairs. In some cases the mutual solubility is predicted ($k_{ij}=0$) satisfactorily. Equally good results are obtained for the three condensates and light-oil-2. In the case of light-oil-1 satisfactory correlation and prediction are obtained for the solubility of light-oil-1 in MEG but the solubility of MEG in light-oil-1 is underestimated. This is partially due to uncertainty in the data and naphthenic nature of the oil. More investigations are required for the data and the modeling of light-oil-1.

For the reservoir-fluid + MEG + water systems satisfactory predictions are obtained using an average temperature independent k_{ij} for all MEG-HC pairs obtained from reservoir-fluid + MEG systems and water-HC k_{ij} from a generalized correlation. CPA can satisfactorily describe the trends in solubilities of reservoir fluids, MEG and water as a function of MEG mole fraction in the polar phase and as a function of temperature. The results are generally correct in order of magnitude. Interestingly the modeling results for light-oil-1 + MEG + water systems are equally good in contrast to light-oil-1 + MEG system where the solubility of MEG in light-oil-1 was under estimated.

Finally a comparison of CPA calculations is made between reservoir fluid and well-defined hydrocarbons in presence of polar chemicals such as water and MEG. It has been seen that modeling results for reservoir fluid systems are as good as for well-defined hydrocarbon

systems. In some cases the modeling results for the systems with reservoir fluid are better than those of the systems with well-defined hydrocarbons.

The deviations from experimental data are attributed to the complexity of the systems with associating and non-associating components and the challenges involved in the measurements and the modeling of very low solubilities on the order of part per million level. In case of reservoir fluid, systems are even more complex as we have numerous well-defined components (about 90 components in C₂-C₉ carbon fractions) and hundreds of ill-defined components in decane plus fraction. The components are paraffinic, naphthenic and aromatic in nature and of a wide range of molar mass and density.

The existing characterization method (proposed by Yan et al.) can satisfactorily predict (as good as for well-defined systems) the mutual solubility of condensates, MEG and water without explicitly taking aromaticity into account. This is because specific gravity difference (ΔSG) of a carbon fraction from normal paraffins is used to take aromaticity into account (in Yan et al. correlations given in Chapter 3). However for the oils with higher decane plus fraction it may be necessary to explicitly taking aromaticity into account by adding salvation term.

Conclusions and Future Work

As crude oil resources decrease, the oil industry demands more sophisticated methods for the exploitation of natural resources. As a result, the use of oil field chemicals is becoming increasingly important.³ These chemicals are classified as drilling, production and injection chemicals. In this project the production chemicals are of interest. These chemicals belong to various families such as alcohols, glycols, alkanolamines, polymers and salts. They are used as gas hydrate inhibitors, corrosion and scale inhibitors and demulsifiers. The distribution of these chemicals is important to the oil and gas industry for economical operation of production facilities, environmental perspective and downstream processing. The purpose of this project is the experimental measurement and the thermodynamic modeling of distribution of complex chemicals (i.e. MEG and methanol) in oil-water systems.

Conclusions

As it is expensive to measure oil-water partition coefficients ($K_{\text{oil-water}}$) for all production chemicals used by oil industry, therefore it is of interest to investigate alternative approaches to estimate them from octanol-water partition coefficients (K_{ow}) or hexane-water partition coefficients (K_{hw}). In order to correlate $K_{\text{oil-water}}$ with K_{ow} or K_{hw} experimental data were collected from different sources. It has been noted that the experimental data of $K_{\text{oil-water}}$ is very rare and the only data available are from Statoil. The experimental data of K_{ow} and K_{hw} are even not available for all the chemicals of interest in this study. K_{ow} cannot be predicted for all the chemicals as their molecular structure is not available to comply with confidentiality agreement with the suppliers. These reasons pose limitations to obtain correlations for all chemical families of interest. However a satisfactory linear correlation was established between $K_{\text{oil-water}}$ and K_{ow} for alcohols (methanol to octadecanol). Similarly satisfactory correlations are obtained between $K_{\text{oil-water}}$ and K_{hw} for light alcohols (methanol to 1-butanol). The correlations for two other chemical families (i.e. glycol and alkanolamine) are less reliable possibly because of a limited number of data points. Therefore more data and molecular structure's information are required to build such correlations.

On the basis of the amount of chemicals used, MEG and methanol are the most important chemicals and it was decided to focus the study on these two hydrate inhibitors, especially MEG. For thermodynamic modeling using CPA methanol is described as 2-site (2B) molecule whereas the four-site (4C) scheme is used for both MEG and water throughout in this work in accordance to previous studies.

In the process of extending CPA EoS to reservoir fluids in presence of polar chemicals it is of interest to investigate the VLE and LLE of binary systems of well-defined hydrocarbons and polar chemicals. The CPA equation of state therefore has been applied to VLE, LLE of binary systems of well-defined hydrocarbons (i.e. methane, n-alkanes and alkylbenzene) and polar chemicals such water or methanol. For aromatic hydrocarbons + water systems satisfactory modeling results are obtained for the mutual solubility of alkylbenzenes and water by obtaining k_{ij} from homomorph alkanes and fitting only the cross-association volume to binary data. For higher alkylbenzenes (i.e. pentylbenzene, hexylbenzene etc.) the solubility of alkylbenzene in water can be predicted satisfactorily but for the solubility of water in alkylbenzene experimental data are not available for comparison. Similarly, the mutual solubility of n-nonane and water as well as water in undecane has been predicted satisfactorily (for available data) using k_{ij} obtained from a generalized correlation as a function of carbon number.

For VLE the of methane + methanol CPA, can satisfactorily predict (using k_{ij} from correlation as a function of temperature obtained in this work) the methane content in methanol over a range of temperature and pressure and methanol content in gas phase especially at high temperature and low pressure. Equally good description is obtained by using a single temperature independent $k_{ij}=0.01$ (from de Hemptinne et al.¹⁰⁰) and $k_{ij}=0.0487$ (from Haghighi et al.⁸⁹) which suggest that higher values of binary interaction parameter do not influence considerably the calculations (for methane + methanol system).

To optimize the hydrate inhibitors injection by minimizing the losses in hydrocarbon phase(s) successful estimation of inhibitor distribution is required. The CPA EoS is therefore applied to multicomponent system of mixture-1 (MIX-1) + water, MIX-1 + water + methanol and MIX-1 + water + MEG. In these systems water, methanol and MEG are polar compounds which can self-associate as well as cross associate with each other. The Elliott combining rule is used for MEG-water and methanol-water in accordance to previous works.

MIX-1 consists of 94 mol % methane, 4 mol % ethane and 2 mol % n-butane. For systems with MIX-1, water and inhibitor contents of the gas phase were modeled over a range of

temperature and pressure. It is shown that CPA can predict ($k_{ij}=0$) satisfactorily the water content in the gas phase of MIX-1 + Water, MIX-1 + Water + Methanol and MIX-1 + Water + MEG systems. The methanol content in vapor phase of MIX-1 + Water + Methanol system could be correlated with % AAD of 16 in comparison to reported experimental uncertainty of 15%.

Mixture-2 (MIX-2) represents a synthetic condensate consisting of 19.5 mol % methane, 5.8 mol % ethane, 9.2 mol % propane, 9.2 mol % n-butane, 13.8 mol % n-heptane, 25.3 mol % toluene and 17.2 mol % n-decane. For systems with MIX-2, the composition of the gas phase and the organic phase are modeled for a temperature range 258 K to 298 K and pressure 5 bar to 37 bar. It is shown that CPA can satisfactorily predict the organic phase compositions in VLE of MIX-2 (synthetic condensate) + water, MIX-2 + Water + Methanol and MIX-2 + Water + MEG systems but less satisfactory predictions for vapor phase are obtained partially due to the reported¹⁰² uncertainty in the experimental data.

To investigate the distribution of MEG in oil-water systems using CPA EoS the experimental data are required but such data are very rare especially for gas-condensates and oils. Therefore experimental work was carried out for condensate, MEG and water systems at Statoil R & D. Experimental data for the mutual solubility of North Sea condensates + MEG are presented. To evaluate the effect of water on mutual solubility, the systems like condensates + MEG + water are experimentally investigated and the LLE data are presented in the temperature range of 275.15 to 323.15 K at atmospheric pressure. In the condensate + MEG systems, the mutual solubility increases with increasing temperature. The solubility of aromatic hydrocarbons is much higher than that of naphthenic and paraffinic hydrocarbons in each carbon fraction. Benzene and toluene contribute a major part to the solubility of reservoir fluids in MEG. Therefore the more aromatic (in C₇-C₉ carbon fraction) the condensate is the higher will be the solubility and vice versa.

In the condensate + MEG + water system, the mutual solubility of MEG and condensate decreases with increasing water content in polar phase and the solubility of some of the components become negligible. The mutual solubility increases with increasing temperature. The solubility of aromatic hydrocarbon is higher than that of naphthenic and paraffinic hydrocarbons. The aromatic components like benzene and toluene contribute almost half of the total solubility of condensate in MEG. The data presented in this project are new data and no data could be found for such systems to make a comparison. However the reproducibility of the data is very satisfactory.

Finally the CPA EoS has been applied to the modeling of the mutual solubility of reservoir fluids, monoethylene-glycol (MEG) and water. The reservoir fluids studied consist of three condensates and two light-oils from the North Sea. Yan et al.¹⁶ correlations are used for characterization of the reservoir fluid.

For the reservoir-fluid + MEG systems excellent correlations are obtained for the mutual solubility of reservoir fluid and MEG as a function of temperature using solely a single average, temperature independent k_{ij} for all MEG-hydrocarbon pairs. In some cases the mutual solubility is predicted ($k_{ij}=0$) satisfactorily. Equally good results are obtained for the three condensates and the light-oil-2. In the case of light-oil-1 satisfactory correlation and prediction are obtained for the solubility of light-oil-1 in MEG but the solubility of MEG in light-oil-1 is underestimated possibly because of experimental uncertainty or relatively more naphthenic character of the light-oil-1. More investigations are required for the data and the modeling of light-oil-1.

For the reservoir-fluid + MEG + water systems satisfactory predictions are obtained using an average temperature independent k_{ij} for all MEG-HC pairs obtained from reservoir-fluid + MEG systems and water-HC k_{ij} from a generalized correlation. CPA can satisfactorily describe the trends in solubilities of reservoir fluids, MEG and water as a function of MEG mole fraction in the polar phase and as a function of temperature. The results are generally correct in order of magnitude. Interestingly the modeling results for light-oil-1 + MEG + water systems are equally good in contrast to light-oil-1 + MEG system where the solubility of MEG in light-oil-1 was under-estimated. The comparison of CPA calculations for reservoir fluid and well-defined hydrocarbons in presence of polar chemicals such as water and MEG has shown that modeling results for reservoir fluid systems are as good as for well-defined hydrocarbon systems.

It is shown that the existing characterization method (proposed by Yan et al.) can satisfactorily predict (as good as for well-defined systems) the mutual solubility of condensates, MEG and water without explicitly taking aromaticity into account. This is because specific gravity difference (ΔSG) of a carbon fraction from normal paraffins is used to take aromaticity into account (in Yan et al. correlations given in Chapter 3). However for the oils with higher decane plus fraction it may be necessary to explicitly taking aromaticity into account by adding salvation term.

It has been shown that the CPA EoS is a flexible model by applying to a variety of phase equilibria such as VLE, LLE and VLLE of binary, multicomponent and reservoir fluid mixtures in presence of polar associating, non-associating and solvating compounds.

7.1 Future Work Recommendations

In order to estimate/ predict octanol-water partition coefficients of production chemicals it is essential to get more information on their molecular structure from chemical suppliers.

More binary data for MEG + alkane and MEG + aromatic hydrocarbons is required in order to develop a fully predictive model for distribution of complex chemical in oil-water systems. As it has been shown that average binary interaction parameter are used for all MEG-HC pairs due to the absence of the binary data. Furthermore data for water + heavy aromatics and MEG + heavy aromatic are required in order to evaluate if solvation is required for decane plus fractions. Therefore experimental work should be carried out to overcome these limitations.

In this project, reservoir fluids are characterized using Yan et al.¹⁶ correlations with a characterization method similar to one proposed by Pedersen et al.^{84,79} however other characterization methods should also be tested such as Whitson et al.⁸⁵ method especially for light oils.

In order to investigate the effect PNA distribution in decane plus fraction of a condensate or oil on distribution of chemical, TBP data with experimental density and molar mass of each cut are required. The density and molar mass of a carbon fraction may be correlated to PNA distribution. This is necessary because using SARA analysis external laboratory results have shown very different aromatic content as 5 % and 35 % for the same light oil sample.

Further investigation should be made both for the experimental and modeling for methanol content in gas phase as it is reported^{89,102} that deviations exists between measured data with high degree of scatter and modeling results from this project have shown deviations at lower temperature and higher pressure.

The distilled water was used in the experiments carried out for mutual solubility of reservoir fluid water and MEG. Further investigations by using formation water should be made to evaluate the effect of ions on such solubilities. To model such systems CPA should be developed to apply for electrolyte systems by adding an additional term such as Debye-Hückel term to account for electrolytic character. The ideal case will be that in the absence of electrolyte, eCPA reduces to original CPA.

8 Bibliography

- (1) Kulkarni, P. Hydrate inhibitors for deepwater flow assurance: Reducing capital investment and operating expenses www.pennenergy.com/index/petroleum **2011**.
- (2) Brustad, S. Løken, K. P. Waalmann, J. G. Offshore Technology Conference, Houston, 2005.
- (3) Fink, J. *Oil Field Chemicals*. 1st ed. Gulf Professional Publishing, 2003.
- (4) Nordstad, E. N. Knudsen, B. L. Sæten, J. O. Aas, N. Eilersten, H. B. *Statoil internal report*, 1998.
- (5) Knudsen, B. L. 8th *International Oil Field Chemical Symposium*, Geilo, 1997.
- (6) Aas, N. Knudsen, B. Sæten, J. O. Nordstad, E. In *Proceedings of SPE International Conference on Health, Safety and Environment in Oil and Gas Exploration and Production*, 2002.
- (7) Hasanov, B. Aliyev, F. Hameed, M. A. Rahman, M. M. *Volumes and Costs of Antihydrates Used in Some of the Main Gas Fields in Norway*, NTNU: Trondheim, Norway, 2010.
- (8) von Son, K. *Reclamation/regeneration of glycols used for hydrate inhibition*, Deep offshore technology 2000, CCR Technologies Inc. USA, Charlie Wallace, Consultant, USA, 2000.
- (9) Wei, Y. S. Sadus, R. J. *AIChE Journal* **2000**, 46, 169-196.
- (10) Oliveira, M. B. Coutinho, J. A. P. Queimada, A. J. *Fluid Phase Equilibria* **2007**, 258, 58-66.
- (11) Folas, G. K. Kontogeorgis, G. M. Michelsen, M. L. Stenby, E. H. Solbraa, E. *Journal of Chemical & Engineering Data* **2006**, 51, 977-983.
- (12) Derawi, S. O. Kontogeorgis, G. M. Stenby, E. H. Haugum, T. Fredheim, A. O. *Journal of Chemical & Engineering Data* **2002**, 47, 169-173.
- (13) Razzouk, A. Naccoul, R. A. Mokbel, I. Duchet-Suchaux, P. Jose, J. Rauzy, E. Berro, C. *Journal of Chemical & Engineering Data* **2010**, 55, 1468-1472.
- (14) Kontogeorgis, G. M. Folas, G. K. *Thermodynamic Models for Industrial Applications: From Classical and Advanced Mixing Rules to Association Theories*, 1st ed. Wiley, 2010.
- (15) Kontogeorgis, G. M. Voutsas, E. C. Yakoumis, I. V. Tassios, D. P. *Industrial & Engineering Chemistry Research* **1996**, 35, 4310-4318.
- (16) Yan, W. Kontogeorgis, G. M. Stenby, E. H. *Fluid Phase Equilibria* **2009**, 276, 75-85.
- (17) Vik, E. A. Berg, J. D. Ofjord, G. D. Reinhard, M. *Environmental Modelling and Software* **1992**, 25, 85-92.
- (18) Vik, E. A. Bakke, S. Bansal, K. M. *Environmental Modelling and Software* **1998**, 13, 529-537.
- (19) Nordstad, E. N. Knudsen, B. Sæten, J. O. Aas, N. Eilersten, H. B. *Chemicals in Value Chain (Kjemikalier i Verdikjeden)*, 1998.
- (20) OECD Partition Coefficient (n-octanol/water). *High Performance Liquid Chromatography*, OECD Guideline 117. 1989.
- (21) Marrero, J. Gani, R. *Industrial & Engineering Chemistry Research* **2002**, 41, 6623-6633.
- (22) Derawi, S. O. Kontogeorgis, G. M. Stenby, E. H. *Industrial & Engineering Chemistry Research* **2001**, 40, 434-443.
- (23) Chen, F. Holten-Andersen, J. Tyle, H. *Chemosphere* **1993**, 26, 1325-1354.
- (24) Sangster, J. *Octanol-Water Partition Coefficients - Fundamentals & Physical Chemistry*, John Wiley & Sons Ltd, 1997.
- (25) Klamt, A. *COSMO-RS: From Quantum Chemistry to Fluid Phase Thermodynamics and Drug Design*, Elsevier Science, 2005.
- (26) Ruelle, P. *Chemosphere* **2000**, 40, 457-512.
- (27) Dearden, J. C. Brensen, G. M. *Quant. Struct. -Act. Relat.* **1988**, 7, 133-144.
- (28) Leo, A. Hansch, C. Elkins, D. *Chemical Reviews* **1971**, 71, 525-616.
- (29) Leo, A. J. In *Molecular Design and Modeling: Concepts and Applications Part A: Proteins, Peptides, and Enzymes*, Academic Press, 1991, 202, 544-591.
- (30) Davis, G. Tomlinson, E. Harrison, G. Dearden, G. C. *Chem. Ind. London* **1967**, 677-683.

- (31) James, M. Davis, S. Anderson, N. J. *Pharm. Pharmacol.* **1981**, 33, 108.
- (32) Kinkel, J. F. M. Tomlinson, E. Smit, P. *International Journal of Pharmaceutics* **1981**, 9, 121-136.
- (33) Meylan, W. M. Howard, P. H. *J Pharm Sci* **1995**, 84, 83-92.
- (34) www.ACD/Labs.com **2009**.
- (35) Spieß, A. C. Eberhard, W. Peters, M. Eckstein, M. F. Greiner, L. Büchs, J. *Chemical Engineering and Processing: Process Intensification* **2008**, 47, 1034-1041.
- (36) Fredenslund, A. Jones, R. L. Prausnitz, J. M. *AIChE Journal* **1975**, 21, 1086.
- (37) Hansen, H. K. Rasmussen, P. Fredenslund, A. Schiller, M. Gmehling, J. *Industrial & Engineering Chemistry Research* **1991**, 30, 2352-2355.
- (38) Magnussen, T. Rasmussen, P. Fredenslund, A. *Ind. Eng. Chem. Process Des. Dev.* **1981**, 20, 133.
- (39) Larsen, B. L. Rasmussen, P. Fredenslund, A. *Industrial & Engineering Chemistry Research* **1987**, 26, 2274-2286.
- (40) Chen, F. Holten-Andersen, J. Tyle, H. *Chemosphere* **1993**, 26, 1325-1354.
- (41) Schulte, J. Dürr, J. Ritter, S. Hauthal, W. H. Quitzsch, K. Maurer, G. *Journal of Chemical & Engineering Data* **1998**, 43, 69-73.
- (42) Renon, H. Prausnitz, J. M. *AIChE Journal* **1968**, 14, 135-144.
- (43) Abrams, D. S. Prausnitz, J. M. *AIChE Journal* **1975**, 21, 116.
- (44) Wertheim, M. S. *J Stat Phys* **1984**, 35, 19-34.
- (45) Wertheim, M. S. *J Stat Phys* **1984**, 35, 35-47.
- (46) Wertheim, M. S. *J Stat Phys* **1986**, 42, 459-476.
- (47) Wertheim, M. S. *J Stat Phys* **1986**, 42, 477-492.
- (48) Chapman, W. G. Gubbins, K. E. Jackson, G. Radosz, M. *Industrial & Engineering Chemistry Research* **1990**, 29, 1709-1721.
- (49) Chapman, W. Jackson, G. Gubbins, K. *Molecular Physics* **1988**, 65, 1057-1079.
- (50) Huang, S. H. Radosz, M. *Industrial & Engineering Chemistry Research* **1990**, 29, 2284-2294.
- (51) Kontogeorgis, G. M. Michelsen, M. L. Folas, G. K. Derawi, S. von Solms, N. Stenby, E. H. *Industrial & Engineering Chemistry Research* **2006**, 45, 4855-4868.
- (52) Yakoumis, I. V. Kontogeorgis, G. M. Voutsas, E. C. Tassios, D. P. *Fluid Phase Equilibria* **1997**, 130, 31-47.
- (53) Voutsas, E. C. Kontogeorgis, G. M. Yakoumis, I. V. Tassios, D. P. *Fluid Phase Equilibria* **1997**, 132, 61-75.
- (54) Hendriks, E. M. Walsh, J. Bergen, A. R. D. *J Stat Phys* **1997**, 87, 1287-1306.
- (55) Yakoumis, I. V. Kontogeorgis, G. M. Voutsas, E. C. Hendriks, E. M. Tassios, D. P. *Industrial & Engineering Chemistry Research* **1998**, 37, 4175-4182.
- (56) Wu, J. Prausnitz, J. M. *Industrial & Engineering Chemistry Research* **1998**, 37, 1634-1643.
- (57) Voutsas, E. C. Yakoumis, I. V. Tassios, D. P. *Fluid Phase Equilibria* **1999**, 158-160, 151-163.
- (58) Kontogeorgis, G. M. V. Yakoumis, I. Meijer, H. Hendriks, E. Moorwood, T. *Fluid Phase Equilibria* **1999**, 158-160, 201-209.
- (59) Polysou, E. N. Louludi, A. E. Kontogeorgis, G. M. Yakoumis, I. V. University of Thessaloniki, Greece, 1999, p. 101.
- (60) Voutsas, E. C. Boulougouris, G. C. Economou, I. G. Tassios, D. P. *Industrial & Engineering Chemistry Research* **2000**, 39, 797-804.
- (61) Pfohl, O. Pagel, A. Brunner, G. *Fluid Phase Equilibria* **1999**, 157, 53-79.
- (62) Kontogeorgis, G. M. Yakoumis, I. V. Vlamos, P. M. *Computational and Theoretical Polymer Science* **2000**, 10, 501-506.
- (63) Michelsen, M. L. Hendriks, E. M. *Fluid Phase Equilibria* **2001**, 180, 165-174.
- (64) Peeters, P. *Nucleation and condensation in gas-vapor mixtures of alkanes and water*, Technical University of Eindhoven: Eindhoven, The Netherlands, 2002.
- (65) von Solms, N. Michelsen, M. L. Kontogeorgis, G. M. *Industrial & Engineering Chemistry Research* **2003**, 42, 1098-1105.

- (66) Derawi, S. O. Michelsen, M. L. Kontogeorgis, G. M. Stenby, E. H. *Fluid Phase Equilibria* **2003**, 209, 163-184.
- (67) Derawi, S. O. Kontogeorgis, G. M. Michelsen, M. L. Stenby, E. H. *Industrial & Engineering Chemistry Research* **2003**, 42, 1470-1477.
- (68) Orr, F. M. Jr. *High resolution prediction of gas injection process performance for heterogeneous reservoirs*. 2003.
- (69) Bruinsma, D. F. M. Desens, J. T. Notz, P. K. Sloan, E. D. *Fluid Phase Equilibria* **2004**, 222-223, 311-315.
- (70) Derawi, S. O. Zeuthen, J. Michelsen, M. L. Stenby, E. H. Kontogeorgis, G. M. *Fluid Phase Equilibria* **2004**, 225, 107-113.
- (71) Folas, G. K. Derawi, S. O. Michelsen, M. L. Stenby, E. H. Kontogeorgis, G. M. *Fluid Phase Equilibria* **2005**, 228-229, 121-126.
- (72) Queimada, A. J. Miqueu, C. Marrucho, I. M. Kontogeorgis, G. M. Coutinho, J. A. P. *Fluid Phase Equilibria* **2005**, 228-229, 479-485.
- (73) Kaarsholm, M. Derawi, S. O. Michelsen, M. L. Kontogeorgis, G. M. *Industrial & Engineering Chemistry Research* **2005**, 44, 4406-4413.
- (74) Folas, G. K. Gabrielsen, J. Michelsen, M. L. Stenby, E. H. Kontogeorgis, G. M. *Industrial & Engineering Chemistry Research* **2005**, 44, 3823-3833.
- (75) Saghir, M. Z. Jiang, C. G. Derawi, S. O. Stenby, E. H. Kawaji, M. *Eur. Phys. J. E* **2004**, 15, 241-247.
- (76) Frøyna, E. W. *Measurement of water content in natural gas*, Norwegian University of Science and Technology: Trondheim, Norway, 2004.
- (77) Folas, G. K. Kontogeorgis, G. M. Michelsen, M. L. Stenby, E. H. *Industrial & Engineering Chemistry Research* **2006**, 45, 1527-1538.
- (78) de Hemptinne, Mougin, Barreau, Ruffine, Tamouza, Inchekel *Application of statistical thermodynamic-based equations of state to petroleum engineering*, IFP: France.
- (79) Pedersen, K. S. Thomassen, P. Fredenslund, A. *Advances in Thermodynamics, C7+ Fraction Characterization*, Taylor & Francis: New York, 1989, Vol. 1.
- (80) Michelsen, M. L. Hendriks, E. M. *Fluid Phase Equilibria* **2001**, 180, 165-174.
- (81) Folas, G. K. *Modeling of Complex Mixtures Containing Hydrogen Bonding Molecules*, DTU: 2800 Kgs Lyngby, Denmark, 2006.
- (82) Suresh, S. J. Elliott, J. R. *Industrial & Engineering Chemistry Research* **1992**, 31, 2783-2794.
- (83) Oliveira, M. B. Coutinho, J. A. P. Queimada, A. J. *Fluid Phase Equilibria* **2007**, 258, 58-66.
- (84) Soave, G. *Fluid Phase Equilibria* **1986**, 31, 203-207.
- (85) Whitson, C. H. Søreide, I. Chorn, L. G. Mansoori, G. A. *Advances in Thermodynamics, C7+ Fraction Characterization*, Taylor & Francis: New York, 1989, Vol. 1.
- (86) Twu, C. H. *Fluid Phase Equilibria* **1984**, 16, 137-150.
- (87) Soave, G. S. *Fluid Phase Equilibria* **1998**, 143, 29-39.
- (88) Inhibitor partitioning: http://www.infochemuk.com/publicat/leaflets/Inhibitor_partitioning.pdf **2009**.
- (89) Haghighi, H. Chapoy, A. Burgess, R. Mazloum, S. Tohidi, B. *Fluid Phase Equilibria* **2009**, 278, 109-116.
- (90) Haghighi, H. Chapoy, A. Burgess, R. Tohidi, B. *Fluid Phase Equilibria* **2009**, 276, 24-30.
- (91) Folas, G. K. Kontogeorgis, G. M. Michelsen, M. L. Stenby, E. H. *Industrial & Engineering Chemistry Research* **2006**, 45, 1516-1526.
- (92) Maczynski, A. Wiśniewska-Gocłowska, B. Goral, M. J. *Phys. Chem. Ref. Data* **2004**, 33, 549-577.
- (93) Goral, M. Wisniewska Gocłowska, B. Maczynski, A. J. *Phys. Chem. Ref. Data* **2004**, 33, 1159-1188.
- (94) Bahadori, A. Vuthaluru, H. B. Tadé, M. O. Mokhatab, S. *Chem. Eng. Technol.* **2008**, 31, 1743-1747.

- (95) Shaw, D. G. Maczynski, A. Goral, M. Wisniewska-Gocłowska, B. Skrzecz, A. Owczarek, I. Blazej, K. Haulait-Pirson, M.C. T. Hefter, G.T. Kapuku, F. Maczynska, Z. Szafranski, A. *J. Phys. Chem. Ref. Data* **2005**, *34*, 2261-2298.
- (96) Shaw, D. G. Maczynski, A. Goral, M. Wisniewska-Gocłowska, B. Skrzecz, A. Owczarek, I. Blazej, K. Haulait-Pirson, M.C. T. Hefter, G.T. Kapuku, F. Maczynska, Z. Szafranski, A. *J. Phys. Chem. Ref. Data* **2005**, *34*, 1489-1553.
- (97) Maczynski, A. Shaw, D. G. Goral, M. Wisniewska-Gocłowska, B. Skrzecz, A. Owczarek, I. Blazej, K. Haulait-Pirson, M.C. T. Hefter, G.T. Kapuku, F. Maczynska, Z. Szafranski, A. *J. Phys. Chem. Ref. Data* **2005**, *34*, 1389-1488.
- (98) Shaw, D. G. Maczynski, A. Goral, M. Wisniewska-Gocłowska, B. Skrzecz, A. Owczarek, I. Blazej, K. Haulait-Pirson, M.C. T. Hefter, G.T. Kapuku, F. Maczynska, Z. Szafranski, A. *J. Phys. Chem. Ref. Data* **2005**, *34*, 2299-2345.
- (99) Chen, H. Wagner, J. *Journal of Chemical & Engineering Data* **1994**, *39*, 679-684.
- (100) de Hemptinne, J.-C. Mougin, P. Barreau, A. Ruffine, L. Tamouza, S. Inchekel, R. *Application of statistical thermodynamic-based equations of state to petroleum engineering*, 2006, pp. 363-386.
- (101) Hong, J. H. Malone, P. V. Jett, M. D. Kobayashi, R. *Fluid Phase Equilibria* **1987**, *38*, 83-96.
- (102) Chapoy, A. H. Mohammadi, A. Valtz, A. Coquelet, C. Richon, D. *GPA Research Report RR-198: Water and Inhibitor Distribution in Gas Production Systems*, 2008.
- (103) *Heriot-Watt University Hydrate model: www.pet.hw.ac.uk/research/hydrate/*.
- (104) Avlonitis, D. A. *Thermodynamics of Gas Hydrate Equilibria*. PhD Thesis, Heriot-Watt University: Edinburgh, UK, 1988.
- (105) Tohidi, B. *Gas Hydrate Equilibria in the Presence of Electrolyte Solutions*. PhD Thesis, Heriot-Watt University: Edinburgh, UK, 1995.
- (106) Valderrama, J. O. *J. Chem. Eng. Japan* **1990**, 87-91.
- (107) Avlonitis, D. Danesh, A. Todd, A. C. *Fluid Phase Equilibria* **1994**, *94*, 181-216.
- (108) ASTM D5134 - 98 Standard Test Method for Detailed Analysis of Petroleum Naphthas through n-nonane by Capillary Gas Chromatography **2008**.
- (109) Staveley, L. A. K. Milward, G. L. *J. Chem. Soc.* **1957**, 4369-4375.
- (110) Riaz, M. Kontogeorgis, G. M. Stenby, E. H. Yan, W. Haugum, T. Christensen, K. O. Solbraa, E. Løkken, T. V. *Fluid Phase Equilibria* **2011**, *300*, 172-181.
- (111) Lindboe, M. Haugum, T. Fredheim, A. O. Solbraa, E. *Measurement and Modeling of Liquid-Liquid Equilibrium in n-Heptane-MEG Systems* **2002**.
- (112) Riaz, M. Kontogeorgis, G. M. Stenby, E. H. Yan, W. Haugum, T. Christensen, K. O. Løkken, T. V. Solbraa, E. *Journal of Chemical & Engineering Data* **2011** (In the press).
- (113) Derawi, S. O. Kontogeorgis, G. M. Stenby, E. H. Haugum, T. Fredheim, A. O. *Journal of Chemical & Engineering Data* **2002**, *47*, 169-173.
- (114) Frost, M. *Measurement and modelling of phase equilibrium in Oil-MEG-Water mixtures*. MSc Thesis, DTU: 2800 Kgs Lyngby, Denmark, 2010.
- (115) Yussuf, M. *Measurement of Phase Equilibria for Oil-Water-MEG Mixtures*. MSc Thesis, DTU: 2800 Kgs Lyngby, Denmark, 2011.
- (116) Pedersen, K. S. Michelsen, M. L. Fredheim, A. O. *Fluid Phase Equilibria* **1996**, *126*, 13-28.
- (117) Kontogeorgis, G. M. Michelsen, M. L. Folas, G. K. Derawi, S. von Solms, N. Stenby, E. H. *Industrial & Engineering Chemistry Research* **2006**, *45*, 4869-4878.
- (118) Folas, G. K. Berg, O. J. Solbraa, E. Fredheim, A. O. Kontogeorgis, G. M. Michelsen, M. L. Stenby, E. H. *Fluid Phase Equilibria* **2007**, *251*, 52-58.
- (119) Folas, G. K. Kontogeorgis, G. M. Michelsen, M. L. Stenby, E. H. *Fluid Phase Equilibria* **2006**, *249*, 67-74.
- (120) Dhima, A. de Hemptinne, J.-C. Moracchini, G. *Fluid Phase Equilibria* **1998**, *145*, 129-150.
- (121) Robinson, D. B. Peng, D.-Y. Chung, S. Y.-K. *Fluid Phase Equilibria* **1985**, *24*, 25-41.
- (122) Søreide, I. Whitson, C. H. *Fluid Phase Equilibria* **1992**, *77*, 217-240.

- (123) Kabadi, V. N. Danner, R. P. *Industrial & Engineering Chemistry Process Design and Development* **1985**, 24, 537-541.
- (124) Kontogeorgis, G. M. Tsivintzelis, I. Michelsen, M. L. Stenby, E. H. *Fluid Phase Equilibria* **2011**, 301, 244-256.
- (125) Stefanis, E. Constantinou, L. Panayiotou, C. *Ind. Eng. Chem. Res.* **2004**, 43, 6253-6261.
- (124) Marrero, J. Gani, R. *Ind. Eng. Chem. Res.* **2002**, 41, 6623-6633.

9 Appendices

9.1 Appendix A: Production Chemicals

Appendix-A presents tables and figures related to work presented in chapter-2: “octanol-water partition coefficient”. The list of production chemicals used by oil and gas industry and related information is given in appendix A. 1. The data and predictions for octanol-water, oil-water and hexane-water partition coefficients used to investigate various correlations among them are given in appendices A. 2 and A. 3. The correlation between carbon number (Nc) of alcohols and $K_{oil-water}/K_{ow}$ or $K_{oil-water}/K_{hw}$ are given in appendices A. 4 and A. 5. Finally calculation results (taken from the literature) of $\log K_{ow}$ for polyfunctional molecules from UNIFAC models and AFC correlations are shown in appendix A. 6.

A. 1: List of Production Chemicals Their Functions, CAS No., $\log K_{ow}$ and $K_{oil-water}$

Compound Name	CAS No.	$\log K_{ow}$	$K_{oil-water}$
pH Regulating Chemical			
Formic acid	64-18-6		0.01
Waxinhibitor			
Aromatic solvent	64742-94-5	4.4	0.01
Alkylamine	27176-87-0	1.4	0.01
Ethylvinyl acetate polymer	N/A	0.0002	0.01
Polyacrylate	N/A	0.0002	0.01
Xylene	1330-20-7	4.0001	0.01
Alkyl ester	N/A	3	0.01
Alkylsulphonate	N/A	0.8	0.01
Alkyl ester	N/A	2	0.01
Alkylarylsulphonate salt	N/A	2	0.01
Ethyl vinyl acetate polymer	N/A	0	0.01
Emulsion Breaker			
Alkylene oxide block polymer 1024	N/A	0.0002	0.01
Polymeric alkoxyate 78	N/A	0.0002	0.01
Butyldiglycolether	112-34-5	1.3	0.01
Alkylene oxide block polymer 9561	N/A	0.0002	0.01
Low aromatic solvent	64742-06-9	5.2	0.01
2-Ethyl hexanol	104-76-7	2.61	114
Alkylbenzenes (C9 - C10)	64742-94-5	4.38	19952
Polymeric alkoxyate 851	N/A	0	0.01
Polymerised polyol 9261	N/A	0	0.01
Alkoxyate quaternary polyamine 3216	N/A	0	0.01
Polyolester 400	N/A	0	0.01
Di-Epoxyde	N/A	0	2754.2287
ISOPROPYLAMINE SALT OF DDBSA	68584-24-7	2.9999	549.5
Polymeric alkoxyate 510	N/A	0	0.01
Hydroxyl Terminated Poly (oxyalkylene) Complex Polyether	9082-00-2	0	0.01
Polyol ester 317	N/A	0	0.01
Polyamine	N/A	0.0002	0.01
			continued..

Alkoxyated polyacrylate	70857-15-7	0.0002	2511
Polyoxyalkylene glycols	68123-18-2	0.0002	60
Polyglycol polyester	N/A	0.0002	1
Polyol ester 208	N/A	0	0.01
Diepoxide	68123-18-2	0.0002	2754.2287
Amine based fatty acid	N/A	0	1000
Di-Epoxide	N/A	0.0002	2754.2287
Ethylene glycol monobutyl ether	111-76-2	1.84	69.1830971
Polyamine	N/A	0.0002	2.38
Corrosion Inhibitor			
Alkyl amine salt	N/A	-0.1	16
Isopropanol	67-63-0		0.012
Butyl glycol	111-76-2	1.1	12.5892541
Amine based fatty acids	N/A	-2.2	0.0063
Sodium carbonate	497-19-8		0.00001
Sodium thiosulphate	10102-17-7		0.00001
Sodium bicarbonate	144-55-8		0.00001
Scale Inhibitor			
Sodium polyaspartate	N/A	-2	0.005
Organo Phosphate	68131-71-5	1.17	14.79
Polycarboxylic acid salt	N/A	-0.0001	0.025
Polyaspartate	N/A	2.75	0.0047
Aminmethylene phosphonic acid ammonium salt	N/A	0	0.01
Potassium hydroxide	1310-58-3		0.01
Others			
Amine ethoxilate	26635-93-8	1.11	12.88
Block polymer	N/A	0.0002	37153
Polyamine	N/A	0.0002	2.38
Siliconglycol	N/A	2	0.09
Dodecyl benzene sulphonic acid	85117-49-3	3.2	2.71
Alkylsulphonate	N/A	0.8	6.3
Defoamer			
Alkyl acetate	N/A	3.9	0.01
Dipropylene Glycol n-butyl ether	29911-28-2	2.28	190.546072
Glycerol oleate	68424-61-3	5.94	870963.59
Alkylacetate	N/A	3.9	0.01
Polydimethyl siloxan (PDMS)	63148-62-9	0.0002	0.01
Fluorosilicone #1	N/A	0	0.01
Alkylcarboxylate	N/A	2.6	398
Fatty acid polyglycol ester	N/A	4.82	50118.7234
Flocculant			
Acrylic copolymer in aqueous emulsion	N/A	1.6299	0.01
Anionic acrylic copolymer	N/A	0.4	2.51
Maleic acid Copolymer	113221-69-5	0	0.01
Acrylic copolymer in aqueous emulsion form	N/A	-0.0001	0.01
			continued..
Polycarboxylic acid salt	N/A	-0.0001	0.01
Alkyl sulphate salt	N/A	2	0.01

Hydrate Inhibitor			
Monoethylenglycol	107-21-1		0.0015
Methanol	67-56-1		0.11
Sodium hydroxide	1310-73-2		0.00001

A. 2: Oil-Water Partition Coefficients ($K_{\text{oil-water}}$) and Octanol-Water Partition Coefficients (K_{ow}) of Production Chemicals.

	Family	Chemical Name	Abb.	Formula	Mol. wt.	Cas No.	Nc	Smile	LogKoil-water	Koil-water	References	LogKow	Kow	Reference
1	Alcohols	Methanol		C1OH		067-56-1	1	CO	-0.959	0.11	Knudsen B. 2000, Statoil Internal Report	-0.77	0.169	Hanach C. et al. 1995 (Softwater Kowwin)
2		Ethanol		C2OH	46.07	064-17-5	2	CCO	-1.009	0.098	calculated from ratio=koil-water/kow=2	-0.31	0.489	Hanach C. et al. 1995 (Softwater Kowwin)
3		2-Propanol		C3OH	60.1	067-63-0	3	CC(O)C	-1.921	0.012	Knudsen B. 2000, Statoil Internal Report	0.05	1.122	Hanach C. et al. 1995 (Softwater Kowwin)
4		1-Propanol		C3OH	60.1	071-23-8	3	CCCO	-0.886	0.13	Knudsen B. 2000, Statoil Internal Report	0.25	1.778	Hanach C. et al. 1995 (Softwater Kowwin)
5		1-Butanol		C4OH	74.12	071-36-3	4	CCCCO	-0.292	0.51	Knudsen B. 2000, Statoil Internal Report	0.88	7.585	Hanach C. et al. 1995 (Softwater Kowwin)
6		1-Pentanol		C5OH	88.15	071-41-0	5	CCCCCO	NA	NA	NA	1.51	32.36	Stangaster 1995 (Software Kowwin)
7		1-Hexanol		C6OH	102.18	111-27-3	6	CCCCCCO	NA	NA	NA	2.03	107.15	Hanach C. et al. 1995 (Softwater Kowwin)
8		Heptanol		C7OH	116.21	111-70-6	7	CCCCCCO	NA	NA	NA	2.64	436	Ruelle,P.Chemosphere 40,2000,457-512
9		n-decanol		C10OH	158.29	112-30-1	10	CCCCCCCCCO	2.057	114	Knudsen B. 2000, Statoil Internal Report	4.57	37153	Hanach C. et al. 1995 (Softwater Kowwin)
10		Octadecanol		C18OH	270.5	NA	18	C18O	3.987	9700	Knudsen B. et al. 1999,5, p.	7.72	52480746	Estimated LogKow (Version 1.67)
11		2-Methylprapan-2-ol							NA	NA	NA	0.36		
12		Benzyle Alcohol							NA	NA	NA	1.08		
13	Glycol/ Glycol ether	Monoethylene glycol	MEG		62.068	107-21-1	2	OCCO	-2.824	0.0015	Knudsen B. 2000, Statoil Internal Report	-1.36	0.043	Hanach C. et al. 1995 (Softwater Kowwin)
14		Triethylene glycol	TEG		150.17	112-27-6	6	C(COCCOCCO)O	-1.509	0.031	Knudsen B. 2000, Statoil Internal Report	-1.75	0.018	Estimated LogKow (Version 1.67)
15		Butyldiglycol			162.23	112-34-5	8	O(CCOCCO)CCCC	-0.252	0.56	Knudsen B. 2000, Statoil Internal Report	0.56	3.63	Funasaki, N, et al. 1984 (Software Kowwin)
16		Butyldiglycoloctate							0.919	8.3	Knudsen B. 2000, Statoil Internal Report			
17	Alkanolamine	Butylethanolamine	BEA		117.19	111-75-1	6	OCCNCCCC	-1.310	0.049	Knudsen B. 2000, Statoil Internal Report	0.33	2.14	Estimated LogKow (Version 1.67)
18		Methyldiethanolamine	MDEA		119.2	105-59-9	5	OCCN(CCO)C	-1.509	0.031	Knudsen B. 2000, Statoil Internal Report	-1.5	0.032	Estimated LogKow (Version 1.67)
19		Mono-Ethanolamine	MEA		61.08	141-43-5	2	NCCO	-1.585	0.026	Knudsen B. 2000, Statoil Internal Report	-1.31	0.049	Hanach C. et al. 1995 (Softwater Kowwin)
	Imidazoline Salt	Imidazoline Salt	K1324						1.690	49	Knudsen B. 2000, Statoil Internal Report			
		Imidazoline Salt	K1350						1.959	91	Knudsen B. 2000, Statoil Internal Report			
		Imidazoline Salt	K1350						1.505	32	Knudsen B. 2000, Statoil Internal Report			
		Imidazoline Salt	PK6050						1.839	69	Knudsen B. 2000, Statoil Internal Report			
	Reagents N/S													
20	Carboxylic Acids	Butanoic Acid							NA	NA	NA	0.79		J. Chem. Soc. Perkin Trans. 2, 1997
21		Pentanoic Acid							NA	NA	NA	1.39		J. Chem. Soc. Perkin Trans. 2, 1997
22	Aromatics	Toluene							NA	NA	NA	2.69		J. Chem. Soc. Perkin Trans. 2, 1997
23		Pyridine							NA	NA	NA	0.65		J. Chem. Soc. Perkin Trans. 2, 1997
24		Phenol							NA	NA	NA	1.49		J. Chem. Soc. Perkin Trans. 2, 1997

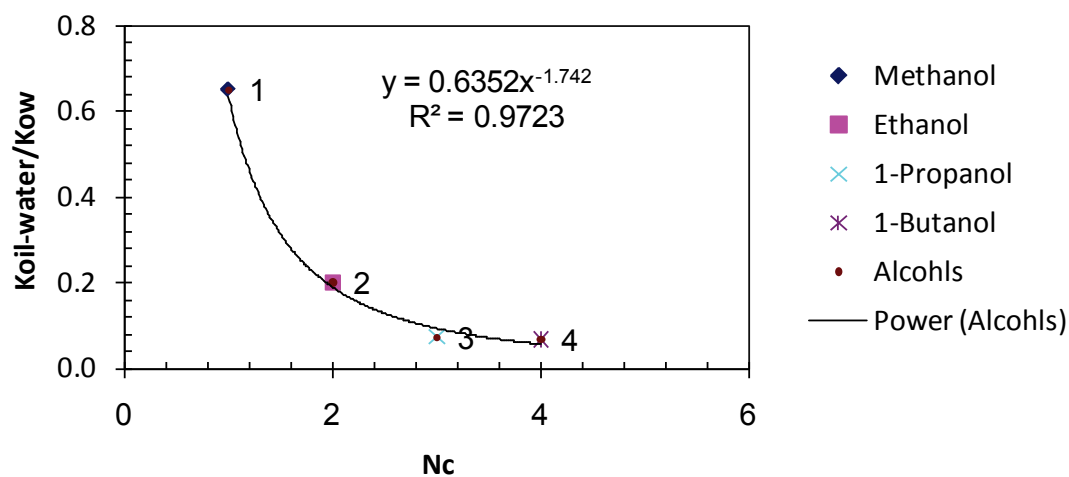
NA not available
 Abb. abbreviation
 Mol. Wt. Molecular Weight

A. 3: Hexane-Water Partition Coefficients (K_{hw}) for Alcohols.^{1,2}

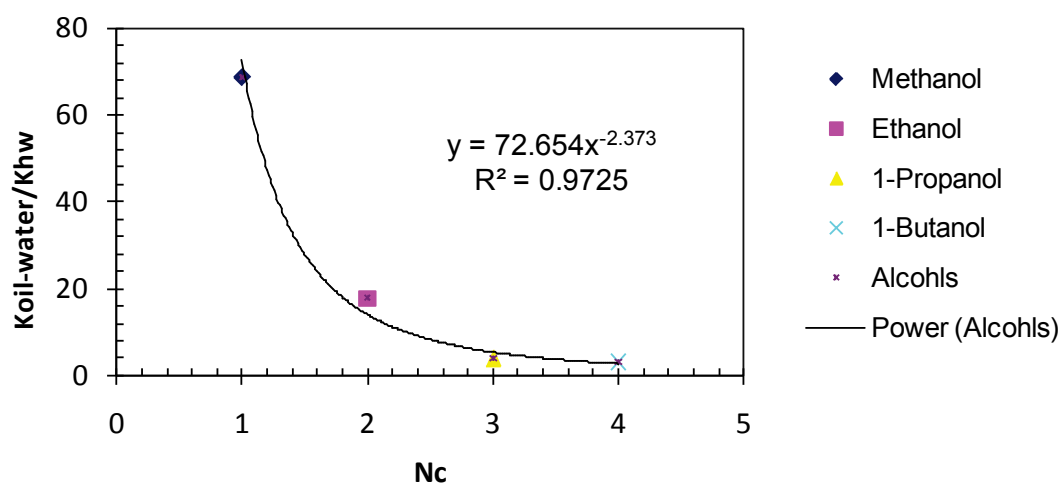
	Family	Chemical Name	Formula	Mol. wt.	CAS No.	Nc	Smile	¹ K_{hw}
1	Alcohals	Methanol	C1OH		067-56-1	1	CO	0.0016
2		Ethanol	C2OH	46.07	064-17-5	2	CCO	0.0055
3		2-Propanol	C3OH	60.1	067-63-0	3	CC(O)C	
4		1-Propanol	C3OH	60.1	071-23-8	3	CCCO	0.0331
5		1-Butanol	C4OH	74.12	071-36-3	4	CCCCO	0.166
6		1-Pentanol	C5OH	88.15	071-41-0	5	CCCCCO	0.398
7		1-Hexanol	C6OH	102.18	111-27-3	6	CCCCCO	2.819
8		Heptanol	C7OH	116.21	111-70-6	7	CCCCCO	16.218

(1) Schulte, J. Dürr, J. Ritter, S. Hauthal, W. H. Quitzsch, K. Maurer, G. *Journal of Chemical & Engineering Data* **1998**, 43, 69-73.

(2) Ruelle, P. *Chemosphere* 40, 2000, 457-512



A. 4: Correlation between carbon number (N_c) of alcohols and $K_{oil-water}/K_{ow}$.



A. 5: Correlation between carbon number (N_c) of alcohols and $K_{oil-water}/K_{hw}$.

A. 6: Calculations of logK_{ow} for Polyfunctional Molecules from UNIFAC Models and AFC Correlations.¹

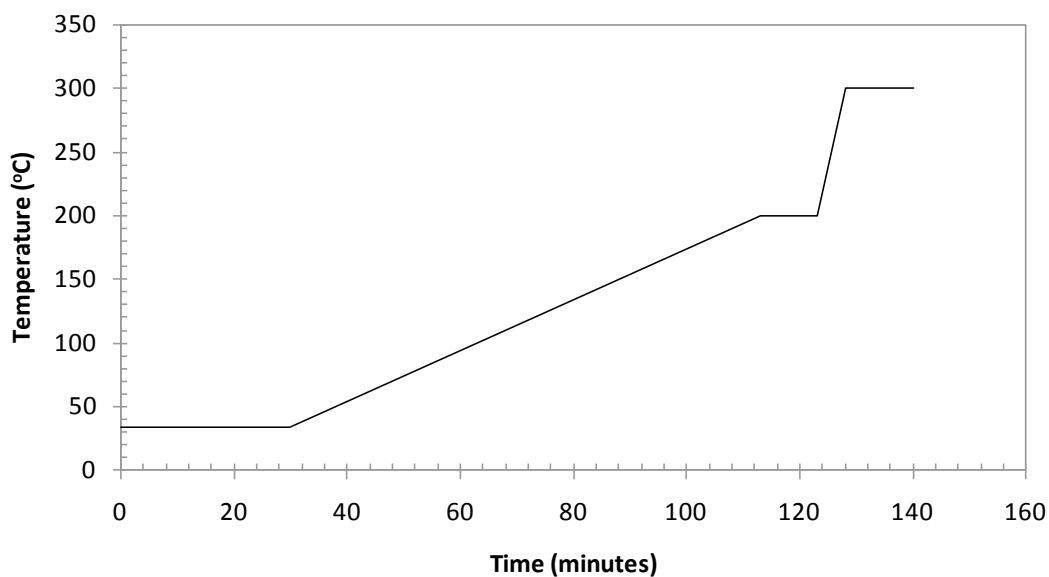
solute	log P_{ow}^{exp}	AAD					
		original UNIFAC VLE-1	UNIFAC LLE	original UNIFAC VLE-2	modified UNIFAC VLE-3	WATER UNIFAC	AFC model
triethylene glycol	-2.08	0.43	-1.11	-0.18	-0.64	-0.63	-1.75
diethanolamine	-1.43	-0.40	na ^a	-0.37	-1.00	-1.68	-1.71
ethylene glycol	-1.36	-0.72	-3.14	0.53	-1.04	-1.14	-1.20
ethanolamine	-1.31	-0.57	na ^a	-0.85	-0.82	na ^a	-1.61
1,3-propanediol	-1.04	-1.15	-1.11	-1.18	-1.22	-0.70	-0.71
triethanolamine	-1.00	-0.28	na ^a	-0.86	-1.18	-1.90	-2.48
propylene glycol	-0.92	-0.46	-0.68	-0.36	-0.64	-0.70	-0.78
2,3-butanediol	-0.92	-1.05	-1.01	-1.09	-1.11	-0.26	-0.36
1,4-butanediol	-0.83	-1.05	-1.01	-1.09	-1.11	na ^a	-0.22
2-methoxyethanol	-0.77	0.35	-0.47	0.41	-0.38	-0.26	-0.91
2-(2-hydroxypropoxy)-1-propanol	-0.67	-0.72	-0.97	-0.94	-0.99	0.29	-0.64
ethylcarbitol	-0.54	-0.12	-1.34	-0.79	-0.96	0.43	-0.69
dimethylcarbitol	-0.36	0.24	-2.10	-0.86	-1.19	0.58	-0.48
2-ethoxyethanol	-0.28	0.79	0.00	0.87	0.02	0.18	-0.42
isopropylcellosolve	0.05	-0.47	-0.98	-0.79	-0.86	0.62	0.00
butylcarbitol	0.56	-0.06	-1.19	-0.72	-0.89	1.31	0.29
isobutylcellosolve	0.75	-0.45	-0.94	-0.77	-0.83	1.05	0.49
1,3-benzenediol	0.80	2.26	0.18	-0.61	-1.36	2.22	1.03
2-butoxyethanol	0.83	1.66	0.95	1.78	0.83	1.05	0.57
diethoxymethane	0.84	-0.20	-1.39	-0.82	-1.02	1.06	0.79
1,2-benzenediol	0.88	2.26	0.18	-0.61	-1.36	2.22	1.03
hexylcarbitol	1.70	-0.03	-1.09	-0.68	-0.86	2.18	1.27
total data points	22	0.85	0.93	0.98	0.86	0.66	0.29

^a na: not available group parameters.

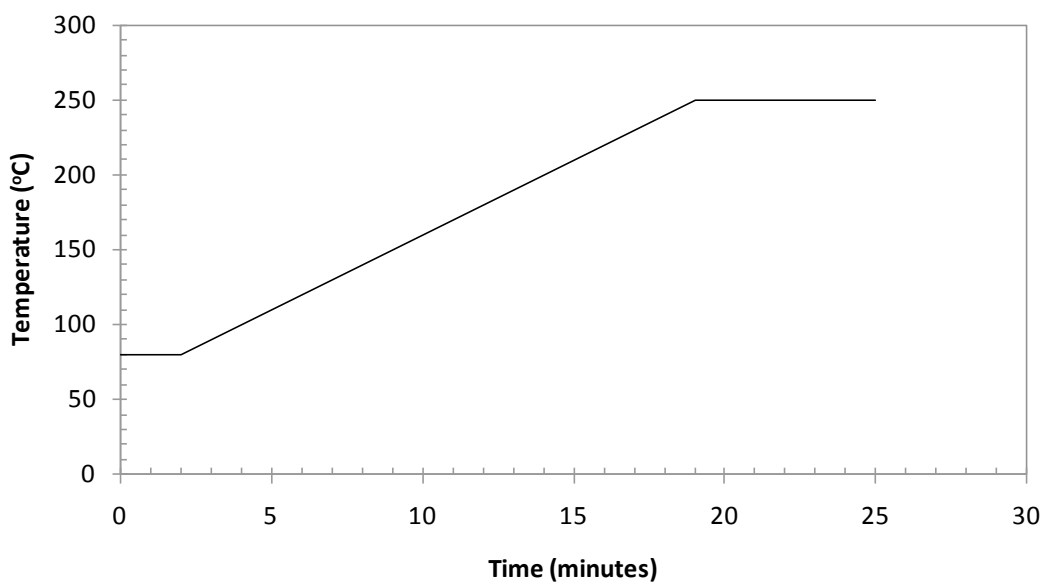
- (1) Derawi, S. O. Kontogeorgis, G. M. Stenby, E. H. *Industrial & Engineering Chemistry Research* **2001**, *40*, 434-443.

9.2 Appendix B: GC Analysis

In this appendix temperature programs used for condensate and glycol GC are shown in (appendices) B. 1 and B. 2. In appendix B. 3 ASTM D5134 Standard used for indentation of peaks in a reservoir fluid is presented.

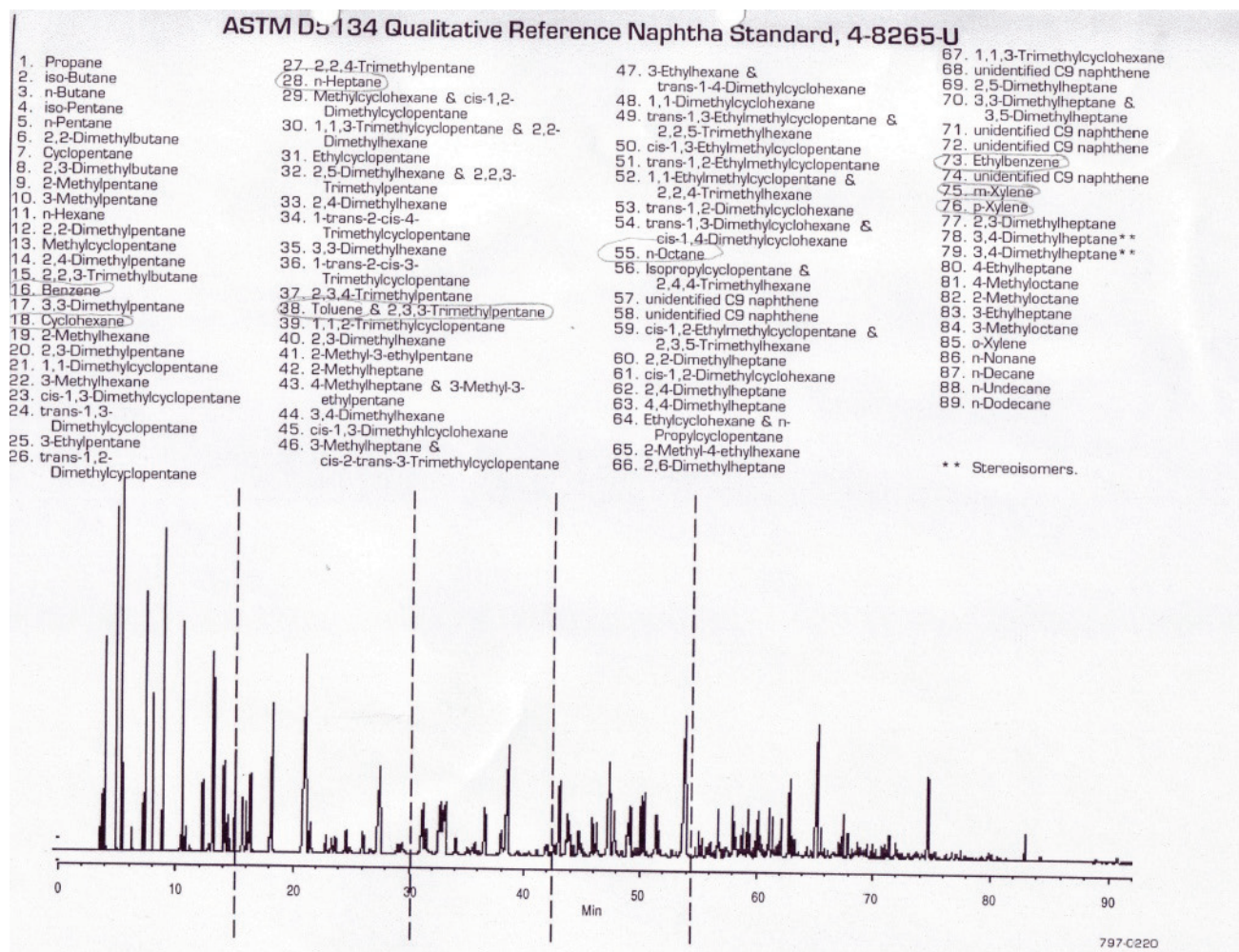


B. 1: The temperature program used for condensate analysis on condensate GC.

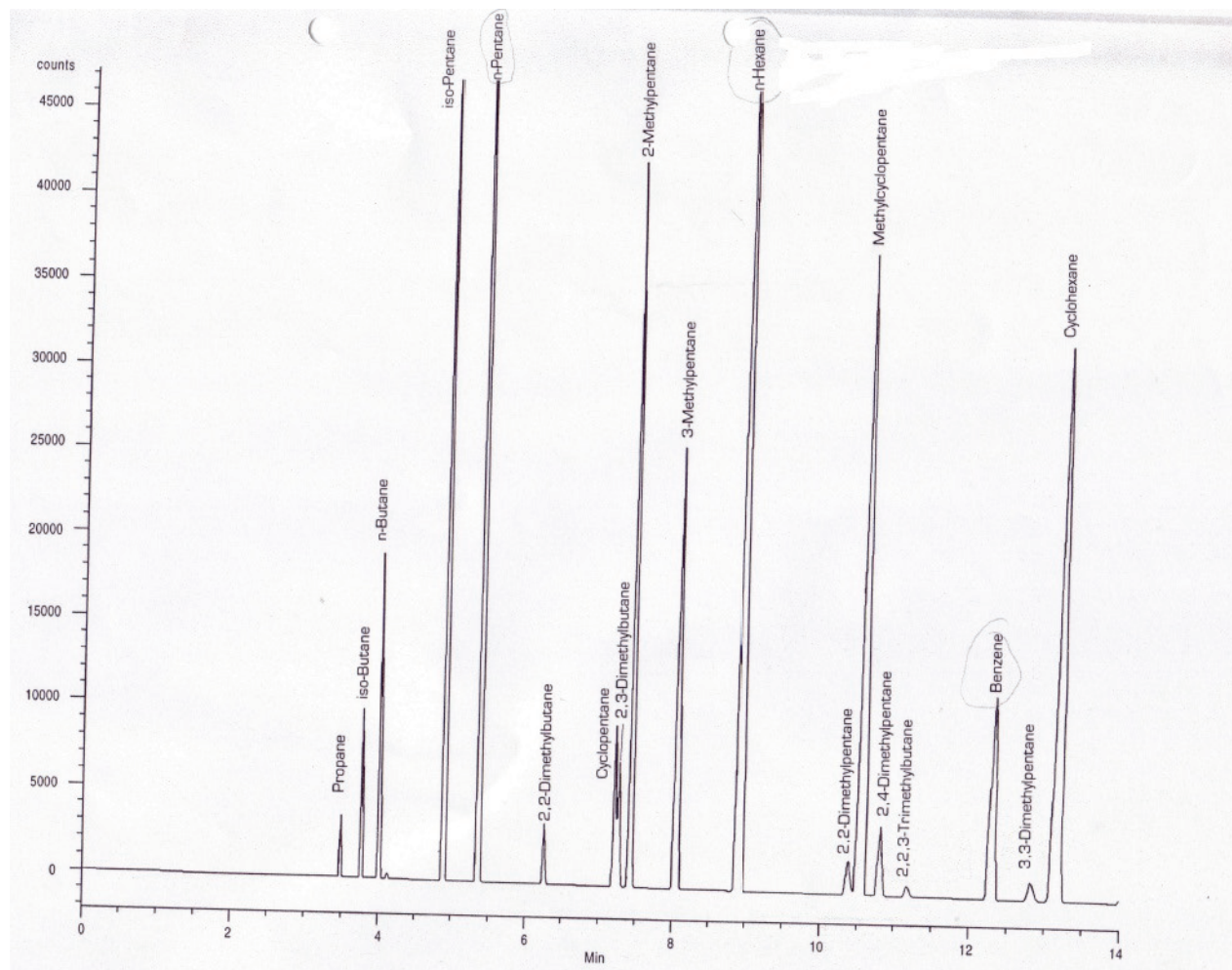


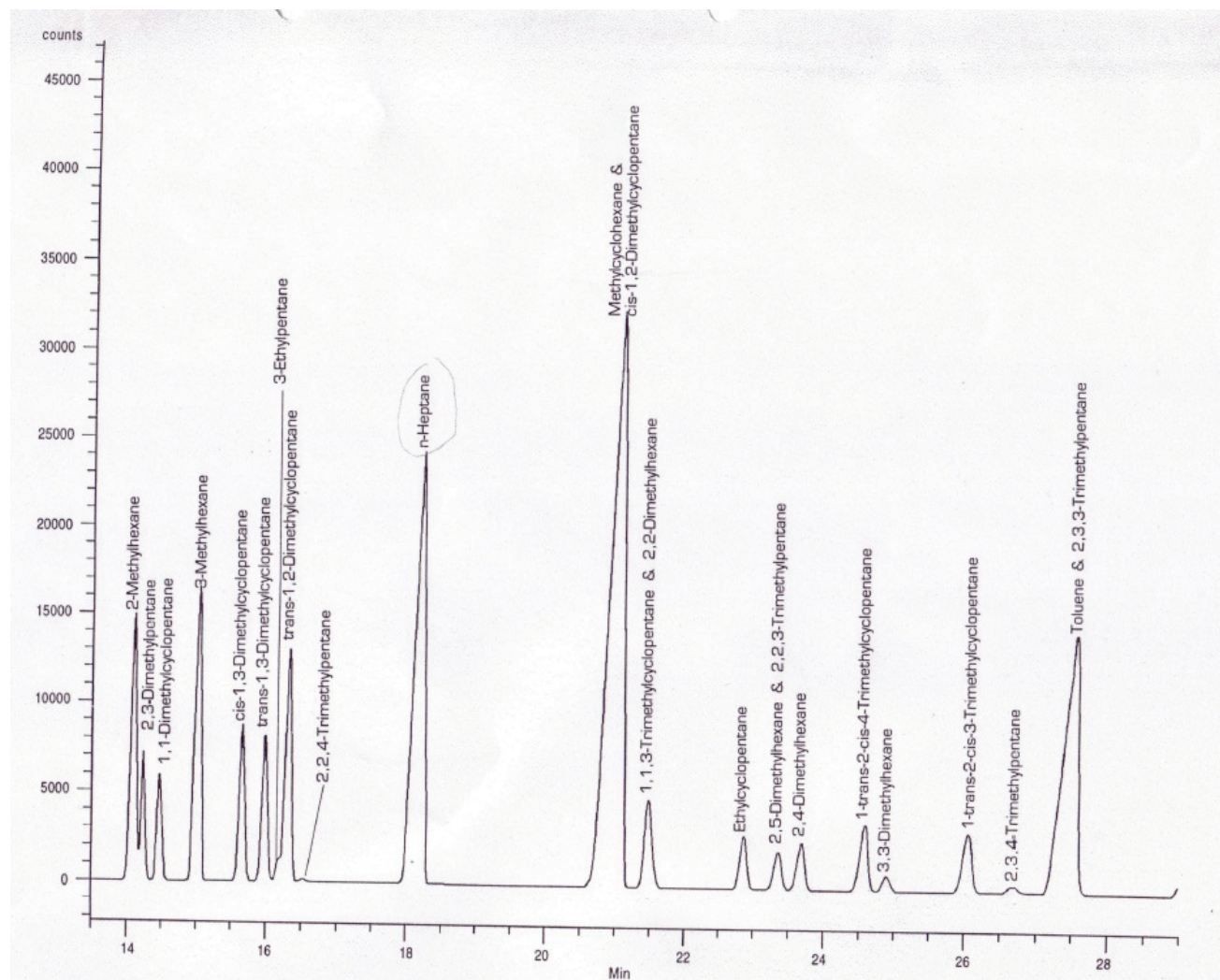
B. 2: The temperature program for glycol GC.

B. 3: ASTM D5134 Standard 1 of 6



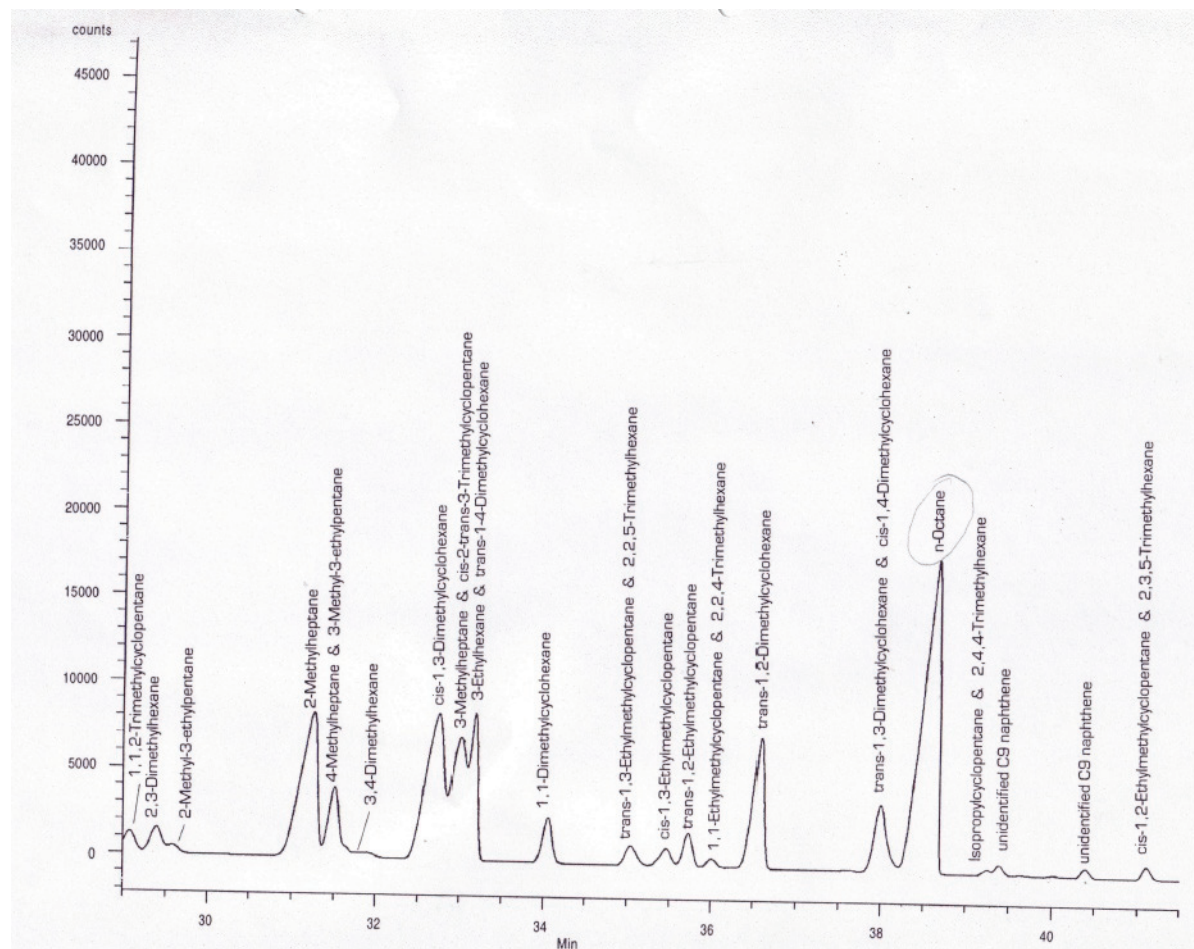
ASTM D5134 Standard 2 of 6

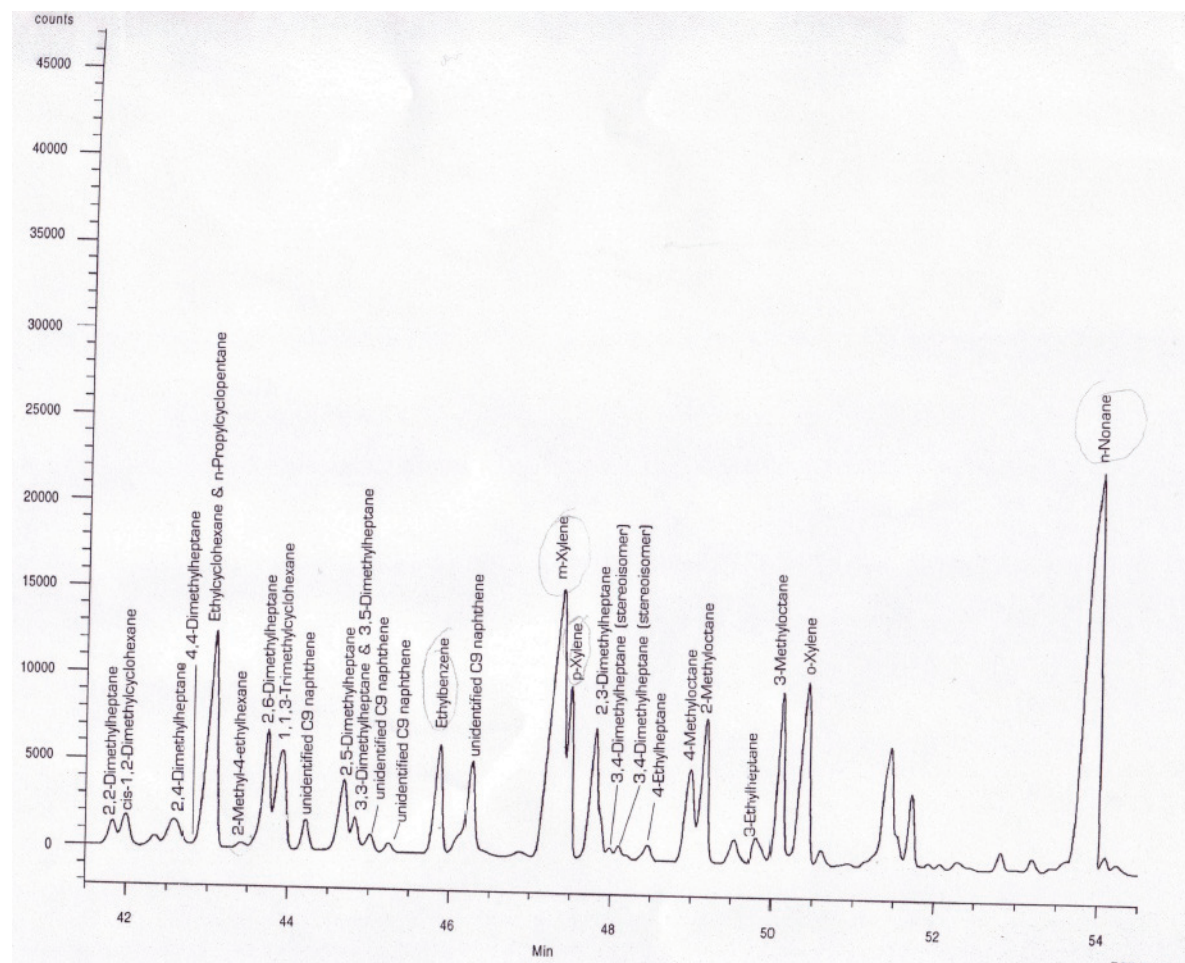




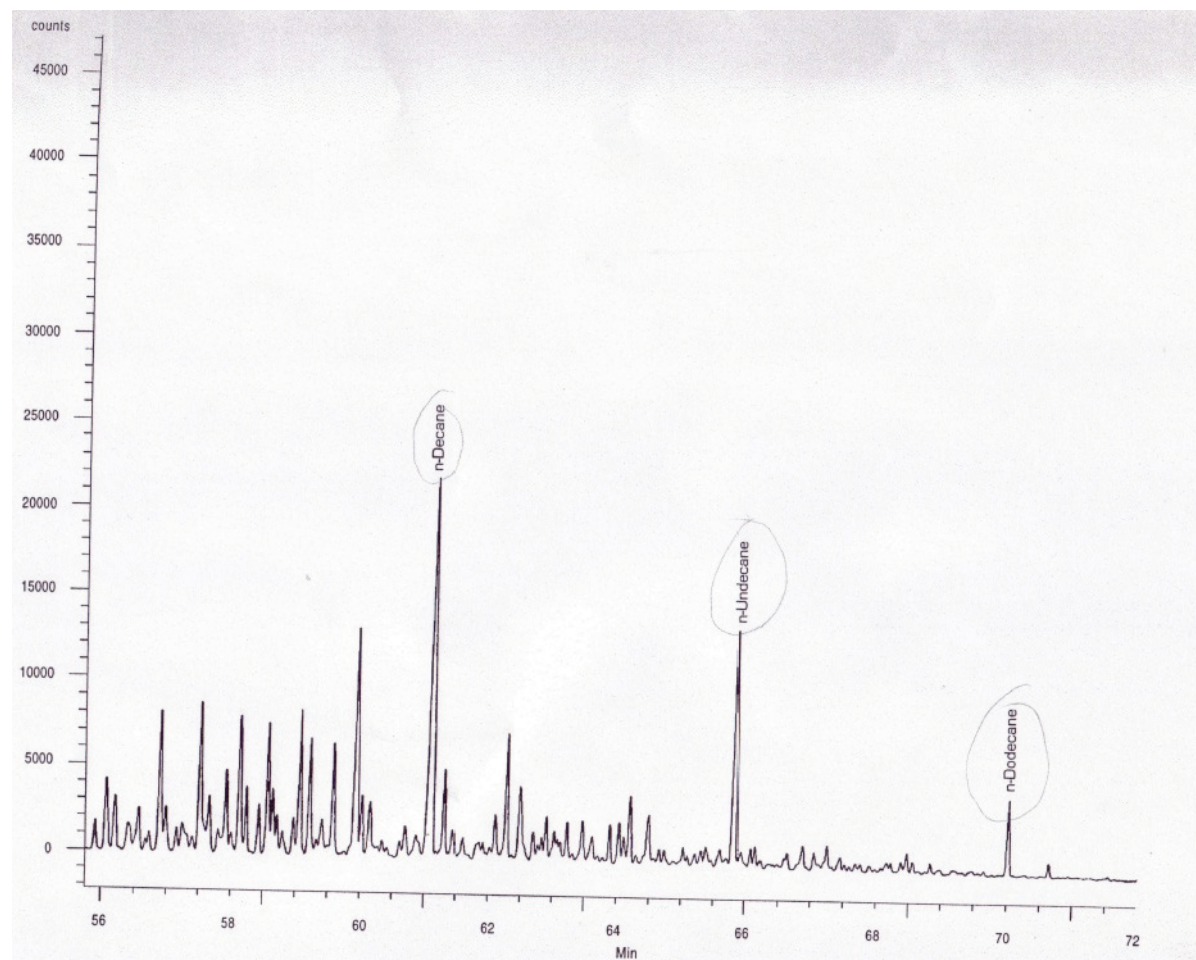
ASTM D5134 Standard

4 of 6





ASTM D5134 Standard 6 of 6



9.3 Appendix C: Thermodynamic Modeling

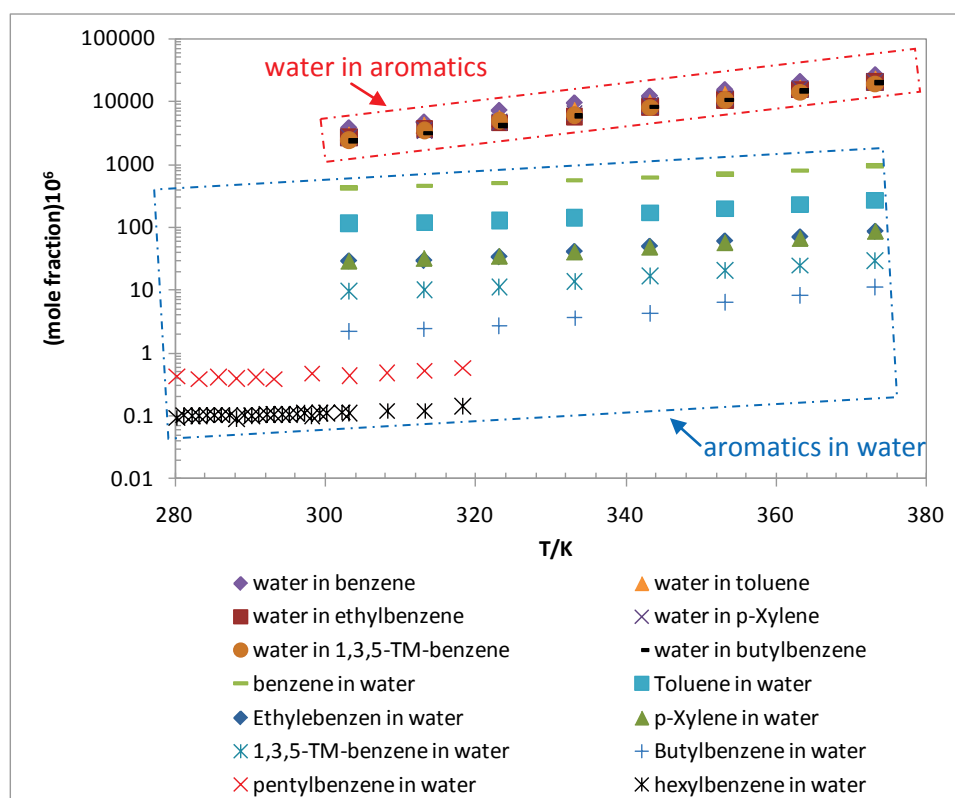
In appendix C work related to the modeling of phase behavior of well-defined hydrocarbon and reservoir fluid systems in presence of polar chemicals is presented.

C. 1: % AAD for Mutual Solubility of Water + Pentylbenzene for $k_{ij} = -0.0945$. The data are not available for water in pentylbenzene therefore corresponding %AAD is not presented.

β_{cross}	Pentylbenzene in Water % AAD	Water in Pentylbenzene % AAD	Global % AAD
0.050	354		
0.040	296		
0.030	239		
0.020	182		
0.010	124		
0	66		

C. 2: % AAD for Mutual Solubility of Water + Hexylbenzene for $k_{ij} = -0.0945$. The data are not available for water in hexylbenzene therefore corresponding %AAD is not presented.

β_{cross}	hexylbenzene in Water % AAD	Water in Hexylbenzene % AAD	Global % AAD
0.040	160		
0.030	140		
0.035	120		
0.020	82		
0.010	42		
0	17		



C. 3: Experimental data and trends in mutual solubility of aromatic hydrocarbons and water systems. It is shown that solubility of water in aromatic hydrocarbon very close to each other whereas solubility of hydrocarbon in water decreases with increasing carbon number. The numerical values of these solubilities are given in Table given below.

C. 4: Experimental Data for Mutual Solubility of Water and Heavy Aromatics Showing That Solubility of Water in HC Lie in the Same Range.

Aromatic	T/K	HC in water (x .10 ⁶)	Water in HC (x. 10 ⁶)
Benzene	303-373	424-950	3840-26500
Toluene	303-373	117-268	2479-19366
p-xylene	303-373	29-87	2710-20200
Ethylbenzene	303-373	29-85	2710-20200
Butylbenzene	303-373	2-11	2360-19900
1,3,5-TM-benzene	303-373	10-29	2470-19000
Pentylbenzene	280-318	0.420-0.575	Not available
Hexylbenzene	278-218	0.102-0.145	Not available

9.4 Appendix D: List of Publications

This appendix presents scientific contributions made during this project in form of journal articles and as conference presentations. Further more I have co-supervised three master theses.

D. 1: Journal Publications

-
- 1 Riaz M. Kontogeorgis G.M. Stenby E.H. Yan W. Haugum T. Christensen K.O. Solbraa E. Løkken T.V., *Mutual Solubility of MEG, Water and Reservoir Fluid: Experimental Measurements and Modeling using the CPA Equation of State*, Journal of Fluid Phase Equilibria 300(2011) 172-181.
 - 2 Riaz M. Kontogeorgis G.M. Stenby E.H. Yan W. Haugum T. Christensen K.O. Solbraa E. Løkken T.V., *Measurement of Liquid-Liquid Equilibria for Condensate + Glycol and Condensate + Glycol + water Systems*, Journal of Chemical & Engineering Data (accepted for publication ID:je-2011-00158c)
-

D. 2: Conference Proceedings

-
- 1 Riaz M. Kontogeorgis G.M. Stenby E.H. Yan W. Haugum T. Christensen K.O. Solbraa E. Løkken T.V., *Distribution of Gas Hydrate Inhibitors in Oil and Gas Production Systems*, Oral Presentation, Presented at 25th European Symposium on Applied Thermodynamics (ESAT), 2011, Saint Petersburg, Russia.
 - 2 Riaz M. Kontogeorgis G.M. Stenby E.H. Yan W. Haugum T. Christensen K.O. Solbraa E. Løkken T.V., *Mutual Solubility of MEG, Water and Reservoir Fluid: Experimental Measurements and Modeling using the CPA Equation of State*, Poster Presentation, Presented at Special Symposium on SAFT, 2010, Barcelona, Spain.
 - 3 Riaz M. Kontogeorgis G.M. Stenby E.H. Yan W. Haugum T. Christensen K.O. Solbraa E. Løkken T.V., *Mutual Solubility of MEG, Water and Reservoir Fluid: Experimental Measurements and Modeling using the CPA Equation of State*, Oral Presentation Presented at CHISA/ECCE7, 2010, Prague, Czech Republic.
 - 4 Riaz M. Kontogeorgis G.M., *Mutual Solubility of MEG, Water and Reservoir Fluid: Experimental Measurements and Modeling using the CPA Equation of State*, Poster Presentation Presented at Danske Kemiingeniør Konference (DK2), 2010, Lyngby, Denmark.
 - 5 Riaz, M. Thomsen, K., *Design and Analysis of Extractive Distillation Processes using Ionic Liquids*, Poster presentation (regarding Master Thesis Work) Presented at: EUCHEM 2008 Conference on Molten Salts and Ionic Liquids, 2008, Copenhagen, Denmark
-

D. 3: Article-1 Published in Journal of Fluid Phase Equilibria.

Mutual solubility of MEG, water and reservoir fluid: Experimental measurements and modeling using the CPA equation of state

Muhammad Riaz^a, Georgios M. Kontogeorgis^{a,*}, Erling H. Stenby^{a,b}, Wei Yan^a, Toril Haugum^c, Kjersti O. Christensen^c, Even Solbraa^c, Torbjørn V. Løkken^c

^a Center for Energy Resources Engineering (CERE), Department of Chemical and Biochemical Engineering, Technical University of Denmark, DK-2800 Lyngby, Denmark

^b Center for Energy Resources Engineering (CERE), Department of Chemistry, Technical University of Denmark, DK-2800 Lyngby, Denmark

^c Statoil ASA, Research and Development Center, N-7005 Trondheim, Norway

ARTICLE INFO

Article history:

Received 4 August 2010

Received in revised form 5 October 2010

Accepted 6 October 2010

Available online 12 October 2010

Keywords:

Reservoir fluid

Monoethylene glycol (MEG)

Water

Experimental data

CPA equation of state

Thermodynamic modeling

Mutual solubility

Polar chemicals

ABSTRACT

This work presents new experimental phase equilibrium data of binary MEG–reservoir fluid and ternary MEG–water–reservoir fluid systems at temperatures 275–326 K and at atmospheric pressure. The reservoir fluid consists of a natural gas condensate from a Statoil operated gas field in the North Sea.

Prediction of mutual solubility of water, MEG and hydrocarbon fluids is important for the oil industry to ensure production and processing as well as to satisfy environmental regulations. The CPA equation of state has been successfully applied in the past to well defined systems containing associating compounds. It also has been extended to reservoir fluids in presence of water and polar chemicals using a Pedersen like characterization method with modified correlations for critical temperature, pressure and acentric factor. In this work CPA is applied to the prediction of mutual solubility of reservoir fluid and polar compounds such as water and MEG. Satisfactory results are obtained for mutual solubility of MEG and gas condensate whereas some deviations are observed for the ternary system of MEG–water–gas condensate.

© 2010 Elsevier B.V. All rights reserved.

D. 4: Article-2 Accepted for Publication in Journal of Chemical and Engineering Data (In the Press).

JOURNAL OF CHEMICAL & ENGINEERING DATA

ARTICLE

pubs.acs.org/jced

Measurement of Liquid–Liquid Equilibria for Condensate + Glycol and Condensate + Glycol + Water Systems

Muhammad Riaz,[†] Georgios M. Kontogeorgis,^{*,†} Erling H. Stenby,[†] Wei Yan,[†] Toril Haugum,[§] Kjersti O. Christensen,[§] Torbjørn V. Løkken,[§] and Even Solbraa[§]

[†]Department of Chemical and Biochemical Engineering, Center for Energy Resources Engineering (CERE), Technical University of Denmark, DK-2800 Lyngby, Denmark

[‡]Department of Chemistry, Center for Energy Resources Engineering (CERE), Technical University of Denmark, DK-2800 Lyngby, Denmark

[§]Statoil ASA, Research and Development Center, N-7005 Trondheim, Norway

ABSTRACT: Today's oil and gas production requires the application of various chemicals in large amounts. To evaluate the effects of those chemicals on the environment, it is of crucial importance to know how much of the chemicals are discharged via produced water and how much is dissolved in the crude oil. The ultimate objective of this work is to develop a predictive thermodynamic model for the mutual solubility of oil, water, and polar chemicals. But for the development and validation of the model, experimental data are required. This work presents new experimental liquid–liquid equilibrium (LLE) data for 1,2-ethanediol (MEG) + condensate and MEG + water + condensate systems at temperatures from (275 to 323) K at atmospheric pressure. The condensate used in this work is a stabilized natural gas condensate from an offshore field in the North Sea. Compositional analysis of the natural gas condensate was carried out by gas chromatography, and detailed separation of individual condensate's components has been carried out. Approximately 85 peaks eluting before nonane were identified by their retention time. Peak areas were converted to mass fraction using 1-heptene as an internal standard. The components were divided into boiling range groups from hexane to nonane. Paraffinic (P), naphthenic (N), and aromatic (A) distributions were obtained for the boiling point fractions up to nonane. The average molar mass and the overall density of the condensate were measured experimentally. For the mutual solubility of MEG and condensate, approximately 72 component peaks could be detected up to nonane and many components from decane plus carbon fraction. Their solubility was quantified, and the sum was reported as solubility of condensate in MEG. A similar procedure was adopted for the MEG, condensate, and water system, but because of the presence of water, the solubility of condensate in the polar phase decreases, and some of the components were not detectable.